

Combinatorial Concepts and Algorithms for Drawing Planar Graphs

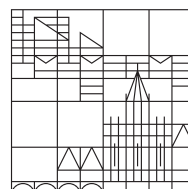
Dissertation

zur Erlangung des akademischen Grades
Doktor der Naturwissenschaften
(Dr. rer. nat.)

vorgelegt von
Melanie Baur

an der

Universität
Konstanz



Mathematisch-Naturwissenschaftliche Sektion
Fachbereich Informatik & Informationswissenschaft

Tag der mündlichen Prüfung: 10. Juli 2012
Erster Referent: Prof. Dr. Ulrik Brandes
Zweite Referentin: PD Dr. Sabine Cornelsen

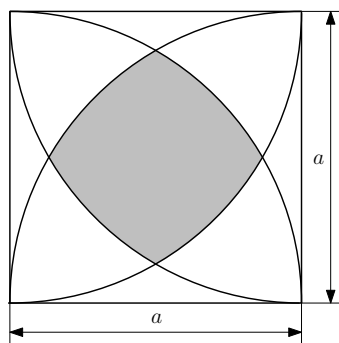
Preface

“I decided to carefully and thoroughly examine
all that has been accomplished on earth.”
Ecclesiastes 1, 13

I remember the time when I wanted to become a detective. I think there is not much difference from being a researcher - combining hints and theories to one truth. Maybe this is why I always loved math and I always will do.

I remember the time when I learned hundreds of digits of π . It sounds to me more beautiful than any poem. Now, I still think it is at least as beautiful as any poem of Annette von Droste-Hülshoff. Maybe this is why I always loved math and I always will do.

I remember the time when my father and I spent hours, indeed days, to calculate the gray area of the following figure:¹



Maybe this is why I always loved math and I always will do.

But now, I know so much more about it. Now, I can represent it as a graph, label and orient the edges, order the vertices, embed it in different surfaces, find bijective functions that map it onto other combinatorial structures, create algorithms that do

¹Bernhard Krohn, Helmut Rattay. *Geometrie*. Verlag Handwerk und Technik.

all this for me, and prove that they really do it in limited time and space. Thanks to *Ulrik Brandes* who discovered and aroused the passion for graphs inside me.

Thanks to my colleagues in chronological order, Daniel for being my favorite piano player (except Ingolf), Christian for smiling his special smile on every pic, Barbara for Italian holidays, Thomas for cycling and climbing, Martin H. for being my first office mate, Jürgen for a prospective raclette, Hendrik for not complaining during hiking, Krists for a graph drawing class, Sabine for sharing muffins and the love to Eugen Jost with me, Sven for Beratersprech, Uwe for the Leipzig bet, Martin M. for being relaxed all the time, Christine for office supplies, Natalie for watching Top Models, Bobo for blues, Andreas for projecting his secret wishes on me, Steffen for the baking skills of his wife, Arlind for remembering my cake, Viviana for SOS.

Thanks to those without whom I would not have been able to come to that point, Steffi for throwing the bridal bouquet to Uli, Uli for suffering even more under her professor than I did, Sonja for choosing me as her maid of honor, Silvi - I do not have so much words to express that all, Ninja for being crazier than I am, Hedi for Italian holidays and an idea.

Thanks to all those who made my PhD time in Konstanz very special, Team Südsee, the name says it all, Stephen for being his Melli, Georg for rock 'n' roll, Wolfgang for run and bike, Bekki for e-mails, Marco for going more often to the toilet than I do, Martin N. for Otto and Australia, Emma and Paula for being the proof that time passes by and life is fun, Martin W. for Argentina, Markus for helium, Uli S. for his TV and physiotherapy, Armin for steaks, Michela and Erica for Italian, Christoph for this pic, Sebi for having passed the SBF See exam, Franzi, Sarah, and Joni for connecting, Martin O. also for connecting, all others from the connect groups I have been over the years, Pia for having another side deep inside, Reinhard for a very good dinner, Achim for listening to my stories on the sailing boat, Olli for knowing more about coffee machines than I do, Eva for exchanging secrets.

Thanks to Manfred and Ronny for bringing me back to life after my accident.

Thanks to my mentors Roman and Philipp for introducing me to the big real world outside.

Last but not least I deeply thank Mom, Dad, and Patrick for being my family, and Michael for giving me his name.

Melanie Badent
April 2012

Deutsche Zusammenfassung

Im Vergleich zu allgemeinen Graphen haben planare Graphen unzählige spezifische kombinatorische Eigenschaften, die einer eingehenden Betrachtung wert sind. Durch das Studium einiger ihrer prägnantesten Charakteristika stießen wir schließlich auf die Eleganz des dreifachen Zusammenhangs und dessen Verbindung zu Polytopen. Dies verführte uns dazu, uns den auf der Klasse der dreifach zusammenhängenden, planaren Graphen besonders wichtigen Konzepten kanonische Ordnung und Schnyder-Wälder zu widmen. Während diese bisher meist getrennt betrachtet wurden, legen wir in dieser Arbeit den Fokus auf ihre Gemeinsamkeiten, und stellen die Zusammenhänge erstmals auf einheitliche Art und Weise vor.

Der Titel *Kombinatorische Konzepte und Algorithmen zum Zeichnen planarer Graphen* spiegelt bereits die zweigeteilte Grundstruktur dieser Arbeit wider. In Teil I *Konzepte* führen wir, nach einer Zusammenfassung wesentlicher Eigenschaften planarer Graphen, die kombinatorischen Konzepte kanonische Ordnung und Schnyder-Wälder ein. Weiterhin zeigen wir deren Zusammenhang zu Kontaktrepräsentationen durch Dreiecke auf. Von den vielfältigen Anwendungsmöglichkeiten konzentrieren wir uns auf das Zeichnen von Graphen, insbesondere auf Dreiecksrepräsentationen, und stellen in Teil II *Algorithmen* detaillierte und einheitliche Algorithmen dazu vor, wobei ein Schwerpunkt auf der Implementierung der linkesten kanonischen Ordnung liegt.

Eigener Beitrag. Die Hauptbeiträge dieser Arbeit sind zum Einen die Einführung des Konzepts der linkesten kanonischen Ordnung und die Herstellung einer Beziehung über geordnete Pfadpartitionen zu minimalen Schnyder-Wäldern, zum Anderen die Bereitstellung von effizienten Algorithmen mit detaillierten, leicht umsetzbaren Pseudocodes. Aufbauend darauf zeigen wir, wie und auf welchen Graphenklassen diese Verfahren Kontaktrepräsentationen mittels homothetischer Dreiecke ermöglichen.

Darüber hinaus geben wir auf einheitliche Art und Weise eine umfangreiche Übersicht über verwandte Konzepte und stellen zu diesen teilweise neue, einfachere oder besser aufeinander aufbauende Beweise und Algorithmen vor. Teile dieser Arbeit wurden bereits in [Badent et al. \[2007, 2010, 2011\]](#) veröffentlicht.

Teil I - Konzepte

Kapitel 1: Planare Graphen. Zuerst führen wir grundlegende Definitionen und Eigenschaften planarer Graphen ein, die im weiteren Verlauf der Arbeit wiederholt verwendet werden. Unser Hauptaugenmerk liegt dabei auf den wesentlichen Grundlagen dreifach zusammenhängender, planarer Graphen. Zum Abschluss dieses Kapitels fassen wir einige Charakterisierungen planarer Graphen zusammen.

Kapitel 2: Kanonische Ordnung. In diesem Kapitel stellen wir Definitionen sowohl von kanonischer Ordnung für verschiedene Klassen von Graphen, nämlich triangulierte und dreifach zusammenhängende, planare Graphen, als auch von speziellen kanonischen Ordnungen, wie beispielsweise linker und linkerster kanonischer Ordnung, vor.

Die von uns eingeführte linkerste kanonische Ordnung ist insbesondere auch eine linke kanonische Ordnung und im Unterschied zu dieser eindeutig bestimmt [Badent et al., 2010, 2011]. Danach zeigen wir die Verbindung der kanonischen Ordnung eines Dualgraphen zur kanonischen Ordnung des Ursprungsgraphen auf [Badent et al., 2010, 2011].

Schließlich behandeln wir kurz verwandte Konzepte wie kanonische Ordnung für zweifach, vierfach und fünffach zusammenhängende, planare Graphen [Harel und Sardas, 1998, Kant und He, 1997, Nagai und Nakano, 2000], kanonische Ordnungsbäume und geordnete Spannbäume [Chuang et al., 1998, He et al., 1999, Chiang et al., 2001, 2005].

Kapitel 3: Schnyder-Wälder. Nun führen wir Schnyder-Wälder für triangulierte und dreifach zusammenhängende, planare Graphen ein und stellen eine Bijektion zwischen Schnyder-Wäldern und Schnyder-Beschriftungen vor, sowie deren Zusammenhang zu kanonischer Ordnung [Schnyder, 1989, 1990, Di Battista et al., 1999, Felsner, 2001]. Um ein besseres Verständnis von der Struktur eines Schnyder-Waldes zu bekommen, betrachten und beweisen wir mehrere seiner Eigenschaften, gehen näher auf duale Aspekte ein und skizzieren eine Idee, um zu beweisen, dass die Menge aller Schnyder-Wälder einen distributiven Verband bildet [Felsner, 2004b].

Schwerpunkt des Kapitels ist die Einführung von Pfadpartitionen, die auf dreifach zusammenhängenden, planaren Graphen bijektiv zu Schnyder-Wäldern sind. Diese Einsicht kann benutzt werden, um auf einfache Art und Weise das minimale Element des Verbandes zu berechnen [Badent et al., 2011].

Kapitel 4: Kontaktrepräsentation durch Dreiecke. Es ist wohlbekannt, dass es für jeden Graph eine Kontaktrepräsentation durch Dreiecke gibt. Wir schränken das Problem auf homothetische Dreiecke ein und zeigen, dass jeder serien-parallele gerichtete Graph mit zwei Endpunkten und jeder teilweise planare 3-Baum eine strenge, homothetische Kontaktrepräsentation durch Dreiecke besitzt [Badent et al., 2007]. Danach führen wir ein neues Ergebnis an, das unsere Forschung auf vierfach zusammenhängende, planare Triangulierungen erweitert [Gonçalves et al., 2011]. Bezugnehmend auf die vorangegangenen Kapitel, betrachten wir Kontaktrepräsentationen durch Dreiecke abschließend im Kontext dualer Konzepte und Schnyder-Wälder [de Fraysseix et al., 1994, Gonçalves et al., 2011].

Teil II - Algorithmen

Kapitel 5: Kanonische Ordnung. Nun beschreiben wir präzise unseren Algorithmus zur Berechnung der linkesten kanonischen Ordnung und präsentieren detaillierte Pseudocodes, die sich einfach in eine konkrete Linearzeit-Implementierung übertragen lassen. [Badent et al., 2010, 2011].

Unter den vielen Anwendungen von kanonischer Ordnung legen wir den Schwerpunkt auf Gitterzeichnungen und erklären die berühmte *Shiftmethode* von Kant [1996]. Als Anwendung neben dem reinen Graphenzeichnen zeigen wir, wie man einen zweifach zusammenhängenden, planaren Graphen gleichzeitig trianguliert und eine kanonische Ordnung für ihn berechnet [Kant, 1993].

Kapitel 6: Schnyder-Wälder. Zuletzt beschreiben wir Algorithmen für die in Kapitel 3 beschriebenen Konzepte, die in Linearzeit ausgeführt werden können. Im Einzelnen legen wir einen Algorithmus dar, der für einen triangulierten, planaren Graphen einen Schnyder-Wald ohne im Uhrzeigersinn orientierte Kreise berechnet. Für dreifach zusammenhängende, planare Graphen beschreiben wir Methoden um einen Schnyder-Wald über die kanonische Ordnung [Di Battista et al., 1999] beziehungsweise über Kantenkontraktionen [Felsner, 2001] zu berechnen.

Weiterhin passen wir unseren Algorithmus zur Berechnung der linkesten kanonischen Ordnung aus Kapitel 5 so an, dass er den minimalen Schnyder-Wald eines dreifach zusammenhängenden, planaren Graphen ausgibt [Badent et al., 2011]. Wir schließen mit Anwendungen aus dem Graphenzeichnen wie Schwerpunktsrepräsentationen von triangulierten Graphen [Schnyder, 1990], konvexen Zeichnungen von dreifach zusammenhängenden, planaren Graphen [Felsner, 2001, 2004a] und der Verbindung von Schnyder-Wäldern zu orthogonalen Oberflächen und geodätischen Einbettungen [Felsner, 2003].

Contents

Introduction	1
I Concepts	5
1 Planar Graphs	7
1.1 Basics	7
1.2 Drawings and Embeddings	15
1.3 Number of Graph Elements	19
1.4 Triangulating Graphs	21
1.5 Triconnected Graphs	22
1.6 Characterization	31
2 Canonical Ordering	37
2.1 Introduction	37
2.2 Special Canonical Orderings	43
2.3 Duality	45
2.4 Related Concepts	49
3 Schnyder Woods	59
3.1 Triangular Graphs	61
3.2 Triconnected Graphs	74
3.3 Characterization of Planar Graphs	84
3.4 Duality	85

3.5	Lattice Structure	88
3.6	Path Partition	91
4	Triangle Contact Representation	97
4.1	Preliminaries	101
4.2	Homothetic Triangle Contact Representation	103
4.3	TTSP-Digraphs	104
4.4	Partial Planar 3-Trees	109
4.5	4-Connected Triangulations	115
4.6	Duality	116
4.7	Schnyder Woods	118
4.8	Notes	121
II	Algorithms	123
5	Canonical Ordering	125
5.1	Computation	125
5.2	Linear-Time Implementation	130
5.3	Applications	136
6	Schnyder Woods	145
6.1	Triangular Graphs	146
6.2	Triconnected Graphs	150
6.3	Drawings	156
	Conclusion	163
	Bibliography	165
	List of Symbols	187
	Index	191

Introduction

“Adventures in cyberspace, the chase is on!
Just wait and cyberchase.”¹

In comparison to general graphs, planar graphs have numerous specific properties that make them worth to be considered thoroughly. After studying fundamental as well as prominent characteristics, we finally encountered the elegance of triconnectivity and its connection to polytopes. This seduced us to devote ourselves to the concepts of canonical ordering and Schnyder woods that are of particular importance to the class of triconnected, planar graphs. Whereas these concepts mostly have been investigated separately so far, we focus this thesis on their similarities and connection points, and present them consistently for the first time.

The title *Combinatorial Concepts and Algorithms for Drawing Planar Graphs* already reflects the twofold structure of this thesis. In Part I *Concepts* we introduce, after giving a summary of fundamental properties of planar graphs, the combinatorial concepts of canonical ordering and Schnyder woods. Furthermore, we reveal their connection to triangle contact representations. Canonical ordering and Schnyder woods have manifold applications in graph encoding, in dimension theory, in the area of counting various kinds of planar maps, and more. We concentrate on graph drawing, in particular on triangle contact representations, and present in Part II *Algorithms* appropriate detailed and consistent algorithms with focus on the implementation of the leftist canonical ordering.

Contribution. Main contributions of this thesis are the introduction of the concept of leftist canonical ordering, the establishing of a connection via ordered path partitions to minimal Schnyder woods, and the provision of efficient algorithms with detailed pseudocodes that ease coding. Based on these, we show how and on which graph classes these methods can be used to determine homothetic triangle contact representations.

¹Cyberchase theme song, <http://pbskids.org/cyberchase/>

Furthermore, we give an extensive overview of related concepts in a consistent manner and provide various new, simpler or more consistent proofs and algorithms. Parts of this thesis are published in [Badent et al. \[2007, 2010, 2011\]](#).

Part I - Concepts

Chapter 1: Planar Graphs. First, we introduce definitions and notations that are used throughout the thesis and state basic theorems about planar graphs, in particular, about triconnected, planar graphs. To conclude this chapter, we summarize characterizations of planar graphs.

Chapter 2: Canonical Ordering. In this chapter, we present definitions of canonical orderings for triangular and triconnected, planar graphs as well as special canonical orderings such as leftmost and leftist canonical ordering.

The leftist canonical ordering introduced by us is in particular a leftmost canonical ordering but in addition, it is uniquely determined [[Badent et al., 2010, 2011](#)]. Thereafter, we show the connection between a canonical ordering of the dual and the canonical ordering of the respective original graph [[Badent et al., 2010, 2011](#)].

Finally, we bring up related concepts such as canonical ordering for biconnected, 4-connected, and 5-connected, planar graphs [[Harel and Sardas, 1998](#), [Kant and He, 1997](#), [Nagai and Nakano, 2000](#)], canonical ordering trees, and orderly spanning trees [[Chuang et al., 1998](#), [He et al., 1999](#), [Chiang et al., 2001, 2005](#)].

Chapter 3: Schnyder Woods. Now, we present Schnyder woods for triangular and triconnected, planar graphs, explain a bijection between Schnyder woods and Schnyder labelings, and describe the relation to canonical orderings [[Schnyder, 1989, 1990](#), [Di Battista et al., 1999](#), [Felsner, 2001](#)]. To increase the understanding of the combinatorial structure of a Schnyder wood, we observe and prove several of its distinctive properties, examine dual aspects and sketch an idea to prove that the set of all Schnyder woods forms a distributive lattice [[Felsner, 2004b](#)].

Since Schnyder woods can be used to prove that a graph is planar if and only if the dimension of its incidence order is at most three [[Schnyder, 1989](#)], we do not withhold this result from the reader and outline the proof of [Felsner \[2004a\]](#).

We complete with the introduction of ordered path partitions that are a generalization of canonical orderings. The gist of this chapter is that certain equivalence classes of ordered path partitions are in one-to-one correspondence with Schnyder woods for triconnected, planar graphs. This bijection can be used to easily compute

the minimal element of the lattice [Badent et al., 2011] that is formed by the set of Schnyder woods.

Chapter 4: Triangle Contact Representation. It is well known that every graph has a triangle contact representation. We restrict this problem to homothetic triangles and show that every two-terminal series-parallel digraph and any partial planar 3-tree has a strict homothetic triangle contact representation [Badent et al., 2007]. Also, we describe a new approach that extends our results to 4-connected, planar triangulations [Gonçalves et al., 2011]. With regard to the previous chapters, we examine triangle contact representations in the context of dual concepts and Schnyder woods [de Fraysseix et al., 1994, Gonçalves et al., 2011].

Part II - Algorithms

Chapter 5: Canonical Ordering. In this chapter, we precisely describe our algorithm to compute the leftist canonical ordering and present detailed pseudocodes that in particular simplify its implementation with linear running time [Badent et al., 2010, 2011].

Of the many applications of canonical orderings in graph drawing, we emphasize grid drawings and present the well-known *shift method* of Kant [1996]. As an application from a slightly other subject, we describe how to triangulate a biconnected, plane graph while computing a canonical ordering at the same time [Kant, 1993].

Chapter 6: Schnyder Woods. Finally, we present algorithms for the concepts explained in Chapter 3 which run in linear time. In more detail, we state an algorithm that computes a Schnyder wood without clockwise oriented cycles on a triangular graph. For triconnected, planar graphs, we explain methods to compute a Schnyder wood via canonical ordering [Di Battista et al., 1999] and via edge contraction [Felsner, 2001], respectively.

Moreover, we adapt our algorithm to determine a leftist canonical ordering of Chapter 5 to output the minimal Schnyder wood of a triconnected, planar graph [Badent et al., 2011]. We conclude with applications in graph drawing such as barycentric representations of triangular graphs [Schnyder, 1990], convex drawings of triconnected, planar graphs [Felsner, 2001, 2004a] and the relation of Schnyder woods to orthogonal surfaces and geodesic embeddings [Felsner, 2003].

Part I
Concepts

Chapter 1

Planar Graphs

This section settles the foundations for this thesis by introducing definitions and notations as well as basic results about planar graphs that are used throughout. For graph-theoretic notations we closely stick to the terminology of [Diestel \[2010\]](#). Other books on graph theory that use the same notations are, e. g., [Harary \[1969\]](#) and [Bondy and Murty \[1976\]](#).

1.1 Basics

By \mathbb{N} we denote the set of natural numbers including zero and by \mathbb{R} we denote the set of real numbers. Let \mathbb{F}_2 denote the field with two elements $\{0, 1\}$.

Topological Prerequisites Let \mathbb{R}^2 denote the *Euclidean plane*, i. e., the two-dimensional Euclidean space together with the natural topology induced by the Euclidean metric. Analogously, let \mathbb{R}^3 denote the *Euclidean space*, i. e., the three-dimensional Euclidean space together with the natural topology induced by the Euclidean metric. Any subset of the Euclidean plane and the Euclidean space, respectively, is assumed to carry the subspace topology.

Speaking about the *plane*, we always refer to the Euclidean plane \mathbb{R}^2 . An element $p \in \mathbb{R}^2$ is written as a vector $p = (p_1, p_2)$, with $p_i \in \mathbb{R}$, $i = 1, 2$. Thus, by a pair of *coordinates* we can uniquely determine a point in the plane. We also denote the coordinates of a point $p = (p_1, p_2) \in \mathbb{R}^2$ by $(x(p), y(p))$, where $p_1 = x(p)$ and $p_2 = y(p)$, respectively.

Analogously, an element $p \in \mathbb{R}^3$ is written as a vector $p = (p_1, p_2, p_3)$ and the coordinates of p are denoted by $(x(p), y(p), z(p))$.

The length of a vector $p = (p_1, p_2) \in \mathbb{R}^2$ is

$$\|p\| = \sqrt{p_1^2 + p_2^2}.$$

The *Euclidean distance* of two points $p = (p_1, p_2) \in \mathbb{R}^2$ and $q = (q_1, q_2) \in \mathbb{R}^2$ in the plane is

$$d(p, q) = d(q, p) = \|p - q\| = \sqrt{(q_1 - p_1)^2 + (q_2 - p_2)^2}.$$

The *Manhattan distance* (or *L_1 distance*, *ℓ_1 norm*, *Taxicab metric*) of two points $p = (p_1, p_2)$ and $q = (q_1, q_2) \in \mathbb{R}^2$ is

$$d_1(p, q) = d_1(q, p) = \|p - q\|_1 = |(q_1 - p_1)| + |(q_2 - p_2)|.$$

Let $p, q \in \mathbb{R}^2$ with $p \neq q$. A *straight-line segment* $s \subseteq \mathbb{R}^2$ has the form

$$s = \{p + \lambda(q - p) \mid 0 \leq \lambda \leq 1\}.$$

Let $\mathbb{I} = [0, 1] = \{p \in \mathbb{R} \mid 0 \leq p \leq 1\}$ be the *closed unit interval*. A *simple polygonal arc* is the union of finitely many straight-line segments and homeomorphic to \mathbb{I} . A *simple arc* (or *Jordan arc*, *open curve*) is the image of a homeomorphic mapping $a: \mathbb{I} \rightarrow \mathbb{R}^2$. The images of 0 and 1 are the *endpoints* of a , all other points are *internal points*. We say that a *joins* $a(0)$ and $a(1)$. A *simple closed curve* (or *Jordan curve*) is a simple arc with $a(0) = a(1)$. Two simple closed curves are *tangent* to each other if and only if both curves share a common tangent line at a common point. This point is called a *contact point*.

Since an arc is the continuous image of \mathbb{I} , it is compact and, therefore, closed in \mathbb{R}^2 . If a is an arc with endpoints p and q , then the set $a \setminus \{p, q\}$ is denoted by \mathring{a} and called *interior* of a .

For an open or closed set $S \subseteq \mathbb{R}^2$, we denote by ∂S the boundary of S .

Let \mathbb{R}^d denote the vector space of all column vectors of length d with real entries. A point set $S \subseteq \mathbb{R}^d$ is *convex* if for any pair of vectors $p, q \in S$ the vector $(1 - \lambda)p + \lambda q \subseteq S$ for all $\lambda \in [0, 1]$. The *convex hull* of some $S \subseteq \mathbb{R}^d$ is

$$\bigcap \{S' \subseteq \mathbb{R}^d \mid S \subseteq S', S' \text{ convex}\}.$$

A *polytope* is the convex hull of a finite set of points in \mathbb{R}^d . See Figure 1.1(a) for an example of a three-dimensional polytope. A *polygon* is a two-dimensional polytope. An example is shown in Figure 1.1(b).

The vertices and edges of a polytope determine a graph, sometimes called *polyhedral graph*.

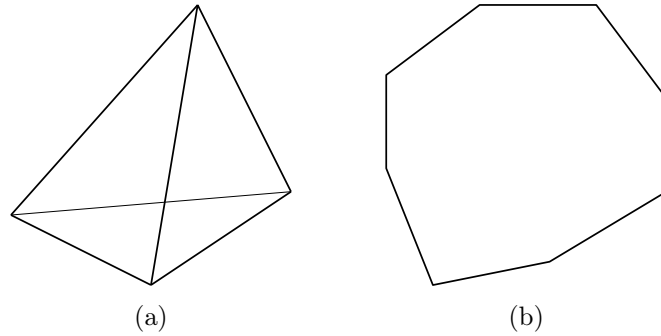


Figure 1.1: (a) Three-dimensional polytope. (b) Convex polygon.

Sets and Relations A set $\mathcal{S} = \{S_1, \dots, S_n\}$ of non-empty subsets of a finite set S is a *partition* of S if $S_1 \cup \dots \cup S_n = S$ and $S_i \cap S_j = \emptyset$, $i, j \in \{1, \dots, n\}$, $i \neq j$. By $[S]^n$ we denote the set of all n -element subsets of S . Sets with n elements are called *n -sets*; subsets with n elements are called *n -subsets*.

Let S_1, \dots, S_n be sets. The *Cartesian product* (or *product set*) of S_1, \dots, S_n is defined as

$$S_1 \times \dots \times S_n = \{(s_1, \dots, s_n) \mid s_i \in S_i \text{ for all } i \in \{1, \dots, n\}\}.$$

A set $R \subseteq S_1 \times \dots \times S_n$ is called a *relation*; a relation $R \subseteq S_1 \times S_2$ is a *binary relation*. If $S_1 = S_2 = S$, then $R \subseteq S \times S$ is called a *binary relation on S* .

A *total order* \preceq (or *linear order*) is a binary relation over a set S that satisfies for all $a, b, c \in S$ the following conditions:

1. $a \preceq b$ or $b \preceq a$ (*total*)
2. If $a \preceq b$ and $b \preceq a$, then $a = b$. (*antisymmetric*)
3. If $a \preceq b$ and $b \preceq c$, then $a \preceq c$. (*transitive*)

A (*non-strict*) *partial order* \preceq is a binary relation over a set S that satisfies for all $a, b, c \in S$ the following conditions:

1. $a \preceq a$ (*reflexive*)
2. If $a \preceq b$ and $b \preceq a$, then $a = b$. (*antisymmetric*)
3. If $a \preceq b$ and $b \preceq c$, then $a \preceq c$. (*transitive*)

A *strict partial order* \prec is a binary relation over a set S that satisfies for all $a, b, c \in S$ the following conditions:

1. $a \not\prec a$ (*irreflexive*)
2. If $a \prec b$, then $b \not\prec a$. (*symmetric*)
3. If $a \prec b$ and $b \prec c$, then $a \prec c$. (*transitive*)

A *partially ordered set* (or *poset* for short) $P = (S, \prec)$ and $P = (S, \preceq)$, respectively, consists of a set S together with a strict and non-strict partial order \prec and \preceq on S , respectively. If not stated otherwise, we always refer to non-strict partial orders. An element $m \in S$ of a poset $P = (S, \preceq)$ is called *maximal* if there is no element $e \in S$ with $m \preceq e$; an element $m \in S$ is called *minimal* if there is no element $e \in S$ with $e \preceq m$. In general, there may be more than one maximal and minimal element, respectively, or none. In a finite poset, there exists always at least one maximal element.

A poset is a *lattice* $L = (S, \preceq)$ if it satisfies the following two conditions:

1. Every $a, b \in S$ has a *join* $c \in S$ (also called *least upper bound* or *supremum*), written as $a \vee b$, i. e.,

$$\begin{aligned} & a \leq c \text{ and } b \leq c \\ \forall c' \in S: & a \leq c', b \leq c' \Rightarrow c \leq c'. \end{aligned}$$

2. Every $a, b \in S$ has a *meet* $c \in S$ (also called *greatest lower bound* or *infimum*), written as $a \wedge b$, i. e.,

$$\begin{aligned} & a \geq c \text{ and } b \geq c \\ \forall c' \in S: & a \geq c', b \geq c' \Rightarrow c \geq c'. \end{aligned}$$

A lattice $L = (S, \preceq)$ is *distributive* if the operations join and meet are distributive. In more detail, for all $a, b, c \in S$ there holds:

$$\begin{aligned} a \wedge (b \vee c) &= (a \wedge b) \vee (a \wedge c) \\ a \vee (b \wedge c) &= (a \vee b) \wedge (a \vee c) \end{aligned}$$

Every bounded lattice has a *greatest element* (also called *maximum* or *maximal element*) and a *least element* (also called *minimum* or *minimal element*).

Graphs A *graph* consists of a set V of vertices (or *nodes*, *points*) and a set E of edges (or *lines*). We denote a graph as a pair $G = (V, E)$ with $V = \{v_1, \dots, v_n\}$ and $E = \{e_1, \dots, e_m\}$, i. e., we only consider *finite*, *non-empty* graphs. We refer to the vertex set of G by $V(G)$ and to its edge set by $E(G)$. If G is an *undirected graph*,

then the set of edges is a set $E \subseteq \{\{u, v\} \mid u, v \in V\}$. An *undirected edge* $e \in E$, denoted by $e = \{u, v\}$, is an edge of an undirected graph. If G is a *directed graph* (or *digraph* for short), then the set of edges is a binary relation on V , i. e., $E \subseteq V \times V$. A *directed edge* $e \in E$, denoted by $e = (u, v)$, is an edge of a directed graph. Then, $e = (u, v)$ is an *incoming edge* of v and an *outgoing edge* of u . Further, u is the *source* of e and v is the *target* of e .

If an edge $e = \{u, v\}$ is directed from u to v as well as from v to u , then it is called *bi-oriented* (or *bi-directed*) edge. If it is directed only in one direction, it is sometimes called *uni-directed* edge.

For $v \in V$, an edge $e = \{v, v\}$ and $e = (v, v)$, respectively, is called a *loop*. If E is a multiset, then the edges of multiplicity greater than one are called *multiple edges*. Graphs without loops and multiple edges are called *simple*, and otherwise *multigraphs*. If not stated otherwise, we only consider simple, undirected graphs.

Two distinct vertices $u, v \in V$ are *adjacent* (or *neighbors*) if there exists an edge $e = \{u, v\} \in E$. The vertices u and v are *incident* to e and called *endvertices* (or *endpoints*) of e . Edge e *links* (or *joins*) its endvertices u and v . If G is a graph with n vertices and all vertices are pairwise adjacent, then G is called *complete graph* and denoted by K_n . A graph K_3 is called a *triangle*.

A graph $G = (V, E)$ is *bipartite* if V admits a partition $\mathcal{V} = \{V_1, V_2\}$ into two sets such that every edge of E has exactly one endvertex in V_1 and one endvertex in V_2 , i. e., there are no adjacent vertices in V_i , $i = 1, 2$. A bipartite graph in which each pair of vertices from different sets is adjacent is called *complete*. If $|V_1| = n$ and $|V_2| = m$, then the complete bipartite graph is denoted by $K_{n,m}$.

The set of neighbors of a vertex v in G is denoted by $N_G(v)$. The *degree* (or *valency*) $\deg_G(v)$ of a vertex v in G is equal to $|N_G(v)|$. A vertex with degree 0 is called *isolated*. If G is a directed graph, the *indegree* $\deg_G^-(v)$ and *outdegree* $\deg_G^+(v)$ of a vertex $v \in V$, respectively, is equal to the number of incoming and outgoing edges of v , respectively. If the underlying graph is clear from the context, we simply drop the index G .

A *subgraph* of a graph $G = (V, E)$ is a graph $G' = (V', E')$ such that $V' \subseteq V$ and $E' \subseteq E$. It is written as $G' \subseteq G$. If $G \neq G'$, we write $G' \subset G$ and say that G' is a *proper subgraph* of G . If $E' \cap [V]^2$, then G' is a *(vertex) induced subgraph* of G , denoted by $G[V']$. Informally expressed, a (vertex) induced subgraph contains exactly the edges $e = \{u, v\} \in E$ with $u, v \in V' \subseteq V$ that link vertices in V' .

For any set of vertices V' , we write $G - V'$ for $G[V \setminus V']$, i. e., $G[V \setminus V']$ is obtained by *removing* vertices and incident edges from G . If $V' = \{v\}$, we also write $G - v$ for $G[V \setminus \{v\}]$. For two graphs G and G' , we write $G - G'$ shortly for $G - V(G')$. Further, for $E' \subseteq [V]^2$, we define $G - E' = (V, E \setminus E')$ and $G + E' = (V, E \cup E')$, i. e., the

edges of E' are *removed* from and *added* to the graph G , respectively. Instead of $G - \{e\}$ and $G + \{e\}$ we write for short $G - e$ and $G + e$, respectively. Also, for two graphs $G = (V, E)$ and $G' = (V', E')$, we set $G \cup G' = (V \cup V', E \cup E')$.

Let V_1, V_2 be two vertex sets with $v_1 \in V_1$ and $v_2 \in V_2$. An edge $\{v_1, v_2\}$ is an V_1 - V_2 -*edge*. The set of all V_1 - V_2 -edges in an edge set E is denoted by $E(V_1, V_2)$. A set of edges E' is a *cut* in G if there exists a partition $\mathcal{V} = \{V_1, V_2\}$ of V such that $E' = E(V_1, V_2)$. A minimal non-empty cut in G is called a *bond*.

Two graphs $G = (V, E)$ and $G' = (V', E')$ are *isomorphic* if there exists a bijection $\phi: V \rightarrow V'$ with $\{u, v\} \in E$ if and only if $\{\phi(u), \phi(v)\} \in E'$. The map ϕ is called an *isomorphism*. If $G = G'$, then ϕ is called an *automorphism*. Since we are only interested in the isomorphism type of a graph, we do not distinguish between isomorphic graphs.

Paths, Cycles, and Wheels A *path* in a graph G is a sequence of distinct vertices $P = \{v_1, \dots, v_k\}$ such that there is an edge between any two consecutive vertices in P . An example of a path is illustrated in Figure 1.2(a). We also denote a path by $P = \langle v_1, \dots, v_k \rangle$. The vertices v_1 and v_k are *linked* by P and are called *endvertices* of P ; the vertices v_2, \dots, v_{k-1} are called *inner vertices*. Path P is also called a v_1 - v_k -path. For sets of vertices V_1, V_2 , we call $P = \langle v_1, \dots, v_k \rangle$ a V_1 - V_2 -path if $V(P) \cap V_1 = \{v_1\}$ and $V(P) \cap V_2 = \{v_k\}$.

The *length* of a path equals its number of edges. A path P *contains* a vertex v (written as $v \in P$) if $v = v_i$ for some $1 \leq i \leq k$. A path P *contains* an edge e (written as $e \in P$) if $e = \{v_i, v_{i+1}\}$ for some $1 \leq i \leq k-1$. A *subpath* P' of a path P is a consecutive subsequence of vertices of P , i. e., $P' = \langle v_i, v_{i+1}, \dots, v_j \rangle$ for some $1 \leq i \leq j \leq k$. Two paths are *disjoint* if they do not have any vertices in common.

If $P = \langle v_1, \dots, v_k \rangle$ is a path, then the graph $C = P + \{v_k, v_1\}$ is called a (*simple*) *cycle*. We write a cycle as $C = \{v_1, \dots, v_k, v_1\}$. See Figure 1.2(b) for an example. The *length* of a cycle equals its number of edges. A cycle of length n is denoted by C_n and called an *n-cycle*. A graph is *acyclic* if it does not contain any cycle.

The graph $W_n = (V(C_n) \cup \{v\}, E(C_n) \cup E)$, where $E = \{\{u, v\} \mid u \in C_n\}$ with $v \notin C_n$, is called *wheel*. An example is shown in Figure 1.2(c).

Connectivity A graph $G = (V, E)$ is *connected* if any two of its vertices are linked by a path. A graph that is not connected is *disconnected*. If $V' \subseteq V$ and $G[V']$ is connected, then we call V' *connected* in G . A *connected component* G' of G is a maximal connected subgraph of G , i. e., no graph $G[V(G') \cup \{v\}]$ is connected for $v \in V \setminus V(G')$.

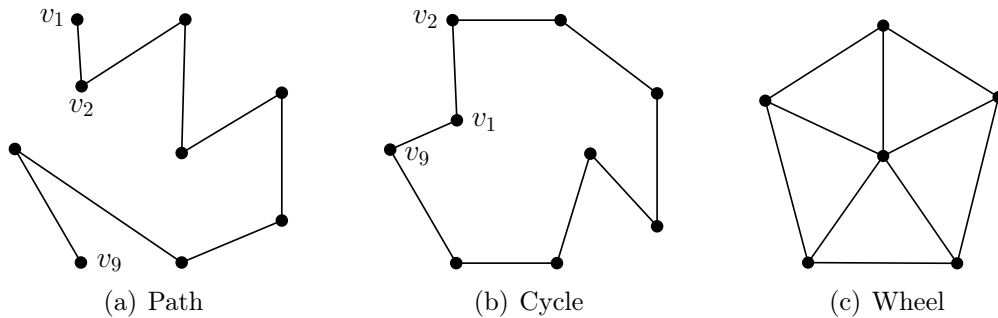


Figure 1.2: (a) A path $P = \langle v_1, v_2, \dots, v_9 \rangle$ of length 8. (b) A cycle $C_9 = \{v_1, v_2, \dots, v_9, v_1\}$. (c) A wheel W_5 .

A set $S \subseteq V \cup E$ *separates* G if $G - S$ is disconnected. If $S \subseteq V$ separates G , then S is called a *separator* (or *cutset*). If $S = \{v\} \subseteq V$ separates a connected component of G , then v is called a *cut vertex*. If $S = \{v, w\} \subseteq V$ separates a connected component of G , then $\{v, w\}$ is called a *separation pair*.

A graph G is *k-vertex connected* if $|V| > k$ and $G - S$ is connected for every $S \subseteq V$ with $|S| < k$, i. e., removing k vertices and their incident edges preserves the connectivity of G . A graph G is *k-edge connected* if $|E| > k$ and $G - S$ is connected for every $S \subseteq E$ with $|S| < k$, i. e., removing k edges from G preserves the connectivity of G . Speaking only about k -connected graphs, we always refer to k -vertex connected graphs.

Connected graphs are, thus, exactly the 1-connected graphs. We also call 2-connected graphs *biconnected*, i. e., the graphs that do not have any cut vertex, and 3-connected graphs *triconnected*, i. e., the graphs without a separation pair.

Menger [1927] shows that the connectivity of a graph is related to the number of disjoint paths linking vertices in the graph. In more detail, he proves the following:

Theorem 1.1 (Menger, 1927). *Let $G = (V, E)$ be a graph with $V_1, V_2 \subseteq V$. Then, the minimum number of vertices separating V_1 from V_2 equals the maximum number of disjoint V_1 - V_2 -paths in G .*

Diestel [2010] presents in his book three different proofs of Menger's theorem.

Forests and Trees An acyclic graph is called a *forest*. A connected forest is called a *tree*. The vertices of degree 1 in a tree are its *leaves*; the vertices of degree greater than 1 are *inner vertices*.

Sometimes one vertex of a tree T is treated specially; then, it is called *root* of T . A tree with a fixed root is a *rooted tree*.

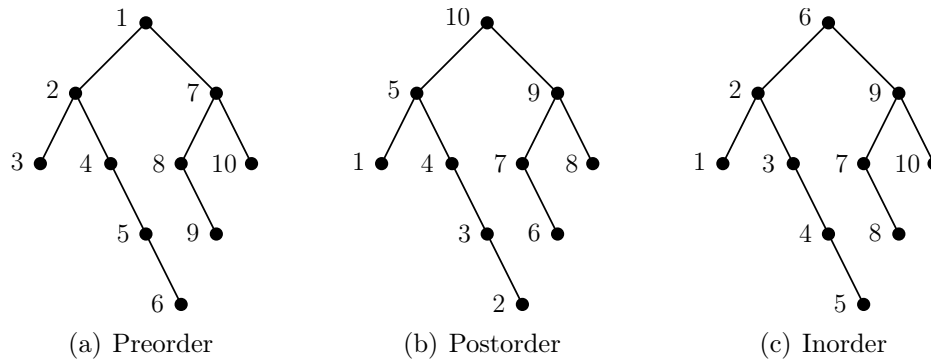


Figure 1.3: Different tree traversals of a binary tree.

In a rooted tree, the *parent* of a vertex v is defined as the neighbor of v on the unique path from v to the root; all other neighbors are its *children*. Any vertex on the path from a vertex v to the root is called an *ancestor* of v . Two vertices u and v of a tree T are *related in T* if either u is an ancestor of v or v is an ancestor of u , and *unrelated in T* otherwise. An edge $e \notin T$ is *unrelated in T* if both of its endvertices are unrelated.

A *spanning tree T* of a connected graph G is a subgraph of G that is a tree with $V(T) = V(G)$ and $E(T) \subseteq E(G)$. Two spanning trees T_1 and T_2 of a graph G with the same root r are *independent* if for each vertex v of G the inner vertices of the two paths $P_1 = \langle v, \dots, r \rangle$ in T_1 and $P_2 = \langle v, \dots, r \rangle$ in T_2 are disjoint. A *spanning forest* is any subgraph that is both a forest and spanning.

The *arboricity* of a graph is the minimum number of spanning forests that is needed to cover all the edges of the graph.

The following lemma is folklore.

Lemma 1.2. *A tree with n vertices has $n - 1$ edges.*

Let T be a rooted and *ordered* tree, i. e., at each vertex v there is given a cyclic ordering of the edges incident to v . Then, T can be traversed in different ways.

1. **Preorder traversal:** First, visit the root, then traverse the subtrees from left to right. See Figure 1.3(a).
2. **Postorder traversal:** First, traverse the subtrees from left to right, then visit the root. See Figure 1.3(b).

If T is a *binary tree*, i. e., each node has at most two children, then there exists a third traversal:

3. **Inorder traversal:** First, traverse the left subtree, then visit the root, and, finally, traverse the right subtree. See Figure 1.3(c).

1.2 Drawings and Embeddings

A *drawing* (or *representation*) of a graph $G = (V, E)$ is a function $\Gamma : V \cup E \rightarrow \mathbb{R}^2$ that maps each vertex $v \in V$ to a distinct point $\Gamma(v) \in \mathbb{R}^2$ and each edge $\{u, v\} \in E$ to a simple arc with endpoints $\Gamma(u), \Gamma(v) \in \mathbb{R}^2$. A drawing is *planar* if for any two edges $e, e' \in E$ the arcs $\Gamma(e)$ and $\Gamma(e')$ do not intersect. A graph is *planar* if it admits a planar drawing, and *non-planar* otherwise. Since each edge is the continuous image of $\mathbb{I} = [0, 1]$, each planar drawing Γ of a graph G corresponds to a closed set in \mathbb{R}^2 .

A planar drawing Γ subdivides the plane into topologically connected regions called *faces*. These are open subsets of \mathbb{R}^2 . Since Γ is bounded, there is exactly one unbounded region, called the *outer face* (or *external face*); all other faces are *inner faces* (or *interior faces*). We denote the set of faces of a planar drawing Γ by $F(\Gamma)$. The *boundary* (or *frontier*) of a face $f \subseteq \mathbb{R}^2$ is ∂f . Since f is open, $\partial f \subseteq \mathbb{R}^2 \setminus f$. Edges and vertices on the boundary of face f are *incident* to f and f is *incident* to the edges and vertices on its boundary. Two faces are *adjacent* if they are incident to the same edge.

The vertices incident to the outer face are *exterior vertices* (or *external vertices*, *outer vertices*), all other vertices are *interior vertices* (or *internal vertices*, *inner vertices*). The edges incident to the outer face are *exterior edges* (or *external edges*, *outer edges*), all other edges are *interior edges* (or *internal edges*, *inner edges*).

Two planar drawings are *equivalent* if there is a homeomorphism of the plane that transforms one into the other. A *topological embedding* is an equivalence class of planar drawings. A topological embedding of G induces for each vertex a counterclockwise circular order of its incident edges that can be described by a *rotation system* (or *rotating system*) $\pi = \{\pi_v \mid v \in V(G)\}$, where π_v is a cyclic permutation of the edges incident to v (compare, e. g., Gross and Tucker [1987], Mohar [1996]). A graph G together with a rotation system is called a *combinatorial embedding* of G .

The notion of planar drawings extends to other surfaces. A graph is *embeddable on a surface S* if it can be drawn in S such that its edges intersect only at common endvertices. A *sphere with k handles* is the surface that is obtained from a sphere by adding k handles and denoted by S_k . The index k is called *genus* of S_k .

The *genus* $\gamma(G)$ of a graph G is the minimum value k such that G is embeddable on a surface with genus k . In Section 1.6 we will see that planar graphs are exactly the graphs with genus 0.

Different topological embeddings can lead to the same combinatorial embedding. However, a topological embedding of a connected, planar graph uniquely determines its embedding on the sphere. Further, an embedding on the sphere determines a combinatorial embedding in the plane up to the choice of the outer face. We call a combinatorial embedding of a connected graph together with a fixed outer face just *embedding*.

For example, let G consist of two connected components G_1 and G_2 , where G_1 is a cycle and G_2 is a path. Then, every planar drawing of G has one bounded and one unbounded face and G_2 can be drawn in the bounded or in the unbounded face. Both drawings have the same rotation system and, thus, the same combinatorial embedding. However, the topological embeddings are different.

Sometimes a drawing of G is called *geometric embedding*. In the remainder of this thesis, we often do not distinguish between a drawing and its underlying graph.

A planar graph together with a fixed embedding is called an *embedded planar graph* or *plane graph*. A plane graph G is *maximal plane* or just *maximal* if no edge can be added to form a plane graph $G' \supset G$ with $V(G') = V(G)$. A *triangular graph* is a maximal plane graph with at least three vertices. The inner faces of a triangular graph are its *elementary triangles*. The *angles* of a triangular graph are the angles of its elementary triangles. Angles are denoted both in clockwise and counterclockwise order. For example, let u, v, w be a triangle. The angle at v , inside the triangle, is then denoted by u, v, w and w, v, u , respectively. A *separating triangle* is a cycle of length 3 that is not a face.

A graph G is *internally triconnected* if it is biconnected and for any separation pair $\{u, v\}$ of G , u and v are exterior vertices and each connected component of $G - \{u, v\}$ contains an exterior vertex. In other words, adding one vertex to the outer face and connecting it to all exterior vertices results in a triconnected graph.

An *outer chain* of a plane graph is a path $P = \langle v_1, \dots, v_k \rangle$ on the outer face such that $\deg(v_1) \geq 3$, $\deg(v_k) \geq 3$, and $\deg(v_2) = \dots = \deg(v_{k-1}) = 2$.

A *chordal path* of a cycle C is a path P that links two vertices of C that are not adjacent in C . Further, no vertex of the chordal path is a vertex of C , and there is no edge e in C such that $P + e$ forms an inner face of C . A chordal path $P = \langle v_1, \dots, v_k \rangle$ is minimal if none of v_2, \dots, v_{k-1} is an end of a chordal path. A *chord* is a chordal path of length 1, i. e., an edge.

Special Drawings When drawing a graph, one can aim to fulfill different *drawing conventions* (compare [Di Battista, Eades, Tamassia, and Tollis \[1998\]](#)) that are fundamental rules that a drawing has to satisfy.

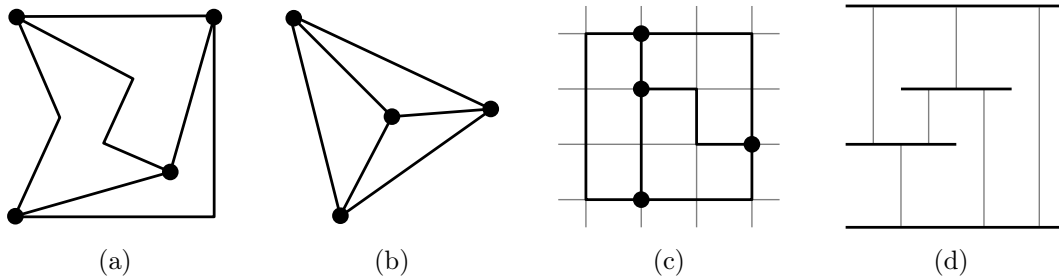


Figure 1.4: Different drawings of K_4 : (a) Polyline drawing (b) Strictly convex, straight-line drawing (c) Orthogonal, polyline, grid drawing (d) Visibility representation

A *polyline drawing* is a drawing where each edge is mapped to a polygonal arc. Examples are shown in Figures 1.4(a)-1.4(c). A point shared by any two consecutive segments of the polygonal arc is called a *bend*. A special case of a polyline drawing is a *straight-line drawing* where each edge is drawn as a straight-line segment as for instance the drawing in Figure 1.4(b).

In a *grid drawing* of a graph G , each vertex is mapped to a point in the plane with an integer coordinate. Similarly, a *grid graph* (or *lattice graph*) is a graph whose vertices have integer coordinates in the plane. An *orthogonal grid drawing* is a polyline drawing such that each segment is drawn on the grid and each bend is a grid point. An example is presented in Figure 1.4(c). We denote the grid size by $W \times H$, where W is the width of the grid and H is the height of the grid.

Let $p = (p_1, p_2)$ and $q = (q_1, q_2)$ be two *grid points* with $p_1 < q_1$, i. e., points that are integers. By $\mu(p, q)$ we denote the intersection of the straight line through p with slope $+1$ and the straight line through q with slope -1 . In more detail,

$$\mu(p, q) = \left(\frac{p_1 - p_2 + q_1 + q_2}{2}, \frac{-p_1 + p_2 + q_1 + q_2}{2} \right).$$

If the Manhattan distance between two grid points p and q is even, then $\mu(p, q)$ is a grid point.

A drawing is *convex* if each face is a convex polygon; it is *strictly convex* if no three vertices that are incident to the same face lie on one straight line. For example, the drawing in Figure 1.4(b) is strictly convex whereas the drawings in Figures 1.4(a) and 1.4(c) are not convex.

Other Representations A *visibility representation* is a mapping which assigns each vertex to a horizontal line segment and each edge to a vertical line segment such that the vertical line segment touches only the two horizontal line segments

that represent its endvertices. An example of such a representation is given in Figure 1.4(d).

In a *barycentric representation*, all except some exterior vertices are placed in the barycenter of their neighbors. More formally, a barycentric representation of a graph $G = (V, E)$ in \mathbb{R}^3 is defined by an injective function

$$v \in V \rightarrow (v_1, v_2, v_3) \in \mathbb{R}^3$$

that satisfies

1. $\sum_{i=1}^3 v_i = 1$ for all $v \in V$, and
2. for each edge $\{u, v\}$ and each vertex $w \neq u, v$, there is some $i \in \{1, 2, 3\}$ for that

$$u_i < w_i \quad \text{and} \quad v_i < w_i.$$

A barycentric representation is *weak* if Condition 2 is modified such that for each edge $\{u, v\}$ and each vertex $w \neq u, v$, there is some $i \in \{1, 2, 3\}$ for that

$$(u_i, u_{i+1}) <_{lex} (w_i, w_{i+1}) \quad \text{and} \quad (v_i, v_{i+1}) <_{lex} (w_i, w_{i+1}).$$

Note that $(u_i, u_{i+1}) <_{lex} (w_i, w_{i+1})$ if $(u_i < w_i)$ or $(u_i = w_i \text{ and } u_{i+1} < w_{i+1})$. An example and more details can be found in Section 6.3.1 in which we describe an algorithm for determining such a representation.

Duality Let $G = (V, E)$ be a plane graph with face set F . A multigraph $G^* = (V^*, E^*)$ with face set F^* is the *dual graph* of G (or *planar dual*) if there exist the following bijections:

$$\begin{aligned} F &\rightarrow V^* : f \mapsto v^*(f) \\ E &\rightarrow E^* : e \mapsto e^* \\ V &\rightarrow F^* : v \mapsto f^*(v) \end{aligned}$$

such that

1. $v^*(f) \in f$ for all $f \in F$,
2. $v \in f^*(v)$ for all $v \in V$,
3. $|e^* \cap G| = |\dot{e}^* \cap \dot{e}| = |e \cap G^*| = 1$ for all $e \in E$, and this point is in e as well as in e^* in the interior.

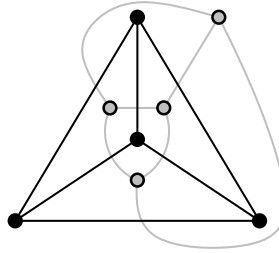


Figure 1.5: K_4 (black graph) and its dual graph (gray graph).

Informally explained, place a new vertex inside each face of G and add edges that link these new vertices as follows. For every edge $e \in E$, add an edge e^* crossing e and linking the vertices that are placed inside the faces that are incident to e . If e is incident to only one face, then create a loop. The resulting plane multigraph G^* is the dual graph of G . Figure 1.5 shows an example of a graph and its dual.

Every connected, plane graph has a dual graph. Moreover, there exists a natural bijection between any two dual graphs. Thus, we can speak of *the* dual graph of G . Details can be found in [Diestel \[2010\]](#).

An *abstract dual* of a graph G is a multigraph G^* such that $E(G^*) = E(G)$ and the bonds in G^* are precisely the edge sets of cycles in G . [Whitney \[1932\]](#) proves that planar duals are equivalent to abstract duals and gives a planarity criterion based on the existence of a dual. We describe this in more detail at the end of this chapter in Section 1.6.3.

1.3 Number of Graph Elements

In this section, we review some early results and basic properties of planar graphs, putting particular emphasis on the number of vertices, edges, and faces of a graph.

We start with the well-known theorem by Euler, called *Euler's polyhedron formula* or simply *Euler's formula*. Since its proof is part of every beginner's course in graph theory, we omit it here and refer to [Eppstein's Geometry Junkyard](#) where 19 different proofs can be found [[Eppstein, 2005](#)], or to any graph theory book, for example [Diestel \[2010\]](#), [Steger \[2007\]](#). Euler's formula gives a simple relation between the number of vertices, edges, and faces in a connected planar graph and can be used to prove many other properties of planar graphs. [Malkevitch \[1984\]](#) discusses to whom the first correct proof is due to.

Theorem 1.3 (Euler, about 1750). *If G is a connected, planar graph with n vertices, m edges, and f faces, then*

$$n - m + f = 2.$$

The next theorems give an upper bound on the number of edges and faces of a planar graph.

Theorem 1.4. *A planar graph G with $n \geq 3$ vertices has at most $3n - 6$ edges. A maximal plane graph G with $n \geq 3$ vertices has exactly $3n - 6$ edges.*

Proof. It suffices to prove the second part of the theorem. Let G be a maximal plane graph with m edges and f faces. Then, every face is incident to three edges and every edge is incident to two faces. Thus, with Theorem 1.3 follows:

$$\begin{aligned} m &= n + f - 2 \\ m &= n + \frac{2}{3}m - 2 \\ m &= 3n - 6 \end{aligned} \quad \square$$

Theorem 1.5. *A planar graph G with n vertices has at most $2n - 4$ faces.*

Proof. Combining Theorem 1.3 with Theorem 1.4 leads to the result. \square

The next lemma is known as the degree sum formula that can be easily proved by double counting. It says that the degrees of all vertices sum up to twice the number of edges.

Lemma 1.6. *Given any graph $G = (V, E)$, then*

$$\sum_{v \in V} \deg(v) = 2|E|.$$

A direct consequence of Lemma 1.6 is that every graph has an even number of vertices of odd degree. This statement is also known as the *handshaking lemma* since at a party the number of guests that shakes hands with an odd number of other guests is even.

Theorem 1.7. *Every planar graph with $n \geq 4$ has at least four vertices with degree at most five.*

Proof. Assume for a contradiction that the graph has three vertices with degree 3 and the remaining vertices have degree 6. Then, by Lemma 1.6 follows:

$$\begin{aligned} 2m &= \sum_{v \in V} \deg(v) \geq 3 \cdot 3 + (n - 3) \cdot 6 = 6n - 9 \\ m &\geq 3n - 4.5 \end{aligned}$$

This contradicts Theorem 1.4. \square

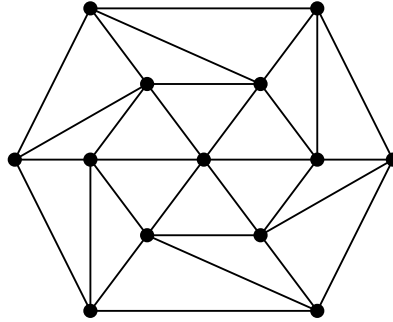


Figure 1.6: Adding one vertex to the outer face and linking it with all exterior vertices yields a 5-connected, planar graph, called *icosahedron*.

This statement implies that there is no 6-connected, planar graph. However, there exist 5-connected, planar graphs. For example, the icosahedron is 5-connected and shown in Figure 1.6.

The next theorem presents two small graphs that are not planar. These graphs will be used in Section 1.6.1 to characterize planar graphs.

Theorem 1.8. K_5 and $K_{3,3}$ are not planar.

Proof. By Theorem 1.4 a graph with five vertices has at most nine edges. Thus, K_5 is not planar since it has ten edges.

If $K_{3,3}$ is planar, it has five faces (Theorem 1.3). However, there is no cycle of length less than four. Hence, every face is incident to at least four edges. Thus, $2m \geq 4f$ and $f \leq (2 \cdot 9)/4 < 5$. This is a contradiction. \square

1.4 Triangulating Graphs

Some applications require its graphs to be triangulated. A prominent example is computer graphics in which the surfaces of objects are often modeled by triangles to simplify the rendering process.

Triangulating a graph is typically done by inserting edges, called *dummy edges*. If a graph $G = (V, E)$ is not triangulated, then there exists a face f of G that is incident to at least four vertices. Let v_1, v_2, v_3, v_4 be these vertices in counterclockwise order around f . Inserting either the edge $\{v_1, v_3\}$ or $\{v_2, v_4\}$ triangulates f . Note that by planarity constraints $\{v_1, v_3\} \notin E$ and $\{v_2, v_4\} \notin E$. Inductive application of this argument yields a triangulated graph.

There exist several linear-time algorithms for triangulating planar graphs. The first one is due to [Read \[1987\]](#). An overview of triangulating algorithms can be found in [Kant \[1993\]](#).

Since all maximal plane graphs have $3n - 6$ edges (Theorem 1.4), the number of edges that has to be added to the graph is fixed. However, other optimization requirements of interest have been investigated.

[Biedl, Kant, and Kaufmann \[1997\]](#) discuss the problem of triangulating a planar graph under the constraint to achieve 4-connectivity of the graph. They develop a linear-time and -space algorithm that triangulates a given input graph into a 4-connected output graph if the input graph does not contain a separating triangle.

[Kant \[1993\]](#) shows that the decision problem of triangulating a planar graph while minimizing the maximum degree of a vertex is \mathcal{NP} -complete for biconnected graphs. He also develops an algorithm to triangulate a biconnected, planar graph that is based on canonical ordering. Canonical orderings are discussed in detail in Chapter 2 and his algorithm is presented in Section 5.3.3.

1.5 Triconnected Graphs

Among all planar graphs, triconnected graphs are especially interesting. In this section, we work properties of triconnected, planar graphs out, discuss triconnected components, show how to make planar and non-planar graphs triconnected, and describe the two most famous construction sequences for triconnected, non-planar graphs and a construction rule for triconnected, planar graphs. For detailed proofs and other aspects of triconnected graphs like certifying algorithms, we refer the interesting reader to the thesis of [Schmidt \[2011\]](#).

1.5.1 Properties

First, we gather some fundamental properties of triconnected, planar graphs that are used in the remainder of this thesis. Most of them are stated without a proof but, of course, we give references where these can be found.

We do not want to step into the theory of polytopes too deeply, however, the following well-known theorem simply cannot be omitted in a section about the properties of triconnected, planar graphs.

Theorem 1.9 (Steinitz’s Theorem; [Steinitz, 1914](#), [Steinitz and Rademacher, 1934](#)). *A graph is the graph of a three-dimensional polytope if and only if it is planar and triconnected.*

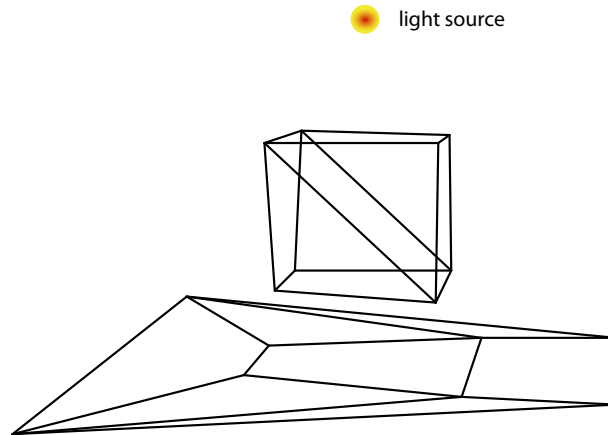


Figure 1.7: Visualizing a three-dimensional polytope in two dimensions by projecting it to the plane with a light source.

Proofs of this theorem can be found in the original paper and in [Barnette and Grünbaum \[1969\]](#).

One way of visualizing Steinitz's theorem is by placing a light source near one face of a three-dimensional polytope and watching the shadows that are formed on a plane on the other side of the polytope, as illustrated in Figure 1.7. The shadows of the edges form a straight-line embedding of a triconnected, planar graph. The face nearest to the light source corresponds to the outer face of the embedded graph.

The following extension of Euler's formula (Theorem 1.3) was first presented in 1852 by [Schläfli \[1950\]](#). Since his proof was not correct, the first correct proof was given by [Bruggesser and Mani \[1971\]](#). Another one and an overview of other proofs can be found in [Nef \[1984\]](#).

Theorem 1.10 (Euler-Poincaré). *Let $P \subset \mathbb{R}^d$ be a polytope. Then,*

$$\sum_{i=0}^d (-1)^i f_i = 1,$$

where f_i is the number of i -dimensional faces of P and $f_d = 1$, i. e., the polytope itself.

The number of vertices, edges, and faces correspond to f_0 , f_1 , and f_2 , respectively. Thus, for polytopes in \mathbb{R}^3 , we get Euler's formula together with Steinitz's theorem (Theorem 1.9).

Without proof, we state the following propositions about biconnected and triconnected graphs. A detailed proof can be found in [Diestel \[2010\]](#).

Proposition 1.11. *In a biconnected, plane graph, every face is bounded by a cycle.*

Proposition 1.12. *In a triconnected, plane graph, the face boundaries are exactly its non-separating cycles.*

As we will prove in Theorem 1.22, any planar graph can be embedded in the sphere and conversely. Thus, there are also many ways to embed a planar graph in the plane. However, the following holds for biconnected, planar graphs.

Theorem 1.13 (Whitney, 1932). *Every biconnected, planar graph can be embedded in the plane such that any specified face is the outer face.*

There is only one way to embed a triconnected, planar graph on the sphere. This implies that fixing a face as the outer face leads to a unique embedding in the plane. Therefore, we do not distinguish between triconnected, planar graphs and triconnected, plane graphs in the following, and often implicitly assume that the graph is given together with an embedding.

Theorem 1.14 (Whitney, 1933). *The embedding of a triconnected, planar graph into the sphere is unique.*

Remark 1.15. *Two incident faces of a triconnected, planar graph share one vertex or one edge. Especially, no face has a chord.*

Triconnected, planar graphs can be represented in a special way. Mapping the vertices of a designated outer face to a convex polygon in the plane and replacing the edges by rubber bands, yields a convex, straight-line drawing. In a physical sense, each vertex is mapped to the center of gravity of its neighbors. Such a representation is often called *rubber band representation*. An example is shown in Figure 1.8.

Theorem 1.16 (Tutte's Theorem; Tutte, 1963). *Every triconnected, planar graph has a representation in the plane such that all edges are straight lines and all inner faces are convex.*

Tutte's theorem can be proved in different ways. Another proof beside the original one is given in Thomassen [1980]. For an overview of the whole topic, see Lovász [2009]. In Ziegler [1995, page 138], Tutte's theorem is proved by representing the graph as the graph of a polytope. More precisely, the graph can be "lifted up" to a polytope that is then projected to the plane.

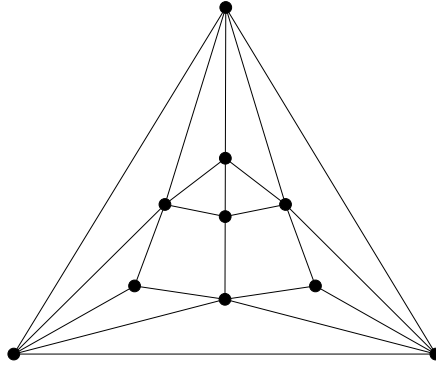


Figure 1.8: Rubber band representation of a triconnected, planar graph.

1.5.2 Triconnected Components

Let $S = \{u, v\} \subseteq V$ be a separation pair of a biconnected graph $G = (V, E)$. The edges of G can be divided into equivalence classes E_1, \dots, E_j such that two edges that lie on a common path not containing any vertex of S except an endvertex are in the same equivalence class. The equivalence classes E_1, \dots, E_j are called the *separation classes* of G with respect to S .

Let $E' = \bigcup_{i=1}^k E_i$ and $E'' = \bigcup_{i=k+1}^j E_i$ be such that $|E'| \leq 2$ and $|E''| \leq 2$. The graphs $G' = (V(E'), E' \cup \{u, v\})$ and $G'' = (V(E''), E'' \cup \{u, v\})$ are called *split graphs* of G with respect to S . The new edge $e = \{u, v\}$ is called *virtual edge*.

Each split graph is again biconnected. Splitting a graph, then splitting its split graphs, and so on until no more split operation is possible results in the *split components* of G that are triconnected. However, they are not necessarily unique.

In order to obtain unique split components, we reassemble the split graphs in the following way. Let $G_1 = (V_1, E_1)$ and $G_2 = (V_2, E_2)$ be two split components containing the same virtual edge e . The graph $G' = (V_1 \cup V_2, E_1 \cup E_2)$ is called *merge graph* of G_1 and G_2 . Replacing two split components G_1 and G_2 by their merge graph is called *merging* G_1 and G_2 .

The *triconnected components* of G are obtained from its split components by merging the triangles into maximal simple cycles and the triple bonds into maximal sets of multiple edges (*bonds*), where a *triple bond* is a set of three multiple edges. Although the split components are not necessarily unique, the triconnected components are.

Lemma 1.17 (Hopcroft and Tarjan, 1972). *The triconnected components of a graph are unique.*

Hopcroft and Tarjan [1972, 1974] present an $\mathcal{O}(n + m)$ -time algorithm that decomposes a graph into its triconnected components. Gutwenger and Mutzel [2001] correct the faulty parts of the algorithm of Hopcroft and Tarjan. Further, they show the connection of triconnected components to SPQR-trees. SPQR-trees are introduced by Di Battista and Tamassia [1989] and can be implemented in linear time. Mader [2008] describes the algorithm of Hopcroft and Tarjan in a more comprehensive manner and gives a visual understanding of it by illustrating the procedure in detail. Miller and Ramachandran [1992] discuss a parallel algorithm on a CRCW PRAM using $\mathcal{O}(n + m)$ processors. Their algorithm runs in $\mathcal{O}(\log^2 n)$ time.

1.5.3 Triconnecting Graphs

We present several results on augmentation problems since many drawing algorithms require the input graph to have a certain degree of connectivity. The *general augmentation problem* is to find a smallest set of edges whose addition to the graph results in a k -connected graph, for any fixed $k \in \mathbb{N}$. The inserted edges are often called *dummy edges*. After drawing the graph, the dummy edges can be removed from the final drawing.

Augmentation problems are introduced by Eswaran and Tarjan [1976] and for general graphs there exist many results. Eswaran and Tarjan [1976] study a lower bound on the number of edges that are required to make a graph biconnected. Hsu and Ramachandran [1991b] give a linear-time algorithm for the general augmentation problem for $k = 2$. Their algorithm corrects the faulty parts of the one of Rosenthal and Goldner [1977]. The general augmentation problem of making a graph triconnected is studied by Watanabe and Nakamura [1990, 1993] who present an $\mathcal{O}(n(n + m)^2)$ -time algorithm. This result is improved by Hsu and Ramachandran [1991a] whose algorithm runs in linear time and consists of two stages. In the first stage, the input graph gets biconnected and, in the second stage, the resulting biconnected graph gets triconnected such that the number of edges that is added in total is as small as possible. In Ishii, Nagamochi, and Ibaraki [1998], an overview of results for the augmentation problem such that the graph becomes ℓ -edge connected and k -vertex connected, respectively, can be found. References for the general augmentation problem for $k \geq 4$ are stated in Zey [2008].

The general augmentation problem with additional edge costs is to find an edge set with minimal costs that makes a graph k -connected. This problem is \mathcal{NP} -hard for all $k > 1$ [Eswaran and Tarjan, 1976, Watanabe and Nakamura, 1993].

Kant and Bodlaender [1991] (and also Kant [1993]) study different augmentation scenarios with the additional requirement that the augmented graphs have to be planar. This problem is called *planar augmentation problem*. In more detail, they prove

that the decision problem whether adding at most K edges to a planar graph yields a biconnected, planar graph is \mathcal{NP} -complete. Further, they present an algorithm that inserts at most twice the number of the required edges and runs in $\mathcal{O}(n \log n)$ time. Zey [2008] shows that the problem is still \mathcal{NP} -hard even if all cutvertices belong to the same biconnected component. If it is further required that the SPQR-tree of the biconnected component that contains all cutvertices has height 1, the problem remains \mathcal{NP} -hard. For this version of the planar augmentation problem, Zey gives an approximation algorithm that inserts at most $\frac{5}{3}$ times the number of edges and that runs in $\mathcal{O}(n^{2.5})$ time.

Kant and Bodlaender also state a $\frac{3}{2}$ -approximation algorithm for the planar biconnectivity augmentation problem with $\mathcal{O}(n^3)$ running time. However, Fialko and Mutzel [1998] show a counterexample for their approach and introduce a new algorithm with performance ratio $\frac{5}{3}$. Thereupon, Zey [2008] spot other incorrect parts in the algorithm of Fialko and Mutzel [1998] and show a counterexample that yields an approximation ratio of 2.

For planar, biconnected graphs, Kant and Bodlaender [1991] present an approximation algorithm for triconnecting the graph with performance ratio $\frac{5}{4}$ and $\mathcal{O}(n^3)$ running time. If all cutvertices of the biconnected graph are part of one triconnected component, then the problem is solvable in polynomial time [Kant, 1993].

If the embedding of a planar graph $G = (V, E)$ is fixed, then Zey [2008] gives an algorithm that computes a smallest set of edges E' such that $G' = (V, E \cup E')$ is biconnected. His algorithm can be carried out in $\mathcal{O}(n + m + \alpha(n)n)$ time, where $\alpha(n) = \min\{k \mid A_k(1) \geq n\}$ and $A_k(j)$ is the *Ackermann function* defined as

$$A_k(j) = \begin{cases} j + 1 & \text{if } k = 0 \\ A_{k-1}^{(j+1)}(j) & \text{if } k \geq 1 \end{cases}$$

The notation A^j denotes that the function A is iteratively applied j times.

1.5.4 Constructing Triconnected Graphs

Constructing a triconnected graph is closely related to deciding whether a graph is triconnected or not since often this question can be answered by applying a reversed valid construction sequence to a graph. A common operation in this method is edge contraction which will be used in several other sections throughout the remainder of this thesis, too.

In more detail, *contracting* an edge $e = \{u, v\}$ means removing the edge from the graph and identifying its endvertices u and v as shown in Figure 1.9. If e is

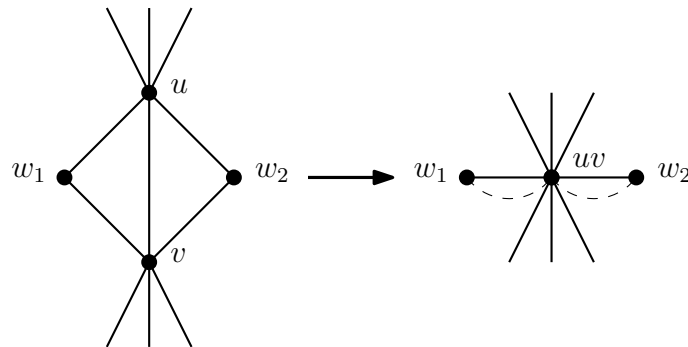


Figure 1.9: Contracting edge $e = \{u, v\}$. Dashed edges are deleted in G/e .

contracted in G , we denote this by G/M_e . If e is contracted in G and all multiple edges are replaced by a single edge, we write G/e .

Following the historic development, we start with a brief review of the construction of non-planar, triconnected graphs and then show how similar concepts are used for planar, triconnected graphs.

Non-Planar Graphs An algorithm that provides evidence that a graph fulfills a certain property is called *certifying algorithm*. [Tutte \[1961\]](#) provides one of the most famous certifying algorithms for triconnectivity by showing that any triconnected graph $G \neq K_4$ can be reduced to a K_4 by a sequence of edge contractions. Such a sequence of edge contractions is called *Tutte's contraction sequence* and can be found in $\mathcal{O}(n^2)$ time.

[Elmasry, Mehlhorn, and Schmidt \[2012\]](#) state that it is still an open problem whether Tutte's contraction sequence can even be found in sub-quadratic time. Moreover, they present a certifying algorithm for Hamiltonian graphs, i. e., graphs possessing a Hamiltonian cycle. [Schmidt \[2011\]](#) recapitulates in his thesis many other construction and certifying algorithms for triconnected graphs that are not necessarily planar.

Here, we follow an approach of Thomassen.

Lemma 1.18 ([Thomassen, 1980](#)). *Every triconnected graph G with at least five vertices contains an edge e such that G/e is triconnected.*

Proof. Suppose for a contradiction that for every edge $e = \{u, v\} \in G$ the graph G/e is not triconnected. Then, there exists a vertex w such that $G - \{u, v, w\}$ is disconnected, and G_1 and G_2 are two connected components of $G - \{u, v, w\}$. Choose e and w such that G_1 has as many vertices as possible and let $x \in V(G_2)$ be a neighbor of w . Such a neighbor exists since otherwise $G - \{u, v\}$ would be

disconnected. By the assumption, $G/\{w, x\}$ is not triconnected, thus, there exists a vertex y such that $G - \{w, x, y\}$ is disconnected. Therefore, $G[V(G_1) \cup \{u, v\}] - y$ is in a connected component G_3 and $|V(G_3)| > |V(G_1)|$. \square

The other way around, this lemma implies that one can generate all triconnected graphs from a K_4 by splitting vertices and adding edges. This generalizes a result of [Tutte](#) who constructs triconnected graphs from a wheel by adding edges and splitting vertices. Such a sequence of operations is called *Tutte's construction sequence*.

More precisely, he proves that all triconnected graphs can be generated from a wheel by iteratively applying of one of the following two operations:

1. **Adding an edge** between two vertices that are not adjacent.
2. **Splitting a vertex** w with $\deg(w) \geq 4$ into two vertices u and v , and adding an edge $\{u, v\}$ such that $\deg(u) \geq 3$ and $\deg(v) \geq 3$.

Lemma 1.19 ([Tutte, 1961](#)). *Applying a vertex splitting operation on a triconnected graph generates a triconnected graph.*

Theorem 1.20 ([Tutte, 1961](#)). *A graph is triconnected if and only if it can be generated from a wheel by repeatedly performing edge addition and vertex splitting operations.*

Albeit we deal with simple graphs in this thesis, we remark that these results can be extended to multigraphs by allowing the insertion of loops and multiple edges.

Shortly afterward, [Thomassen, Barnette and Grünbaum \[1969\]](#) generate triconnected graphs starting with a K_4 . Their set of operations is slightly different from the one of [Tutte](#) and allows, besides adding new edges, subdividing existing edges by introducing new vertices. In more detail, it comprises the following three operations which are called *Barnette-Grünbaum operations* and are depicted in [Figure 1.10](#):

1. **Adding an edge** between two distinct vertices.
2. **Subdividing one edge** $\{u, v\}$ into the edges $\{u, x\}$ and $\{x, v\}$ by adding a new vertex x , and add an edge $\{x, y\}$ with $y \notin \{u, v\}$.
3. **Subdividing two edges** e and e' that have at most one vertex in common by adding the new vertices x and y , respectively, and add an edge $\{x, y\}$.

Note that multiple edges can be created in this process but we prohibit loops.

These operations do not only preserve the triconnectivity of the graph, they also lead to a complete characterization of triconnected graphs as stated in the next theorem.

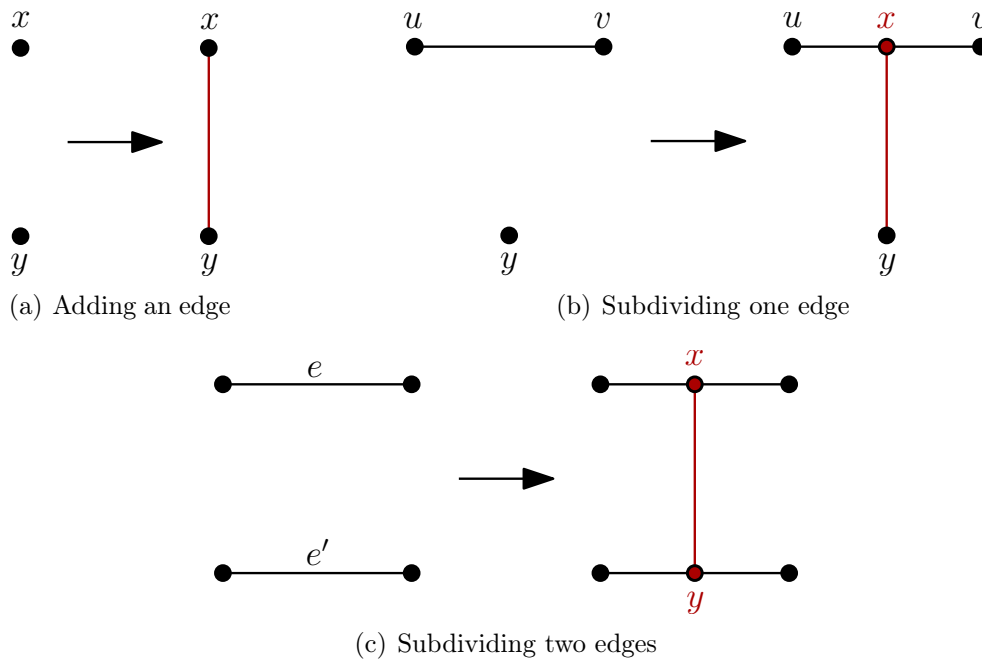


Figure 1.10: The Barnette-Grünbaum operations. (a) Adding a new edge $\{x, y\}$. (b) Subdividing the edge $\{u, v\}$ and adding a new edge $\{x, y\}$. (c) Subdividing the edges e and e' and adding a new edge $\{x, y\}$.

Theorem 1.21 (Barnette and Grünbaum, 1969). *A multigraph without loops is triconnected if and only if it can be constructed from the K_4 by using Barnette-Grünbaum operations.*

A sequence of Barnette-Grünbaum operations is called *Barnette's and Grünbaum's construction sequence*. Schmidt [2010] shows that the Barnette's and Grünbaum's construction sequence can be transformed into Tutte's sequence of contractions in linear time.

Planar Graphs Läuchli [1981] generates all k -connected, planar graphs for $0 \leq k \leq 3$ by using two operations that are similar to the operations of Tutte, however, the conditions when the operations can be applied are different. In full detail, Läuchli's two operations are:

1. **Adding an edge** between two vertices that are not adjacent and that are on the boundary of the same face. In addition, for $k = 0$, they have to be in the same connected component.

2. **Splitting a vertex** w into two vertices u and v and add an edge $e = \{u, v\}$. In addition, for $k = 3$, guarantee that $\deg(w) \geq 4$, $\deg(u) \geq 3$, and $\deg(v) \geq 3$.

Läuchli proves that all topological embeddings of a desired graph can be generated using his two operations with the following initial graphs :

connectivity	initial graph
$k = 0$	a single vertex for each desired component
$k = 1$	a single vertex
$k = 2$	a triangle
$k = 3$	any wheel $W_i, i \geq 3$

Even before, **Montanari** [1970] generated all planar graphs using web grammars. Another way to create triconnected, planar graphs is to generate a three-dimensional polytope and then consider its polyhedral graph since by Steinitz's theorem (Theorem 1.9) every triconnected, planar graph is the graph of a three-dimensional polytope. This is explained in detail, e. g., in **Barnette and Grünbaum** [1969].

1.6 Characterization

We dedicate this section to the characterization of planar graphs and start giving a tabular overview of the characterizations presented throughout the following.

A graph is planar if and only if	Theorem [author]
it has a planar embedding on the sphere.	Theorem 1.22
it contains no subdivision of K_5 or $K_{3,3}$.	Theorem 1.25 [Kuratowski, 1930]
the dimension of its incidence order is ≤ 3 .	Theorem 1.28 [Schnyder, 1989]
it has an abstract dual.	Theorem 1.29 [Whitney, 1932]
its cycle space has a sparse basis.	Theorem 1.30 [Mac Lane, 1937]

In contrast to these comprehensive characterizations, there are some properties that are necessary but not sufficient conditions of planar graphs. Amongst them is the well-known Fary's theorem that states that every planar graph admits a straight-line drawing and which is discussed in more detail in the next section. Here, we briefly prove the following descriptive condition.

Theorem 1.22 (e. g., **Bondy and Murty** [1976], page 138). *A graph is planar if and only if it has a planar embedding on the sphere. Consequently, planar graphs have genus 0.*

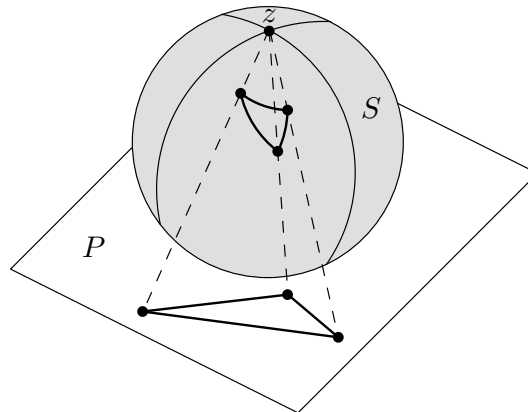


Figure 1.11: Stereographic projection from a graph on the sphere to the plane and vice versa.

Proof. Consider a sphere S resting on a plane P and denote by z the point of S that is to the opposite of the contact point of S and P . Let $\pi : S \setminus \{z\} \rightarrow P$ be defined by $\pi(s) = p \Leftrightarrow z, s, p$ are collinear. This function is called the *stereographic projection from z* and visualized in Figure 1.11.

Suppose that G has an embedding Γ on the sphere and choose a point z such that it is not in Γ . Then, the image under π is an embedding of G in the plane.

The converse is proved in the same way. \square

1.6.1 Theorems of Kuratowski and Fary

Kuratowski's and Fary's theorems are among the most famous theorems about the characterization of planar graph. [Kuratowski \[1930\]](#) characterized planar graphs in terms of forbidden subgraphs. The first short proof is due to [Dirac and Schuster \[1954\]](#) and many other proofs have been established over the years (compare for example [Thomassen \[1981\]](#)).

Fary's theorem, that is independently proved by [Fáry \[1946\]](#), [Stein \[1951\]](#), and [Wagner \[1936\]](#), states that any planar graph admits a straight-line drawing. [Tutte \[1960, 1963\]](#) extends Fary's result and proves that every triconnected, planar graph and its dual have simultaneous straight-line drawings. We present a proof of both theorems at once that is due to [Thomassen \[1980\]](#). It builds on some characterization of triconnected graphs that can also be used to construct them (compare Lemma 1.18). Later, this lemma is used to construct Schnyder woods.

Before we start, we need the following definition. A *subdivision* of a graph $G = (V, E)$ is obtained as follows: replace some edges of G with new paths that

link the endvertices of the replaced edges such that none of these paths has an inner vertex in V or on another path.

Theorem 1.23 (Thomassen, 1980). *A triconnected, planar graph that contains no subdivision of K_5 or $K_{3,3}$ has a convex drawing in the plane.*

Proof. We prove the theorem by induction on the number of vertices n of a tri-connected, planar graph G . The idea of the proof is sketched in Figure 1.12. The statement is obviously true for $n = 4, 5$, so assume that $n \geq 6$.

Let $e = \{u, v\}$ be an edge of G such that G/e is triconnected and let w be the vertex that is obtained by contracting e and identifying u and v . If G/e has a subdivision of K_5 or $K_{3,3}$, then G does, too. So we can assume by the induction hypothesis that G/e has a convex drawing in the plane, denoted by Γ . In addition, $G - w$ is biconnected.

Let f be the inner face of $\Gamma \setminus \{w\}$ that emerges when removing w from Γ . Furthermore, let $N_G(u) = \{x_1, \dots, x_k\}$ be the vertices adjacent to u in G in counterclockwise order around u and note that each $x_i \in N_G(u)$ is incident to f . For $i = 1, \dots, k$, let P_i be the path with endvertices x_i and x_{i+1} ($x_{k+1} = x_1$), such that no other vertex of $N_G(u)$ is an inner vertex of P_i , and such that all edges of P_i are incident to f .

If all neighbors of v other than u are contained in one single path P_i , then the drawing can be easily modified such that it is convex. If v is adjacent to three or more vertices of $N_G(u)$, then G contains a subdivision of K_5 . If v is adjacent to an inner vertex of P_i and to a vertex of $P_j \neq P_i$, then G contains a subdivision of $K_{3,3}$.

A similar argumentation holds for the outer face. □

Lemma 1.24 (Thomassen, 1980). *If a graph G contains no subdivision of K_5 or $K_{3,3}$ but the addition of any edge to G creates such a subdivision, then G is triconnected.*

Proof. We prove the theorem by induction on the number of vertices n of G . For $n = 4, 5$ the statement is obviously true, so assume that $n \geq 6$.

Clearly, G is biconnected. Also, if $G - \{u, v\}$ is disconnected for two vertices $u, v \in V$, then u and v are adjacent. So, assume for a contradiction that there exists $V' = \{u, v\} \subset V$ such that $G - V'$ is disconnected. Let $G'_1 = (V'_1, E'_1)$ and $G'_2 = (V'_2, E'_2)$ be the two connected components of $G - V'$. Let $G_1 = G[V'_1 \cup V']$ and $G_2 = G[V'_2 \cup V']$, i. e., $G = G_1 \cup G_2$; and G_1 and G_2 have precisely u, v , and the edge $\{u, v\}$ in common. Then, the addition of an edge to G_1 or G_2 creates a subdivision of K_5 or $K_{3,3}$. By the induction hypothesis, G_1 and G_2 are triconnected. For $i = 1, 2$, let Γ_i be a convex drawing of G_i in the plane (compare Theorem 1.23),

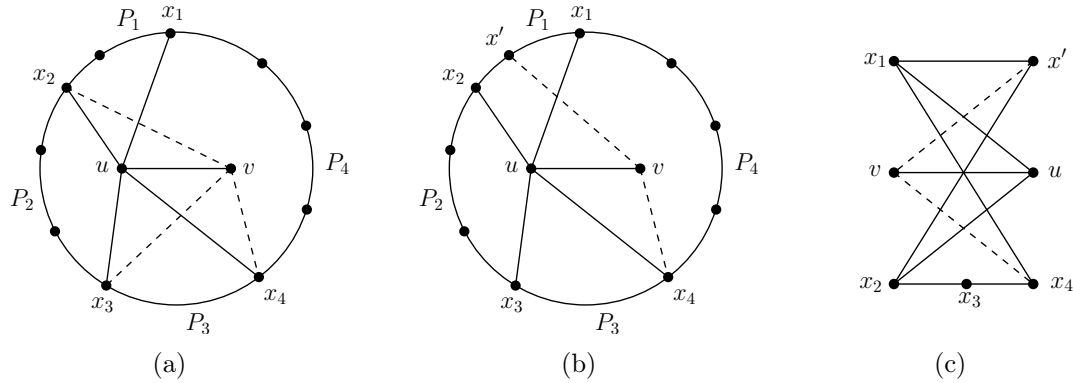


Figure 1.12: (a) Graph contains a subdivision K_5 . (b-c) Graph contains a subdivision of $K_{3,3}$.

let f_i be a face of Γ_i that is incident to $\{u, v\}$, and let $w_i \neq u, v$ be a vertex incident to f_i . Then, $G + \{w_1, w_2\}$ has a subdivision of K_5 or $K_{3,3}$ (by assumption). If all vertices of degree at least three of the subdivision of K_5 or $K_{3,3}$ are in G_1 and G_2 , respectively, then G_1 and G_2 contain a subdivision of K_5 or $K_{3,3}$, respectively. Since K_5 and $K_{3,3}$ are triconnected, it is not possible that two vertices of K_5 or $K_{3,3}$ of degree at least three are in $V(G_1) \setminus V(G_2)$ and two are in $V(G_2) \setminus V(G_1)$. Thus, G_1 (G_2) contains exactly one vertex of degree at least three and the subdivision is a $K_{3,3}$ since K_5 is 4-connected. Adding a new vertex x and the edges $\{u, x\}$, $\{v, x\}$, and $\{w_1, x\}$ to G_1 creates a $K_{3,3}$ (and analogously with edge $\{w_2, x\}$ for G_2). In contrast, Γ_1 (Γ_2) can be extended to a drawing of this graph. \square

Combining Theorem 1.23 and Lemma 1.24 leads simultaneously to Kuratowski's and Fary's theorems.

Theorem 1.25 (Kuratowski's Theorem; Kuratowski, 1930). *A graph is planar if and only if it contains no subdivision of K_5 or $K_{3,3}$.*

Theorem 1.26 (Fary's Theorem; Fary, 1946, Stein, 1951, Wagner, 1936). *A planar graph has a straight-line representation.*

1.6.2 Schnyder's Theorem

Schnyder [1989] characterizes planar graphs in terms of their dimension. Before we state his theorem at the end of this section, we give the required definitions of realizers and dimension.

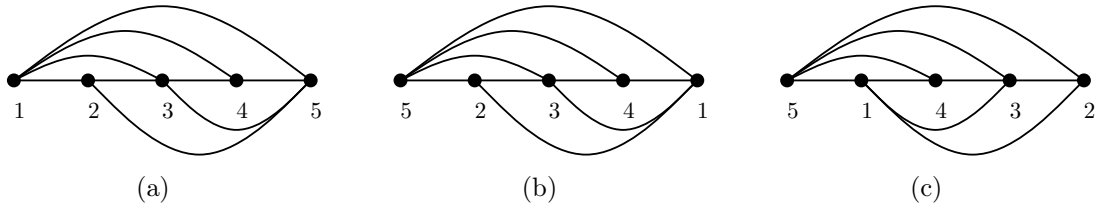


Figure 1.13: Realizer consisting of three linear orders for the $K_5 - \{2, 4\}$.

Definition 1.27 (realizer). *A non-empty family \mathcal{R} of total orders on V is called a realizer of G if for every edge $e = \{u, v\} \in E$ and every vertex $w \in V$ that is not incident to e , there is some $L \in \mathcal{R}$ so that $u \prec w$ and $v \prec w$ in L .*

The (order-)dimension of G , denoted by $\dim(G)$, is defined as the smallest positive integer t for which G has a realizer of cardinality t . If G' is a subgraph of G , then $\dim(G') \leq \dim(G)$. In this sense, the dimension is *monotone*.

For example, the dimension of a K_5 is 4. Removing any edge from a K_5 reduces the order to 3 as shown in Figure 1.13. Also, the dimension of a $K_{3,3}$ is 4. Again, removing any edge reduces the order to 3.

Let $G = (V, E)$ be K_5 without the edge $\{2, 4\}$, i.e., $V = \{1, 2, 3, 4, 5\}$ and $E = \{\{1, 2\}, \{1, 3\}, \{1, 4\}, \{1, 5\}, \{2, 3\}, \{2, 5\}, \{3, 4\}, \{3, 5\}, \{4, 5\}\}$. The next table shows with reference to Figure 1.13 that indeed there exists for every edge $\{u, v\} \in E$ and every vertex $w \in V$ a linear order such that $u \prec w$ and $v \prec w$.

	1	2	3	4	5
$\{1, 2\}$	x	x	(a)	(a)	(a)
$\{1, 3\}$	x	(c)	x	(a)	(a)
$\{1, 4\}$	x	(c)	x	(a)	(a)
$\{1, 5\}$	x	(c)	(c)	(c)	x
$\{2, 3\}$	(b)	x	x	(a)	(a)
$\{2, 5\}$	(b)	x	(b)	(b)	x
$\{3, 4\}$	(b)	(c)	x	x	(a)
$\{3, 5\}$	(b)	(c)	x	(b)	x
$\{4, 5\}$	(b)	(c)	(c)	x	x

Note that a graph has dimension less than 3 if and only if it is a subgraph of a path [Schnyder, 1989]. Felsner [2004a] shows that, if a graph G contains a cycle, then $\dim(G) \geq 3$.

Theorem 1.28 (Schnyder's Theorem; Schnyder, 1989). *A graph is planar if and only if the dimension of its incidence order is at most three.*

The proof is given in Section 3.3 since it uses the notion of Schnyder woods that we present in Chapter 3.

1.6.3 Other Characterizations

One of the first characterizations of planar graphs is due to Whitney [1932]. He characterizes planar graphs in terms of the existence of its dual graph.

Theorem 1.29 (Whitney, 1932). *A graph is planar if and only if it has an abstract dual.*

Mac Lane [1937] gives a characterization of planar graphs in terms of cycle spaces. Let $G = (V, E)$ be a graph and let $\mathcal{E}(G)$ denote the vector space of the function $E \rightarrow \mathbb{F}_2$. This vector space is called the *edge space* of G . Its elements correspond to the subsets of E , its *standard basis* is $\{\{e_1\}, \dots, \{e_m\}\}$ and its dimension is m .

A subset of the edge space is called *sparse* if every edge of G lies in at most two sets of the subset. The *cycle space* is the subspace of $\mathcal{E}(G)$ that is spanned by all cycles in the graph.

Theorem 1.30 (Mac Lane, 1937). *A graph is planar if and only if its cycle space has a sparse basis.*

A short proof of Mac Lane's planarity criterion is due to O'Neil [1973]. From this abstract criterion one can get back a pure graph-theoretic planarity criterion due to Tutte [1963] and Kelmans [1980].

Theorem 1.31 (Tutte, 1963, Kelmans, 1980). *A triconnected graph is planar if and only if each of its edges is contained in exactly two induced non-separating cycles.*

Thomassen [1980] extends Tutte's criterion to infinite graphs and describes the infinite graphs that satisfy Mac Lane's criterion. He also studies Whitney's theorem for infinite graphs. A proof of the theorems presented in this section can be found, beside in the original papers, also in Diestel [2010].

Chapter 2

Canonical Ordering

A prerequisite of many planar layout algorithms is an appropriate processing sequence of the vertices. Prominent examples are topological ordering, *st*-ordering, and canonical ordering.

In this chapter, we present fundamental definitions of different vertex orderings with focus on canonical ordering and some basic properties related to them. We give definitions of *st*-ordering for biconnected graphs, and canonical orderings for triangular, bi-, tri-, and 4-connected, planar graphs, and for 4- and 5-connected, triangular graphs. We rephrase most of the definitions of canonical ordering to stress their relationship to *st*-ordering and to present them in a uniform way. We newly define the leftist canonical ordering of a triconnected, planar graph that is in particular a leftmost canonical ordering and prove that the leftist canonical ordering corresponds to the leftist canonical ordering of the dual graph. Most of these results can be found in [Badent et al. \[2011\]](#). As a last point, we briefly summarize concepts that are related to canonical ordering such as canonical ordering tree and orderly spanning trees.

2.1 Introduction

The first linear-time algorithm to compute an *st*-ordering from a given biconnected graph G is due to [Even and Tarjan \[1976, 1977\]](#). [Ebert \[1983\]](#) presents a slightly simpler algorithm that is further simplified by [Tarjan \[1986\]](#). A new approach for *st*-ordering the vertices of a graph without a preprocessing step is given by [Brandes \[2002\]](#). In general, an *st*-ordering is not unique, and the choice of some special *st*-ordering often affects the application.

One of the first applications of the concept of st -ordering is the planarity test of [Lempel, Even, and Cederbaum \[1967\]](#). Applications in graph drawing include visibility representations [[Rosenstiehl and Tarjan, 1986](#), [Tamassia and Tollis, 1986](#), [He and Kao, 1995](#), [Zhang and He, 2003](#)] or orthogonal drawings [[Papakostas and Tollis, 1998](#)]. Other applications can be found, e. g., in network routing [[Annexstein and Berman, 2000](#), [Akon et al., 2004](#)].

As mentioned above, specific st -orderings may lead to especially pleasant drawings. For example, the length of the longest s - t -path affects the height of a visibility representation. [He and Kao \[1995\]](#) state the problem of minimizing the length of the longest s - t -path for two given vertices s and t on the outer face of a biconnected, plane graph. [Zhang and He \[2005b,c, 2007\]](#) give various theoretical bounds on the length of the longest path of st -orientations for plane graphs. [Papamantou and Tollis \[2006, 2010\]](#) study parametrized st -orientations. Finally, [Sadasivam and Zhang \[2010\]](#) show that the corresponding decision problem, i. e., finding an s - t -path with length less than or equal to K , for $K \in \mathbb{N}$, for a given biconnected, plane graph with two vertices s and t on the outer face, is \mathcal{NP} -complete.

Definition 2.1 (st -ordering). *Let $G = (V, E)$ be a biconnected graph with $\{s, t\} \in E$. An ordering $s = v_1, \dots, v_n = t$ of the vertices of G is an st -ordering if for all vertices v_k , $1 < k < n$, there are*

$$1 \leq i < k < j \leq n \text{ such that } \{v_i, v_k\}, \{v_k, v_j\} \in E.$$

An example of an st -ordering of a planar graph is shown in [Figure 2.1\(a\)](#).

Lemma 2.2 ([Lempel et al., 1967](#)). *A graph $G = (V, E)$ is biconnected if and only if it has an st -ordering for each $\{s, t\} \in E$.*

Another characterization of biconnected graphs is due to [Whitney \[1932\]](#) who shows that a graph is biconnected if and only if it has an open ear decomposition. An *open ear decomposition* is a sequence of paths P_0, \dots, P_s inducing graphs $G_i = (V_i, E_i)$ with $V_i = \cup_{j=0}^i V(P_j)$ and $E_i = \cup_{j=0}^i E(P_j)$, $0 \leq i \leq s$, such that $E(P_0), \dots, E(P_s)$ is a partition of E and for each $P_i = \langle v_0, \dots, v_k \rangle$, $\{v_0, v_k\} \subseteq V_{i-1}$ and $\{v_1, \dots, v_{k-1}\} \cap V_{i-1} = \emptyset$. Open ear decompositions for triconnected graphs are mentioned in [Chapter 3](#).

An st -orientation (also called *bipolar orientation*) is obtained from an st -ordering in linear time by orienting the edges from lower-numbered to higher-numbered vertices. Also, an st -orientation can be transformed into an st -ordering in linear time by topological sorting [compare, e. g., [Knuth, 2011](#)].

Further properties of st -orientations are studied by [de Fraysseix, Ossona de Mendez, and Rosenstiehl \[1995\]](#).

Canonical orderings are introduced for triangular graphs by [de Fraysseix, Pach, and Pollack \[1988, 1990\]](#). They establish an $\mathcal{O}(n \log n)$ -time algorithm that embeds a triangular graph with n vertices on a $(2n - 4) \times (n - 2)$ integer grid by computing a canonical ordering of the vertices and then inserting them on a grid using this ordering. Later, [Chrobak and Payne \[1995\]](#) show how to execute this algorithm in linear time. Recently, [Aleardi, Devillers, and Fusy](#) extend canonical orderings to triangulations on cylinders.

In the following, we establish a new definition of canonical ordering for triangular graphs to emphasize its relation to *st*-orderings. This definition rephrases the one of [de Fraysseix, Pach, and Pollack \[1988, 1990\]](#).

Definition 2.3 (canonical ordering). *Let $G = (V, E)$ be a triangular graph and let v_1, v_2 , and v_n be the vertices on the outer face of G in counterclockwise direction. An ordering v_1, v_2, \dots, v_n of the vertices is a canonical ordering of (G, v_1) if for each $k = 3, \dots, n - 1$, there are*

$$1 \leq i_1 < i_2 < k < j \leq n \text{ such that } \{v_{i_1}, v_k\}, \{v_{i_2}, v_k\}, \{v_k, v_j\} \in E.$$

For an example of a canonical ordering of a triangular graph, see [Figure 2.1\(b\)](#). The next lemma shows that the above definition is equivalent to the definition of [de Fraysseix et al. \[1988, 1990\]](#). For $k = 1, \dots, n$, let $G_k = G[V_k] = (V_k, E_k)$ be the subgraph induced by v_1, \dots, v_k , and let C_k be the outer face of G_k .

Lemma 2.4. *Let $G = (V, E)$ be a triangular graph and let v_1, v_2 , and v_n be the vertices on the outer face of G in counterclockwise direction. An ordering v_1, \dots, v_n is a canonical ordering of (G, v_1) if and only if for $k = 3, \dots, n - 1$ holds:*

1. *The subgraph G_k is biconnected.*
2. *C_k is a simple cycle.*
3. *The vertex v_{k+1} is in the outer face of G_k such that its neighbors form a subpath of the path $C_k - e$, with $e = \{v_1, v_2\}$.*

Proof. Let v_1, \dots, v_n be a canonical ordering. We prove by induction on k that all three properties are fulfilled. Clearly, this is true for $k = 3$.

Let $k > 3$. Since v_k has at least two different neighbors in G_{k-1} , G_k is biconnected. From [Definition 2.3](#), v_k has a neighbor v_j with $k < j$. Thus, v_{k+1} must lie in the outer face of G_k and C_k is a simple cycle. Further, since G is triangular, the neighbors of v_{k+1} form a subpath of C_k . Thus, all three conditions are fulfilled.

Let now be given an ordering v_1, \dots, v_n that fulfills the three conditions stated in the lemma. We have to show that the ordering is canonical.

Since v_k is in the outer face of G_{k-1} and since G_k is biconnected, vertex v_k has at least two neighbors v_{i_1} and v_{i_2} in G_k with $i_1, i_2 < k$. As v_k is in the outer face of G_{k-1} and as C_k is a simple cycle, v_k is a vertex of C_k . By the triangulation of G , v_k has a neighbor v_j with $j > k$. \square

We use the next lemma to prove that every triangular graph has a canonical ordering. For this purpose we need the definition of inside and outside chords. An *inside chord* and an *outside chord* is a chord that is an interior and exterior edge of a cycle, respectively.

Lemma 2.5 (de Fraysseix et al., 1988, 1990). *Let G be a triangular graph and let $C = \{v_1 = c_1, \dots, c_k = v_2, v_1\}$ be a cycle of G . Then, there exists a vertex $c \neq v_1, v_2$ on C that is not incident to an inside or outside chord, respectively.*

Proof. Assume the cycle has an inside chord. Let $\{c_i, c_j\}$ be an inside chord with $i + 1 < j$ and such that $j - i$ is minimal. Then, $c_{i+1} = c$ cannot be incident to an inside chord of the cycle $\{c_i, \dots, c_j, c_i\}$ by the minimality of $j - i$. By the planarity of G , it cannot be incident to any inside chord of C . The case that the cycle has an outside chord is analogous. \square

We are now ready to prove the following theorem.

Theorem 2.6 (de Fraysseix et al., 1988, 1990). *Every triangular graph has a canonical ordering.*

Proof. We prove the theorem by reverse induction on k , making use of Lemma 2.5.

Let $G_{n-1} = G - v_n$. Let $c_\ell = v_1, \dots, v_2 = c_r$ be the neighbors of v_n . Since G is triangulated, $\{c_\ell = v_1, \dots, v_2 = c_r, v_1\}$ forms a cycle that determines the boundary of the outer face G_{n-1} .

Let $k < n$. We remark that C_k has no outside chord. By Lemma 2.5, there exists a vertex $v_k \neq v_1, v_2$ on C_k that is not incident to an inside chord. Thus, v_k is not incident to any chord. Then, v_k has at least two neighbors v_{i_1}, v_{i_2} with $i_1 < i_2 < k$, namely, the left and right neighbor of v_k on C_k . Since G is triangulated, v_k has at least one neighbor $v_j \in G \setminus G_k$. \square

Kant [1996] generalizes canonical orderings to triconnected, planar graphs and presents a linear-time algorithm to construct a straight-line convex grid embedding of a triconnected, planar graph on a $(2n - 4) \times (n - 2)$ grid. This grid size is improved by Chrobak and Kant [1997] to $(n - 2) \times (n - 2)$. More about applications of canonical ordering to graph drawing can be found in Chapter 5.

In the following, we rephrase Kant's generalization to triconnected, planar graphs.

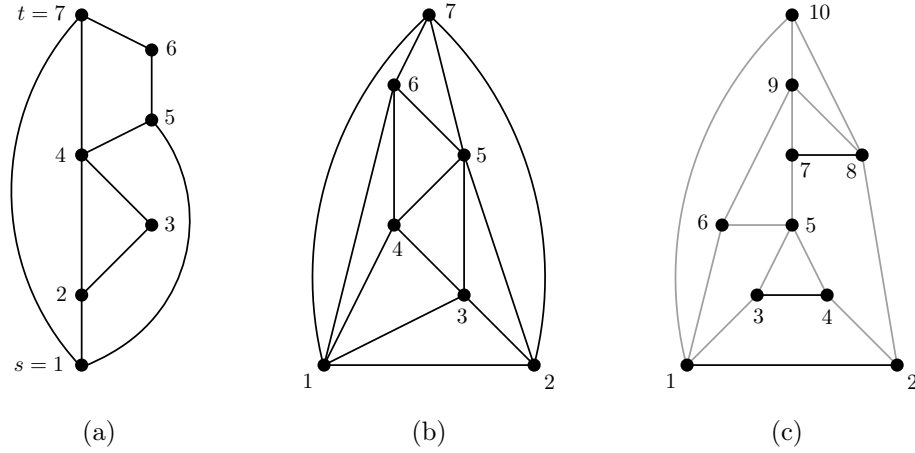


Figure 2.1: (a) An st -ordering of a biconnected graph. (b) Canonical ordering of a triangular graph. (c) Canonical ordering of a triconnected, planar graph. Black paths are chains.

Definition 2.7 (canonical ordering). *Let $G = (V, E)$ be a triconnected, planar graph with $n \geq 3$ vertices. Let $\Pi = (P_0, \dots, P_s)$ be a partition of V into paths and let $P_0 = \langle v_1, v_2 \rangle$, $P_s = \langle v_n \rangle$ such that $\langle v_2, v_1, v_n \rangle$ is a path on the outer face of G in clockwise direction. For $k = 0, \dots, s$ let $G_k = G[V_k] = (V_k, E_k)$ be the subgraph induced by $V_k = P_0 \cup \dots \cup P_k$, let C_k be the outer face of G_k . Partition Π is a canonical ordering of (G, v_1) if for each $k = 1, \dots, s - 1$:*

1. C_k is a simple cycle.
2. Each vertex z_i in P_k has a neighbor in $V \setminus V_k$.
3. $|P_k| = 1$ or $\deg_{G_k}(z_i) = 2$ for each vertex z_i in P_k .

P_k is called a singleton if $|P_k| = 1$ and a chain otherwise.

A canonical ordering Π is refined to a *canonical vertex ordering* v_1, \dots, v_n by ordering the vertices in each P_k , $k > 0$, according to their clockwise appearance on C_k . For an example of a canonical vertex ordering of a triconnected, planar graph, see Figure 2.1(c).

The following observations help to build an intuitive understanding of canonical orderings. Each path P_k encloses an interval of consecutive faces of G_k adjacent to C_{k-1} on the outside of G_{k-1} . This interval consists of exactly one face if P_k is a chain and of one or more faces if P_k is a singleton. Iterative application of

Condition 2 of Definition 2.7 guarantees that for each $z_i \in P_k$ there is a path to v_n in $G[V \setminus V_k] \cup \{z_i\}$, i. e., a path not using a vertex in $V_k \setminus \{z_i\}$.

Lemma 2.8. *For $k = 1, \dots, s - 1$:*

1. P_k has no chord.
2. For each vertex z in P_k there is a z - v_n -path $z = z_{k_0}, \dots, z_{k_p} = v_n$ where each z_{k_i} is in P_{k_i} and $k_i < k_j$ for $0 \leq i < j \leq p$. Especially:
 - (a) $G[V \setminus V_k]$ is connected.
 - (b) If $\deg_{G_k}(z) = 2$, then v is in C_k .
 - (c) P_k is on C_k .
3. (a) A singleton P_{k+1} and a path of C_k bound some faces or
 (b) a chain P_{k+1} and a path of C_k bound one face.
4. G_k is biconnected.
5. If $\{v, w\}$ is a separation pair of G_k , then both are on C_k .

Proof. The properties are directly implied by the fact that G is triconnected and by Definition 2.7. \square

Similarly to the proof of Theorem 2.6, Kant [1996] proves that every triconnected, planar graph has a canonical ordering. However, one has to carefully determine which is the next path that can be shelled off from the outer face. We give a new and constructive proof of the existence of a canonical ordering of a triconnected, planar graph in Section 5.1 that computes it from the low numbers to the high numbers.

Theorem 2.9 (Kant, 1996). *Every triconnected, planar graph has a canonical ordering.*

Definition 2.10 (length of a canonical ordering). *Let $\Pi = (P_0, \dots, P_s)$ be a canonical ordering. The length of a canonical ordering is the number of paths of the partition, i. e., the length is $s + 1$.*

Remark 2.11. *There exists a triconnected, planar graph G such that there are canonical orderings of (G, v_1) with different lengths. See Figure 2.2.*

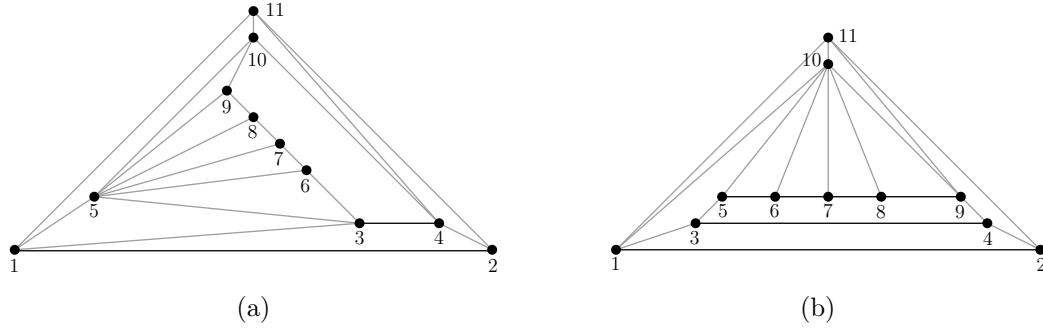


Figure 2.2: Different canonical orderings of the same graph. Black paths are chains. The length of the canonical ordering is (a) 9 and (b) 5.

2.2 Special Canonical Orderings

Throughout this section, let $G = (V, E)$ be a triconnected, planar graph. Since in general a canonical ordering of (G, v_1) is not uniquely defined, Kant [1996] introduces a leftmost (and rightmost) canonical ordering of (G, v_1) . However, these canonical orderings are only unique with respect to a given partition. Therefore, we newly define a leftist (and rightist) canonical ordering that is uniquely determined. The leftist (rightist) canonical ordering is in particular a leftmost (rightmost) canonical ordering.

2.2.1 Leftmost Canonical Ordering

Let P_0, \dots, P_s be a canonical ordering of (G, v_1) and let $e = \{u_1, u_2\}$ be an edge of G such that there are $k_1 < k_2$ with $u_i \in P_{k_i}, i = 1, 2$. Then, e is an *outgoing edge* of u_1 and an *incoming edge* of u_2 . Kant [1996] requires that a leftmost canonical ordering may be constructed by reordering a given canonical ordering only if the incoming and outgoing edges are maintained.

In particular, a canonical ordering defines a partial order \prec on the paths of Π . First, define $P_k \prec P_{k'}$ if $k < k'$, $k = 1, \dots, s$, and there is an edge between a vertex of P_k and a vertex of $P_{k'}$. Then, extend \prec to its transitive closure. Moreover, a leftmost canonical ordering is a total order that respects the partial order \prec of Π by not changing incoming and outgoing edges, respectively, and by taking paths from left to right.

More precisely, let P_0, \dots, P_k be a sequence of paths that can be extended to a canonical ordering of G . A path P of G is a *feasible candidate* for the step $k+1$ if also P_0, \dots, P_k, P can be extended to a canonical ordering. Let $v_1 = c_1, c_2, \dots, c_q = v_2$

be the vertices from left to right on C_k . Let c_ℓ be the neighbor of P on C_k such that ℓ is as small as possible and let c_r be the neighbor of P on C_k such that r is as large as possible. We call c_ℓ the *left neighbor* and c_r the *right neighbor* of P .

Definition 2.12 (leftmost canonical ordering). *A canonical ordering P_0, \dots, P_s is called leftmost (rightmost) if for $k = 0, \dots, s - 1$ the following is true. Let c_ℓ be the left neighbor of P_{k+1} and let $P_{k'}$, $k + 1 \leq k' \leq s$, be a feasible candidate for the step $k + 1$ with left neighbor $c_{\ell'}$. Then,*

1. $\ell \leq \ell'$ ($\ell \geq \ell'$) or
2. $P_{k+1} \prec P_{k'}$.

An example of a leftmost canonical ordering is presented in Figure 2.3(b).

Note that once a canonical ordering is known, a simple linear-time algorithm can be used to rearrange its paths so that it becomes leftmost [Kant, 1996]. Also note that Kant did not use Condition 2 of a leftmost canonical ordering in his definition but in his reordering algorithm.

While leftmost canonical orderings are particularly useful for many applications, we stress that the rearrangement is applicable to any canonical ordering and that a leftmost canonical ordering is only unique with respect to a given partition.

2.2.2 Leftist Canonical Ordering

Our goal is to develop a canonical ordering that is unique irrespective of a given partition. In the leftist canonical ordering we add in each step the leftmost possible path where the choice is not only within an already given partition.

Definition 2.13 (leftist canonical ordering). *A canonical ordering P_0, \dots, P_s is called leftist (rightist) if for $k = 0, \dots, s - 1$ the following is true. Let c_ℓ be the left neighbor of P_{k+1} and let P be a feasible candidate for the step $k + 1$ with left neighbor $c_{\ell'}$. Then $\ell \leq \ell'$ ($\ell \geq \ell'$).*

Examples of a leftist and rightist canonical ordering are shown Figures 2.3(c) and 2.3(a).

Note that a feasible candidate for the step $k + 1$ needs not to be a feasible candidate for the step $k + 2$ anymore. Also note that the leftist canonical ordering is unique irrespective of a given partition and it is a leftmost canonical ordering. Figure 2.3 illustrates that leftmost and leftist canonical orderings do not have to be the same. A similar concept related to Schnyder labelings without clockwise cycles is defined for triangular graphs in Brehm [2000] (compare also Sections 3.1 and 6.1).

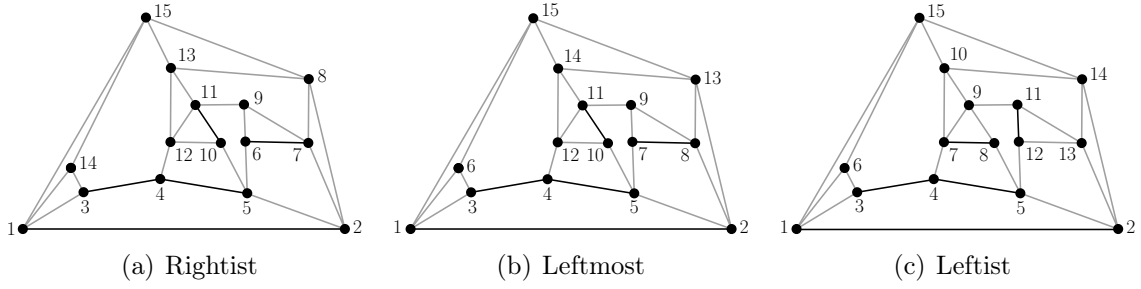


Figure 2.3: Different canonical orderings. Black paths are chains. (b) Leftmost canonical ordering of the canonical ordering of (a).

We show in Section 5.1 how to compute the leftist canonical ordering of a tri-connected, planar graph and give detailed pseudocodes for a clear understanding of the algorithm and an easy implementation.

2.3 Duality

[Kant \[1993\]](#) shows that a leftmost canonical ordering corresponds to a leftmost canonical ordering of the dual graph. In this section, we extend this concept to the leftist canonical ordering and show that the leftist canonical ordering can also be found by choosing always the rightmost face or singleton in the algorithm of [Kant \[1996\]](#). We conclude that the dual of the leftist canonical ordering is the leftist canonical ordering of the dual graph.

A similar concept for st -orientations is investigated by [Rosenstiehl and Tarjan \[1986\]](#) (see also [Tamassia and Tollis \[1986\]](#)).

Let $\langle v_2, v_1, v_n \rangle$ be a path on the outer face of G in clockwise direction. Let $\Pi = (P_0, \dots, P_{k-1})$ with $P_0 = \langle v_1, v_2 \rangle$, $P_{k-1} \neq \langle v_n \rangle$ and $\Pi = (P_{k+1}, \dots, P_s)$ with $\langle v_1, v_2 \rangle \neq P_{k+1}$, $P_s = \langle v_n \rangle$, respectively, be a sequence of paths of G that can be extended to a canonical ordering of (G, v_1) . We say that P_k is a *feasible extension* of Π if P_0, \dots, P_k and P_k, \dots, P_s , respectively, can also be extended to a canonical ordering of (G, v_1) .

Let $G_k = G[V \setminus (P_{k+1}, \dots, P_s)]$. [Kant \[1996\]](#) proves that the path P_k is a feasible extension for P_{k+1}, \dots, P_s if and only if the following is true:

1. All vertices of P_k are adjacent to some vertex in P_{k+1}, \dots, P_s .
2. If P_k is a chain, then all vertices of P_k have degree 2 in G_k .
3. $G_{k-1} = G[V \setminus (P_k \cup \dots \cup P_s)]$ is biconnected.

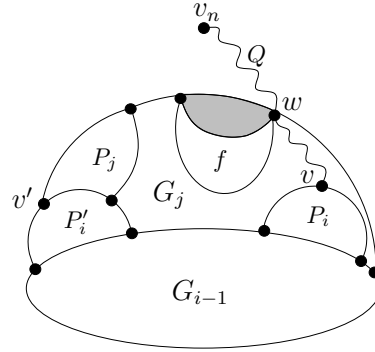


Figure 2.4: Illustration of the proof of Theorem 2.16. The gray component has to be eliminated before w can become part of a feasible extension.

An inner face of G_k is called a *separation face* if its incidence with the outer face of G_k is not only a single path.

Remark 2.14. *The following two conditions are equivalent for a path P_k on the outer face of G_k , $k \geq 2$:*

1. $G[V \setminus (P_k \cup \dots \cup P_s)]$ is biconnected.
2. (a) P_k is not incident to a separation face and
 (b) P_k is a singleton with degree greater than 2 or P_k is a maximal sequence of vertices of degree 2 on the outer face of G_k .

Definition 2.15 (upper rightist canonical ordering). *A canonical ordering P_0, \dots, P_s of (G, v_1) is called upper rightist if for $k = s - 1, \dots, 0$ the following is true. Let $P \neq P_k$ be a feasible extension of P_{k+1}, \dots, P_s . Then, P is between v_1 and P_k on the clockwise outer facial cycle C_k around G_k .*

Theorem 2.16. *The upper rightist canonical ordering of a triconnected, planar graph with a fixed vertex on the outer face equals its leftist canonical ordering.*

Proof. Let $\Pi = (P_0, \dots, P_s)$ be the upper rightist canonical ordering and let $\Pi' = (P_0, \dots, P_{i-1}, P'_i, \dots, P'_{s'-1}, P'_{s'})$ be the leftist canonical ordering of (G, v_1) . For $k = 0, \dots, s$ let again $G_k = G[V \setminus (P_{k+1} \cup \dots \cup P_s)] = G[P_0 \cup \dots \cup P_k]$. The idea of the proof is illustrated in Figure 2.4.

Assume that $P_i \neq P'_i$. Then, both P_i and P'_i are feasible extensions of P_0, \dots, P_{i-1} and P'_i is to the left of P_i on C_{i-1} . Hence, it is not possible that one of the two is contained in the other. Let $v \in P_i \setminus P'_i$ and $v' \in P'_i \setminus P_i$. Since P'_i is feasible, it

follows that $G[V \setminus (P_0 \cup \dots \cup P_{i-1} \cup P'_i)]$ is connected. Thus, there is a path Q from v to v_n that contains no vertices of P'_i or G_{i-1} .

Let $i < j < s$ be such that $v' \in P_j$. Let w' be the first vertex of Q not in G_j and let w be the vertex that is immediately before w' in Q . Then, w is to the right of v' on the outer facial cycle C_j of G_j . Further, w is adjacent to the vertex w' in $P_{j+1} \cup \dots \cup P_s$.

Assume first that w is not incident to a separation face. If w has degree 2 in G_j , let P be a maximal sequence of vertices of degree 2 in C_j containing w . Otherwise, let $P = \langle w \rangle$. In both cases, P is a feasible extension of P_{j+1}, \dots, P_s on the right of P_j .

Assume now that w is incident to a separation face f . Consider the separator S of G_j consisting of all the vertices that are incident to both, f and the outer face and consider the components of G_j with respect to S . Then, there is one component that contains G_{i-1} and v' . All other components have to be eliminated before w can become part of a feasible extension. Hence, all these components have to contain a feasible extension. But all these components are to the right of v' . Thus, P_j was not the rightmost feasible extension. \square

Let $G^* = (V^*, E^*)$ be the dual graph of $G = (V, E)$. Let v_1^* be the dual vertex of the outer face of G and let v_1 be on the outer face of G^* . Kant [1993] shows that a leftmost canonical ordering of (G, v_1) induces a leftmost canonical ordering on (G^*, v_1^*) . We rephrase Kant's construction and show that the result can be extended to the leftist canonical ordering.

Let $\Pi = (P_0, \dots, P_s)$ be a canonical ordering of (G, v_1) . Let E_i be the set of edges of $G_i = G[P_0 \cup \dots \cup P_i]$, $i = 0, \dots, s$, and let $E(P_0) = E_0$, $E(P_i) = E_i \setminus E_{i-1}$, $i = 1, \dots, s$. In more detail, $E(P_i)$ consists of all edges that are incident to two vertices in P_i and of all cut edges of G_{i-1} that are incident to a vertex of P_i .

Analogously, if $\Pi^* = (P_0^*, \dots, P_s^*)$ is a partition of the set V^* of faces of G , let E_i^* be the set of edges of $G_i^* = G^*[P_0^* \cup \dots \cup P_i^*]$, $i = 0, \dots, s$, and let $E^*(P_0) = E_0^*$, $E^*(P_i^*) = E_i^* \setminus E_{i-1}^*$, $i = 1, \dots, s$. For $E' \subset E$ let E'_* be the set of dual edges of E' . Further, let v_2^* be the neighbor of v_1^* on the outer facial cycle of G^* in counterclockwise direction.

Definition 2.17 (dual canonical ordering). *A partition $\Pi^* = (P_0^*, \dots, P_s^*)$ of V^* into paths is the dual canonical ordering of a canonical ordering $\Pi = (P_0, \dots, P_s)$ of (G, v_1) if and only if $P_0^* = \langle v_1^*, v_2^* \rangle$ and*

$$\begin{aligned} E^*(P_0^*) \cup E^*(P_1^*) &= E(P_s)_* \\ E^*(P_k^*) &= E(P_{s-k+1})_*, & k = 2, \dots, s-1 \\ E^*(P_s^*) &= E(P_1)_* \cup E(P_0)_*. \end{aligned}$$

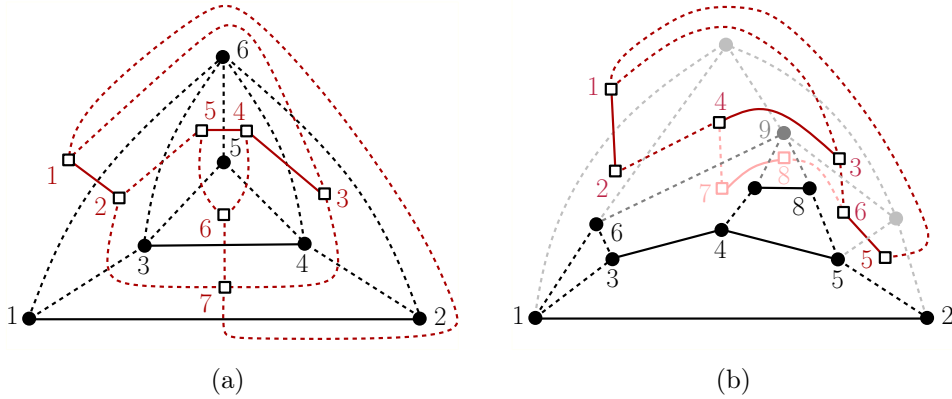


Figure 2.5: (a) A graph G and its leftist canonical ordering Π with $P_0 = \langle 1, 2 \rangle$ and $P_s = \langle 6 \rangle$, and the dual graph G^* and its leftist canonical ordering Π^* with $P_0^* = \langle 1, 2 \rangle$ and $P_s^* = \langle 7 \rangle$. Black solid paths are chains in Π , red solid paths are chains in Π^* . (b) Illustration of the proof of Theorem 2.18.

Theorem 2.18. *Let Π be a canonical ordering of (G, v_1) .*

1. *A dual canonical ordering Π^* of Π exists and is uniquely determined. It is a canonical ordering of (G^*, v_1^*) .*
2. *Π is the leftist canonical ordering of (G, v_1) if and only if Π^* is the leftist canonical ordering of (G^*, v_1^*) .*

Proof. Let $\Pi = (P_0, \dots, P_s)$.

1. Let v_n^* be the face of G bounded by P_0 and P_1 . Then $P_s^* = \langle v_n^* \rangle$. By the definition of the dual canonical ordering, $P_0^* = \langle v_1^*, v_2^* \rangle$. Further, $\langle v_2^*, v_1^*, v_n^* \rangle$ is a path on the outer face of G^* in clockwise direction.

Again by the definition of a dual canonical ordering, it follows that the subgraph induced by P_0^* and P_1^* is the simple cycle bounding the face of G^* in which v_n is located. Hence, Conditions 1 and 3 of Definition 2.7 are fulfilled for $k = 1$. Condition 2 is fulfilled by the triconnectivity of G^* .

Let C_k^* be the boundary of the outer face of $G_k^* = G^*[P_0^* \cup \dots \cup P_k^*]$, $k = 1, \dots, s$. We will prove the following observation by induction on k while proving Theorem 1. The remark is certainly true for $k = 1$.

Remark 2.19. *Let $k = 1, \dots, s$. The edges of the simple cycle C_k^* are the duals of the cut edges of G_{s-k} and it holds that the vertices of $P_s \cup \dots \cup P_{s-k+1}$ are inside the cycle C_k^* and the vertices of G_{s-k} are outside C_k^* .*

Let now $k = 2, \dots, s-1$ and let w_1^*, \dots, w_t^* be the faces bounded by P_{s-k+1} and C_{s-k} in the order in which they occur around P_{s-k+1} . Then $P_k^* = \langle w_1^*, \dots, w_t^* \rangle$. Since each vertex in P_{s-k+1} is adjacent to at least one vertex in $P_{s-k+2} \cup \dots \cup P_s$, it follows that C_k^* is a simple cycle. Since each of these faces is incident to at least one edge in C_{s-k} , it follows that w_i^* , $i = 1, \dots, t$, is adjacent to at least one vertex in $P_{k+1}^* \cup \dots \cup P_s^*$. Assume now that P_k^* is a chain, i. e., that P_{s-k+1} is a singleton $\langle v \rangle$ with more than two neighbors in G_{s-k} . See Figure 2.5(b) for an illustration. Since C_{s-k} is a simple cycle it follows that all vertices in P_k^* have degree 2 in G_k^* . Finally, the vertices of G inside C_k^* are exactly those that had been inside C_{k-1}^* plus the vertices in P_{s-k+1} . Hence, Remark 2.19 is true for k .

2. From the construction in Theorem 1 follows that Π^* is the upper rightist canonical ordering of (G^*, v_1^*) and, hence, with Lemma 2.16 that Π^* is the leftist canonical ordering of (G^*, v_1^*) . \square

2.4 Related Concepts

In the remainder of this chapter, we give a brief overview on other concepts that are related to canonical orderings such as canonical ordering for biconnected graphs, 4-, and 5-connected graphs, canonical ordering trees, and orderly spanning trees.

2.4.1 Biconnected Graphs

Harel and Sardas [1998] relax the definition of de Fraysseix et al. [1988, 1990] of canonical ordering for triangular graphs to a canonical ordering for biconnected, plane graphs, called *biconnected canonical ordering*. They use it to draw a biconnected, plane graph on a $(2n-4) \times (n-2)$ grid in linear time.

Let G_k and C_k be defined as usual. Let $v_1 = c_1, c_2, \dots, c_q = v_2$ be the vertices from left to right on C_k .

Definition 2.20 (right, left, legal support). *Let v be a vertex of $G - G_k$ that has exactly one neighbor c_i on C_k , $1 \leq i \leq q$.*

1. *Vertex v has a right support (left support) if $\{c_i, v\}$ follows $\{c_i, c_{i+1}\}$ ($\{c_i, c_{i-1}\}$) in counterclockwise (clockwise) order around c_i , $1 \leq i \leq q-1$ ($2 \leq i \leq q$).*
2. *Vertex v has a legal support on C_k if $i = 1$ and v has a right support, or $i = q$ and v has a left support, or $1 < i < q$ and v has a right support or a left support.*

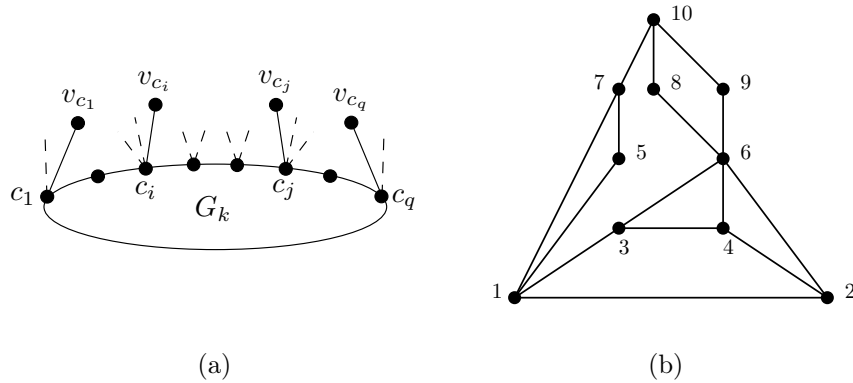


Figure 2.6: (a) Vertices c_1 and c_q have a legal support, v_{c_i} has a right support, v_{c_j} has a left support. (b) Biconnected canonical ordering.

Right, left, and legal supports are illustrated in Figure 2.6(a).

Definition 2.21 (biconnected canonical ordering). *Let G be a biconnected, plane graph with $n \geq 2$ vertices. Let $\Pi = (P_0, \dots, P_s)$ be a partition of V into paths and let $P_0 = \langle v_1, v_2 \rangle$ such that $\{v_1, v_2\}$ is an edge on the outer face of G . Partition Π is a biconnected canonical ordering of (G, v_1) if for each $k = 1, \dots, s - 1$:*

1. G_k is connected.
2. All vertices in $G - G_k$ are on the outer face of G_k .
3. Each vertex z_i in P_{k+1} has a neighbor in V_k . If z_i has exactly one neighbor in V_k , then it has a legal support on C_k .

An example of a biconnected canonical ordering is shown in Figure 2.6(b). Note that a biconnected canonical ordering is not necessarily an st -ordering.

2.4.2 4-Connected Graphs

Let $G = (V, E)$ be a 4-connected, planar graph with four vertices v_1, v_2, v_{n-1}, v_n on the outer face of G in counterclockwise direction. Let all inner faces be triangulated.

Kant and He [1997] add the edge $\{v_2, v_n\}$ to the graph in order to triangulate it. They introduce the definition of canonical ordering for 4-connected, triangular graphs and use this kind of canonical ordering to compute regular edge labelings and visibility representations.

We rephrase the definition of **Kant and He [1997]** that is similar to the definition of **Chen, Hung, and Lu [2009]**.

Definition 2.22 (4-canonical ordering). *Let $G = (V, E)$ be a 4-connected, triangular graph with three vertices $v_1, v_2,$ and v_n on the outer face of G such that $\{v_1, v_2\} \in E$. An ordering v_1, \dots, v_n of the vertices is a 4-canonical ordering of (G, v_1) if for each $k = 3, \dots, n - 2$, there are*

$$1 \leq i_1 < i_2 < k < j_1 < j_2 \leq n \text{ such that } \{v_{i_1}, v_k\}, \{v_{i_2}, v_k\}, \{v_k, v_{j_1}\}, \{v_k, v_{j_2}\} \in E.$$

The following lemma shows that the above definition is equivalent to the definition of [Kant and He \[1997\]](#). Again, for $k = 1, \dots, n$, let $G_k = G[V_k] = (V_k, E_k)$ be the subgraph induced by v_1, \dots, v_k and let C_k be the outer face of G_k .

Lemma 2.23. *Let $G = (V, E)$ be a 4-connected, triangular graph with three vertices $v_1, v_2,$ and v_n on the outer face of G such that $\{v_1, v_2\} \in E$. An ordering v_1, \dots, v_n is a 4-canonical ordering of (G, v_1) if and only if for $k = 3, \dots, n - 2$ holds:*

1. *The subgraph G_k is biconnected.*
2. *The outer face C_k is a simple cycle.*
3. *The vertex v_{k+1} is in the outer face of G_k such that its neighbors form a subpath of the path C_k .*
4. *If $k \leq n - 2$, then v_k has at least two neighbors in $G - G_{k-1}$.*

Proof. Let v_1, \dots, v_n be a 4-canonical ordering of (G, v_1) . Then, according to the proof of [Lemma 2.4](#), the first three conditions are true. Since in [Definition 2.22](#) the existence of two edges $\{v_k, v_{j_1}\}, \{v_k, v_{j_2}\} \in E$ with $k < j_1 < j_2 \leq n$ is required, also the fourth condition is fulfilled.

Let now be given an ordering v_1, \dots, v_n that fulfills the four conditions stated in the lemma. Combining the fourth condition with the proof of [Lemma 2.4](#) results in a 4-canonical ordering. \square

Note that [Definition 2.22](#) is stronger than [Definition 2.3](#) since in the first definition each vertex v_k has to have at least one neighbor in $G - G_k$ while in the latter one each vertex v_k is required to have at least two neighbors in $G - G_k$ [[Kant and He, 1997](#), [He, 1997](#)], for $k = 3, \dots, n - 2$.

[Kant and He \[1997\]](#) show how to compute a regular edge labeling from a canonical ordering. A *regular edge labeling* of a 4-connected, internally triangulated graph G with four vertices on the outer face is an orientation and labeling of the interior edges of G with labels 1 and 2 such that:

1. The edges incident to an interior vertex v appear in counterclockwise order around v as follows:

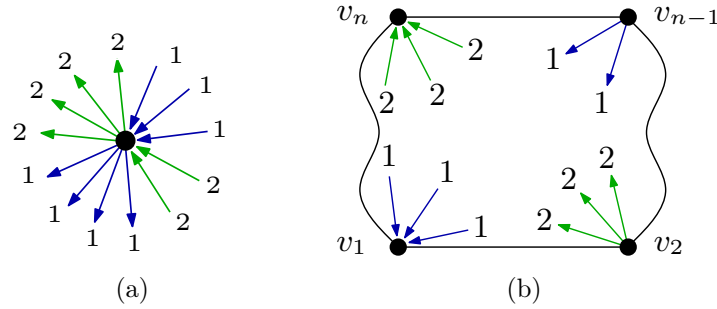


Figure 2.7: Edge orientations and labels (a) at an interior vertex. (b) at the four vertices v_1, v_2, v_{n-1}, v_n on the outer face.

- a set of outgoing edges with label 1
- a set of incoming edges with label 2
- a set of incoming edges with label 1
- a set of outgoing edges with label 2

See Figure 2.7(a).

2. Let v_1, v_2, v_{n-1}, v_n be the four vertices on the outer face in counterclockwise order. Then,
 - all interior edges incident to v_1 are labeled 1 and entering v_1 .
 - all interior edges incident to v_2 are labeled 2 and leaving v_2 .
 - all interior edges incident to v_{n-1} are labeled 1 and leaving v_{n-1} .
 - all interior edges incident to v_n are labeled 2 and entering v_n .

See Figure 2.7(b).

We will see in Chapter 3 that regular edge labelings are closely related to Schnyder woods.

Nakano, Rahman, and Nishizeki [1997] introduce the definition of a 4-canonical ordering that holds for not necessarily internally triangulated graphs. Here, we cite the variant of the definition of Miura, Nakano, and Nishizeki [2000b]. For 4-connected graphs that are internally triangulated, both definitions are equivalent.

Definition 2.24 (4-canonical ordering). *Let $G = (V, E)$ be a 4-connected, planar graph with four vertices v_1, v_2, v_{n-1}, v_n on the outer face of G in counterclockwise direction such that $\{v_1, v_2\}, \{v_{n-1}, v_n\} \in E$. Let $\Pi = (P_0, \dots, P_s)$ be a partition of V into paths such that $P_0 = \langle v_1, v_2 \rangle$, $P_s = \langle v_{n-1}, v_n \rangle$. For $k = 0, \dots, s$ let*

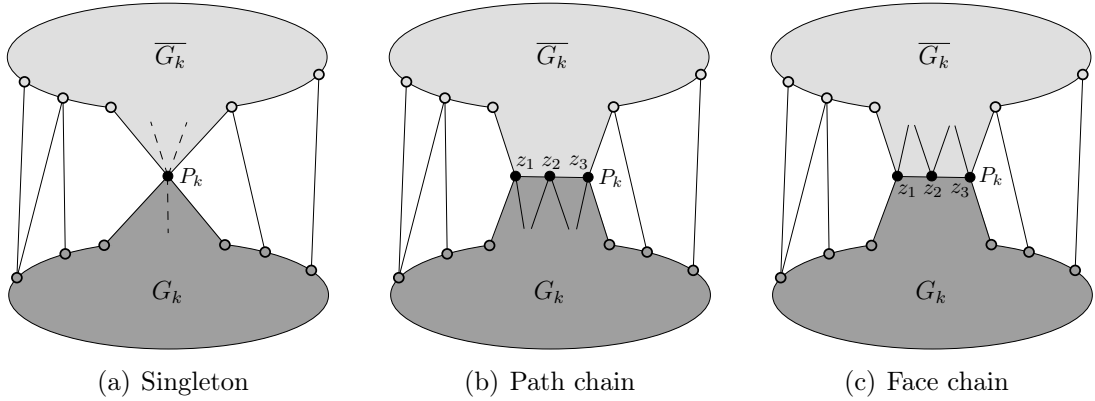


Figure 2.8: Different scenarios of a 4-canonical ordering.

$G_k = G[V_k] = (V_k, E_k)$ be the subgraph induced by $V_k = P_0 \cup \dots \cup P_k$ and for $k = 1, \dots, s$ let $\overline{G}_k = G - G_{k-1}$. Let C_k be the outer face of G_k , let \overline{C}_k be the outer face of \overline{G}_k . Partition Π is a 4-canonical ordering of (G, v_1, v_n) if for each $k = 1, \dots, s-1$:

1. G_k and \overline{G}_k are biconnected.
2. (a) $|P_k| = \langle z \rangle$, $\deg_{G_k}(z) \geq 2$ (see Figure 2.8(a)) or
 (b) $|P_k| > 1$, $\deg_{G_k}(z_i) = 2$, $\deg_{\overline{G}_k}(z_i) \geq 3$ for each vertex z_i in P_k (see Figure 2.8(b)) or
 (c) $|P_k| > 1$, $\deg_{G_k}(z_i) \geq 3$, $\deg_{\overline{G}_k}(z_i) = 2$ for each vertex z_i in P_k (see Figure 2.8(c)).

P_k is called a singleton if $|P_k| = 1$, and a chain otherwise. We distinguish two types of chains: path chains (case 2b) and face chains (case 2c).

Note that if z is a singleton, then $\deg_{\overline{G}_k}(z) \geq 2$ since \overline{G}_k is biconnected.

In more detail, a singleton P_k has at least two neighbors in $V \setminus V_k$ and at least two neighbors in V_{k-1} as shown in Figure 2.8(a)). Let $P_k = \langle z_1, \dots, z_p \rangle$ be a chain. Then, z_1 and z_p have exactly one neighbor in $V \setminus V_k$ and z_2, \dots, z_{p-1} have no neighbor in $V \setminus V_k$ (see Figure 2.8(b)) or z_1 and z_p have exactly one neighbor in V_{k-1} and z_2, \dots, z_{p-1} have no neighbor in V_{k-1} (see Figure 2.8(c)).

Miura, Nakano, and Nishizeki [2000b] refine a 4-canonical ordering to a 4-canonical vertex ordering v_1, \dots, v_n by ordering the vertices in each P_k , $k > 0$, according to their clockwise appearance on C_k . An example is presented in Figure 2.9.

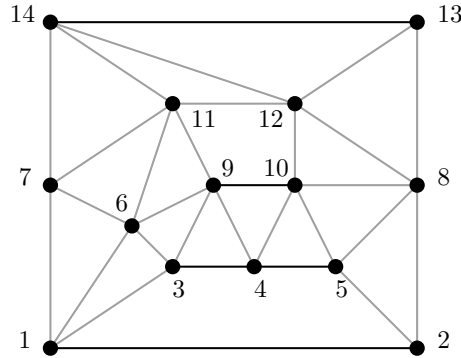


Figure 2.9: A 4-canonical vertex ordering. Black paths are chains, $\langle 3, 4, 5 \rangle$ is a face chain, $\langle 9, 10 \rangle$ is a path chain.

Kant and He [1997] show that every 4-connected, triangulated, planar graph has a 4-canonical ordering (see also Nishizeki and Rahman [2004]). Also, they present an algorithm that computes a canonical ordering in $\mathcal{O}(n)$ time. A more general version of the proof is due to Nakano et al. [1997].

Theorem 2.25 (Nakano et al., 1997). *Let $G = (V, E)$ be a 4-connected, planar graph with four vertices v_1, v_2, v_{n-1}, v_n on the outer face of G in counterclockwise direction such that $\{v_1, v_2\}, \{v_{n-1}, v_n\} \in E$. Then, G has a 4-canonical ordering.*

Nakano et al. [1997] use 4-canonical orderings to 4-partition a graph in linear time. In more detail, let be given a 4-connected, planar graph $G = (V, E)$ with four distinct vertices v_1, \dots, v_4 on the outer face and four natural numbers n_1, \dots, n_4 such that $\sum_{i=1}^4 n_i = |V|$. A *four-partition* $\mathcal{V} = \{V_1, \dots, V_4\}$ is a partition of the vertex set V such that $v_i \in V_i$, $|V_i| = n_i$, and each V_i induces a connected subgraph of G , for each $i = 1, \dots, 4$.

Also several drawing algorithms make use of 4-canonical orderings. He [1997] uses a 4-canonical ordering to construct a straight-line grid embedding of 4-connected, planar graphs with grid size $W + H \leq n$, $W \leq \frac{n+3}{2}$, and $H \leq 2\frac{n-1}{3}$. Miura, Nakano, and Nishizeki [2000b] draw a 4-connected, triangulated, planar graph on an integer grid of width $\lceil \frac{n}{2} \rceil - 1$ and height $\lceil \frac{n}{2} \rceil$. Miura, Nakano, and Nishizeki [2000a] construct a convex grid drawing of a 4-connected, planar graph on an integer grid with $W + H \leq n - 1$. All of these methods can be carried out in linear time.

2.4.3 5-Connected Graphs

Nagai and Nakano [2000] give a linear-time algorithm to compute five independent spanning trees of a 5-connected, triangular graph. These five trees may be rooted at any vertex. Their algorithm builds on canonical ordering for 5-connected, triangular graphs that we briefly announce in the following.

Let $G = (V, E)$ be a 5-connected, triangular graph and let v_1, v_2 , and v_n be the vertices on the outer face of G in counterclockwise direction. By $n_1, \dots, n_{\deg(v_n)}$ we denote the neighbors of v_n in counterclockwise direction on the outer face of $G - v_n$ such that $n_1 = v_1$ and $n_2 = v_2$. Construct a graph G' by removing the edges $\{n_1, v_n\}$, $\{n_2, v_n\}$, and $\{n_3, v_n\}$ and by inserting a new vertex v_0 on the outer face of G that is adjacent to n_1, n_2 , and n_3 . This construction is illustrated in Figure 2.10(a).

For $k = 0, \dots, s$, let $G_k = G[V_k] = (V_k, E_k)$ be the graph induced by $V_k = \{v_0\} \cup P_0 \cdots \cup P_k$ and for $k = 1, \dots, s$, let $\overline{G}_k = G' - G_{k-1}$. Let C_k be the outer face of G_k .

Definition 2.26 (5-canonical ordering). *A partition $\Pi = (P_0, \dots, P_s)$ of V into paths is called 5-canonical ordering of (G, v_1) if for each $k = 1, \dots, s - 1$:*

1. $P_0 = \langle n_1, n_2, n_3 \rangle$, $P_1 = \langle z_1, \dots, z_p \rangle$, where z_i are the neighbors of n_2 in \overline{G}_1 , for $i = 1, \dots, p$, and $P_s = \langle n_{\deg(v_n)}, n_{\deg(v_n)-1} \rangle$.
2. G_k is biconnected and \overline{G}_k is triconnected.
3. (a) $P_k = \langle z \rangle$, $\deg_{G_k}(z) \geq 3$, $\deg_{\overline{G}_k}(z) \geq 2$ (see Figure 2.10(b)) or
 (b) $|P_k| \geq 2$, $\deg_{G_k}(z_i) = 3$, and $\deg_{\overline{G}_k}(z_i) \geq 3$ for each vertex z_i in P_k (see Figure 2.10(c)).

P_k is called a singleton if $|P_k| = 1$, and a chain otherwise.

Theorem 2.27 (Nagai and Nakano, 2000). *Let G be a 5-connected, triangular graph and let G' be defined as above. Then, G' has a 5-canonical ordering that can be computed in linear time.*

2.4.4 Canonical Ordering Tree

The term canonical ordering tree (also called canonical spanning tree) appears for the first time in Chuang, Garg, He, Kao, and Lu [1998] and He, Kao, and Lu [1999]. Canonical ordering trees are often used for graph encoding [Chuang et al., 1998, He et al., 1999, Zhang and He, 2005d, Barbay et al., 2007]. An interesting application

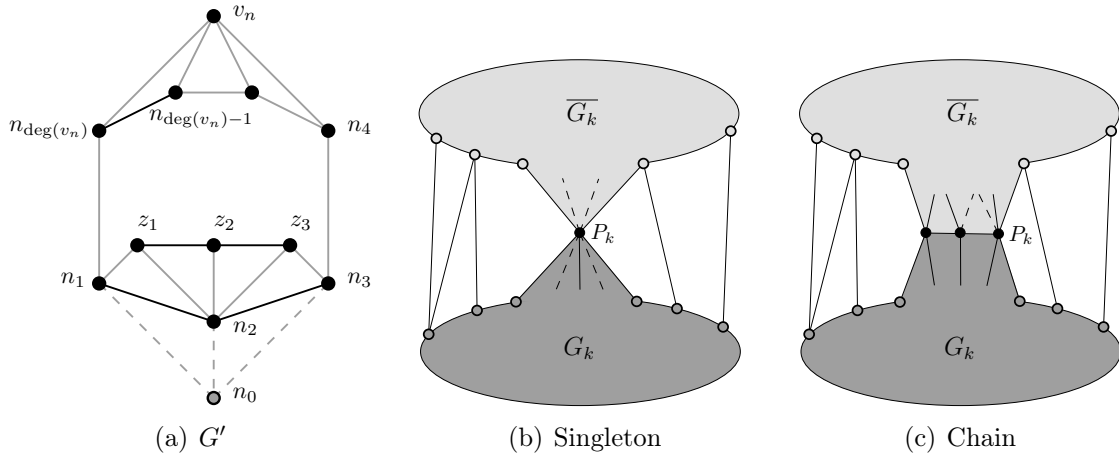


Figure 2.10: (a) Construction of G' . $P_0 = \langle n_1, n_2, n_3 \rangle$, $P_1 = \langle z_1, z_2, z_3 \rangle$, $P_s = \langle n_{\deg(v_n)}, n_{\deg(v_n)-1} \rangle$. (b-c) Different scenarios of a 5-canonical ordering.

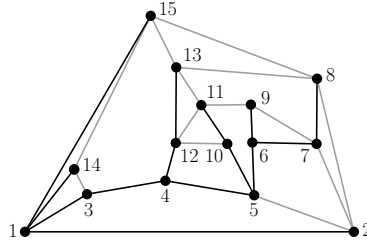


Figure 2.11: Canonical ordering tree T of graph G . The underlying canonical ordering is the rightist canonical ordering. Black edges are tree edges, gray edges are edges of $G - T$.

in graph drawing are visibility representations for triangular graphs. Zhang and He [2005a] construct an st -ordering from a canonical ordering tree to guarantee a bound on the longest directed path in the graph.

Let $G = (V, E)$ be a triconnected, planar graph with $n \geq 3$ vertices, let v_1 be a vertex on the outer face of G , and let $\Pi = (P_0, \dots, P_s)$ be a canonical ordering of (G, v_1) . Again, let c_ℓ be the left neighbor of $P_k = \langle z_1, \dots, z_p \rangle$. Detailed definitions can be found in Sections 2.1 and 2.2.

Definition 2.28 (Canonical Ordering Tree). *Let $\Pi = (P_0, \dots, P_s)$ be a canonical ordering of (G, v_1) . Then, P_0 together with the union of the paths $P_k + \{c_\ell, z_1\}$ for $k = 1, \dots, s$ is called canonical ordering tree of (G, v_1) .*

In Figure 2.11 an example of a canonical ordering tree is shown.

In the following lemma, some properties of canonical ordering trees are stated.

Lemma 2.29 (Chuang et al., 1998). *A canonical ordering tree T of (G, v_1) has the following properties:*

1. *Let $\{u, v\}$ be an edge in $G - T$. Then, u and v are unrelated in T .*
2. *The edges incident to each v in G have the following pattern in counterclockwise order around v : an edge to its parent in T , a block of non-tree edges to lower-numbered vertices, a block of tree edges to its children in T , a block of non-tree edges to higher-numbered vertices. Blocks might be empty.*

For example in Figure 2.11, vertex 7 has the following neighbors in counterclockwise order: an edge to its parent vertex 6, an edge to an unrelated vertex 2, an edge to its child vertex 8, an edge to an unrelated vertex 9.

Theorem 2.30 (Chuang et al., 1998). *For every triconnected, planar graph the preorder of any canonical ordering tree is also a canonical ordering of the graph.*

2.4.5 Orderly Spanning Tree

Chiang, Lin, and Lu [2001, 2005] generalize canonical ordering trees to orderly spanning trees. Applications of orderly spanning trees are graph encoding [Chiang et al., 2001, 2005], visibility representations [Chiang et al., 2001, 2005], floor planning [Liao et al., 2003], and other [Chen et al., 2003].

Definition 2.31 (Orderly Spanning Tree). *Let $G = (V, E)$ be a plane graph and let T be a spanning tree of G . Let v_1, \dots, v_n be the preorder of the vertices of G with respect to T .*

1. *A vertex v_i is orderly with respect to T if the edges incident to v_i in G have the following pattern in counterclockwise order around v_i :*
 - *an edge to its parent in T*
 - *a block of non-tree edges to lower-numbered vertices*
 - *a block of tree edges to its children in T*
 - *a block of non-tree edges to higher-numbered vertices*

Blocks might be empty. See Figure 2.12.

2. *T is called an orderly spanning tree of G if v_1 is an exterior vertex, and each v_i , $1 \leq i \leq n$, is orderly with respect to T .*

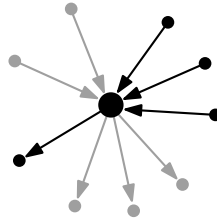


Figure 2.12: Orderly vertex: edges are oriented from higher to lower numbered vertices. Black edges are tree edges, gray edges are non-tree edges.

Zhang and He [2005a] summarize different properties of orderly spanning trees in the following lemma.

Lemma 2.32. *Let $G = (V, E)$ be a triangular graph with $n \geq 3$ vertices and let v_1 , v_2 , and v_n be the vertices on the outer face of G in counterclockwise order.*

- *Let T be an orderly spanning tree of G . Then, the preorder of T is a canonical ordering of G . Thus, T is a canonical ordering tree of G .*
- *A canonical ordering tree of G is also an orderly spanning tree of G .*

Bonichon, Gavaille, and Hanusse [2011] introduce the concept of *well-orderly trees*, a special case of orderly spanning trees [Chiang et al., 2001], that is used for graph encoding.

Chapter 3

Schnyder Woods

Schnyder woods are originally introduced by [Schnyder \[1989, 1990\]](#) under the name realizer for triangular graphs as a combinatorial structure to characterize planar graphs as the graphs whose incidence relation is the intersection of at most three total orders as well as an alternative method for straight-line drawings. A Schnyder wood of a triangular graph is a partition of the interior edges into three trees such that each tree spans all interior vertices and is rooted at an external vertex. Additionally, the incoming and outgoing edges of an interior vertex form a special pattern around it. There exist several equivalent formulations of Schnyder woods, such as Schnyder labelings (also known as normal labelings), α -orientations, and more that are presented in this chapter.

The problem of decomposing a graph into forests is rather old. [Nash-Williams \[1961, 1964\]](#) develop a formula to determine the arboricity of any graph. However, his proof does not provide a construction. From his result follows that planar graphs have arboricity at most three. [Kampen \[1976\]](#) does the spread work for Schnyder's result by showing that any triangular graph can be decomposed into three edge-disjoint trees. [Grossi and Lodi \[1998\]](#) partition general, planar graphs into three edge-disjoint forests in $\mathcal{O}(n \log n)$ -time.

[Itai and Rodeh \[1988\]](#) connect independent spanning trees with st -orientations. They show that for each biconnected graph G and for each vertex r of G there exist two independent spanning trees of G rooted at r . [Di Battista, Tamassia, and Vismara \[1999\]](#) use independent spanning trees to perform 2-paths queries on biconnected graphs. Independent spanning trees on triconnected graphs are investigated by [Zehavi and Itai \[1989\]](#) and [Cheriyán and Maheshwari \[1988\]](#). They independently prove that for each triconnected graph G and for each vertex r of G there exist three independent spanning trees of G rooted at r using st -orientations and non-separating ear decompositions, respectively. At the same time, [Cheriyán and Maheshwari \[1988\]](#)

extend a result of [Whitney \[1932\]](#) by showing that every triconnected graph has a non-separating open ear decomposition.

However, the problem of partitioning a graph into trees or other graphs with special properties is a research field on its own. Some results can be found, e. g., in [[Ringel, 1993](#), [Ringel et al., 1997](#), [Biedl and Brandenburg, 2007](#)].

Another linking of *st*-orderings and Schnyder woods is discovered by [Zhang and He \[2003\]](#) who show how to obtain an *st*-numbering from a Schnyder wood of a triangular graph via canonical ordering trees. They claim that an *st*-ordering obtained from a canonical ordering tree yields visibility representations with a low height.

[Di Battista et al. \[1999\]](#) and [Felsner \[2001\]](#) extend Schnyder woods to triconnected, planar graphs and present a linear-time algorithm to construct a Schnyder wood. While the algorithm of [Di Battista et al. \[1999\]](#) uses canonical ordering, the one of [Felsner \[2001\]](#) extends the technique of [Schnyder \[1990\]](#). Also, [Felsner \[2001, 2003, 2004b\]](#), [Felsner and Zickfeld \[2008\]](#) do some pioneering work in the field of Schnyder woods for triconnected, planar graphs. They characterize them as those graphs that admit a rigid geodesic embedding and show a bijection between Schnyder woods and rigid geodesic embeddings. Further, they investigate connections to orthogonal surfaces and give an alternative proof for the Brightwell-Trotter theorem that is an extension of Schnyder's characterization to embedded planar multigraphs. More aspects of Schnyder woods and related concepts are highlighted in [Zickfeld \[2007\]](#). [Aleari, Fusy, and Lewiner \[2008\]](#) extend Schnyder woods to graphs embedded on surfaces of arbitrary genus.

To my knowledge, Felsner also wrote the first book dealing with Schnyder woods and related combinatorial concepts [[Felsner, 2004a](#)]. One of these nice combinatorial properties is that the set of Schnyder woods has a lattice structure [[Brehm, 2000](#), [de Fraysseix and Ossona de Mendez, 2001](#), [Felsner, 2004b](#)]. To prove the structure of a distributive lattice for triconnected, planar graphs, [Felsner \[2004b\]](#) shows how a Schnyder wood of a graph induces a Schnyder wood on the dual graph. Also, this insight reveals relations of Schnyder woods to Eulerian orientations and spanning trees - other combinatorial sets that have a lattice structure.

Another question that arises with the fact that the set of Schnyder woods forms a distributive lattice is the one of finding the minimal element. [Brehm \[2000\]](#) provides an algorithm that computes the minimal and maximal Schnyder wood of a triangular graph, respectively, i. e., the Schnyder wood without clockwise and counterclockwise cycles, respectively. [Felsner \[2004b\]](#) shows how to iteratively reverse the direction of cycles to obtain the minimal Schnyder wood of a triconnected, planar graph. [Fusy, Schaeffer, and Poulalhon \[2008\]](#) develop an algorithm with a long case distinction that directly computes the minimal Schnyder wood of a triconnected, planar graph. Using their result, [Badent, Brandes, and Cornelsen \[2011\]](#) present an

intuitive algorithm that builds on the ideas of leftist canonical ordering and outputs a Schnyder wood without clockwise and counterclockwise cycles, respectively.

In this chapter, we present Schnyder woods for triangular graphs and show that they are bijective to Schnyder labelings, 3-orientations, and canonical orderings. We show how to modify a Schnyder wood to get a different one and also Schnyder woods with special properties, i. e., Schnyder woods without clockwise and counterclockwise cycles, respectively.

We transfer the results of triangular graphs to triconnected, planar graphs. In more detail, after giving definitions of Schnyder woods and Schnyder labelings of triconnected, planar graphs and proving that these two structures are bijective, we present different properties of them. Also, we characterize planar graphs via the dimension of their incidence order. In [Felsner \[2004a, Chapter 2\]](#) most of Section 3.2 is summarized.

Then, we extend the concept of Schnyder woods to the dual graph and construct a bijection to path partitions [[Badent et al., 2011](#)]. Since the set of Schnyder woods of a graph and its dual forms a distributive lattice, we present the theoretical foundations to find the minimal element of the lattice. The corresponding algorithms are presented in Chapter 6.

3.1 Triangular Graphs

In this section, let $G = (V, E)$ be a triangular graph and let v_1, v_2 , and v_n be the vertices on the outer face of G in counterclockwise direction. For simplicity, we sometimes denote $v_1 = a_1, v_2 = a_2, v_n = a_3$ and assume on the labels $i = 1, 2, 3$ a cyclic structure so that $3 + 1 = 1$ and $1 - 1 = 3$.

We announce the notion of Schnyder woods, Schnyder labelings, and 3-orientations for triangular graphs and show that they are in one-to-one correspondence [[Schnyder, 1989, 1990, de Fraysseix and Ossona de Mendez, 2001](#)].

Definition 3.1 (Schnyder wood). *A Schnyder wood (or realizer) of (G, v_1) is an orientation and labeling of the interior edges of G with labels 1, 2, and 3 (alternatively with labels blue, green, and red) such that:*

1. *Every interior vertex v has outdegree one in each label.*
2. *The labels i of the three outgoing edges $e_i, i = 1, 2, 3$, of an interior vertex v occur in counterclockwise order.*
3. *Each incoming edge of vertex v with label i enters v in the clockwise sector from e_{i-1} to e_{i+1} .*

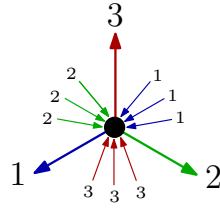


Figure 3.1: Edge orientations and labels at an interior vertex.

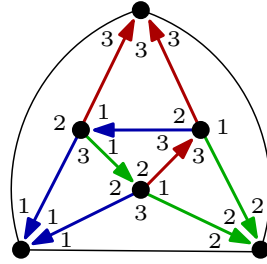


Figure 3.2: Schnyder wood and Schnyder labeling of a triangular graph. Blue edges have label 1, green edges have label 2, and red edges have label 3.

4. The edges $\{v, a_i\}$ are oriented from v to a_i with label i .

Figure 3.1 explains the edge orientations and labels at an interior vertex and Figure 3.2 presents an example of a Schnyder wood.

Definition 3.2 (Schnyder labeling). A Schnyder labeling (or normal labeling) of (G, v_1) is a labeling of the angles of G with labels 1, 2, and 3 (alternatively with labels blue, green, and red) such that:

1. Rule of vertices: The labels of the angles at each interior vertex form in counterclockwise order non-empty intervals of 1's, 2's, and 3's. See Figure 3.3(a).
2. Rule of faces: Each inner face has an angle with label 1, an angle with label 2, and an angle with label 3 appearing in counterclockwise order. See Figure 3.3(b).
3. All interior angles at a_i are colored i , for $i = 1, 2, 3$.

An example of a Schnyder labeling is shown in Figure 3.2.

Definition 3.3 (3-orientation). A 3-orientation of a triangular graph is an orientation of the interior edges such that each interior vertex has outdegree 3.

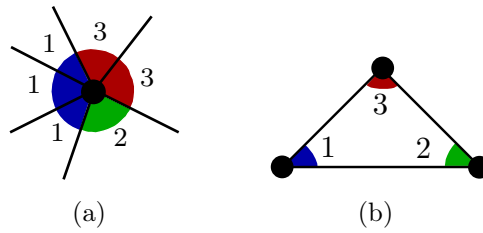


Figure 3.3: (a) Rule of vertices. (b) Rule of faces.

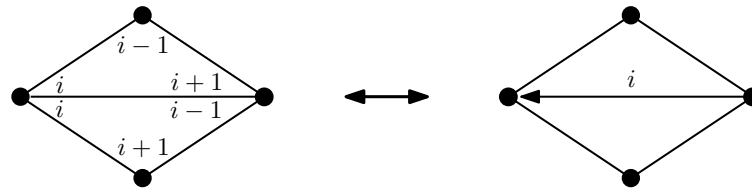


Figure 3.4: Angle labels and edge orientation.

3.1.1 Bijections

We show that each Schnyder wood corresponds to exactly one Schnyder labeling and vice versa. This correspondence is illustrated in Figures 3.2 and 3.4.

In a Schnyder labeling, each interior edge is incident to two faces and, therefore, has one end with two distinct labels and one end with the same label i . Then, the edge is oriented from the end with distinct labels to the end with identical labels and gets label i . The other way round, if an edge $e = (u, v)$ is labeled i in a Schnyder wood, then the angle at the source u of e to the right of e is labeled $i + 1$ and the angle at u to the left of e is labeled $i - 1$. The angles at the target v of e are both labeled i .

From Schnyder woods to Schnyder labelings. It is easy to see that from Definition 3.1 follows the rule of vertices (Property 3.2(1)).

Let u, v, w be a triangle of G in counterclockwise order. Without loss of generality, let $\{u, v\}$ be an outgoing edge of vertex u labeled 1 (the other cases are symmetric). Then, $\{u, w\}$ is either an outgoing edge of vertex u and labeled 2, or an incoming edge of vertex u and labeled 3. In the same way, $\{v, w\}$ is either an outgoing edge of vertex v and labeled 2, or an incoming edge of vertex v and labeled 1. In all scenarios, the rule of faces (Property 3.2(2)) is fulfilled. See Figure 3.5.

Property 3.1(4) directly corresponds to Property 3.2(3).

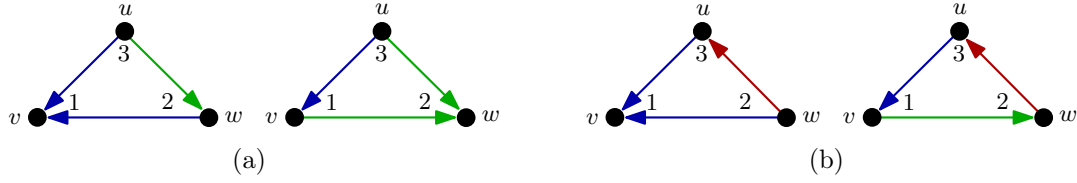


Figure 3.5: From Schnyder woods to Schnyder labelings: Rule of faces is in all cases fulfilled.

From Schnyder labelings to Schnyder woods. Apply the construction stated above to a Schnyder labeling. Let T_i denote the oriented subgraph of G induced by the edges having label i . The rule of vertices (Property 3.2(1)) guarantees that each T_i , $i = 1, 2, 3$, satisfies Properties 3.1(1)-3.1(3). Property 3.2(3) directly corresponds to Property 3.1(4). Thus, each Schnyder labeling induces a Schnyder wood.

Clearly, a Schnyder wood also defines a 3-orientation. Moreover, a 3-orientation defined by a Schnyder wood is sufficient to reconstruct the Schnyder wood. In fact, Schnyder woods and 3-orientations are in one-to-one correspondence.

Theorem 3.4 (de Fraysseix and Ossona de Mendez, 2001). *Schnyder woods are in bijection with 3-orientations.*

Proof. We show how to map a Schnyder wood to a 3-orientation and vice versa such that the composition of the two maps yields the identity.

From Schnyder woods to 3-orientations. In a Schnyder wood, each interior vertex has outdegree one in each of the three labels. Thus, the orientation of the edges in a Schnyder wood is a 3-orientation.

From 3-orientations to Schnyder woods. Orient the external edges as a circuit. A *balanced chain* is a directed path whose inner vertices have one outgoing edge at each side of the path. First, we show that no simple cycle is the union of less than three balanced chains. Let C be a simple cycle and let $G' = (V', E')$ be the graph induced by the vertices of C and the vertices that lie on the outer face of C . Each face of G' except the one defined by C is a triangle. Thus, G' has the following number of edges:

$$|E'| = 3|V'| - |V(C)| - 3$$

Every subgraph H of a triangular graph G has

$$\sum_{v \in V(H)} \deg_G^+(v) - |E(H)|$$

many edges that are not in $E(H)$ and directed to vertices of $G \setminus H$. Further,

$$\sum_{v \in V'} \deg_G^+(v) = 3|V'| - 6$$

as G' contains the three external vertices that have outdegree 1.

Combining these three equations yields

$$\sum_{v \in V'} \deg_G^+(v) = |E'| + |V(C)| - 3$$

and, therefore,

$$|V(C)| - 3$$

edges are directed to vertices in the interior of C . Thus, there are three vertices that do not have an outgoing edge to a vertex inside C . As each vertex of C is incident to a balanced chain, there are three vertices of C that are not inner vertices of a balanced chain.

Now, given an edge e , consider a maximal balanced chain ending with e . Since this balanced chain does not include a cycle, it ends at an external vertex. Depending on the label of this endvertex, all edges on the chain get the same label. In more detail, if a_i is the endvertex of the balanced chain, then all edges incident to the balanced chain are labeled i , for $i = 1, 2, 3$. This clearly defines a tripartition of the internal edges of the graph and all other properties of a Schnyder wood are fulfilled, too.

It is easy to see that the two constructions are inverse to each other. □

The next lemma will help us to discover 3-orientations without clockwise (counterclockwise) oriented triangles. It will turn out that the Schnyder wood without clockwise (counterclockwise) oriented cycles plays a crucial role in the combinatorial structure of this concept. Details are shown in Section 3.1.4. In Section 6.1 we present an algorithm that is based on the leftist canonical ordering to construct such a Schnyder wood.

Lemma 3.5 (Brehm, 2000). *Let G be a triangular graph with a 3-orientation \mathcal{T} . If \mathcal{T} contains a directed cycle, then it contains a directed face that is oriented in the same direction.*

Proof. If a cycle C has no interior edge that is an outgoing edge for a vertex on C , then we show with Theorem 1.4 that C is a triangle. Let c be the number of vertices of C , let n' and m' be the number of interior vertices and edges of C , respectively.

Since C is a cycle, it has c edges. To triangulate the outer face, $c - 3$ additional edges are required. Then, by Theorem 1.4 follows:

$$\begin{aligned} m' + c + (c - 3) &= 3(n' + c) - 6 \\ c &= m' - 3n' + 3 \end{aligned}$$

As every vertex is incident to three outgoing edges, it holds that $m' = 3n'$. From this follows $c = 3$.

Without loss of generality, let C be a counterclockwise cycle in \mathcal{T} such that there are as few faces inside the triangle as possible. Assume for a contradiction that there is a vertex $v \in C$ that is incident to an outgoing, interior edge. Consider the balanced chain starting at this vertex and ending at an external vertex (compare proof of Theorem 3.4). Then, this directed path must cross C at a vertex w . But such a path cannot exist since otherwise one could find a cycle containing less faces than C . \square

3.1.2 Properties

Lemma 3.6 (Schnyder, 1990). *All angles at an exterior vertex have the same label and distinct exterior vertices have distinct labels. The exterior vertices whose angles are labeled 1, 2, and 3 appear in counterclockwise order.*

Proof. A triangular graph G has exactly $3n - 6$ edges in total (Theorem 1.4). Since G has three exterior edges, it has $3n - 9$ interior edges. Further, G has $n - 3$ interior vertices. Using the bijection from Schnyder labelings to Schnyder woods (Section 3.1.1) yields that every interior vertex has three outgoing edges and, thus, all exterior vertices have only incoming edges. From this follows, that all angles at an exterior vertex have the same label. By the fact that each exterior edge belongs to one inner face and by Definition 3.2 follows the second part of the statement. \square

The consequence of Lemma 3.6 and Theorem 3.4 is the following property of 3-orientations.

Lemma 3.7. *In a 3-orientation the exterior vertices have outdegree 0.*

We come back to edge contractions, now for triangular graphs (compare Section 1.5). An edge $\{u, v\}$ is *contractible* if u and v have exactly two common neighbors w_1 and w_2 . Contracting e means in this sense, replacing the vertices u and v with a new vertex uv , replacing the edges $\{u, w_i\}$ and $\{v, w_i\}$ with $\{uv, w_i\}$, $i = 1, 2$, and all other edges incident to u and v , respectively, become edges that are incident to uv . See again Figure 1.9.

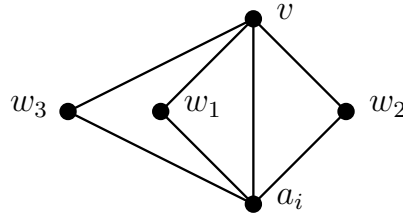


Figure 3.6: Illustration of the proof of Lemma 3.8: The contraction of $e = \{a_i, v\}$ would create a multiple edge. However, inside the triangle a_i, v, w_1 must exist a contractible edge.

If G is triangular, has at least four vertices, and $e = \{u, v\}$ is a contractible edge of G , then G/e is again a triangular graph. Compare Lemma 1.18. Now, we want to perform edge contractions such that one endvertex of the contracted edge is an exterior vertex. This will help us to expand a Schnyder labeling of a triangle to a Schnyder labeling of a larger graph.

Lemma 3.8 (Kampen, 1976). *Let G be a triangular graph with at least four vertices and with the three exterior vertices a_1, a_2 , and a_3 . Then, there exists a neighbor $v \neq a_{i-1}, a_{i+1}$ of a_i such that the edge $\{a_i, v\}$ is contractible.*

Proof. If $G = (V, E)$ has exactly four vertices, the lemma is true. So assume that $|V| > 4$. Let a_i be an external vertex of G and assume for a contradiction that there is no neighbor v such that $e = \{a_i, v\}$ is contractible. Since $|V| > 4$, $\{a_i, v\}$ is incident to two distinct elementary triangles a_i, v, w_1 and a_i, v, w_2 . Since G/e is not triangular, the contraction of e creates a multiple edge. Thus, e must be incident to another triangle a_i, v, w_3 . Without loss of generality, let w_1 lie in the interior region of the triangle a_i, v, w_3 . Then, w_2 lies in the exterior region. Deleting all vertices and edges in the exterior region of a_i, v, w_3 yields a graph G' with less than n vertices. Thus, the lemma holds by induction hypothesis. Since w_3 and a_i are adjacent in G' , there exists a vertex y in the interior region of a_i, v, w_3 such that $\{a_i, y\}$ is contractible. This edge is contractible in G as well. See Figure 3.6. \square

With the help of contractible edges, we can show the following theorem.

Theorem 3.9 (Schnyder, 1989). *Each triangular graph G has a Schnyder wood.*

Proof. Since Schnyder woods and Schnyder labelings are in one-to-one correspondence, we show that every triangular graph has a Schnyder labeling. Let a_1 be an exterior vertex of $G = (V, E)$. We inductively construct a Schnyder labeling such that all angles at a_1 have label 1.

If $n = |V| = 3$, the construction is trivial. So, let $n \geq 4$ and assume that the theorem is true for all triangular graphs with less than n vertices.

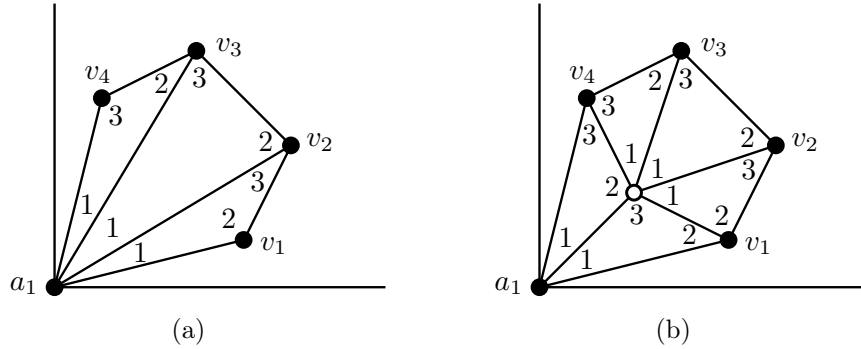


Figure 3.7: Schnyder labeling in (a) is extended to the Schnyder labeling in (b).

By Lemma 3.8, there exists a neighbor v of a_1 such that v is an interior vertex and such that $e = \{a_1, v\}$ is contractible. Let a_1, v_1, \dots, v_k be the neighbors of v in counterclockwise order. By induction hypothesis, G/e has a Schnyder labeling such that all angles at a_1 have label 1. We extend the Schnyder labeling of G/e to a Schnyder labeling of G as follows:

1. Label the angles v_{i+1}, v, v_i with label 1, $i = 1, \dots, k - 1$.
2. Label the angle a_1, v, v_1 with label 3, and the angle a_1, v, v_k with label 2.
3. Label the angle v_1, a_1, v and v, a_1, v_k with label 1.

This procedure is shown in Figure 3.7.

In terms of Schnyder woods this means that a Schnyder wood of G/e is extended to a Schnyder wood of G in the following way. Let (u, v) denote the directed edge from u to v and let $\text{label}(u, v) = i$ indicate that (u, v) has label i .

1. $\text{label}(v, a_1) = 1, \text{label}(v_i, v) = 1, i = 2, \dots, k - 1$
2. $\text{label}(v, v_1) = 2, \text{label}(v, v_k) = 3$

This construction is illustrated Figure 3.8. □

A Schnyder wood consists of three trees. More precisely, let T_i denote the oriented subgraph of G induced by the edges having label i , $i = 1, 2, 3$.

Lemma 3.10 (Schnyder, 1990). *Each T_i is a tree including all internal vertices and exactly one external vertex. All edges of T_i are directed towards this external vertex. Moreover, a_i is the root of T_i , $i = 1, 2, 3$.*

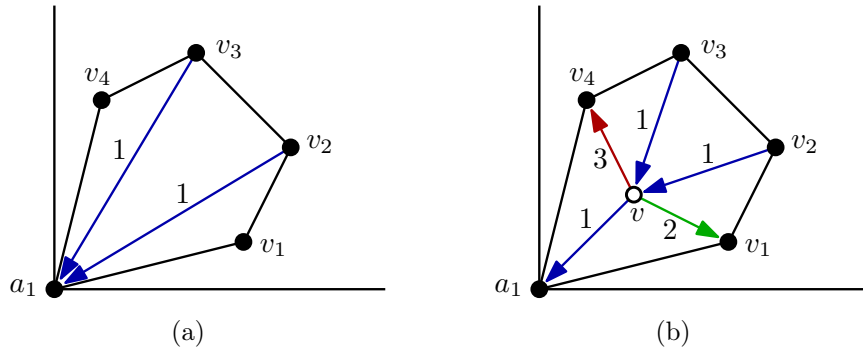


Figure 3.8: Schnyder wood in (a) is extended to the Schnyder wood in (b).

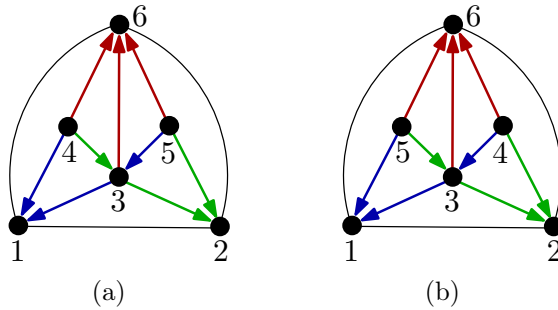


Figure 3.9: Two different canonical orderings inducing the same orientation on the edges and, therefore, the same Schnyder wood.

Proof. This holds for a triangular graph with four vertices. Using the expansion technique from the proof of Theorem 3.9 the statement remains true. \square

3.1.3 Canonical Ordering

To close the cycle to Chapter 2, we now show that Schnyder woods are in one-to-one correspondence to the equivalence classes of canonical orderings, a result that we extend in Section 3.6 to triconnected, planar graphs.

A canonical ordering $\Pi = (v_1, \dots, v_n)$ induces an *orientation* on the interior edge of G as follows. Let $e = \{v_i, v_j\}$ be an interior edge of G such that $i < j$. Then, e is an *outgoing edge* of v_i and an *incoming edge* of v_j .

Definition 3.11 (equivalence of canonical orderings). *Two canonical orderings Π and Π' are equivalent if and only if Π and Π' induce the same orientation on the interior edges. See Figure 3.9.*

Theorem 3.12. *There is a bijection between the equivalence classes of the canonical orderings of (G, v_1) and the Schnyder woods of (G, v_1) .*

Proof. We show how to map the equivalence classes of canonical orderings to a Schnyder wood and a Schnyder wood to the equivalence classes of canonical orderings such that the composition of the two maps yields the identity.

From Canonical orderings to Schnyder woods. Let $\Pi = (v_1, \dots, v_n)$ be a canonical vertex ordering of (G, v_1) . For $k = 3, \dots, n$, let c_ℓ be the left neighbor of v_k and let c_r be the right neighbor of v_k . Remember that right and left neighbors are defined in Section 2.2.1. Let (u, v) denote the directed edge from u to v and let $\text{label}(u, v) = i$ indicate that (u, v) has label i . A Schnyder wood can be constructed by assigning labels and orientations to the interior edges of G by processing the vertices in canonical ordering as follows:

1. $\text{label}(v_k, c_\ell) = 1$
2. $\text{label}(v_k, c_r) = 2$
3. $\text{label}(c_i, v_k) = 3$, for $i = \ell + 1, \dots, r - 1$

See also Algorithm 7 and Figure 6.1 in Chapter 6.

Construction yields a Schnyder wood. In Theorem 6.2 we prove that the construction yields a Schnyder wood without clockwise cycles if the canonical ordering is leftist.

Independence of representatives. Two canonical orderings are only equivalent if they induce the same orientation. Therefore, they induce the same Schnyder wood.

From Schnyder woods to canonical orderings. Let a Schnyder wood of (G, v_1) be given. From Lemma 3.7 we know that the exterior vertices of G have outdegree 0. Let v_1, v_2 , and v_n be the roots of the three trees T_1, T_2 , and T_3 (Lemma 3.10).

We define a partial order \prec on the vertices of G such that the transitive closure yields a canonical ordering. Further, the set of all linear extensions of \prec defines an equivalence class of canonical orderings.

Let $e = \{v_i, v_j\}$ be an interior edge of G . Then, $v_i \prec v_j$ if $\text{label}(v_i, v_j) = 3$ or $\text{label}(v_j, v_i) = 1$ or $\text{label}(v_j, v_i) = 2$.

\prec is **acyclic**. Let T_i denote the oriented subgraph of G induced by the edges having label i , and let T_i^{-1} be the graph that is obtained by reverting all edges of T_i , $i = 1, 2, 3$. We have to show that the graph $T_3 \cup T_1^{-1} \cup T_2^{-1}$ is acyclic.

Assume for a contradiction that there is a cycle in $T_3 \cup T_1^{-1} \cup T_2^{-1}$.

Choose such a cycle C that encloses the minimum number of faces. We show that this cycle must be a face. Suppose the interior region of C contains a vertex v . This vertex has a v - v_n -path where all edges are labeled 3. However, this path contains a vertex of C . By the minimality of C , it contains exactly one vertex of C . Similarly, there exists a v_1 - v - and a v_2 - v -path, respectively. Also, each of these paths contains a vertex of C and, by the minimality of C , it contains exactly one vertex of C . But then subpaths of the v - v_n -path, v_2 - v -path, and C form a cycle that encloses less faces than C . If C contains an interior edge, this edge would also form a cycle enclosing less faces. Thus, the cycle is a face. It is easy to see that such a face contradicts Definition 3.1.

$\Pi = (v_1, \dots, v_n)$ is a **canonical ordering**. Since every internal vertex has two outgoing edges labeled 1 and 2 that are reverted in \prec , and one outgoing edge labeled 3, the properties of Definition 2.3 are fulfilled.

Finally, the two constructions are inverse to each other. □

We remark that this result is also obtained by [de Fraysseix and Ossona de Mendez \[2001\]](#). In detail, they show that any Schnyder wood can be obtained from a *standard shelling order*, i.e., a canonical ordering that is obtained from the preorder of the tree induced by the edges with label 1. The advantage of our proof is that it can be extended to triconnected, planar graphs as shown in Section 3.6.

Orderly Spanning Trees We briefly add a result that demonstrates a connection of orderly spanning trees and Schnyder woods (compare [Zhang and He \[2005a\]](#) and Lemma 2.32).

Lemma 3.13. *Let G be a triangular graph with the three exterior vertices a_1 , a_2 , and a_3 in counterclockwise order and let T_1 , T_2 , and T_3 be the three trees of a Schnyder wood such that each T_i is rooted at a_i , for $i = 1, 2, 3$.*

Then, $T_i \cup \{\{a_i, a_{i+1}\}, \{a_i, a_{i-1}\}\}$ is an orderly spanning tree of G .

3.1.4 Cycles

[Zickfeld \[2007\]](#) shows that a triangulation has a unique Schnyder wood if and only if it is a stacked triangulation. A detailed definition of stacked triangulation is given

in Section 4.4. Consequently, in general there exist several Schnyder woods of a graph. We show how to construct new Schnyder woods from a given one and start with the following introductory results for 3-orientations.

Lemma 3.14 (Brehm, 2000). *Reversing the direction of an oriented cycle in a 3-orientation yields again a 3-orientation.*

Proof. Let C be an oriented cycle. After reverting the direction of the edges of C , all vertices on C still have outdegree 3. For all other vertices, there is no change at all. \square

Lemma 3.15 (Brehm, 2000). *If a triangular graph G has more than one 3-orientation, every 3-orientation contains directed cycles. More precisely, if \mathcal{S} and \mathcal{T} are two different 3-orientations of G , then there exists a cycle which is clockwise in one of \mathcal{S} or \mathcal{T} and counterclockwise in the other.*

Proof. Let \mathcal{S} and \mathcal{T} be two different 3-orientations of G . Let (v_1, v_2) be an edge in \mathcal{S} and let (v_2, v_1) be an edge in \mathcal{T} . Since the outdegree of v_2 is 3 in both \mathcal{S} and \mathcal{T} , there must exist another edge (v_2, v_3) in \mathcal{S} such that (v_3, v_2) in \mathcal{T} . Following this argument inductively, we end up at an already processed vertex. The constructed paths form a clockwise cycle in one and a counterclockwise cycle in the other 3-orientation.

Note that such a path cannot end up at an exterior vertex since this would contradict Lemma 3.7. \square

Theorem 3.16 (Brehm, 2000). *In every triangular graph G , there exists at most one 3-orientation without clockwise and counterclockwise cycles, respectively.*

Proof. Suppose G has two different 3-orientations that both have, without loss of generality, no clockwise cycle. By Lemma 3.15 there exists a cycle in both of them with different orientations, a contradiction. \square

Reverting the direction of all edges of a face that is a directed cycle from counterclockwise (clockwise) to clockwise (counterclockwise) is called a *face flip* (*face flop*). For constructing new Schnyder woods from old ones, it is not only necessary to flip and flop the faces, respectively, but also to change the additional label information.

In more detail, if a face is flipped (flopped) the labels are cyclically rotated in clockwise (counterclockwise) order. Figure 3.10 demonstrates this. It is easy to see that the resulting orientation and labeling of the edges yields again a Schnyder wood.

Using this technique, we can prove the following, more general theorem that states that even general cycles can be flipped and flopped, respectively. Brehm's

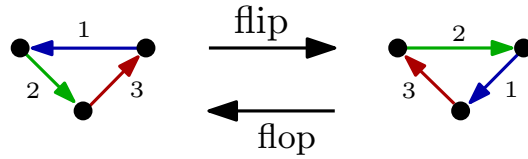


Figure 3.10: Face flip and flop.

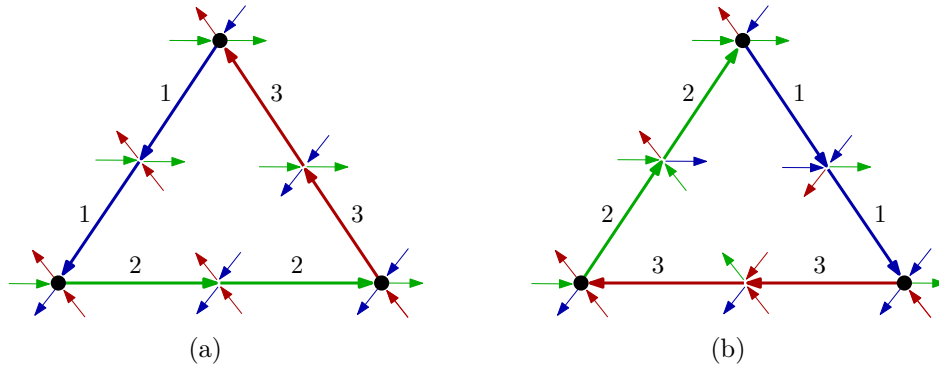


Figure 3.11: Blue edges have label 1, green edges have label 2, red edges have label 3. (a) Counterclockwise cycle in a Schnyder wood. (b) Rotated cycle from (a) with adjusted edge labels according to Theorem 3.17.

proof uses the fact that reverting a cycle can be mimicked by flipping each face inside the cycle once. In contrast, we directly show how to change the labels and colors of the edges on and inside the cycle to obtain the desired Schnyder wood. This procedure is illustrated in Figure 3.12.

Theorem 3.17 (Brehm, 2000). *Let G be a triangular graph together with a Schnyder wood \mathcal{S} and let C be a counterclockwise cycle in \mathcal{S} . Then, a new Schnyder wood can be obtained by*

1. reversing the direction of the edges of C ,
2. setting for each edge with label i on C the new label $i + 1$,
3. setting for each edge with label i inside C the new label $i - 1$,
4. leave all other labels unchanged.

Proof. Figure 3.11 shows that the properties of Definition 3.1 are fulfilled for all vertices on C . One can easily verify that they also hold for the vertices inside C . \square

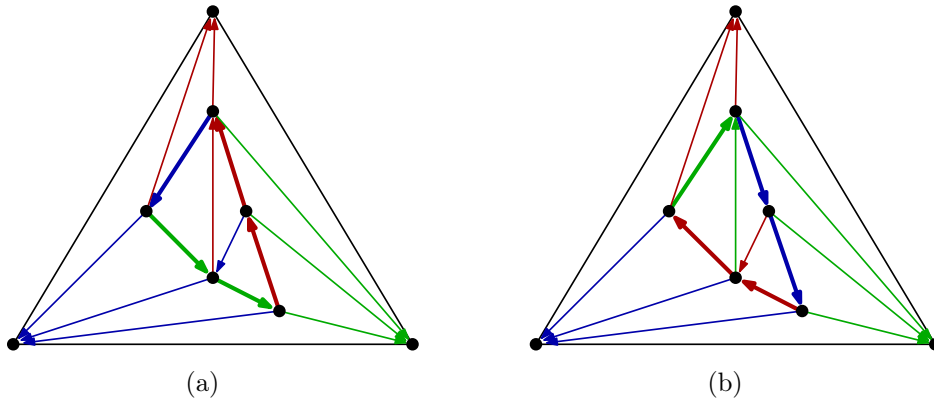


Figure 3.12: Blue edges have label 1, green edges have label 2, red edges have label 3. (a) Schnyder wood with a counterclockwise cycle (bold edges). (b) Cycle from Schnyder wood of (a) is flipped.

Moreover, using face potentials, i. e., how often a face can be flipped and flopped, respectively, [Brehm \[2000\]](#) shows that the set of all Schnyder woods forms a distributive lattice L (it is also shown independently by [Ossona de Mendez \[1994\]](#)), where the partial order of L is defined as follows: Let \mathcal{S} and \mathcal{T} be two different Schnyder woods of (G, v_1) . Then, $\mathcal{S} \preceq \mathcal{T}$ in L if and only if \mathcal{S} can be obtained from \mathcal{T} by flopping some faces.

In particular, there exists a unique minimal and maximal element, respectively, that corresponds to the Schnyder wood without clockwise and counterclockwise cycles, respectively. More about the lattice structure of Schnyder woods is explained in [Section 3.5](#). In [Chapter 6](#) we present an algorithm to construct a Schnyder wood without clockwise and counterclockwise cycles, respectively.

Note that sometimes the lattice L is defined such that $\mathcal{S} \preceq \mathcal{T}$ in L if and only if \mathcal{S} can be obtained from \mathcal{T} by flipping some faces. Then, the minimal element corresponds to the Schnyder wood without counterclockwise cycles.

3.2 Triconnected Graphs

Throughout this section, we consider only triconnected, planar graphs and extend the results of [Section 3.1](#) from triangular graphs to triconnected, planar graphs. In more detail, we show that Schnyder woods are in one-to-one correspondence with Schnyder labelings on triconnected, planar graphs. We conclude with some properties of Schnyder woods.

Some of the following introductory definitions and lemmas are also summarized in Felsner [2004a]. However, we stick with our definitions closer to the relation to canonical ordering, i. e., we require $\langle v_2, v_1, v_n \rangle$ to be a path on the outer face of G in clockwise direction while in the original definition of Felsner [2001] just three arbitrary vertices on the outer face are selected.

We sometimes denote $v_1 = a_1$, $v_2 = a_2$, $v_n = a_3$ and assume on the labels $i = 1, 2, 3$ a cyclic structure so that $3 + 1 = 1$ and $1 - 1 = 3$.

Definition 3.18 (closure). *The closure of (G, v_1) is the graph G_∞ that is obtained from G by adding a new vertex v_∞ to the outer face of G and the edges $\{v_1, v_\infty\}$, $\{v_2, v_\infty\}$, and $\{v_n, v_\infty\}$.*

Definition 3.19 (Schnyder wood). *A Schnyder wood of (G, v_1) is an orientation and labeling of the edges of the closure G_∞ of (G, v_1) with labels 1, 2, and 3 (alternatively with labels blue, green, and red) such that:*

1. *Every edge is oriented by one or two opposing directions. If an edge is bi-oriented, then the two directions have distinct labels.*
2. *The three edges $\{a_i, v_\infty\}$ are oriented towards v_∞ and labeled i , $i = 1, 2, 3$.*
3. *Every vertex $v \neq v_\infty$ has outdegree one in each label. The labels i of the three outgoing edges e_i , $i = 1, 2, 3$, of a vertex v occur in counterclockwise order. Each incoming edge of v with label i enters v in the clockwise sector from e_{i-1} to e_{i+1} . See Figure 3.1.*
4. *There is no inner face whose boundary is a directed cycle in one label.*

Schnyder woods are often defined on the *suspension* of G , i. e., the graph that is obtained by adding half-edges to each vertex v_1 , v_2 , and v_n that reach into the outer face. Sloppily, we often construct Schnyder woods on a triconnected, planar graph G and assume that graph is implicitly augmented to the closure G_∞ . When proving that a construction yields a Schnyder wood, we prove the properties for all vertices of G and assume that the implicit edges $\{a_i, v_\infty\}$ are oriented towards v_∞ and labeled i , $i = 1, 2, 3$.

In Section 6.2 we present two methods to compute a Schnyder wood of a triconnected, planar graph. Moreover, in Theorem 6.3 we prove the following:

Theorem 3.20 (Di Battista et al., 1999, Felsner, 2001). *Every triconnected, planar graph G has a Schnyder wood that can be computed in linear time and space.*

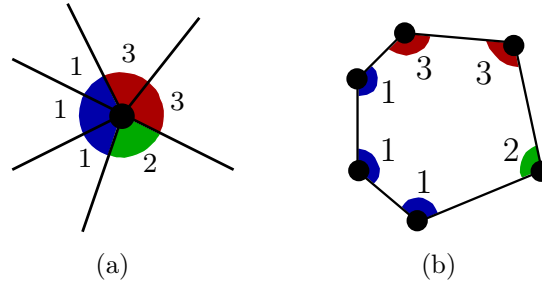


Figure 3.13: (a) Rule of vertices. (b) Rule of faces.

3.2.1 Schnyder Labelings

Note that we define Schnyder labelings on the closure G_∞ rather than on the suspension [Felsner, 2004a] or on the graph itself [Felsner, 2001]. However, the angles at v_∞ receive no labels.

Definition 3.21 (Schnyder labeling). *A Schnyder labeling of (G, v_1) is a labeling of the angles of the closure G_∞ of (G, v_1) with labels 1, 2, and 3 (alternatively with labels blue, green, and red) such that:*

1. *The two angles of the edge $\{a_i, v_\infty\}$ at a_i have labels $i + 1$ and $i - 1$ in counterclockwise order, and the angles at v_∞ have no labels.*
2. *Rule of vertices: The labels of the angles at each vertex except v_∞ form in counterclockwise order non-empty intervals of 1's, 2's, and 3's. See Figure 3.13(a).*
3. *Rule of faces: The labels of the angles at each face except the faces incident to v_∞ form in counterclockwise order non-empty intervals of 1's, 2's, and 3's. See Figure 3.13(b).*

The following lemma reveals a nice property of Schnyder labelings. Further, it is used to show that Schnyder woods and Schnyder labelings are in one-to-one correspondence.

Lemma 3.22 (Felsner, 2001). *Let G_∞ be the closure of a triconnected, planar graph G together with a Schnyder labeling (G, v_1) . The four angles of each edge of G contain all three labels 1, 2, and 3. Moreover, each edge is of one of the two edge types shown in Figure 3.14(a).*

Proof. We delete the three edges $\{a_i, v_\infty\}$, $i = 1, 2, 3$, and distribute the two labels of the edges $\{a_i, v_\infty\}$ at a_i , $i = 1, 2, 3$, to the two exterior edges of G of this angle. Therefore, we need to prove the lemma only for the angles and edges of G .

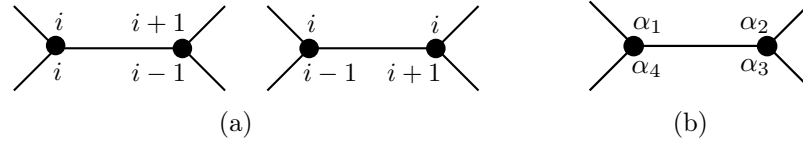


Figure 3.14: (a) Edge types in a Schnyder labeling. (b) Illustration of the proof of Lemma 3.22.

Let n , m , and f denote the number of vertices, edges, and faces of G . By Definition 3.21 the sum of the edges incident to the vertex whose angles have distinct labels at each vertex is three except for the three vertices a_i , $i = 1, 2, 3$, where it is two. The sum of the different labels of the boundary edges of each inner face of G equals also three. Then, by Euler's formula (Theorem 1.3), the sum S of different labels at vertices and faces is:

$$S = 3(n - 3) + 2 \cdot 3 + 3(f - 1) = 3n + 3f - 6 = 3m$$

The same number S can be obtained by counting the changes of labels around the edges. Hence, the average contribution of each edge of G is three.

Let $\alpha_1, \alpha_2, \alpha_3, \alpha_4$ be the four angles of an edge in clockwise order as shown in Figure 3.14(b). Define $\varepsilon_1, \varepsilon_2, \varepsilon_3, \varepsilon_4$ such that

$$\begin{aligned} \alpha_1 &= \alpha_4 + \varepsilon_4 \\ \alpha_2 &= \alpha_1 + \varepsilon_1 \\ \alpha_3 &= \alpha_2 + \varepsilon_2 \\ \alpha_4 &= \alpha_3 + \varepsilon_3 \end{aligned}$$

By Properties 3.21(2) and 3.21(3), $\varepsilon_j \in \{0, 1\}$, $j = 1, 2, 3, 4$. Also, $\sum_{j=1}^4 \varepsilon_j = 0 \pmod 3$. Therefore, either $\sum_{j=1}^4 \varepsilon_j = 0$ or $\sum_{j=1}^4 \varepsilon_j = 3$. Remember that the average contribution of the edges of G to S is 3. Rotational symmetry then leads to the two cases shown in Figure 3.14(a). \square

The next corollary directly follows from Definition 3.21 and Lemma 3.22.

Corollary 3.23 (Felsner, 2001). *In a Schnyder labeling all interior angles of G at the special vertex a_i are labeled i , $i = 1, 2, 3$.*

3.2.2 Bijection

We use the construction depicted in Figure 3.15 to construct Schnyder woods from Schnyder labelings and vice versa.

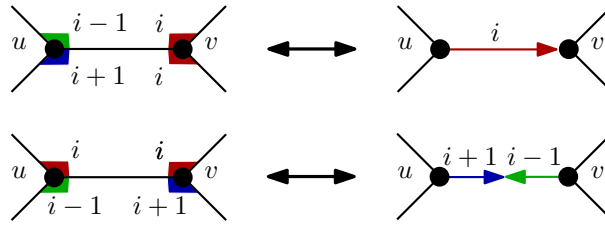


Figure 3.15: Labeling and orientation of an edge according to its angular labels and vice versa.

From Schnyder labelings to Schnyder woods. If an edge $\{u, v\}$ in a Schnyder labeling has different angular labels i and j at vertex u , then direct the edge from u to v in the third label k . Note that this can yield bi-oriented edges.

From Schnyder woods to Schnyder labelings. If an edge (u, v) is labeled i in a Schnyder wood, then label both angles at v with label i , the angle at u to the left of (u, v) with $i - 1$, and the angle at u to the right of (u, v) with $i + 1$. If an edge $\{u, v\}$ is bi-oriented such that (u, v) is labeled $i + 1$ and (v, u) is labeled $i - 1$ in a Schnyder wood, then label the angle at u to the right of (u, v) with $i - 1$, and the angle at u to the left of (u, v) with i as well as label the angle at v to the right of (v, u) with i , and the angle at v to the left of (v, u) with $i + 1$. The angles of the three edges $\{a_i, v_\infty\}$ at v_∞ are not labeled.

Theorem 3.24 (Felsner, 2003). *The correspondence stated above is a bijection between Schnyder labelings and Schnyder woods.*

Proof. We show that the two constructions stated above have the desired properties. It is obvious that they are inverse to each other.

From Schnyder labelings to Schnyder woods. Assume we have given a Schnyder labeling and perform the construction stated above to define orientations and labels of the edges. We have to show that all four properties of Definition 3.19 are fulfilled. By Lemma 3.22, Property 3.19(1) is satisfied. Property 3.21(1) directly corresponds to Property 3.19(2) as well as Property 3.21(2) corresponds to Property 3.19(3). To show that Property 3.19(4) is also true, we assume that there exists an inner face whose boundary is a directed cycle. But then the labels of all interior angles would be the same which contradicts Property 3.21(3). Thus, the construction yields indeed a Schnyder wood.

From Schnyder woods to Schnyder labelings. Now, we have given a Schnyder wood and perform the construction stated above to define angular labels. We

have to show that all three properties of Definition 3.21 are fulfilled. Again, Property 3.19(2) corresponds to Property 3.21(1) as well as Property 3.19(3) corresponds to Property 3.21(2). It remains to show that also Property 3.21(3) holds.

We use a similar technique as in the proof of Lemma 3.22 and count the changes of labels at the vertices, edges, and faces. As usual, let n , m , and f denote the number of vertices, edges, and faces of G . At every vertex, there are three label changes according to Property 3.19(3). Thus, the contribution is $3n$. Each of the three edges $\{a_i, v_\infty\}$ contributes two, the edges of G contribute three. Let F be a face of G and let $\deg(F)$ be the sum of label changes around F . Processing the angles of an inner face in counterclockwise direction, an angle labeled i is either followed by an angle again labeled i or by an angle labeled $i + 1$. Thus, F is a multiple of 3. By Property 3.19(4), $\deg(F) \neq 0$. The outer face of G has a label change at each edge $\{a_i, v_\infty\}$, $i = 1, 2, 3$. Hence, $\deg(F) = 3$.

Then, by Euler's formula (Theorem 1.3):

$$\begin{aligned} 3n + \sum_F \deg(F) &= 3m + 3 \cdot 2 \\ 3n - 3m + \sum_F \deg(F) &= 6 \\ \sum_F \deg(F) &= 3f \end{aligned}$$

This is only possible, if $\deg(F) = 3$ for every face F of G and, thus, Property 3.21(3) follows. \square

We point out that some of the previous results and other equivalent notations are summarized in [Miura, Azuma, and Nishizeki \[2005\]](#).

3.2.3 Properties

Let G be a triconnected, planar graph together with a Schnyder wood of (G, v_1) . Let T_i denote the oriented subgraph of G induced by the edges having label i , and let T_i^{-1} be the graph that is obtained by reverting all edges of T_i , $i = 1, 2, 3$. For each interior vertex $v \in G$, let $P_i(v)$ denote the path $\langle v, \dots, a_i \rangle$ whose edges are in T_i , $i = 1, 2, 3$. This path is unique since every interior vertex has outdegree one in T_i .

Lemma 3.25 ([Felsner, 2001](#)). *For $i = 1, 2, 3$, the directed graph $D_i = T_i \cup T_{i+1}^{-1} \cup T_{i-1}^{-1}$ is acyclic.*

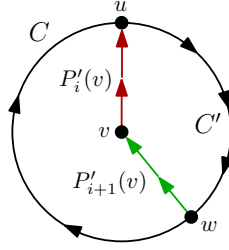


Figure 3.16: Illustration of the proof of Lemma 3.25.

Proof. Let C be a clockwise cycle enclosing the minimum number of faces. We show that C is already a face. An illustration of the proof is depicted in Figure 3.16. Assume for a contradiction, there exists a vertex v inside C . Then, $P_i(v)$ and C have a common vertex u . The same holds for $P_{i+1}(v)$. Let this common vertex be w . Let $P'_i(v)$ be the path from v to u in $P_i(v)$ and let $P'_{i+1}(v)$ be the path from v to w in $P_{i+1}(v)$ such that the direction of all edges is reversed. This means that $P'_{i+1}(v)$ is a path from w to v . Let C' be the path on C from u to w in clockwise direction. Then, $P'_i(v) \cup P'_{i+1}(v) \cup C'$ is a cycle containing less faces than C . The same argumentation holds for $P_{i-1}(v)$ and also for counterclockwise cycles. Also, C contains no chordal edge since this would easily lead again to a cycle enclosing less faces than C . Therefore, C is a face.

If the traversal of a face is in counterclockwise and in clockwise direction, respectively, then no angle of the face has label $i + 1$ and $i - 1$, respectively. This is a contradiction to Property 3.21(3). \square

From Lemma 3.25 we get that a Schnyder wood consists of three trees. More precisely:

Corollary 3.26 (Felsner, 2001). *For $i = 1, 2, 3$, T_i is a directed tree rooted at v_∞ in G_∞ and rooted at a_i in G , respectively.*

Moreover, also the next lemma follows from Lemma 3.25.

Lemma 3.27 (Di Battista et al., 1999). *For each $v \in V$, the paths $P_1(v)$, $P_2(v)$, and $P_3(v)$ have only vertex v in common.*

Let v be an interior vertex of G . By Lemma 3.27, $P_1(v)$, $P_2(v)$, and $P_3(v)$ divide G into three regions $R_1^O(v)$, $R_2^O(v)$, and $R_3^O(v)$, where $R_i^O(v)$ denotes the region bounded by $P_{i-1}(v)$ and $P_{i+1}(v)$. If the two paths $P_{i-1}(v)$ and $P_{i+1}(v)$ are included, we denote the regions by $R_i(v)$, $i = 1, 2, 3$. This is illustrated in Figure 3.17(a).

Lemma 3.28 (Felsner, 2001). *Let u and v be interior vertices. If $u \in R_i(v)$, then $R_i(u) \subseteq R_i(v)$. If $u \in R_i^O(v)$, then $R_i(u) \subset R_i(v)$.*

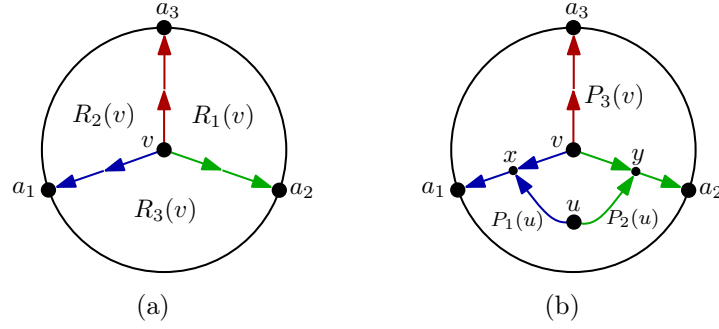


Figure 3.17: (a) Three regions of a vertex v . (b) Illustration of Lemma 3.28.

Proof. Consider the case $i = 3$. This situation is illustrated in Figure 3.17(b). The argumentation for $i = 1, 2$ is symmetric. Let v be an interior vertex of G and assume $u \in R_3^O(v)$. Let x be the first vertex of $P_1(u)$ that is also on $P_1(v) \cup P_2(v)$. By Property 3.19(3), x is on $P_1(v)$. Similarly, let y be the first vertex of $P_2(u)$ that is also on $P_1(v) \cup P_2(v)$. Then, y is on $P_2(v)$. Thus, $R_3(u) \subset R_3(v)$.

Assume now that $u \in R_3(v) \setminus R_3^O(v)$ and that u is on $P_1(v)$. The argumentation for u on $P_2(v)$ is again symmetric. If the outgoing edge of u with label 2 is different from the incoming edge with label 1, then again $R_3(u) \subset R_3(v)$. Otherwise, let u' be the other endvertex of the bi-oriented edge. Then, $R_3(u) = R_3(u')$. If there is a bi-oriented path from u to v such that the edges on $\langle u, u', \dots, v \rangle$ are labeled 2 and the edges on $\langle v, \dots, u', u \rangle$ are labeled 1, then $R_3(u) = R_3(v)$. However, it always holds that $R_3(u) \subseteq R_3(v)$. \square

From this lemma we get some useful properties about the inclusions of regions:

- Let $e = \{u, v\}$. If $\text{label}(u, v) = i$ and e is a uni-directed edge, then $R_i(u) \subset R_i(v)$, $R_{i-1}(u) \supset R_{i-1}(v)$, and $R_{i+1}(u) \supset R_{i+1}(v)$.
- Let $e = \{u, v\}$. If $\text{label}(u, v) = i$ and $\text{label}(v, u) = i - 1$, then $R_{i+1}(u) = R_{i+1}(v)$, $R_i(u) \subset R_i(v)$, and $R_{i-1}(u) \supset R_{i-1}(v)$.

The regions of a vertex can be used to assign coordinates to the vertices. In more detail, in Section 6.3.1 we will assign coordinates to the vertices that count triangles and vertices, respectively. This assignment will lead to a barycentric representation of the graph.

Di Battista et al. [1999] use notations similar to the regions of a vertex to devise data structures that support output-sensitive 3-path queries.

Next, we mention some more interesting properties that help to build an understanding of Schnyder woods.

Lemma 3.29 (Di Battista et al., 1999). *An inner face f of G can be decomposed into six clockwise consecutive paths $e_{31}, P_{21}, e_{23}, P_{13}, e_{12}, P_{32}$, where e_{ij} consists of exactly one edge that is either bi-oriented and labeled i in clockwise direction and labeled j in counterclockwise direction around f , or it is uni-directed and labeled i in clockwise direction around f , or it is uni-directed and labeled j in counterclockwise direction around f , and P_{ij} consists of a possibly empty sequence of edges with label i in clockwise and label j in counterclockwise direction around f . See Figure 3.18.*

Proof. Consider the most general case where no vertex a_1, a_2, a_3 belongs to f . By Properties 3.19(1) and 3.19(3), each vertex of f is incident to an outgoing edge that does not belong to f . Also, for $i = 1, 2, 3$ there exists a vertex of f whose i -labeled outgoing edge does not belong to f . Otherwise, there would exist an i -labeled cycle that contradicts Property 3.19(4) or the two directions of a bi-oriented edge would have the same label that contradicts Property 3.19(1).

We prove that for $i = 1, 2, 3$ there exists at least one vertex $v \in f$ such that $f \subseteq R_i(v)$. Consider the case $i = 3$. The argumentation for $i = 1, 2$ is symmetric. Let $\langle u, v, w \rangle$ be a path on f in clockwise direction.

There are three different cases (see Figure 3.19). Namely, the edges around v are in the following circular clockwise order:

1. The edge $\{v, u\}$, the outgoing edge with label 1, the outgoing edge with label 3, the outgoing edge with label 2, and the edge $\{v, w\}$. Possibly $\{v, u\}$ coincides with the outgoing edge with label 1 and $\{v, w\}$ coincides with the outgoing edge with label 2. Then, $f \subseteq R_3(v)$. See Figure 3.19(a).
2. The edge $\{v, u\}$, the outgoing edge with label 2, the outgoing edge with label 1, the outgoing edge with label 3, and $\{v, w\}$. Possibly $\{v, u\}$ coincides with the outgoing edge with label 2. Then, $f \not\subseteq R_3(v)$. However, by Property 3.19(3) $\{w, v\}$ is an outgoing edge with label 2 for w , followed in circular clockwise order around w by an outgoing edge with label 3, and an outgoing edge with label 1. Then, $f \subseteq R_3(w)$. See Figure 3.19(b).
3. The edge $\{v, u\}$, the outgoing edge with label 3, the outgoing edge with label 2, the outgoing edge with label 1, and $\{v, w\}$. Possibly $\{v, w\}$ coincides with the outgoing edge with label 1. Then, $f \not\subseteq R_3(v)$. However, again by Property 3.19(3), $\{u, v\}$ is an outgoing edge with label 2 for u , followed in circular clockwise order around u by an outgoing edge with label 1, and an outgoing edge with label 3. Then, $f \subseteq R_3(u)$. See Figure 3.19(c).

Now, we prove the claim for e_{31}, P_{21}, e_{23} by making use of the insights gained above. We remark that if $f \subseteq R_i(v)$, then $f \not\subseteq R_j(v)$, $i, j = 1, 2, 3$, $i \neq j$.

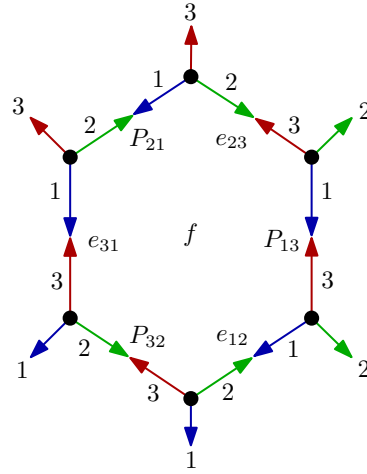


Figure 3.18: Labeling and orientation of the edges of an inner face.

1. Let v be the only vertex of f such that $f \subseteq R_3(v)$. The outgoing edge of v with label 1 either follows $\{v, u\}$ in circular clockwise order around v or it coincides with $\{v, u\}$. In the first case, by Property 3.19(3), $\{u, v\}$ is an outgoing edge of u with label 3, and in the latter one, by Property 3.19(3), $\{u, v\}$ might be bi-oriented and also an outgoing edge of u with label 3. However, in both cases $e_{31} = \{u, v\}$ fulfills the requirements.

The same argumentation holds for e_{23} . Note that P_{21} might be empty.

2. Let v_1, \dots, v_k be vertices of f such that $f \subseteq R_3(v_i)$, $i = 1, \dots, k$. By the proof of Lemma 3.28, we know that all vertices v_1, \dots, v_k are consecutive on f and that $R_3(v_1) = \dots = R_3(v_k)$. So assume that $\langle u, v_1, \dots, v_k, w \rangle$ is a path on f in clockwise direction. Then, $\{v_i, v_{i+1}\}$ is an outgoing edge with label 2 for v_i and an outgoing edge with label 1 for v_{i+1} , $i = 1, \dots, k - 1$. Thus, $P_{21} = \langle v_1, \dots, v_k \rangle$, $e_{31} = \{u, v\}$, and $e_{23} = \{v, w\}$.

The proof for e_{23}, P_{13}, e_{12} and e_{12}, P_{32}, e_{31} is analogous. □

Lemma 3.30 (Di Battista et al., 1999). *Every Schnyder wood of $G = (V, E)$ has $3n - m - 3$ bi-oriented edges, where $|V| = n$ and $|E| = m$.*

Proof. Since the edges $\{a_i, v_\infty\}$ are uni-directed, we only consider G instead of G_∞ . Every triconnected, planar graph has at most $3n - 6$ edges (Theorem 1.4) and every tree with n vertices has $n - 1$ edges (Lemma 1.2). Thus, the total number of possibly bi-oriented edges is $3(n - 1) > m$. From Property 3.19(1) follows that $3n - 3 - m$ edges are bi-oriented. □

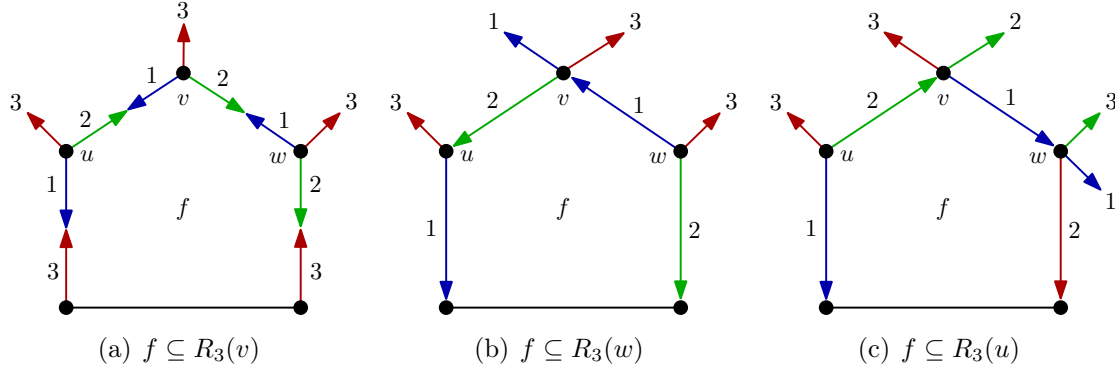


Figure 3.19: Illustration of the proof of Lemma 3.29.

3.3 Characterization of Planar Graphs

We are now ready to prove Schnyder's theorem that was already stated in Section 1.6.2 (Theorem 1.28). We follow the proof of Felsner [2004a].

Theorem 3.31 (Schnyder, 1989). *A graph is planar if and only if the dimension of its incidence order is at most three.*

Proof. We show both directions of the theorem.

G planar $\Rightarrow \dim(G) \leq 3$ Assume that $G = (V, E)$ is a triangular graph (we remark that the dimension is monotone) and consider a Schnyder wood of G . Let T_1 , T_2 , and T_3 be the three trees of the Schnyder wood according to Lemma 3.10. Since a Schnyder wood of a triangular graph has no bi-oriented edges, $R_i(u) \subset R_i(v)$ for every $u \in R_i(v)$. This order induces an order Q_i on the vertices, $i = 1, 2, 3$. In more detail, let $u \prec v$ in Q_i if and only if $R_i(u) \subset R_i(v)$, for $i = 1, 2, 3$. Then, for every edge $e = \{u, v\} \in E$ and every vertex $w \in V$ that is not incident to e , the edge e is in one of the regions $R_i(w)$, $i = 1, 2, 3$. Thus, $u \prec w$ and $v \prec w$ in Q_i .

Choosing any linear extension L_i of Q_i produces a realizer of G , for $i = 1, 2, 3$.

$\dim(G) \leq 3 \Rightarrow G$ planar We show the contraposition by contradiction. Suppose that G is non-planar and has $\dim(G) \leq 3$. Let $\{L_1, L_2, L_3\}$ be a realizer of G and let v_i denote the position of vertex v in L_i , $i = 1, 2, 3$.

For an edge $e = \{u, v\}$, let $e_i = \max(u_i, v_i)$. We define an embedding of G in \mathbb{R}^3 where the scalars s_i are specified later, for $i = 1, 2, 3$.

$$\begin{aligned}\phi: G = (V, E) &\rightarrow \mathbb{R}^3 \\ v \in V &\mapsto (s_1 v_1, s_2 v_2, s_3 v_3) \\ e \in E &\mapsto (s_1(e_1 + \frac{1}{2}), s_2(e_2 + \frac{1}{2}), s_3(e_3 + \frac{1}{2}))\end{aligned}$$

Then, $\phi(v)_i < \phi(e)_i$ for $i = 1, 2, 3$ if and only if $v \in e$ (by Definition 1.27). (\star)

Now we adjust the scalars s_i such that under the orthogonal projection π to the plane all points in $\phi(V \cup E)$ are projected to distinct points and these points are in general position, i. e., no three points are collinear.

Draw G in the plane by joining $\pi(\phi(v))$ and $\pi(\phi(e))$ with a straight-line segment whenever $v \in e$. Assume that G has no planar representation. Then, there are two segments $[\pi(\phi(v)), \pi(\phi(e))]$ and $[\pi(\phi(u)), \pi(\phi(e'))]$ that cross each other with $v \notin e'$ and $u \notin e$. Let p the point where they cross each other. A ray starting at p and leaving the plane orthogonally meets $[\pi(\phi(v)), \pi(\phi(e))]$ in \mathbb{R}^3 at the point x not later than it meets $[\pi(\phi(u)), \pi(\phi(e'))]$ at the point y . Consider the path formed by the straight segments from $\phi(v)$ to x to y to $\phi(e')$. This path is increasing in each coordinate, hence $v \in e'$ by property (\star) that is a contradiction.

Note that this part is also proved by Babai and Duffus [1981]. \square

3.4 Duality

Di Battista et al. [1999] show that a Schnyder wood of a triconnected, planar graph (G, v_1) induces a Schnyder wood of the dual graph (G_∞^*, v_1^*) , where v_1^* is the dual vertex of the face bounded by v_2, v_n, v_∞ , using the properties of Lemma 3.28 and 3.29. Felsner [2004b] shows that the Schnyder woods of (G, v_1) are in one-to-one correspondence with the Schnyder woods of the dual graph (G_∞^*, v_1^*) and with the α_0 -orientations of the primal dual superimposition G^\times that we define later. To prove the bijection of Schnyder woods and Schnyder woods of the dual, Felsner makes use of the fact that Schnyder woods are also in one-to-one correspondence to Schnyder labelings. Given only the orientations of a Schnyder wood of a triconnected, planar graph (G, v_1) , the labels cannot be reconstructed from the underlying orientation in contrast to the case of triangular graphs. An example is shown in Figure 3.20.

Definition 3.32 (dual of the closure). *Let G_∞ be the closure of (G, v_1) and let G_∞^* be its dual such that v_1^* is the dual vertex of the face with boundary v_2, v_n, v_∞ ; v_2^* is the dual vertex of the face with boundary v_1, v_n, v_∞ ; and v_n^* is the dual vertex of the*

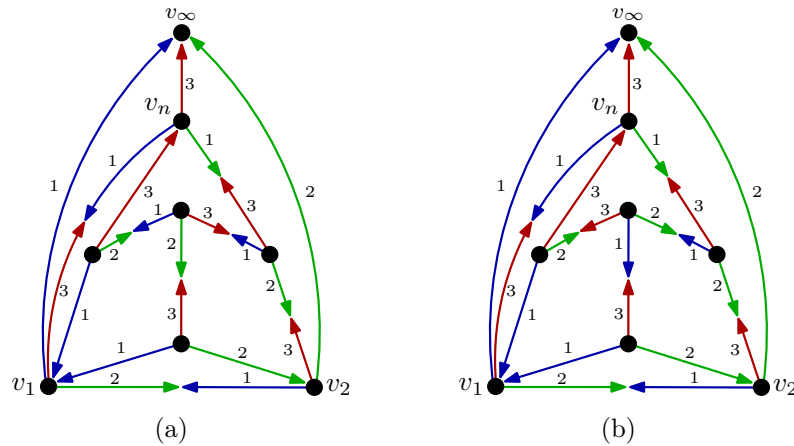


Figure 3.20: Two different Schnyder woods with the same underlying orientation.

face with boundary v_1, v_2, v_∞ . Then, the dual of the closure G_∞^* is the dual graph of G_∞ together with the vertex v_∞ and the three edges $\{v_1^*, v_\infty\}$, $\{v_2^*, v_\infty\}$, and $\{v_n^*, v_\infty\}$.

Definition 3.33 (primal dual superimposition). *The primal dual superimposition $G^\times = (V^\times, E^\times)$ of (G, v_1) is constructed as follows: Superimpose the closure G_∞ of (G, v_1) with its dual G_∞^* such that v_∞ of G_∞ is identified with v_∞ of G_∞^* and such that exactly every edge of G_∞ crosses with its dual edge of G_∞^* and insert edge-vertices at those crossings.*

Theorem 3.34 (Felsner, 2004b). *Let G_∞ be the closure of a triconnected, planar graph G . Then, there exists a bijection between the Schnyder woods of G_∞ and the Schnyder woods of the dual of the closure G_∞^* .*

Proof. By Theorem 3.24 it suffices to show the statement for Schnyder labelings. However, for Schnyder labelings there is an obvious one-to-one correspondence between a graph and its dual. Let G^\times be the primal dual superimposition of G . Let f be a face in G^\times that is not incident to v_∞ . If the angle of f incident to the primal vertex is labeled i in G , then the angle of f incident to the dual vertex is also labeled i , for $i = 1, 2, 3$. Hence, any Schnyder labeling of G induces a Schnyder labeling of G^* and vice versa. Clearly, the decomposition of both yields the identity. \square

An example of a Schnyder wood of G_∞ and its corresponding Schnyder wood of G_∞^* is shown Figure 3.21. The four edges incident to the edge-vertices have the pattern indicated in Figure 3.22.

As mentioned at the beginning of Section 3.1.4, a triangular graph has a unique Schnyder wood if and only if it is a stacked triangulation. Zickfeld [2007] presents

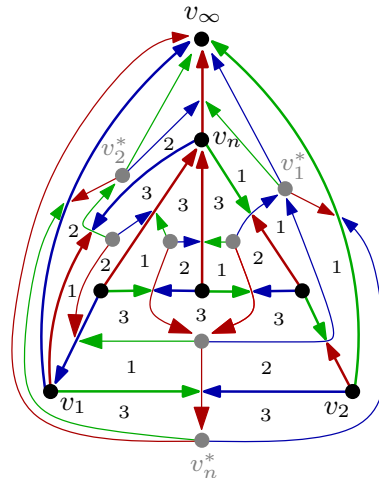


Figure 3.21: A graph and its dual graph with both Schnyder wood and Schnyder labeling.

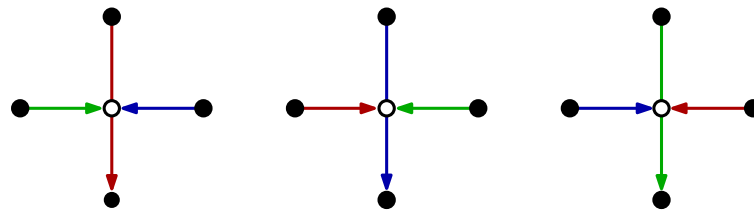


Figure 3.22: Different scenarios of the incident edges of an edge-vertex. Black vertices correspond to vertices of G , white vertices correspond to edge-vertices.

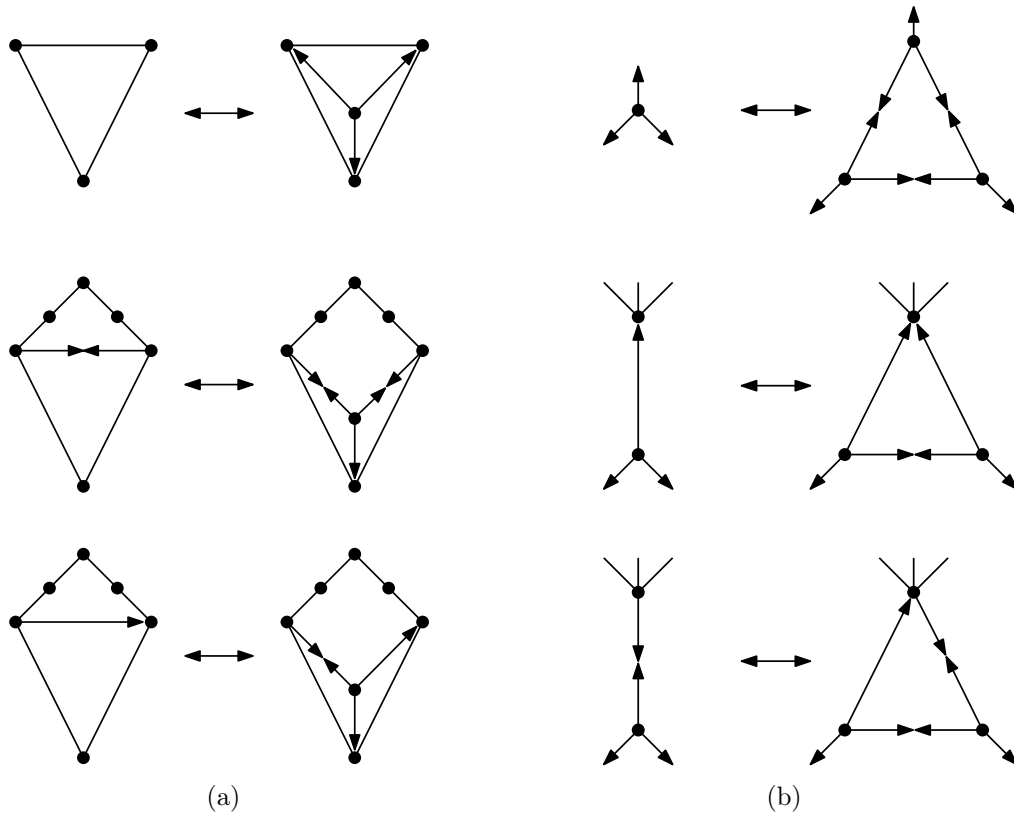


Figure 3.23: Every graph that has a unique Schnyder wood can be constructed by using the three operations in (a), and their duals in (b).

a construction how to obtain a triconnected, planar graph with a unique Schnyder wood.

Theorem 3.35 (Zickfeld, 2007). *All triconnected, planar graphs with a unique Schnyder wood can be constructed from the unique Schnyder wood on the triangle by the six operations shown in Figure 3.23.*

3.5 Lattice Structure

Ossona de Mendez [1994] and Brehm [2000] independently show that the set of Schnyder labelings of a planar triangulation has the structure of a distributive lattice. Felsner [2004b] extends this result to triconnected, planar graphs that we briefly review in this section.

Definition 3.36 (α -orientation). *Let $G = (V, E)$ be a plane graph and let $\alpha : V \rightarrow \mathbb{N}$ be a function such that each vertex $v \in V$ has exactly $\alpha(v)$ outgoing edges. An orientation of the edges E that fulfills this property is called α -orientation. We call α feasible if an α -orientation of G exists.*

The connection to Section 3.1.4, in that we investigated cycles of triangular graphs, is the following one: Let X be an α -orientation of a plane graph G and let C be a directed cycle in X . Let X^C be the orientation that is obtained by reversing all edges of C . Then, X^C is also an α -orientation of G . Since G is planarly embedded, we can distinguish between clockwise and counterclockwise cycles. If C is a clockwise cycle of X , then $X^C \prec X$. The transitive closure of \prec is the order relation which makes the set of α -orientations to a distributive lattice.

Theorem 3.37 (Felsner, 2004b, Ossona de Mendez, 1994). *Let G be a plane graph and $\alpha : V \rightarrow \mathbb{N}$ feasible. The set of α -orientations of G carries an order relation which is a distributive lattice.*

Let us come back to Schnyder woods. A pair of corresponding Schnyder woods of G_∞ and G_∞^* induces an α -orientation of G^\times . Moreover, [Felsner, 2004b] shows that this is an α_0 -orientation that is defined as follows:

Definition 3.38 (α_0 -orientation). *Let $\alpha_0 : V^\times \rightarrow \mathbb{N}$ be a function such that $\alpha_0(v) = 3$ for all primal and dual vertices v , $\alpha_0(v_e) = 1$ for all edge-vertices v_e , and $\alpha_0(v_\infty) = 0$. An orientation of the elements of E^\times is called α_0 -orientation if each vertex $v \in V^\times$ has exactly $\alpha_0(v)$ outgoing edges.*

Theorem 3.39 (Felsner, 2004b). *The Schnyder woods of (G, v_1) are in bijection with the α_0 -orientations of G^\times .*

The next lemma is not only the basis of the proof of Theorem 3.39, it also gives insights how to assign labels to every edge of an α_0 -orientation of G^\times in order to obtain a Schnyder wood.

A straight path of an edge e in G^\times (see See Figure 3.24 for an illustration) is defined as follows:

- If e is the incoming or outgoing edge of an edge-vertex, continue with the other half-edge of the underlying primal or dual edge. This half-edge might be an incoming or outgoing edge of the edge-vertex.
- If e is the incoming edge of a primal or dual vertex, continue with the opposite outgoing edge.

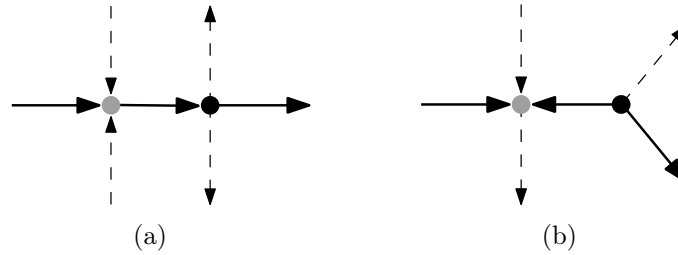


Figure 3.24: Illustration of the straight path (solid edges): (a) Straight path has an incoming edge of the gray edge-vertex, and leaves to the opposite; then enters the black primal or dual vertex and leaves again to the opposite. (b) Straight path has an incoming edge of the gray edge-vertex, and leaves to the opposite; then it is an outgoing edge of the black primal or dual vertex and leaves to the right.

- If e is the outgoing edge of a primal or dual vertex, then the edge-vertex for which e is an incoming edge has one outgoing edge. If this edge is to the right (left) of the straight path, then continue at the primal or dual vertex also with the right (left) outgoing edge.

Lemma 3.40 (Felsner, 2004b). *Let X be an α_0 -orientation of G^\times and $e \in X$ be a directed edge. The straight path whose first edge is e leads to v_∞ where it ends. Further, if x is a primal or dual vertex and p and q are two straight paths leaving x on different edges, then p and q meet only at v_∞ .*

With the directed edge e consider the straight path that is ending at v_∞ . The last vertex on the straight path before v_∞ is either one of v_1, v_2, v_n , then it is a primal edge, or one of v_1^*, v_2^*, v_n^* , then it is a dual edge. All edges on the straight path receive the label of this vertex. More precisely, if (a_i, v_∞) is the last edge, then all edges on the path are labeled i , $i = 1, 2, 3$. The same holds also for the dual vertices, where we denote $v_1^* = a_1^*$, $v_2^* = a_2^*$, $v_n^* = a_3^*$. Felsner [2004b] proves that this mapping yields a pair of Schnyder woods.

Combining Theorems 3.39 and 3.37 leads to the final result of this section:

Theorem 3.41 (Felsner, 2004b). *The set of Schnyder woods of a primal dual superimposition forms a distributive lattice.*

Since the set of all α_0 -orientations of G^\times forms a distributive lattice, there exists a unique α_0 -orientation without clockwise cycles of the primal dual superimposition G^\times . This is the *minimal α_0 -orientation*. An α_0 -orientation can be made minimal by iteratively reversing clockwise cycles. A *minimal Schnyder wood* is a Schnyder wood that is associated with the minimal α_0 -orientation.

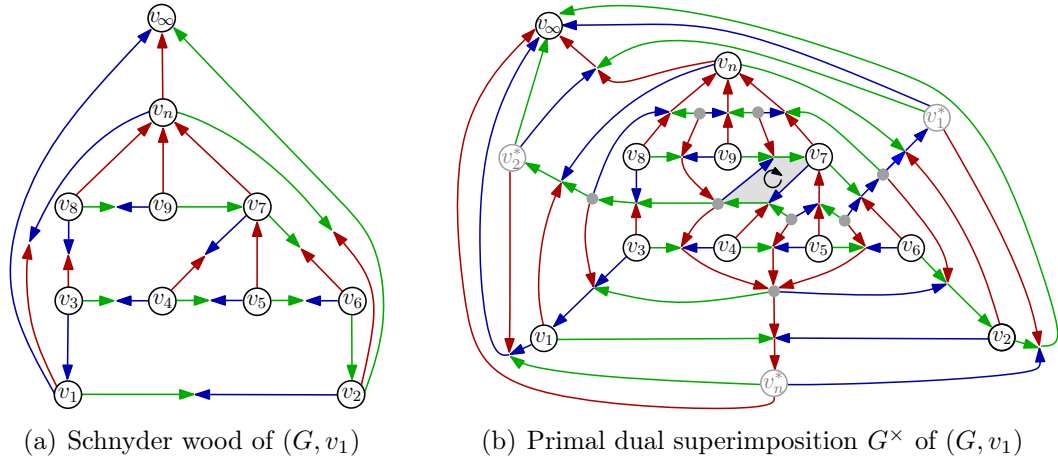


Figure 3.25: Schnyder wood associated with the leftist canonical ordering; the corresponding α_0 -orientation contains a clockwise cycle.

While the minimal Schnyder wood of a triangular graph is the one associated with the leftist canonical ordering [Brehm, 2000], this observation does not hold for triconnected, planar graphs any more as shown in Figure 3.25. Moreover, the minimal Schnyder wood cannot always be reconstructed from a canonical ordering. This is also illustrated in Figure 3.25. The graph has one canonical ordering and at least two different Schnyder woods. Remember that Theorem 3.35 states all triconnected, planar graphs that have a unique Schnyder wood.

3.6 Path Partition

Canonical orderings do not seem to be the right concept to construct a bijection to Schnyder woods since a graph can have more Schnyder woods than canonical orderings. In Section 3.1.3, we constructed a bijection between the equivalence classes of canonical orderings and the Schnyder woods of a triangular graph. In this section, we generalize the definition of a canonical ordering for triconnected, planar graphs to ordered path partitions and show that certain equivalence classes of ordered path partitions are in bijection with Schnyder woods. Further, we show that the leftist ordered path partition corresponds to the minimal Schnyder wood.

Definition 3.42 (ordered path partition). *Let $P_0 = \langle v_1, v_2 \rangle$, let $P_s = \langle v_n \rangle$, and let V_k and C_k be defined as in Definition 2.7. An ordered partition $\Pi = (P_0, \dots, P_s)$ of V into paths is called ordered path partition of (G, v_1) if for each $k = 1, \dots, s - 1$:*

1. C_k is a simple cycle.

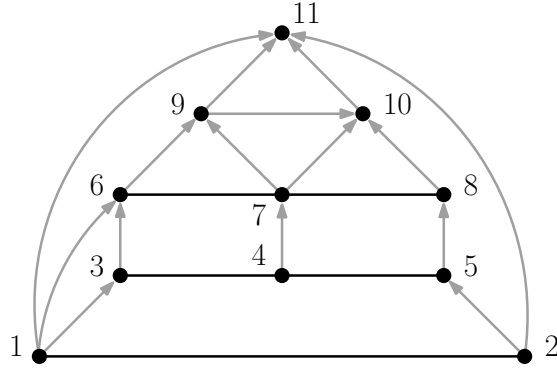


Figure 3.26: Ordered path partition and induced orientation. $P_0 = \langle 1, 2 \rangle$, $P_1 = \langle 3, 4, 5 \rangle$, $P_2 = \langle 6, 7, 8 \rangle$, $P_3 = \langle 9 \rangle$, $P_4 = \langle 10 \rangle$, $P_5 = \langle 11 \rangle$.

2. Each vertex in P_k has a neighbor in $V \setminus V_k$.
3. Each vertex on C_k has at most one neighbor on P_{k+1} .

An ordered path partition $\Pi = (P_0, \dots, P_s)$ of (G, v_1) induces an *orientation* on the edges of G that are not in the paths P_0, \dots, P_s . More precisely, let $e = \{u_1, u_2\}$ be an edge of G such that there are $k_1 < k_2$ with $u_i \in P_{k_i}$, $i = 1, 2$. Then, e is an *outgoing edge* of u_1 and an *incoming edge* of u_2 .

An example of an ordered path partition and the induced orientation is illustrated in Figure 3.26.

Definition 3.43 (equivalence of ordered path partitions). *Two ordered path partitions $\Pi = (P_0, \dots, P_s)$ and $\Pi' = (P'_0, \dots, P'_s)$ are called equivalent if and only if $\{P_0, \dots, P_s\} = \{P'_0, \dots, P'_s\}$ as well as Π and Π' induce the same orientation on the edges.*

Theorem 3.44. *There is a bijection between the equivalence classes of the ordered path partitions of (G, v_1) and the Schnyder woods of (G, v_1) .*

Proof. We show how to map equivalence classes of ordered path partitions to Schnyder woods and Schnyder woods to equivalence classes of ordered path partitions such that the composition of the two maps yields the identity.

From ordered path partitions to Schnyder woods. We extend the construction of Theorem 3.12. Let $\Pi = (P_0, \dots, P_s)$ be an ordered path partition. Let (u, v) denote the directed edge from u to v and let $\text{label}(u, v) = i$ indicate that (u, v) has label i . Then, set $\text{label}(a_i, v_\infty) = i$, for $i = 1, 2, 3$, $\text{label}(a_1, a_2) = 2$ and

$\text{label}(a_2, a_1) = 1$. Let $k = 1, \dots, s$ and let $P_k = \langle z_1, \dots, z_p \rangle$ have left neighbor c_ℓ and right neighbor c_r . We label and orient the edges of P_k and between P_k and C_{k-1} as follows (see Figure 3.27):

1. $\text{label}(z_1, c_\ell) = 1$
2. $\text{label}(z_p, c_r) = 2$
3. $\text{label}(z_i, z_{i+1}) = 2$ and $\text{label}(z_{i+1}, z_i) = 1, i = 1, \dots, p - 1$
4. For all $c \in C_{k-1}$ that are incident to a vertex $z \in P_k$ but not to a vertex in $V \setminus V_k$, set $\text{label}(c, z) = 3$.

Construction yields a Schnyder wood. If the end vertices of an edge e are in the paths P_i and $P_j, i \leq j$, then e is oriented and labeled in step j . Therefore, Property 3.19(1) is true since every edge is oriented exactly once with one or two opposing directions by construction. Property 3.19(2) is obviously true.

Since every vertex is contained in exactly one path, every vertex has outdegree one in label 1 and 2. Let z be a vertex of $P_k, k < s$, and let k' be maximal such that z has a neighbor z' in $P_{k'}$. Then, $k' > k$. Therefore, z has an outgoing edge to z' with label 3. Since z has at most one neighbor in $P_{k'}$, this is the only outgoing edge of z with label 3. Also, since $k' > k$, the edge $\{z, z'\}$ appears in the adjacency list of z in the clockwise sector between the outgoing edge with label 1 and the outgoing edge with label 2. By construction, the incoming edges with label 3 appear in the clockwise sector of the outgoing edges with label 2 and 1.

Assume that z has an incoming edge $e = \{\hat{z}, z\}$ with label 1 that appears in the clockwise sector between the outgoing edges with label 1 and 3. Since $\text{label}(\hat{z}, z) = 1$, it follows that \hat{z} is the leftmost vertex of a path $P_{\hat{k}}$ with $\hat{k} > k$ and that z is the left neighbor of $P_{\hat{k}}$. Since $C_{\hat{k}}$ is a simple cycle and by the planarity of G , the assumption implies that the outgoing edge of z with label 3 is an incoming edge of $P_{\hat{k}}$ to the right of \hat{z} . By Definition 3.42, z has at most one vertex on $P_{\hat{k}}$. This is a contradiction. The same argumentation holds for the incoming edges with label 2. This completes Property 3.19(3).

We show by induction that there is no cycle in one label (Property 3.19(4)). This is for sure true for the first path $P_0 = \langle v_1, v_2 \rangle$. Assume that in G_{k-1} there is no cycle in one label and that P_k is the next path. When adding P_k , there does not exist a directed path in any label between two vertices on C_{k-1} using vertices of P_k .

Independence of representatives. All representatives have the same paths. Two ordered path partitions are only equivalent if they induce the same orientation and, therefore, induce the same Schnyder wood.

From Schnyder woods to ordered path partitions. Let be given a Schnyder wood of (G, v_1) . A path $P = \langle z_1, \dots, z_p \rangle$ of G is a *1-2-labeled path* if the edges $\{z_i, z_{i+1}\}$, $i = 1, \dots, p - 1$, are oriented from z_i to z_{i+1} with label 2, and from z_{i+1} to z_i with label 1. We define a partial order \prec on the partition of V into maximal 1-2-labeled paths. Let e be an edge between two maximal 1-2-labeled paths P and P' . Then, $P \prec P'$ if

1. e is oriented from P to P' and labeled 3 or
2. e is oriented from P' to P and labeled 1 or 2.

We will show that the transitive closure of these two conditions indeed yields a partial order. We will then show that the set of all linear extensions $\Pi = (P_0, \dots, P_s)$ of this partial order \prec defines an equivalence class of ordered path partitions. This will be the image of the given Schnyder wood.

\prec **is acyclic.** Assume that there is a sequence $Q_0 \prec \dots \prec Q_k = Q_0$ of ascending maximal 1-2-labeled paths such that the first and the last element is the same. Then there is a cycle $C = \{c_0, \dots, c_p, c_0\}$, $p > 2$, in G such that the edges $\{c_i, c_{i+1}\}$, $i = 0, \dots, p - 1$, are oriented from c_i to c_{i+1} and labeled 3 or oriented from c_{i+1} to c_i and labeled 1 or 2. Note that some edges of C may also be bi-oriented. Especially, C may contain edges of the 1-2-labeled paths. However, this contradicts Lemma 3.25.

$\Pi = (P_0, \dots, P_s)$ **is an ordered path partition.** $\langle v_1, v_2 \rangle$ is a maximal 1-2-labeled path. From each vertex there is an oriented path to v_1 and labeled 1. Hence, $P_0 = \langle v_1, v_2 \rangle$. All edges incident to v_n are labeled 3. Hence, $\langle v_n \rangle$ is a maximal 1-2-labeled path. From each vertex there is an oriented path to v_n and labeled 3. Hence, $P_s = \langle v_n \rangle$. Next, we prove by induction that C_k , $k = 1, \dots, s - 1$, is a simple cycle and that C_k , $k = 0$, consists of a single edge. This claim is certainly true for $k = 0$. For $k > 0$, let c_i be the vertex not in P_k that is incident to the edge labeled i and oriented away from P_k , $i = 1, 2$. By the definition of \prec , we have $c_1, c_2 \in V_{k-1}$. Again by the definition of \prec , the paths $P_3(u)$, u on P_k may not intersect C_{k-1} . Hence, P_k is contained in the exterior of C_{k-1} and, thus, c_1 , and c_2 are on C_{k-1} . By Lemma 3.27, it follows that $c_1 \neq c_2$. Hence, P_k has at least two neighbors on C_{k-1} . Thus, C_k is a simple cycle.

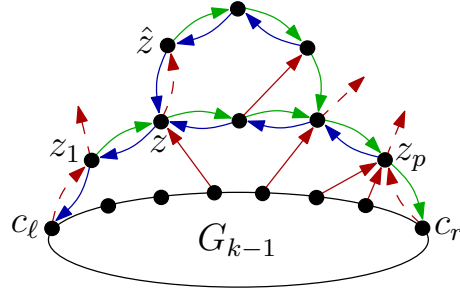


Figure 3.27: Construction of a Schnyder wood from an ordered path partition.

Let now $k = 1, \dots, s - 1$ and let u be a vertex of P_k . Then, there is an edge labeled 3 and oriented away from u . This edge is incident to a vertex of $V \setminus V_k$.

From the definition of Schnyder woods and of \prec , it follows that among the edges between C_{k-1} and P_k there are exactly two that are oriented towards C_{k-1} , one with label 1 and one with label 2. All other edges are labeled 3 and oriented towards P_k . Assume now that there is a vertex c on C_{k-1} that has two neighbors $u, u' \in P_k$. The edges $\{c, u\}$ and $\{c, u'\}$ cannot both be labeled 3. Otherwise, c has two outgoing edges with the same label. By Lemma 3.27, $\{c, u\}, \{c, u'\}$ cannot be labeled 1 and 2, respectively. So assume that $\{c, u\}$ is labeled 1 and that $\{c, u'\}$ is labeled 3. Consider the cycle C bounded by $\{c, u\}, \{c, u'\}$ and a part of P_k . By Property 3.19(3) there have to be vertices $x_i, i = 1, 2$, in the interior of C such that the edges $\{c, x_i\}$ are oriented towards x_i and labeled i . Then, on the one hand, $x_i \in V_{k-1}$ and, on the other hand, the simple cycle C_{k-1} cannot bound a region that contains c, x_1, x_2, v_1 , and v_2 , but does not intersect P_k . The case in which $\{c, u\}$ is labeled 2 is symmetric.

It is easy to see that the two constructions are inverse to each other. □

Definition 3.45 (leftist ordered path partition). *An ordered path partition P_0, \dots, P_s is called leftist if for $k = 0, \dots, s - 1$ and an ordered path partition $P'_0, \dots, P'_{s'}$ with $P_i = P'_i, i = 0, \dots, k$, the following is true. Let c_ℓ (c_r) be the left (right) neighbor of P_{k+1} and $c_{\ell'}$ ($c_{r'}$) be the left (right) neighbor of P'_{k+1} . Then, $\ell \leq \ell'$ and $r \leq r'$.*

Note that in the above definition ℓ and r can be simultaneously minimized. Assume that P'_{k+1} is contained in P_{k+1} with $\ell < \ell'$ and $r' < r$. Let z_1 be the neighbor of c_ℓ in P_{k+1} and z_p the neighbor of $c_{r'}$ in P_{k+1} . Then, the subpath $P = \langle z_1, \dots, z_p \rangle$ of P_{k+1} fulfills the properties of Definition 3.42, has the same left neighbor as P_{k+1} , and a right neighbor that is to the left of c_r . Moreover, analogously to canonical orderings, a sequence P_0, \dots, P_i of paths can be extended to an ordered path partition if and only if P_0, \dots, P_i fulfill the properties of Definition 3.42 and

$G[V \setminus (P_0 \cup \dots \cup P_i)]$ is connected. The latter is fulfilled for P since P is a subpath of P_{k+1} , $G[V \setminus (P_0 \cup \dots \cup P_{k+1})]$ is connected, and each vertex of P_{k+1} is adjacent to a vertex of $G[V \setminus (P_0 \cup \dots \cup P_{k+1})]$.

We now show that the leftist ordered path partition corresponds to the minimal Schnyder wood. The algorithm of [Fusy et al. \[2008\]](#) to compute the minimal element of an α_0 -orientation reuses the idea of the algorithm of [Kant \[1996\]](#). Let G_k and C_k be as in Definition 2.7. A vertex v on C_k is *eligible* if

1. it is incident to at least one edge in $G[V \setminus V_k]$ and
2. it is not incident to a separation face.

[Fusy et al. \[2008\]](#) iteratively eliminate the rightmost eligible vertex and its incident faces from the outer face of G^\times until the graph is shrunk to the edge $\{v_1, v_2\}$. The vertices v_1 and v_2 are considered to be blocked until only the edge $\{v_1, v_2\}$ is left. Let v be the rightmost eligible vertex that is eliminated in step $s - k + 1$. Let P_k be the path that consists of v and a maximal chain of vertices with degree two on C_k to the left of v . Then, P_k is the next path that is eliminated and $\Pi = (P_0, \dots, P_s)$ is the corresponding ordered path partition. It follows that Π is the upper rightist ordered path partition in the following sense:

Definition 3.46 (upper rightist ordered path partition). *An ordered path partition P_0, \dots, P_s of (G, v_1) is called upper rightist if for $k = 1, \dots, s$ and an ordered path partition P'_0, \dots, P'_s with $P_{s-i} = P'_{s-i}$, $i = 0, \dots, k - 1$, the following is true. Let $P_{s-k} = \langle z_1, \dots, z_p \rangle$ and let $P'_{s-k} = \langle z'_1, \dots, z'_{p'} \rangle$, then z'_1 is between v_1 and z_1 , and $z'_{p'}$ is between v_1 and z_p on the clockwise outer facial cycle C_{s-k} around G_{s-k} .*

Theorem 3.47. *The leftist ordered path partition corresponds to the minimal Schnyder wood.*

Proof. It remains to show that the upper rightist ordered path partition equals the leftist ordered path partition. Let $\Pi = (P_0, \dots, P_s)$ be the upper rightist ordered path partition, let $\Pi' = (P_0, \dots, P_{i-1}, P'_i, \dots, P'_{s-1}, P'_s)$ be the leftist ordered path partition of (G, v_1) , and assume $P_i \neq P'_i$.

If P_i is contained in P'_i or P'_i is contained in P_i , then P'_i does not fulfill the requirements of a leftist ordered path partition. Otherwise, the argumentation is the same as in Theorem 2.16. \square

Chapter 4

Triangle Contact Representation

A *contact system* \mathcal{Q} is a set of simple closed or open curves in the plane such that two curves have at most one contact point. If all curves are open, then it is called *contact system of arcs*. A *contact representation* $\mathcal{C} = \{c_v \mid v \in V\}$ of a planar graph $G = (V, E)$ is a contact system \mathcal{Q} such that two curves $c_u, c_v \in \mathcal{Q}$ are tangent to each other if and only if their corresponding vertices $u, v \in V$ are adjacent in G .

Let $G = (V, E)$ be a planar graph, let \mathcal{C} be a contact representation of G , and let \mathcal{C}^* be a contact representation of G^* . For $v \in V$, let c_v be the curve corresponding to $v \in V$. Further, let $e = \{u, v\}$ be an edge incident to two faces f and g . If the intersection of the curves c_u and c_v coincides with the intersection of the curves c_f and c_g , then $(\mathcal{C}, \mathcal{C}^*)$ is a *primal dual contact representation* of G . A *contact point* of a primal dual contact representation is either a contact point of \mathcal{C} or a contact point of \mathcal{C}^* .

The most famous theorem on contact representations is the circle packing theorem of [Koebe \[1936\]](#), [Andreev \[1970\]](#), and [Thurston \[2002\]](#) that states that every planar graph has a contact representation by circles. This is also known as the circle packing theorem. It is extended by [Brightwell and Scheinerman \[1993\]](#) to a unique primal dual contact representation by circles for triconnected graphs. An example is shown in [Figure 4.1](#). While [Brightwell and Scheinerman](#) just prove the existence of such a representation, [Mohar \[1997\]](#) gives a polynomial-time algorithm to construct it. From the theorem of [Brightwell and Scheinerman](#) one can deduce that a triconnected graph and its dual can be represented simultaneously in the plane such that primal and dual edges cross at right angles except for the edges that are incident to the vertex representing the outer face. A generalization of the circle packing theorem is proved in [Schramm \[1991\]](#).

[Sachs \[1994\]](#) reviews some famous theorems about circle representations, their connection to polyhedra, and conformal mappings. Further, he mentions different

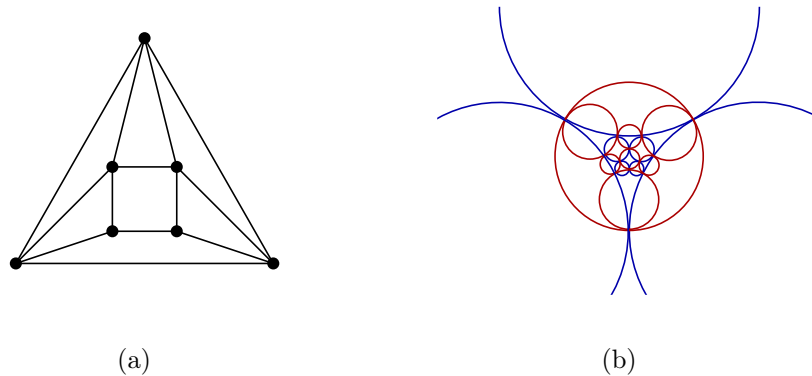


Figure 4.1: Example of a primal dual contact representation by circles. (a) Input graph. (b) Blue circles correspond to the contact representation of the primal graph, red circles correspond to the contact representation of the dual graph.

proofs and their development over the years. More about circle packings can be found in [Stephenson \[2005\]](#). Results about coin representations are also summarized in [Lovász \[2009\]](#).

A direct consequence of the circle packing theorem is Fary's theorem ([Theorem 1.26](#)). Placing vertices at the centers of the circles and drawing straight edges between neighbors, leads to a straight-line, planar drawing of the graph.

The circle packing theorem also implies that every planar graph admits a contact representation by convex polygons. As a consequence, contact representations with different curves are studied. [De Fraysseix, Ossona de Mendez, and Rosenstiehl \[1994\]](#) show that every triangular graph has a triangle contact representation and they prove that the triangles can be chosen as isosceles over a horizontal basis. Details are explained in [Section 4.1](#). If the objects of the contact system are not restricted to be simple curves, they derive that every planar graph may be represented by a contact system of T-shaped and Y-shaped objects, respectively.

The following theorem by [Schramm \[2007\]](#) is needed to prove one of the main results of this chapter, namely, that every 4-connected, planar triangulation admits a contact representation by homothetic triangles.

Theorem 4.1 ([Schramm, 2007](#)). *Let $G = (V, E)$ be a planar triangulation. For each vertex $v \in V$, let there be a convex set a_v in the plane containing more than one point. Then, there exists a (possibly degenerated) contact system in the plane $\mathcal{Q} = \{c_v \mid v \in V\}$, where each c_v is either a point or homothetic to a_v and such that G is a subgraph of the graph induced by \mathcal{Q} .*

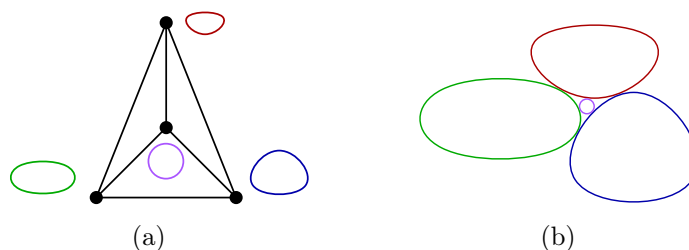


Figure 4.2: Illustration of **Schramm's** Theorem: (a) Convex sets corresponding to the vertices. (b) Contact representation of the graph of (a).

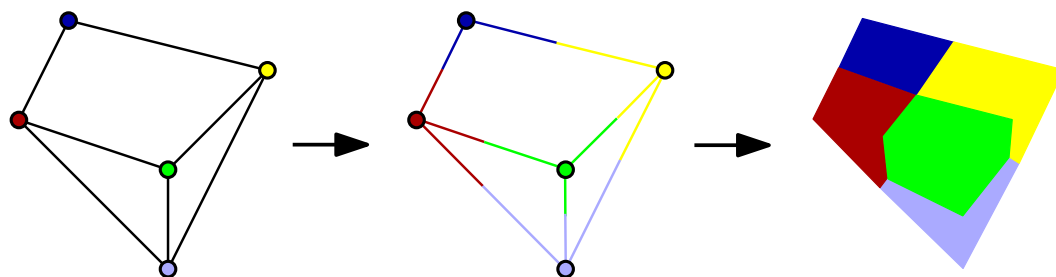


Figure 4.3: A planar graph can be transformed into a touching polygon representation.

Another concept similar to contact representations are touching representations. Vertices are represented by polygonal shapes and two vertices are adjacent if and only if the sides of the polygons touch. Every planar graph can easily be represented with touching polygons. Cut the edges into halves and adjust the faces to form polygons as shown in Figure 4.3 (compare, e. g., **Gansner, Hu, Kaufmann, and Kobourov [2010]**). Since these polygons may have many sides, it is natural to ask whether one can limit the number of sides of the polygons.

Thomassen [1984] shows that there are cubic, triconnected, planar graphs that have no touching representation by pentagons. Further, he proves that every triconnected, planar graph has a touching representation by polygons with six sides. **Gansner et al. [2010]** present a linear-time algorithm that represents every planar graph by touching hexagons.

Gansner, Hu, and Kobourov [2011] study which classes of graphs can be represented by touching triangles. They show that outerplanar graphs and subgraphs of a square or hexagonal grid have such a representation and they present linear-time algorithms for their construction.

Alam, Biedl, Felsner, Kaufmann, and Kobourov [2012] study proportional contact and touching representations. Let $G = (V, E)$ be a graph and let $\omega: V \rightarrow \mathbb{R}^+$ be a *weight function*, i. e., a function that assigns a weight to each vertex of G . Then, G

admits a *proportional contact* and *proportional touching representation*, respectively, if there exists a contact and touching representation of G , respectively, where the area of the polygon for each vertex $v \in V$ is proportional to its weight $\omega(v)$. They show that non-convex quadrilaterals are necessary and sufficient for proportional contact representations for any planar graph. Further, they give results for contact and touching representation, respectively, for special classes of graphs.

Let $\mathcal{F} = \{S_1, \dots, S_n\}$ be a family of multisets, i.e., $S_i = S_j$ is allowed even if $i \neq j$. The *intersection graph* of \mathcal{F} is the graph with vertex set \mathcal{F} and there is an edge between two vertices if and only if $S_i \cap S_j \neq \emptyset$, $i \neq j$. A graph $G = (V, E)$ is an *intersection graph* if there exists a family of multisets \mathcal{F} such that $V = \{v_1, \dots, v_n\}$, where each v_i corresponds to S_i and $E = \{\{v_i, v_j\} \mid S_i \cap S_j \neq \emptyset\}$ (compare, e.g., [McKee and McMorris \[1999\]](#)). The sets can also be derived from specific geometric configurations such as intervals, triangles, etc.

[Erdős, Goodman, and Pósa \[1966\]](#) prove that for any graph $G = (V, E)$ there exists a set S with $\frac{n^2}{4}$ elements and a family of n subsets of S such that two vertices $v_i, v_j \in V$ are joined by an edge $e \in E$ if and only if $i \neq j$ and $S_i \cap S_j \neq \emptyset$.

[Chalopin and Gonçalves \[2009\]](#) prove Scheinerman's conjecture [[Scheinerman, 1984](#)] that says that every planar graph is the intersection graph of some segments in the plane.

In 2007, Katharina Lehmann conjectures that every planar graph is an intersection graph of homothetic triangles (compare [Badent et al. \[2007\]](#)). [Gonçalves et al. \[2011\]](#) prove that this is true. In more detail, they prove that a graph is planar if and only if it has an intersection representation of homothetic triangles where no three triangles intersect in one point. More about intersection graphs can be found, e.g., in [Scheinerman \[1983, 1985a,b\]](#).

Representing vertices by geometrical objects in the plane leads also to the idea of representing vertices by d -dimensional boxes in \mathbb{R}^d . The *boxicity* of a graph G is defined as the smallest d such that G can be represented as the intersection graph of axis-parallel d -dimensional boxes in \mathbb{R}^d . In more detail, a graph has boxicity d if and only if there exists a bijection between the vertices of the graph and the set of boxes such that two boxes intersect if and only if the corresponding vertices are adjacent in G .

A graph has boxicity at most 1 if and only if it is an interval graph. In [McKee and McMorris \[1999\]](#) it is said that [Scheinerman \[1984\]](#) prove that every outerplanar graph has boxicity at most 2. A result of [Thomassen \[1986\]](#) shows that every planar graph has boxicity at most 3. [Felsner and Francis \[2011\]](#) strengthen this result by showing that the boxes can be chosen as cubes. [Roberts \[1969\]](#) shows that a graph with $2n$ vertices that is formed by removing a perfect matching from a complete

graph on $2n$ vertices has boxicity n . More about boxicity can also be found in [Felsner and Francis \[2011\]](#).

In this chapter, we first prove that every planar graph has a triangle contact representation [[de Fraysseix et al., 1994](#)]. Then, we focus on homothetic triangle contact representations and show that two terminal series-parallel digraphs and partial planar 3-trees admit a homothetic triangle contact representation [[Badent et al., 2007](#)]. We continue with a recent result of [Gonçalves et al. \[2011\]](#) who prove that every 4-connected, planar triangulation has a contact representation by homothetic triangles. We summarize this chapter by bringing these results in relation to dual graphs and Schnyder woods.

4.1 Preliminaries

A *triangle contact system* is a contact system where each curve is a closed triangle. A triangle contact system is *strict* if each *contact point of two triangles* is a contact point that is the node of exactly one triangle. In more detail, let A and B be two triangles. Then, a contact point of A and B is a node of triangle A that belongs to the side of triangle B but is not a node of B . It is obvious that any triangle contact system defines a simple graph. A triangle contact system is *non-strict* if there exists a contact point that is the node of more than one triangle. If not specified otherwise, we always refer to strict triangle contact systems.

[De Fraysseix, Ossona de Mendez, and Rosenstiehl \[1994\]](#) show that any simple plane graph may be represented by a triangle contact system. Further, they prove that these representations for triangular graphs are in one-to-one correspondence with Schnyder woods that is proved in [Section 4.7](#).

An example of the construction of [Theorem 4.2](#) is shown in [Figure 4.4](#). The triangles are chosen to be isosceles over a horizontal basis.

Theorem 4.2 ([de Fraysseix et al., 1994](#)). *Each planar graph G has a triangle contact representation.*

Proof. First, we show that any triangular graph has a triangle contact representation. Let $\Pi = (v_1, \dots, v_n)$ be a canonical ordering of G and let $\tau(v_k)$ denote the triangle representing vertex v_k . Construct a Schnyder wood according to [Theorem 3.12](#). Let $\pi_i(v_k)$ denote the canonical ordering label of the parent of v_k in T_i , $i = 1, 2, 3$. We remark that T_1 , T_2 , and T_3 are the three trees of the Schnyder wood according to [Lemma 3.10](#).

Iteratively, we construct drawings Γ_k of G_k , $1 \leq k \leq n$, such that $G_n = G$ and $\Gamma_n = \Gamma$, where Γ is the resulting drawing of the graph. In Γ_k each vertex v is

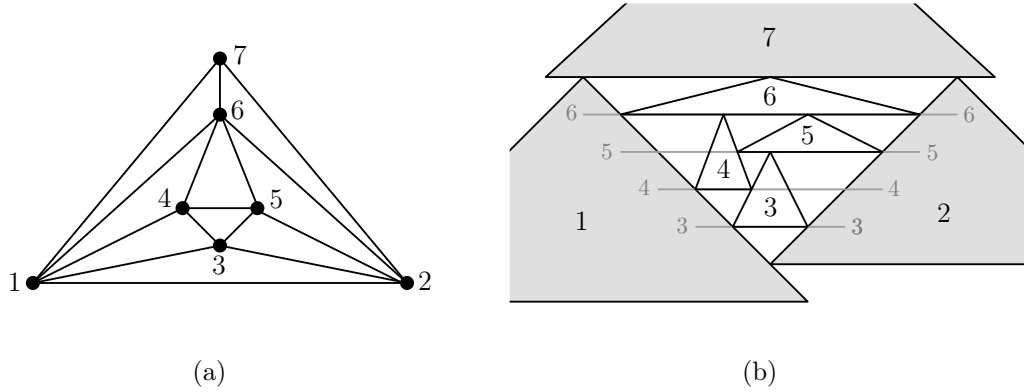


Figure 4.4: (a) A triangular graph. (b) Triangle contact representation of the graph of (a).

represented as an isosceles triangle $\tau(v)$, whose base is parallel to the x -axis, with top corner a_v , bottom left corner b_v , and bottom right corner c_v . Also, $\tau(v)$ is such that the length of $\overline{a_v b_v}$ is equal to the length of $\overline{b_v c_v}$.

We draw the triangles $\tau(v_k)$, $k = 1, \dots, n$, in a coordinate system such that $\overline{b_{v_k} c_{v_k}}$ is parallel to the x -axis with y -coordinate k . Further, the corner a_{v_k} has y -coordinate $\pi_3(v_k)$, for $k = 1, \dots, n - 1$. The corner a_{v_n} has a y -coordinate greater than n .

At the beginning, draw the triangles $\tau(v_1)$, $\tau(v_2)$, and $\tau(v_n)$ such that b_{v_2} is a contact point of $\tau(v_1)$, c_{v_2} is a contact point of $\tau(v_n)$, and c_{v_1} is a contact point of $\tau(v_n)$.

Let c_ℓ be the left neighbor and c_r be the right neighbor of v_k in Γ_{k-1} . See Section 2.2.1 for details of this definition. Using the notation of Schnyder woods, the canonical ordering label of c_ℓ and c_r equals $\pi_1(v_k)$ and $\pi_2(v_k)$, respectively. Let x_ℓ and x_r denote the x -coordinate of the point of $\overline{a_{c_\ell} c_{c_\ell}}$ and $\overline{a_{c_r} b_{c_r}}$, respectively, that has y -coordinate k . Then, the vertices of the triangle $\tau(v_k)$, $3 \leq k \leq n - 1$, receive the following coordinates:

$$a_{v_k} = \left(\frac{1}{2}x_\ell + \frac{1}{2}x_r, \pi_3(v_k)\right), b_{v_k} = (x_\ell, k), c_{v_k} = (x_r, k)$$

By the properties of a canonical ordering, this drawing yields a triangle contact representation.

If G is not triangular, then augment it to a triangular graph G' by adding dummy vertices and dummy edges that are incident to the dummy vertices and original vertices. Then, a triangle contact representation of G follows from a triangle contact representation of G' by removing the triangles corresponding to the dummy vertices. □

The technique used in the proof of Theorem 4.2 can be easily adapted such that all triangles have a right angle. De Fraysseix et al. [1994] further show that a triangle contact representation can be computed in $\mathcal{O}(n^{1+\varepsilon})$ time for any given $\varepsilon > 0$.

4.2 Homothetic Triangle Contact Representation

In this section, we study the problem of computing triangle contact representations of planar graphs under the restriction that the triangles are homothetic. Two triangles are *homothetic* if they only differ in a geometric contraction or expansion. In more detail, a *homothety* is a transformation with respect to a fixed point c , called *center*, and a constant $k \neq 0$, called *ratio*, such that all distances from the center are multiplied by k . The center is mapped to itself and each other point p is mapped to a point q such that c, p, q are collinear and such that $\vec{c}q = k \cdot \vec{c}p$, where $\vec{c}p$ and $\vec{c}q$ denote the directed length from c to p and from c to q , respectively. Then, two triangles are homothetic if there exists a homothety that maps one onto the other.

Conversely, if in any two figures the corresponding sides are parallel, then there exists a homothety that maps one of them onto the other and its center is the point of concurrence of the lines joining corresponding vertices.

We prove that every two-terminal series-parallel digraph and any partial planar 3-tree has a homothetic triangle contact representation [Badent et al., 2007]. This result is extended by Gonçalves, Lévêque, and Pinlou [2011] who answer a conjecture from Jan Kratochvíl stated in 2007¹ that any 4-connected, planar triangulation has a homothetic triangle contact representation.

Our interest in homothetic triangles is motivated by an observation of Kaufmann, Kratochvíl, Lehmann, and Subramanian [2006] that the so-called max-tolerance graphs are exactly the intersection graphs of homothetic triangles in the plane. A *max-tolerance graph* is a graph where each vertex v_i is assigned a closed interval I_i . Further, an interval I_i is associated with a *tolerance* t_i such that an overlap between two intervals I_i and I_j induces an edge between the corresponding vertices v_i and v_j if and only if $|I_i \cap I_j| \geq \max(t_i, t_j)$.

Max-tolerance graphs have interesting applications in molecular biology. DNA sequences are represented as vertices and two vertices are adjacent if and only if the corresponding sequences overlap on at least one position [Benzer, 1959]. The resulting graph is an *interval graph* [Fulkerson and Gross, 1965]. However, for achieving meaningful results, one has to increase the tolerance that leads to the notion of max-tolerance graphs [Lehmann, Kaufmann, Steigle, and Nieselt, 2006].

¹Bertinoro Workshop on Graph Drawing and Computational Geometry, 2007, personal communication

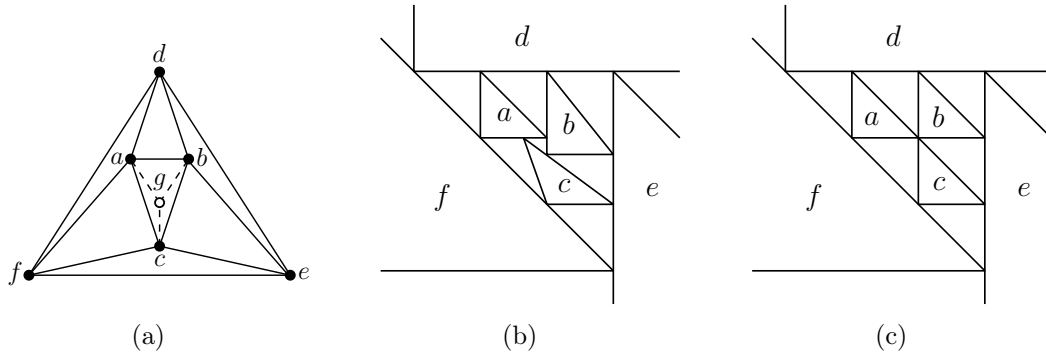


Figure 4.5: (a) A graph that does not admit a homothetic triangle contact representation. (b) Triangle contact representation that is not homothetic. (c) Non-strict homothetic triangle contact representation of the 4-connected, planar graph from (a) without vertex g .

In view of Theorem 4.2, it is self-evident to check whether every planar graph has a contact representation by homothetic triangles. However, one quickly sees that this is not the case. Consider, for example, the octahedron with eight vertices inscribed each in one face as shown in Figure 4.5(a). In any contact representation, a triangle of the octahedron - say a, b, c - must be represented inside the region bounded by the representation of the opposite face, denoted by d, e, f (see Figure 4.5(b)). If all triangles are homothetic, then the triangles a, b, c meet in one point as depicted in Figure 4.5(c) and it is not possible to insert the triangle g that should represent the vertex inscribed in the face abc of the octahedron.

4.3 TTSP-Digraphs

A *two terminal series-parallel digraph* (TTSP-digraph for short) is a planar digraph that has one source and one sink, called *poles*. Figure 4.6(a) shows an example of a TTSP-digraph that is recursively defined as follows:

- *Base case:* A digraph that consists of a single edge is a TTSP-digraph.
- *Parallel composition:* Let G' and G'' be two TTSP-digraphs. The digraph G obtained by identifying the source of G' with the source of G'' and the sink of G' with the sink of G'' is a TTSP-digraph.
- *Series composition:* Let G' and G'' be two TTSP-digraphs. The digraph G obtained by identifying the sink of G' with the source of G'' is a TTSP-digraph.

The underlying undirected graph of a TTSP-digraph is called a *series-parallel graph*.

In this section, we show that any TTSP-digraph admits a strict homothetic triangle contact representation [Badent et al., 2007].

A TTSP-digraph G is associated with a binary tree T that is called the *decomposition tree* of G . An example is shown in Figure 4.6(b). The nodes of T are of three types, Q -nodes, S -nodes, and P -nodes. A Q -node represents a single edge, an S -node represents a series composition, and a P -node represents a parallel composition. More formally, the tree T is defined recursively as follows:

- If G is a single edge, then T consists of a single Q -node.
- If G is created by a series composition of TTSP-digraphs G' and G'' , where the sink of G' is identified with the source of G'' , let T' and T'' be the decomposition trees of G' and G'' , respectively. Then, the root of T is an S -node and has left subtree T' and right subtree T'' .
- If G is created by a parallel composition of TTSP-digraphs G' and G'' , where G' is to the left of G'' in the embedding, let T' and T'' be the decomposition trees of G' and G'' , respectively. Then, the root of T is a P -node and has left subtree T' and right subtree T'' .

Observe that, according to the definition above, the leaves of T are its Q -nodes, while each internal node of T is either an S -node or a P -node. The order of the children of P -nodes defines the embedding of the graph G .

It is well known that the decomposition tree of G has $\mathcal{O}(n)$ nodes and can be constructed in $\mathcal{O}(n)$ time [Valdes et al., 1982].

Without loss of generality, we assume that a child node that has the same type as its parent is preferentially chosen as right child. Also, since G is a simple graph, any maximal set of connected P -nodes may have at most one Q -node as a child. Consider such a maximal set of connected P -nodes that has one Q -node as a child. Let p be the P -node such that the length of the path from p to the root of T is as small as possible among all P -nodes in this set. Then, tree T can be rearranged in such a way that the Q -node is the left child of P -node p which we call a *final P -node*. A P -node that is not final is called *non-final*.

We show that any TTSP-digraph admits a homothetic triangle contact representation and that such a representation can be computed in linear time.

Theorem 4.3. *Let G be a TTSP-digraph with n vertices. There exists an $\mathcal{O}(n)$ -time algorithm that computes a strict homothetic triangle contact representation of G .*

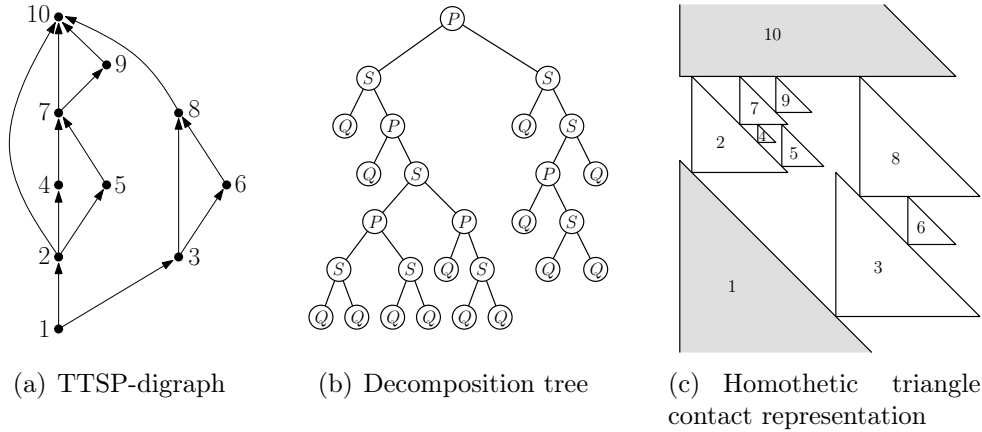


Figure 4.6: Decomposition tree and homothetic triangle contact representation of a TTSP-digraph.

Proof. Assume that G consists of more than one edge, otherwise the statement trivially holds. We describe an algorithm that visits T from bottom to top and incrementally constructs a homothetic triangle contact representation Γ of G . Namely, let $\mu_1, \mu_2, \dots, \mu_k$ be the internal nodes (S - and P -nodes) of T ordered according to a postorder traversal of T . Also, let $G_i \subseteq G$ denote the TTSP-digraph whose decomposition tree is the subtree rooted at μ_i ($1 \leq i \leq k$), and denote by s_i, t_i the source pole and the sink pole of G_i , respectively.

The drawing algorithm performs k steps. In each step i , $1 \leq i \leq k$, a drawing Γ_i of G_i is computed. Since μ_k is the root of T , $G_k = G$ and $\Gamma_k = \Gamma$. In Γ_i , each vertex v is represented as a right triangle $\tau(v)$ with top corner a_v , bottom left corner b_v , and bottom right corner c_v . The right angle is at the bottom left corner b_v . Also, $\tau(v)$ is such that the length of $\overline{a_v b_v}$ is equal to the length of $\overline{b_v c_v}$ (i. e., $\angle c_v a_v b_v = \angle b_v c_v a_v = 45$ degrees). We call *size of* $\tau(v)$ or *side length of* $\tau(v)$ the length of $\overline{b_v c_v}$.

The drawing Γ_i will have the following properties:

P1: Γ_i is a homothetic triangle contact representation of G_i .

P2: In Γ_i , the triangles $\tau(s_i)$ and $\tau(t_i)$ have the same size; all triangles distinct from $\tau(s_i)$ and $\tau(t_i)$ are contained in a polygon with points p_1, p_2, p_3, p_4 such that $\overline{p_1 p_2}$ is properly contained in $\overline{b_{t_i} c_{t_i}}$, $\overline{p_3 p_4}$ is properly contained in $\overline{a_{s_i} c_{s_i}}$, and p_1, p_3 (p_2, p_4) have the same x -coordinate. We call such a polygon the *inner polygon* of Γ_i . The *height* of the inner polygon is the distance between p_1 and p_3 .

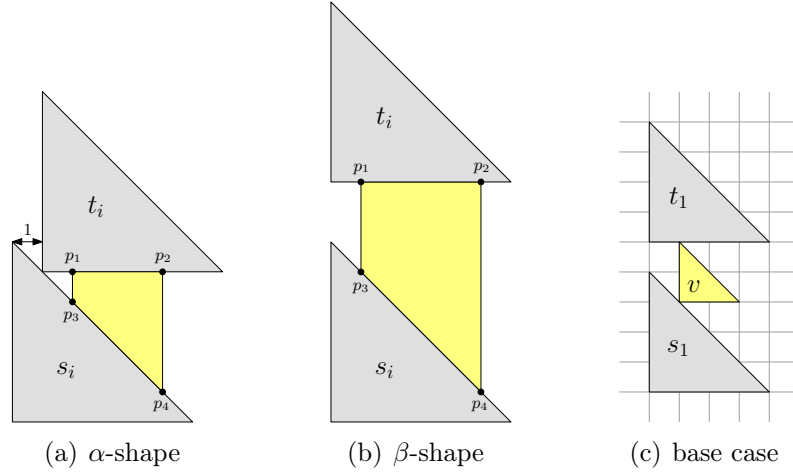


Figure 4.7: Different shapes of the drawing Γ_i .

P3: If μ_i is a final P -node, then drawing Γ_i has a shape like the one depicted in Figure 4.7(a) that we call an α -shape. Namely, b_{t_i} is the contact point of $\tau(s_i)$ and $\tau(t_i)$. It coincides with the point of $\overline{a_{s_i}c_{s_i}}$ that has horizontal distance 1 from $\overline{a_{s_i}b_{s_i}}$. Otherwise (μ_i is either an S -node or a non-final P -node), drawing Γ_i has a shape like the one depicted in Figure 4.7(b) that we call a β -shape. Namely, b_{s_i} and b_{t_i} have the same x -coordinate.

Since G is a simple graph, the base case of the algorithm is an S -node μ_1 with two Q -nodes as children. Let (s_1, v) and (v, t_1) be the two edges that form G_1 . We obtain a β -shape drawing Γ_1 for μ_1 satisfying Properties P1–P3 as depicted in Figure 4.7(c).

Assume by induction that Γ_j satisfies Properties P1–P3, for any $j < i$ and $i \geq 2$. We show how to construct Γ_i that also satisfies Properties P1–P3.

We distinguish three cases:

- μ_i is a final P -node: In this case, the children of μ_i are a Q -node v (corresponding to the edge (s_i, t_i)) and a node μ_j , $j < i$, that is either an S -node or a non-final P -node. By the inductive hypothesis, Γ_j has a β -shape. To construct Γ_i , we modify Γ_j as follows. Triangle $\tau(s_j)$ is scaled-up by extending segment $\overline{a_{s_j}c_{s_j}}$ in the north-west direction until $y(a_{s_j}) = y(b_{t_j}) + 1$. Triangle $\tau(t_j)$ is scaled-up by extending $\overline{b_{t_j}c_{t_j}}$ first in the west direction until $\tau(t_j)$ touches $\tau(s_j)$, and then in the east direction by one unit. By simple geometric considerations it is easy to verify that Properties P1–P3 hold for Γ_i . See Figure 4.8(a).

- μ_i is a non-final P -node: Denote by μ_j and μ_h , $j, h < i$, the children of μ_i . By definition of non-final P -node, each of μ_j and μ_h is either an S -node or a non-final P -node and, therefore, by the inductive hypothesis, Γ_j and Γ_h have β -shapes. Without loss of generality, assume that the height of the inner polygon of Γ_h is less than the height of the inner polygon of Γ_j (if this is not the case, permute μ_j and μ_h).

We construct Γ_i by modifying and composing Γ_j and Γ_h . More precisely, we draw the inner polygon of Γ_h to the right of the inner polygon of Γ_j at one unit horizontal distance. Then, we scale-up the inner polygon of Γ_h (and the drawing inside it) in the south-east direction until its side p_3p_4 coincides with the prolongation of segment $\overline{a_{s_j}c_{s_j}}$. After that, we possibly scale-up the triangles $\tau(s_i)$ in the south-east direction and $\tau(t_i)$ in the east direction so that they have the same size and $x(c_{t_i})$ is equal to the x -coordinate of the rightmost vertical side of the inner polygon of Γ_h plus one (see Figure 4.8(b)). Again, it is immediate to verify that Properties P1–P3 hold for Γ_i .

- μ_i is an S -node: Denote by μ_j and μ_h , $j, h < i$, the children of μ_i where G_h is placed on top of G_j in the series composition. If one of G_j or G_h (say G_h) is a single edge, add a new triangle on top of Γ_j and suitably scale $\tau(s_j)$. Otherwise, we distinguish between two different cases: Γ_h has a β -shape or Γ_h has an α -shape.

Assume first that Γ_h has a β -shape. If the size of $\tau(s_h)$ is smaller than the size of $\tau(t_j)$, then we place Γ_h on top of Γ_j by making a_{s_h} coincident with a_{t_j} , and then redraw $\tau(t_h)$ equal to $\tau(s_j)$. Also, if Γ_j has a β -shape a further scale-up of $\tau(t_h)$ in the north-west direction and of $\tau(s_j)$ in the south-west direction is performed to restore Property P2 (see Figure 4.9(a)). Conversely, if Γ_j has an α -shape, a scale-up of $\tau(t_h)$ in the north-east direction and of $\tau(s_j)$ in the south direction is performed to restore Property P2 (see Figure 4.9(b)). If the size of $\tau(s_h)$ is greater than the size of $\tau(t_j)$, then we place Γ_h on top of Γ_j by making b_{s_h} coincident with b_{t_j} . After that, we perform scaling operations on $\tau(s_j)$ and $\tau(t_h)$ according to the shape of Γ_j in order to restore Property P2 as illustrated by Figure 4.10.

Assume now that Γ_h has an α -shape. In this case, Γ_h cannot be freely scaled-up in the west direction because it is constrained by $\tau(s_h)$. To avoid this problem, we first apply a simple transformation on Γ_h (refer to Figure 4.11). Namely, we first translate $\tau(t_h)$ so that it still touches $\tau(s_h)$ and $x(a_{s_h}) = x(b_{t_h}) + 1$. During this operation, the inner polygon of Γ_h is translated with $\tau(t_h)$, and then it is translated again in the east direction by one unit. Notice that, at the end of this transformation, it may happen that the point p_2 of the inner polygon has x -coordinate greater than or equal to the one of $c(t_h)$. If so, we

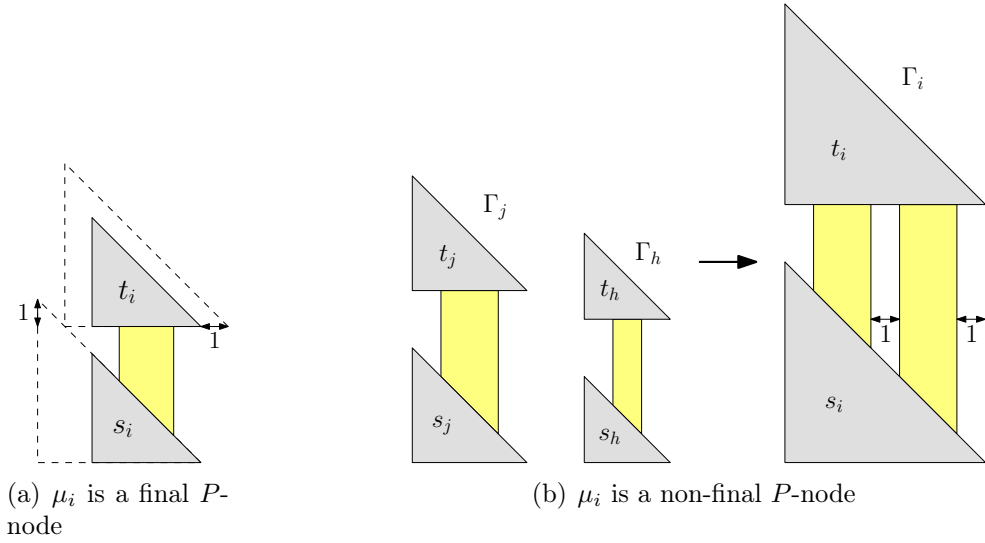


Figure 4.8: Parallel composition.

again scale-up $\tau(t_h)$ and $\tau(s_h)$ until the x -coordinate of p_2 is smaller than the x -coordinate of $c(t_h)$. After this transformation, Γ_i can be constructed by placing Γ_h on top of Γ_j with a technique similar to the one described for the case in which Γ_h has a β -shape. Hence, Properties P1–P3 hold for Γ_i .

The postorder traversal of T takes $\mathcal{O}(n)$ time and the operations required for each series- and parallel-composition can be computed in constant time. \square

4.4 Partial Planar 3-Trees

A *planar 3-tree* is a graph obtained from a complete graph with three vertices by repeating the following operation:

- Choose a bounded triangular face and add a new vertex to this face connecting it to all three vertices of the chosen face.

In this section, we show that any planar 3-tree admits a strict homothetic triangle contact representation [Badent et al., 2007].

The class of graphs does not change if the chosen face is also allowed to be the outer face. However, for our purpose, the given definition is much more handy. Planar 3-trees are also known as *stacked triangulations*. The construction of a triangle

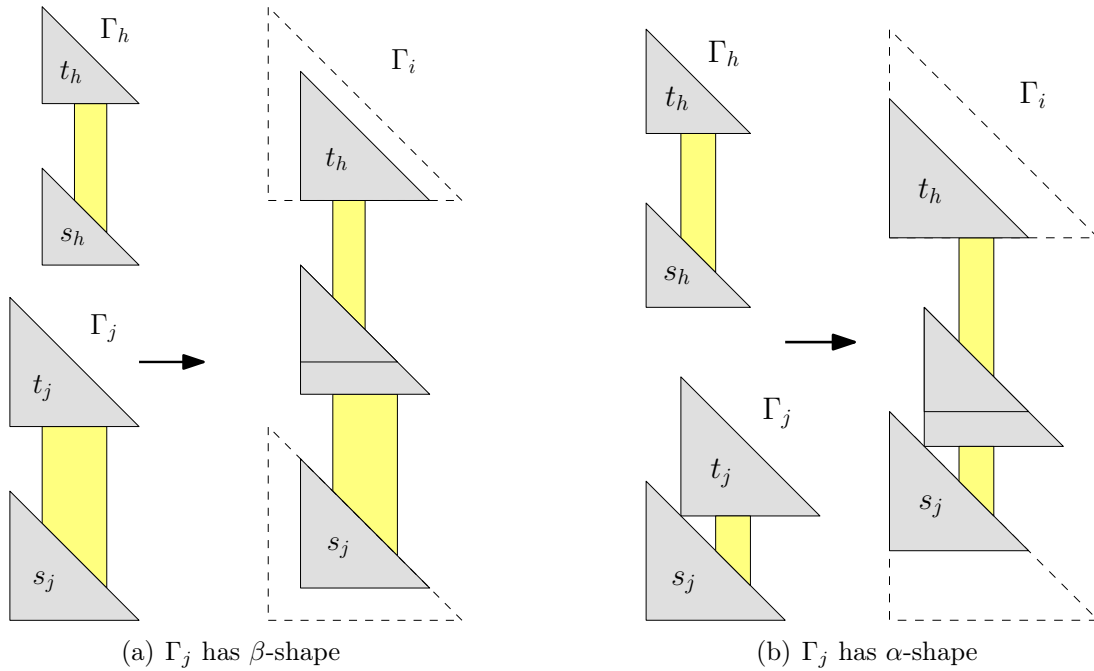


Figure 4.9: Series composition: Γ_h has a β -shape, and the size of $\tau(s_h)$ is smaller than the size of $\tau(t_j)$.

contact representation of a planar 3-tree can be obtained along the construction sequence of the graph. The part of the plane left uncovered by the three triangles of the initial graph consists of an unbounded region and a bounded region. The bounded region is a triangle which is homothetic to the shape of a point reflection of the triangle used to represent the vertices. Let this be called a *triangle of co-shape* (*co-shape* for short). An example is shown in Figure 4.12(a). Actually, the following strong property holds:

- Let C be a non-separating 3-cycle of a graph G . If G has a triangle contact representation, then the three triangles representing the vertices of C enclose a co-shaped empty triangle. The bounding edges of this empty triangle belong to the triangles representing the three vertices of C .

A triangle representing a vertex can be fitted inside a triangle of co-shape such that the corners touch the three bounding edges of the enclosing triangle. This is exactly the operation needed for the inductive construction of a strict triangle contact representation of a planar 3-tree along the construction sequence.

Theorem 4.4. *Every planar 3-tree with n vertices has a strict triangle contact representation that is computable in $\mathcal{O}(n)$ time.*

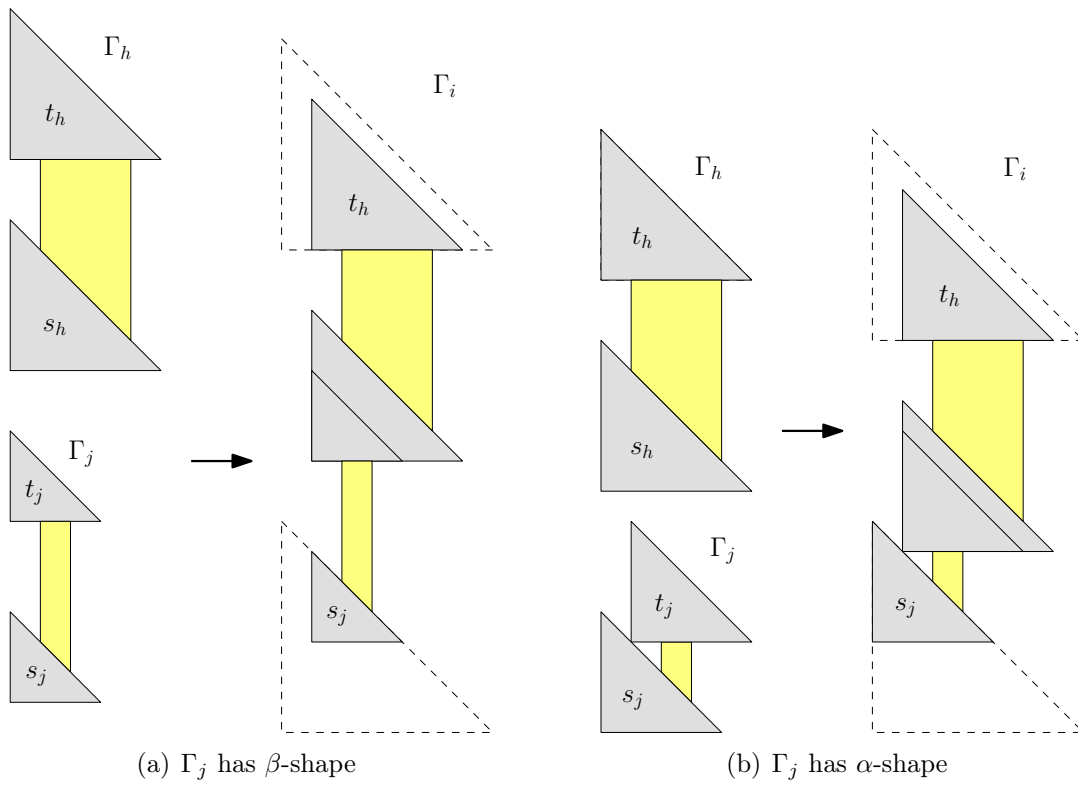


Figure 4.10: Series composition: Γ_h has a β -shape, and the size of $\tau(s_h)$ is greater than the size of $\tau(t_j)$.

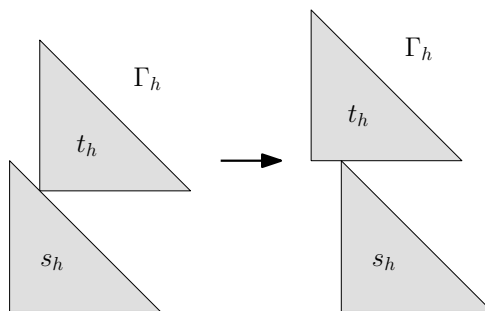


Figure 4.11: Transformation if Γ_h has an α -shape.

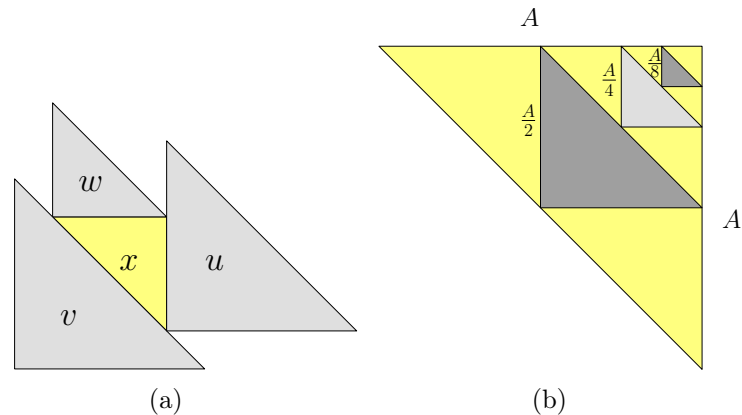


Figure 4.12: (a) Triangle x has co-shape. (b) Side lengths of the triangles inside a triangle of co-shape.

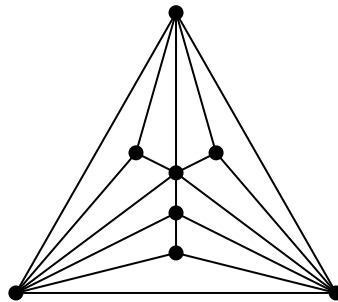


Figure 4.13: A partial planar 3-tree.

A graph G is a *partial planar 3-tree* if it is a subgraph of a planar 3-tree G^+ , i. e., the graph G can be obtained by removing edges and vertices from G^+ . An example of a partial planar 3-tree is shown in Figure 4.13. We will show that a construction of a strict triangle contact representation of G^+ can be used to get a strict triangle contact representation of G .

The removal of vertices from G^+ is reflected by the removal of the corresponding triangles from the representation. Though the basic idea is again easy, the removal of edges is slightly more subtle. Recall that an edge is represented by the contact of a corner of one triangle and a side of another. The idea for removing an edge is to slightly shrink the triangle contributing the corner and to simultaneously move it away so that the contacts of the other two edges are preserved. The plan is to go along a construction of a triangle contact representation of G^+ and to adapt size and placement of a triangle when it appears in the representation. This idea can lead into problems if at some later stage the gap opened by an edge removal is too big compared to the size of a new triangle. This is demonstrated in Fig-

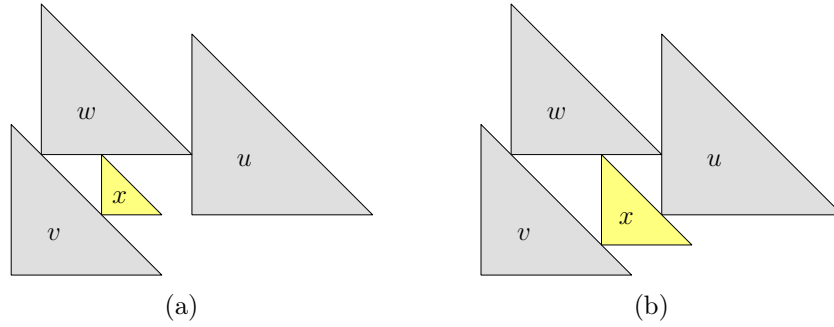


Figure 4.14: The gap opened to remove edge $\{u, v\}$ turns out to be too big for x .

Figure 4.14(a). Actually, it is possible to place the triangle x such that it touches all of u , v , and w , however, the contact between x and u would be of the wrong type making it impossible to place a common neighbor of u , v , and x later as shown in Figure 4.14(b).

To avoid this problem, we have to quantify the side length of the triangles that is denoted by L . Without loss of generality, we can assume that G^+ has n vertices and that the triangles used for the representation are equilateral. Let the side length of the co-shape enclosed by the first three vertices be A . The first (inner) triangle placed during the construction will have side length $L = \frac{A}{2}$ and the second has side length $L = \frac{A}{4}$. For further triangles we can give the following bound: The k -th triangle in the construction sequence of G^+ has side length $L \geq \frac{A}{2^k}$. This is demonstrated in Figure 4.12(b). We choose $A = 2^n$. Thus, the side length of all triangles involved are powers of two and the side length of the smallest triangles are greater or equal to 8 because there are only $n - 3$ inner triangles.

If a triangle that has side length B is to be shrunk, we reduce its side length by 1. Note that the side length of each of the three co-shapes formed by placing the re-sized triangle have side length $L \geq B - 1$. Hence, the size of a triangle fitting into one of these co-shapes is $L \geq \frac{B-1}{2}$.

Starting with the initial co-shape of side length $L = A$, we see that the k -th triangle still has size

$$L \geq (\dots ((A - 1)\frac{1}{2} - 1)\frac{1}{2} \dots - 1)\frac{1}{2} = \frac{1}{2^k}(A - 1 - 2 - \dots - 2^k) > \frac{A}{2^k} - 2.$$

With $A = 2^n$ we get no problems because all triangles have side length at least 6 and gaps are of size ≤ 1 . Hence, there is never the problem that a triangle could fit through a gap.

To actually compute a triangle contact representation for a partial planar 3-tree G , we need a corresponding host G^+ . If G^+ is given, we can compute a con-

struction sequence for G^+ . Along this construction sequence, a triangle contact representation is constructed that avoids contacts for all edges $\{u, v\}$ of $G^+ - G$. These edges are not in G but the vertices u and v are in G . Given such a triangle contact representation, it remains to remove the triangles of vertices that do not belong to G . This yields a triangle contact representation of G .

Theorem 4.5. *Every partial planar 3-tree G has a strict triangle contact representation. If G is given together with a planar 3-tree G^+ that has G as a subgraph, a triangle contact representation of G can be computed in $\mathcal{O}(n)$ time, where n is the number of vertices of G^+ .*

Note that this result provides an alternative structural proof of Theorem 4.3 in terms of the following proposition.

Proposition 4.6. *Every series-parallel graph is a partial planar 3-tree.*

Proof. We show by induction the following statement: Every series-parallel graph G with poles x and y is a subgraph of a plane triangulation G' with x, y , and z on the boundary of the outer face such that

- vertex z does not belong to G and
- G' can be reduced to the outside triangle by iteratively deleting simplicial vertices (i. e., its neighbors form a clique) of degree 3.

This is certainly true if G is a single edge. Then, just add a new vertex z and let G' be the triangle xyz .

If G is obtained by a series composition of G_1 with poles w, x and G_2 with poles x, y , let us suppose that G'_1 has the outer face wxu and G'_2 has the outer face xyv . We construct G' by adding a vertex z adjacent to u, v, w, x, y , and by adding the edge $\{w, y\}$. Then, G' has a planar drawing with wyz being the outer face and it can be reduced (by induction hypothesis) to the skeleton graph $G'[x, y, z, u, v, w]$ that can further be reduced to the triangle wyz by deleting degree 3 vertices u, v , and x . Observe that z does not belong to G . See Figure 4.15(a).

If G is obtained by a parallel composition of G_1 and G_2 with poles x and y , let us suppose that G'_1 has the outer face xyz and G'_2 has the outer face xyv . Observe that, by induction hypothesis, z does not belong to G_1 and v does not belong to G_2 . We construct G' by inserting the graph G'_2 inside the inner triangular face of G'_1 adjacent to the edge $\{x, y\}$ while identifying the vertex v with the common neighbor of x and y in G'_1 . Then, G' has a planar drawing with the outer face xyz , and G' can be reduced to xyz by first reducing G'_2 to xyv inside G'_1 and then reducing G'_1 . See Figure 4.15(b). \square

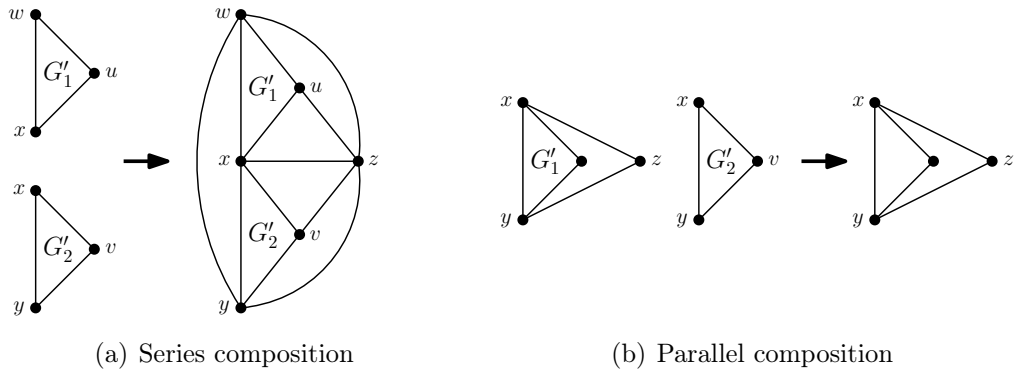


Figure 4.15: Illustration of the proof of Proposition 4.6.

4.5 4-Connected Triangulations

Gonçalves, Lévêque, and Pinlou [2011] finally prove that every 4-connected, planar triangulation admits a non-strict contact representation by homothetic triangles. The proof is surprisingly short and based on Theorem 4.1. An example is shown in Figure 4.5(c).

Theorem 4.7 (Gonçalves et al., 2011). *Every 4-connected, planar triangulation has a non-strict contact representation by homothetic triangles.*

Proof. Let the convex sets in the plane of Theorem 4.1 be homothetic triangles. Let the curves a_x, a_y, a_z be in that way such that they can be sides of homothetic triangles added in the outer face. Then, the contact system of homothetic triangles can be such that

- a triangle might be reduced to a point,
- and it induces a graph $G' \supseteq G$.

Therefore, we have to show the following two conditions.

No triangle is reduced to a point. Assume for a contradiction that there is a vertex v such that its triangle Q_v is reduced to a point p . Let C be a sufficiently small circle around p . Then, C intersects at most three non-degenerate triangles which is a contradiction to the 4-connectedness of G .

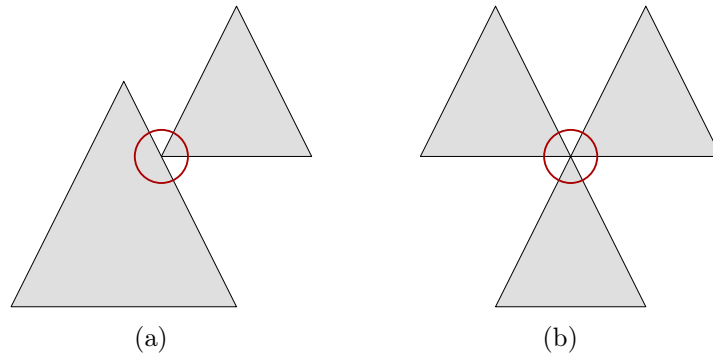


Figure 4.16: Contact points are the contact of (a) two triangles or (b) three triangles.

$\mathbf{E}(G') = \mathbf{E}(G)$. Since no triangle is reduced to a point, either two or three triangles meet in one contact point as demonstrated in Figure 4.16. Thus, a contact point corresponds to either one or three edges in G . Then,

$$|E(G')| \leq 3 + 3(n - 3) = 3n - 6 = |E(G)|. \quad \square$$

It is still unknown whether a representation by homothetic triangles for a given 4-connected triangulation is unique. Therefore, it is not possible to get a unique Schnyder wood from it.

Another interesting result can be derived from Theorem 4.7.

Theorem 4.8 (Gonçalves et al., 2011). *A graph G is planar if and only if it has an intersection representation by homothetic triangles where no three triangles intersect.*

An example of an intersection representation by homothetic triangles is presented in Figure 4.17(a).

Using Theorem 4.8, one can construct a touching representation by hexagonal polygons as shown in Figure 4.17(b). A result that is also obtained by Thomassen [1984] and Gansner et al. [2010].

4.6 Duality

A primal dual contact representation by triangles is *tiling* if the triangles corresponding to vertices and those corresponding to bounded faces form a tiling of the triangle corresponding to the outer face. A primal dual contact representation by triangles is *strict* if each contact point is a vertex of exactly three triangles corresponding to vertices or faces. An example of a strict primal dual contact representation is shown

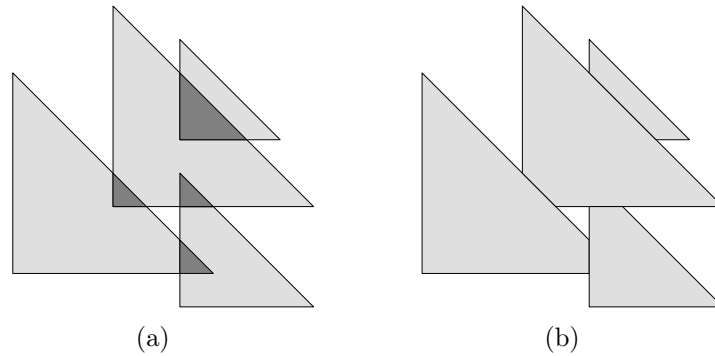


Figure 4.17: (a) Representation by intersecting homothetic triangles. (b) Representation by touching hexagons.

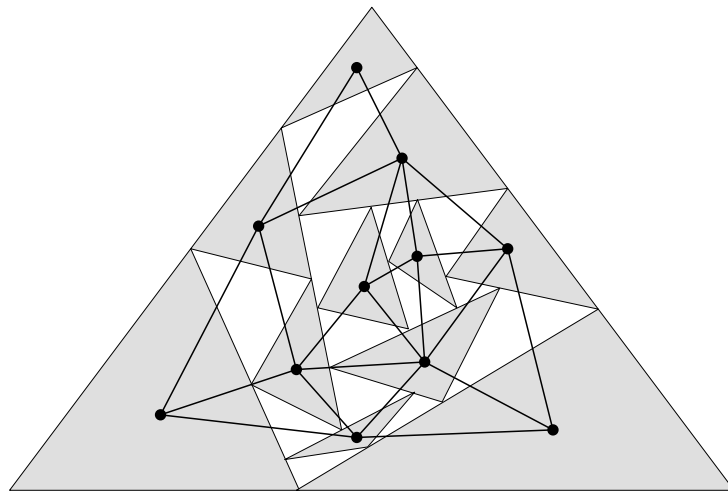


Figure 4.18: A strict tiling dual contact representation by triangles.

in Figure 4.18. A contact system is *stretchable* if there exists a homeomorphism which transforms it into a contact system whose simple arcs are straight-line segments. An *extremal point* of a contact system is a point of the union of the arcs which is interior to no arc.

In this section, we briefly review the result from [Gonçalves, Lévêque, and Pinlou \[2011\]](#) that every triconnected, planar graph admits a strict tiling primal dual contact representation by triangles. [De Fraysseix and Ossona de Mendez \[2007\]](#) connect stretchable systems to barycentric representations.

Let $G = (V, E)$ be a triconnected, planar graph together with a Schnyder wood and its corresponding Schnyder labeling. The contact system of arcs *corresponding* to the Schnyder wood is constructed as follows:

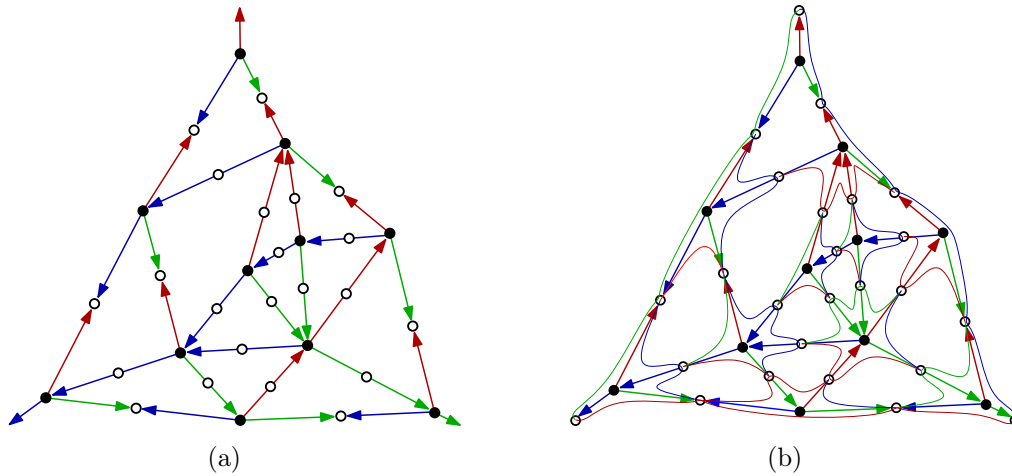


Figure 4.19: (a) Schnyder wood and contact points of the triangle contact representation of Figure 4.18. (b) Contact system of arcs corresponding to the Schnyder wood of (a).

- Each $v \in V$ is represented by three arcs $a_i(v)$, where a_i is labeled i , for $i = 1, 2, 3$. The arcs $a_i(v)$ represent the interval of angles of v that are labeled i .
- Choose for every $e \in E$ an interior point $p(e)$ that represents the contact point.
- The arcs are defined as follows: For each angle at v labeled i between the edges e and e' , there is a subarc of $a_i(v)$ from $p(e)$ to $p(e')$. Then, each contact point is the endpoint of four subarcs. See Figure 4.19 for an example.

Using the results from Section 3.4, one can see that this construction defines a contact system.

Lemma 4.9 (Gonçalves et al., 2011). *The contact system of arcs corresponding to a Schnyder wood is stretchable.*

Theorem 4.10 (Gonçalves et al., 2011). *Every triconnected, planar graph admits a strict tiling primal dual contact representation by triangles. Moreover, a planar graph admits a strict tiling primal dual contact representation by triangles if and only if it is internally triconnected.*

4.7 Schnyder Woods

A triangle contact system is *maximal* if and only if each hole is delimited by exactly three triangles. Notice that a graph that is defined by a maximal triangle contact

system is a triangular graph, however, the reverse is not true. A *free vertex* is a vertex of a triangle that is not a contact point. In this section, we show the following theorem.

Theorem 4.11 (de Fraysseix et al., 1994). *Maximal triangle contact systems are in one-to-one correspondence with Schnyder woods of triangular graphs.*

Proof. We show how to map Schnyder woods of triangular graphs to triangle contact representations and vice versa such that its concatenation yields the identity.

From Schnyder woods to triangle contact representations. Let be given a Schnyder wood of a triangular graph $G = (V, E)$. Remark that the equivalence classes of canonical orderings are in one-to-one correspondence with Schnyder woods for triangular graphs (Theorem 3.12). Then, using the construction from Theorem 4.2 yields a triangle contact representation of G .

From triangle contact representations to Schnyder woods. Let be given a triangle contact representation of triangular graph with three external triangles a_1, a_2, a_3 in counterclockwise order. Let τ be an internal triangle with three vertices a, b, c . Let a have a contact point with a triangle τ' and let a', b', c' be the three vertices of τ' . Define a path inductively for a as follows:

- If a has a contact point with $\overline{b'c'}$, then the next vertex on the path is a' .
- If a has a contact point with $\overline{a'c'}$, then the next vertex on the path is b' .
- If a has a contact point with $\overline{a'b'}$, then the next vertex on the path is c' .

More precisely, the path continues always on the opposite side of the triangle where it enters the triangle with a vertex. If such a path has a cycle, then this is a contradiction to Lemma 2.2 of de Fraysseix et al. [1994] since the difference between the number of triangles adjacent to the inside of the cycle and the number of free vertices belonging to the boundary of the cycle equals 3.

The same construction is also applied for paths starting at the vertices b and c of τ , respectively. Thus, each of these three paths is acyclic and ends at one of the three special vertices a_1, a_2, a_3 . If a path ends at a_i , then all edges are labeled i and directed towards a_i .

This construction clearly fulfills all properties of Definition 3.1. An example is shown in Figure 4.20(a).

Finally, the two constructions are inverse to each other. □

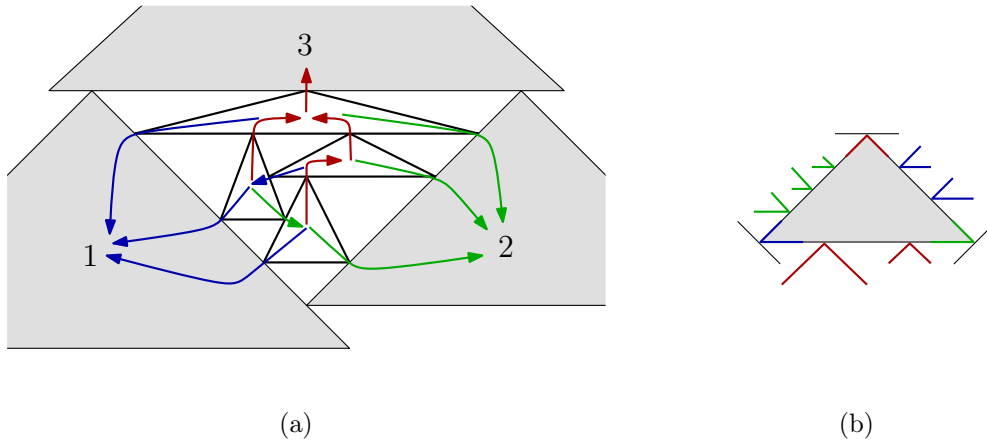


Figure 4.20: (a) A maximal triangle contact system and its Schnyder wood. (b) Triangle contacts induce the labels and orientation of the edges of a Schnyder wood.

Gonçalves et al. [2011] extend the result of de Fraysseix et al. [1994] to triconnected graphs. As we have already seen in Chapter 3, Schnyder woods for triangular graphs are in bijection to 3-orientations (Theorem 3.4), whereas the information about the orientation of the primal edges is not sufficient to uniquely determine a Schnyder wood for triconnected, planar graphs. Therefore, the primal dual superimposition G^\times was introduced (Definition 3.33). Then, the Schnyder woods of a triconnected, planar graph are in bijection with the α_0 -orientations of G^\times (Theorem 3.39).

Theorem 4.12 (Gonçalves et al., 2011). *The strict tiling primal dual contact representations by triangles of a triconnected, planar graph are in one-to-one correspondence with its Schnyder woods.*

Sketch of Proof: We sketch how to map strict tiling primal dual contact representations to Schnyder woods and vice versa such that the concatenation yields the identity. An example is illustrated in Figure 4.21.

From strict tiling primal dual contact representations by triangles to Schnyder woods. Let be given a strict tiling primal dual contact representations by triangles of a triconnected, planar graph G . Construct its corresponding primal dual superimposition G^\times . The α_0 -orientation is then obtained as follows: If two triangles in the primal or dual graph have a vertex-vertex contact, then the corresponding edge in G^\times is bi-oriented. If a contact point in the primal or dual graph is a vertex of one triangle $\tau(v)$ and a side of another triangle $\tau(v')$, then the edge $\{v, v'\}$ is directed from v to v' . Since α_0 -orientations are in one-to-one correspondence with Schnyder woods, we are done.

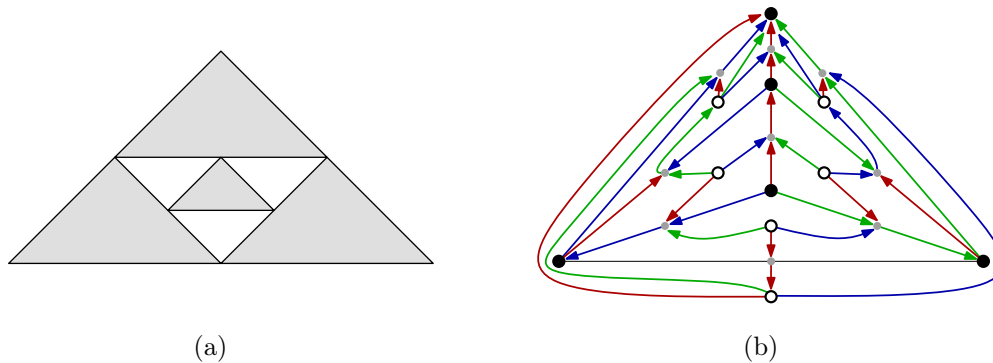


Figure 4.21: (a) A strict tiling primal dual contact representations by triangles. (b) Corresponding Schnyder wood of the primal dual superimposition.

From Schnyder woods to strict tiling primal dual contact representations by triangles. Construct a contact system of arcs according to Figure 4.19(b). By Lemma 4.9, it is stretchable and the curves become triangles. \square

4.8 Notes

Gonçalves et al. [2011] conjecture that every triconnected, planar graph has a strict tiling primal dual contact representation by right triangles. Further, they conjecture that every graph has a contact representation by equilateral triangles.

Felsner [2003] shows that Schnyder woods are in one-to-one correspondence with rigid geodesic embeddings. In Figure 4.22, the results of Felsner [2003] and Gonçalves et al. [2011] are combined. In more detail, the figure illustrates the close connection of strict tiling primal dual contact representations by triangles, Schnyder woods, and rigid geodesic embeddings. Compare also Section 6.3.3.

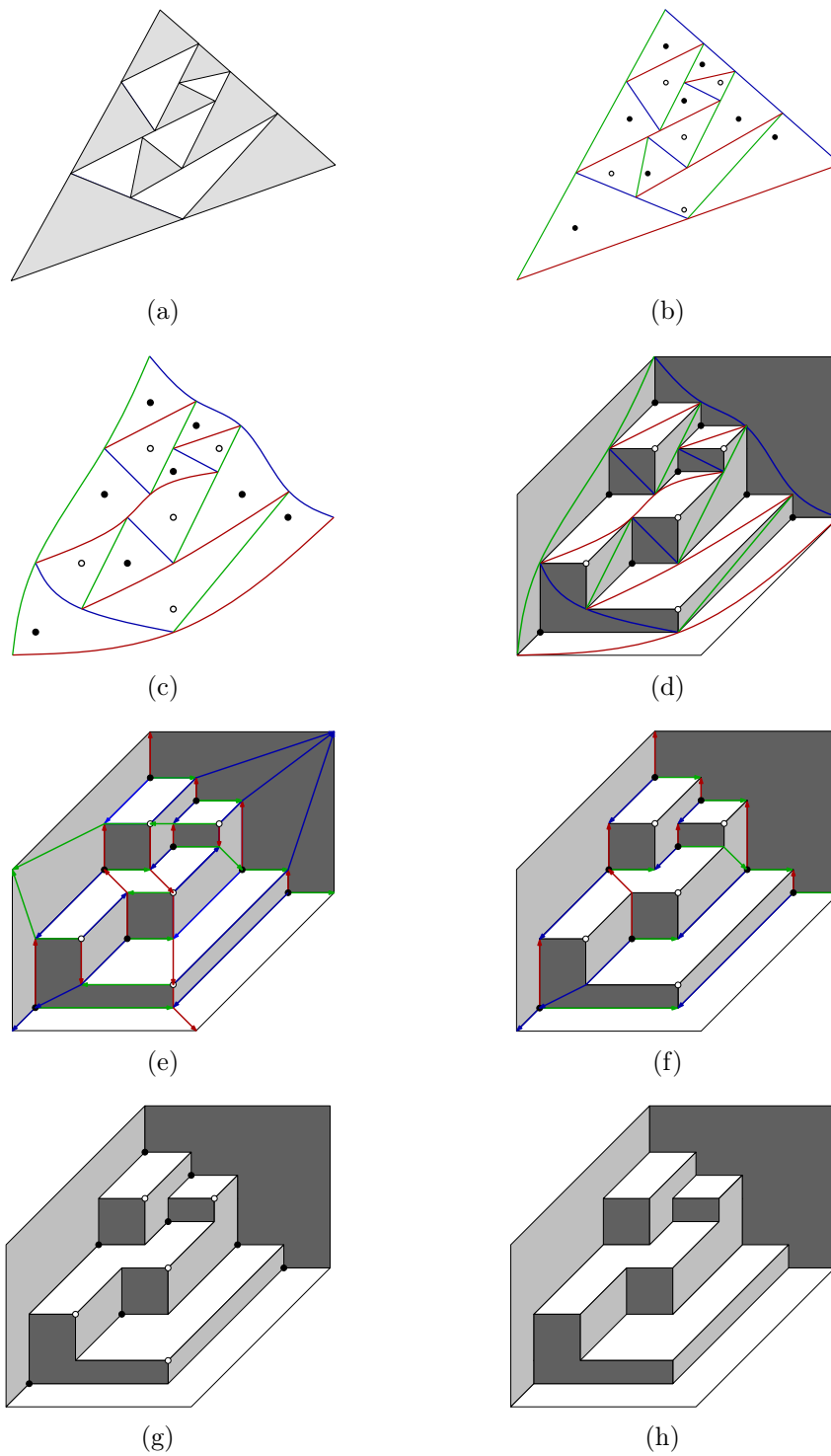


Figure 4.22: Illustration of the construction of an orthogonal surface and its connection to triangle contact representations and Schnyder woods.

Part II

Algorithms

Chapter 5

Canonical Ordering

Canonical vertex orderings are originally introduced by [de Fraysseix, Pach, and Pollack \[1988, 1990\]](#) for triangular graphs and generalized by [Kant \[1996\]](#) to triconnected, planar graphs. Definitions and introductory information can be found in [Chapter 2](#).

[Kant \[1996\]](#) shows constructively that every triconnected, planar graph has a canonical ordering and presents a linear-time algorithm. While several implementations of this algorithm are available, it is rather complicated to understand and implement, and the output is not uniquely determined.

Based on a simple and intuitive criterion, we present a new algorithm that computes the newly defined leftist canonical ordering of a triconnected, planar graph which is a uniquely determined leftmost canonical ordering. We present detailed pseudocodes and show how to implement our algorithm in linear time [[Badent et al., 2010, 2011](#)].

Finally, we review some applications of canonical ordering in planar graph drawing and beyond. We single out grid drawings and give a detailed overview of different algorithms. Then, we give a new description of the shift method of [Kant \[1996\]](#). We finish with a brief outline how to triangulate a biconnected, planar graph while computing a canonical ordering simultaneously [[Kant, 1993](#)].

5.1 Computation

We present an algorithm that computes the unique leftist canonical ordering from scratch, i. e., without any reordering, and we compute it from the low numbers to the high numbers contrary to the previous algorithm that builds the canonical ordering from the end by shelling off paths from the outer face. A similar approach for

biconnected canonical orderings can be found in [Harel and Sardas \[1998\]](#). The main advantage of our algorithm compared to the one of [Kant \[1996\]](#) is that we neither use the dual graph nor any face labels. Also, our proof of correctness includes a new proof of the existence of a canonical ordering for triconnected, planar graphs.

Starting from $P_0 = \langle v_1, v_2 \rangle$, we build the canonical ordering by adding P_1, \dots, P_s in this order. In step $k + 1$, the “belt” around G_k , i. e., the sequence of vertices not in G_k that lie on faces of G incident to G_k , is considered. Then, a candidate not causing any “self-intersection” within the belt is chosen. Before we give the details, we start with a recursive definition of which paths will be considered in the step $k + 1$.

Definition 5.1 (cut faces and locally feasible candidates). $P_0 = \langle v_1, v_2 \rangle$ is a locally feasible candidate. Let P_0, \dots, P_k be a sequence of locally feasible candidates and V_k, G_k , and C_k as in the Definition of canonical ordering (Definition 2.7). A cut face f of G_k is an inner face of G that is incident to some vertex on C_k but is not a face of G_k . Let P_f be the clockwise sequence of vertices incident to f that are not in V_k . If f is incident to an edge on C_k , then f is called a candidate face and P_f is called a candidate for the step $k + 1$. A candidate face f and the candidate P_f are locally feasible for the step $k + 1$ if

1. v_n is not in P_f or P_0, \dots, P_k, P_f is a partition of V ,
2. $G[V \setminus (V_k \cup P_f)]$ is connected, and
3. P_f is a singleton or the degree of each vertex of P_f in $G[V_k \cup P_f]$ is two.

In the remainder of this section, we will see that the locally feasible candidates are exactly the feasible candidates that were defined in Section 2.2.1. We start with the following lemma which is a direct consequence of Definitions 2.7 and 5.1 and the triconnectivity of G .

Lemma 5.2. 1. A canonical ordering is a sequence of locally feasible candidates.

2. If a sequence of locally feasible candidates partitions the whole vertex set of a triconnected, planar graph, then it is a canonical ordering.

Proof. 1. It follows directly from the Definition of canonical ordering (Definition 2.7) and Lemma 2.8(2a) that each canonical ordering is a sequence of locally feasible candidates.

2. Let P_0, \dots, P_s be a sequence of locally feasible candidates partitioning the whole vertex set of a triconnected, planar graph $G = (V, E)$. We show by induction on $k = 0, \dots, s$ that P_k fulfills the condition of a canonical ordering.

$P_0 = \langle v_1, v_2 \rangle$ and v_n is in P_s . By triconnectivity and Condition 3 of a locally feasible candidate, P_s consists only of v_n .

Let now $0 < k < s$. Since P_{k+1} is a candidate and the outer face of G_k is a simple cycle by the inductive hypothesis, it follows that the outer face of G_{k+1} is a simple cycle. Condition 3 of a locally feasible candidate corresponds to Condition 3 of a canonical ordering (Definition 2.7).

By the triconnectivity of G , each vertex has at least degree 3. Hence, if P_{k+1} is a chain, each vertex of P_{k+1} is connected to $V \setminus V_{k+1}$. By the connectivity of $G[V \setminus V_k]$, a singleton has to be connected to some vertex in $V \setminus V_{k+1}$. \square

In the following, we consider the vertices on C_k to be from left to right between v_1 and v_2 . Accordingly, we also consider the cut faces from left to right: A *cut edge* of G_k is an edge of G that is incident to one vertex in V_k and one vertex in $V \setminus V_k$. Let f and f' be two cut faces. Let c and c' be the leftmost vertices on C_k that are incident to f and f' , respectively. We say that f is to the left of f' if c is to the left of c' on C_k or if $c = c'$, then the cut edges of f are to the left of the cut edges of f' in the incidence list of c .

Algorithm 1: Leftist Canonical Ordering

begin

 Let $v_2, v_1, v_3, \dots, v_p$ be the boundary of the inner face incident to $\{v_1, v_2\}$

$P_0 \leftarrow \langle v_1, v_2 \rangle, P_1 \leftarrow \langle v_3, \dots, v_p \rangle, k \leftarrow 1$

while $|V_k| < n - 1$ **do**

 Let f be the leftmost locally feasible candidate face

$P_{k+1} \leftarrow P_f$

$k \leftarrow k + 1$

$P_{k+1} \leftarrow \langle v_n \rangle$

end

Corollary 5.3. *If Algorithm 1 terminates, it computes the leftist canonical ordering of a triconnected, planar graph.*

Before we prove that in each step there exists a locally feasible candidate face, we describe locally feasible candidates in terms of “self-intersection” of the belt. Let P_0, \dots, P_k be a sequence of locally feasible candidates. The *belt* of G_k is the sequence of vertices not in G_k that are incident to the cut faces of G_k from left to right. In more detail, let f_1, \dots, f_t be the cut faces of G_k ordered from left to right. Let P_{f_0} be the vertices in $V \setminus V_k$ that are incident to the outer face in counterclockwise order. The concatenation of P_{f_1}, \dots, P_{f_t} and P_{f_0} is the belt of G_k . For example, in Figure 5.1, $P_2 = \langle 6, 7 \rangle$, $P_3 = \langle 8 \rangle$, and the belt of G_3 is 15, 14|14|14, 15, 13, 12|12, 10|10, 11, 9|9|9, 11, 13|13, 15|15.

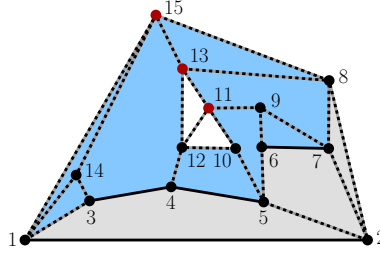


Figure 5.1: State of the algorithm at step $k = 3$: $P_0 = \langle 0, 1 \rangle$, $P_1 = \langle 3, 4, 5 \rangle$, $P_2 = \langle 6, 7 \rangle$, $P_3 = \langle 8 \rangle$; G_3 is gray, cut faces are blue, and forbidden vertices are red.

Definition 5.4 (forbidden, singular, stopper). *A vertex v of the belt of G_k is*

- forbidden if the occurrences of v are not consecutive in the belt of G_k ,
- singular if v occurs more than twice in the belt of G_k and its occurrences are consecutive, and
- a stopper if it is forbidden or singular.

In the above example, vertices 15, 13, and 11 are forbidden and vertices 14 and 9 are singular. Note that v_n is always the first and last vertex of the belt. Hence, it remains forbidden until the end.

It will turn out that the locally feasible candidates are those that do not contain a stopper or that are singular singletons.

Lemma 5.5. *Let P_0, \dots, P_k be a sequence of locally feasible candidates. Let f be a candidate face for the step $k + 1$ and let $P = P_f$.*

1. *If a vertex v of P is adjacent to more than two vertices in $V_k \cup P$, then v occurs more than twice in the belt.*
2. *If $G[V \setminus (V_k \cup P)]$ is not connected, then P contains a forbidden vertex.*
3. *If a vertex v of P is singular, then v is a locally feasible singleton.*
4. *If P contains a forbidden vertex v , then $G[V \setminus (V_k \cup P)]$ is not connected or P contains another vertex with more than two neighbors in $V_k \cup P$.*

Proof. 1. First, assume $v \neq v_n$. Let e be an edge incident to v and a vertex in $V_k \cup P$ that is not incident to f . By Remark 1.15, edge e is a cut edge and, hence, incident to two cut faces. Thus, v is incident to at least three cut faces. If $v = v_n$, then v is the first and the last vertex of the belt and occurs also in f in the belt.

2. Let W be the set of vertices in a connected component of the graph induced by $V \setminus (V_k \cup P)$ and not containing v_n . Since $V \setminus V_k$ was connected, W is adjacent to P and there is a path from P to v_n not intersecting W . By the triconnectivity of G , there is an edge between W and the part of C_k not contained in f . Further, there is at least a third vertex on $C_k \cup P$ adjacent to W . Let w be the rightmost vertex on $C_k \cup P$ that is adjacent to W and let v be the leftmost such vertex. Assume that w is on C_k . Then, v is on P . Consider the face f' containing v and w . Then, the belt contains some vertices of W between the occurrences of v for the belt faces f and f' (see Figure 5.2(a)).
3. If v is singular, then it is a candidate. By Lemma 5.5(2), $G[V \setminus (V_k \cup \{v\})]$ is connected.
4. Since v is forbidden, there is a cut face f' containing v and a cut face h between f and f' such that P_h contains a vertex $w \neq v$. If w is not incident to f , then w and v_n are in two connected components of $G[V \setminus (V_k \cup P)]$ (see Figure 5.2(b)). So assume now that for all faces h' between f and f' the path $P_{h'}$ contains only vertices incident to f . Among these faces let h be the face that is next to f . By Remark 1.15, P_h consists of one vertex $w \neq v$ and w is singular (see Figure 5.2(c)). \square

Corollary 5.6. 1. *A candidate that is a chain is locally feasible if and only if it does not contain any stopper.*

2. *A vertex of the belt is a locally feasible singleton if and only if it is singular.*

For example, the locally feasible candidates for the step $k + 1 = 4$ in Figure 5.1 are $\langle 14 \rangle$, $\langle 12, 10 \rangle$, and $\langle 9 \rangle$.

Theorem 5.7. *Algorithm 1 computes the leftist canonical ordering of a triconnected, planar graph.*

Proof. By Corollary 5.3, it remains to show that in each step of the algorithm there is a locally feasible candidate. By Corollary 5.6(2), if there are any singular vertices, we have a locally feasible candidate. So, assume now we do not have any singular vertices. By Corollary 5.6, we have to show that there is a candidate that does not contain any forbidden vertex.

Let f be a candidate face and let $P = P_f$. Assume that P contains a forbidden vertex v . Let f' be a cut face containing v such that the belt contains a vertex other than v between the occurrence of v in P_f and the occurrence of v in $P_{f'}$. Let f, h_1, \dots, h_t, f' be the sequence of cut faces between f and f' . We show by induction on the number of forbidden vertices in P_{h_1}, \dots, P_{h_t} that there is a locally feasible candidate among P_{h_1}, \dots, P_{h_t} .

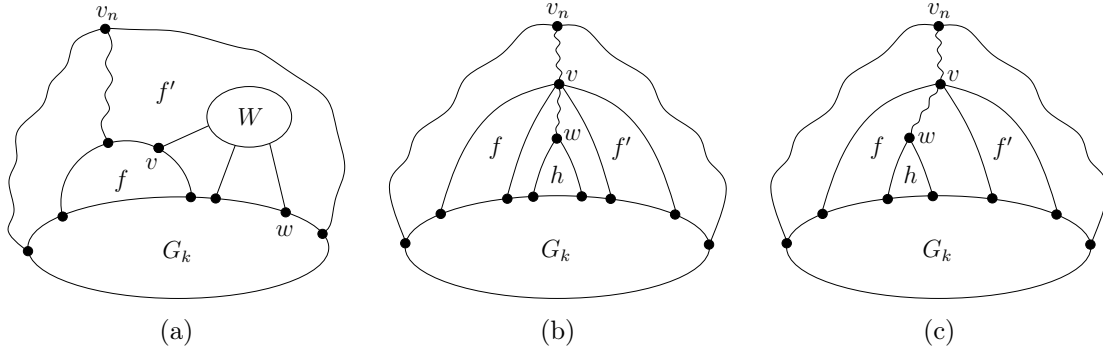


Figure 5.2: Illustration of the proof of Lemma 5.5. (a) W is a connected component of $G[V \setminus (V_k \cup P_f)]$ not containing v_n . Faces f and f' are not consecutive in the belt of G_k . Thus, f contains a forbidden vertex v . (b, c) If v is forbidden, then (b) $G[V \setminus (V_k \cup P_f)]$ is not connected or (c) there is a singular vertex w .

By the choice of f' and by triconnectivity of G , there is at least one $i = 1, \dots, t$ such that P_{h_i} is a candidate that does not contain v . If v is the only forbidden vertex in P_{h_1}, \dots, P_{h_t} , then P_{h_i} is locally feasible.

If P_{h_i} contains a forbidden vertex w (recall that by our assumption there are no singular vertices), there is a cut face $h \neq h_i$ among f, h_1, \dots, h_t, f' incident to w such that the belt contains a vertex other than w between the occurrence of w in P_{h_i} and in P_h . The cut faces between h and h_i do not contain v . Hence, by the induction hypothesis, one of them is a locally feasible candidate. \square

5.2 Linear-Time Implementation

In this section, we give detailed pseudocodes such that the algorithm for the leftist canonical ordering can be easily implemented.

In order to guarantee linear running time, we maintain a list BELT that represents the cut faces from left to right. For a simpler implementation, BELT contains lists of edges rather than one list of vertices and each cut face f is represented by a *belt item* which is a pair consisting of

- a list CHAIN of f 's incident edges not in G_k in clockwise order and
- the rightmost stopper of P_f (if any).

We traverse the list BELT using a pointer CANDIDATE. To decide whether a vertex is a stopper, we maintain two counters. Let $\text{CUTFACES}(v)$ be the number of cut

faces and $\text{CUTEDGES}(v)$ the number of cut edges to which v is incident. In order to make the following lemma true also for v_n , we will count the outer face twice in $\text{CUTFACES}(v_n)$.

Lemma 5.8. *A vertex v in the belt of G_k is*

- *forbidden if and only if $\text{CUTFACES}(v) > \text{CUTEDGES}(v) + 1$ and*
- *singular if and only if $2 < \text{CUTFACES}(v) = \text{CUTEDGES}(v) + 1$.*

Proof. A vertex occurs once for each cut face it is incident to in the belt. Two occurrences of a vertex v in the belt are consecutive if and only if the corresponding cut faces share a cut edge incident to v . So, all occurrences of v in the belt are consecutive if and only if v is only incident to one more cut face than to cut edges. \square

The algorithm `canonicalOrdering` (Algorithm 2) now works as follows (a detailed illustration of the algorithm is shown in Figure 5.3). We start with a copy of G in which each undirected edge $\{v, w\}$ is replaced by the two directed edges (v, w) and (w, v) . In the beginning, the belt is initialized by $(\langle (v_2, v_1), (v_1, v_2), (v_2, v_1) \rangle, \text{NIL})$. Thus, `leftmostFeasibleCandidate` (Algorithm 3) chooses $P_0 = \langle v_1, v_2 \rangle$ as the first path.

In general, each iteration in Algorithm 2 consists of three steps: (1) We choose the new leftmost locally feasible candidate P_k , (2) we find the new cut faces incident to P_k , and (3) we replace P_k by its incident cut faces in the belt and update its neighbors. In full detail:

leftmostFeasibleCandidate We traverse `BELT` from the current cut face `CANDIDATE` to the right doing the following: If `CANDIDATE` is a candidate face, traverse `CANDIDATE.CHAIN` from right to left until a stopper is found. If so, store it. If `CANDIDATE.CHAIN` contains no stopper or it is a singular singleton, it is the next locally feasible candidate. Otherwise, go to the next face. See Algorithm 3.

beltExtension To find the new cut faces, we traverse `CANDIDATE.CHAIN` from left to right. The outer repeat-loop iterates over all vertices incident to two edges of `CANDIDATE.CHAIN`. Each iteration finds the new cut faces incident to such a vertex and increments the counter `CUTEDGES`. In the inner repeat-loop, we traverse all new edges of a new cut face and store them in the list `CHAIN`. Here the counter `CUTFACES` is incremented. Each list `CHAIN` is finally appended to the list `EXTENSION` that stores all new belt items incident to `CANDIDATE.CHAIN`. See Algorithm 5.

updateBelt We replace CANDIDATE (and all its copies if it was a singleton) by the new cut faces found by **beltExtension**. The last edge of the predecessor and the first edge of the successor of CANDIDATE are removed since they are now contained in G_k . If the predecessor of CANDIDATE was not a candidate face before or it lost its stopper, then we go one step to the left in BELT and set CANDIDATE to its predecessor. See Algorithm 4.

Theorem 5.9. *Algorithm 2 computes the leftist canonical ordering of a triconnected, planar graph in linear time.*

Proof. Linear running time: Each edge is touched at most twice in the algorithm **beltExtension**. In the algorithm **leftmostFeasibleCandidate** each candidate is scanned from right to left until the first stopper occurs. All the scanned edges will have been deleted from the list when the candidate will be scanned the next time. In total only $2m$ edges will be added to BELT.

Correctness: While scanning BELT from left to right, we always choose the leftmost locally feasible candidate: Assume that at step $k + 1$ we scan a face f and there are no locally feasible candidates to the left of f . The face f is omitted because it is not a candidate or it contains a stopper. None of the two properties changes if no direct neighbor in BELT had been added to G_k . Hence, as long as f is not locally feasible, no face to the left of f has to be considered. Further, the number of incident cut faces or cut edges of a vertex never decreases. We show that a candidate can only become locally feasible after his rightmost stopper has become singular.

Let v be the rightmost stopper of P_f and assume v is forbidden. Let f_ℓ be the leftmost and f_r be the rightmost cut face containing v . We can conclude from the proof of Theorem 5.7 that all occurrences of v between f_ℓ and f are consecutive and that Algorithm 2 finds the locally feasible candidates between f and f_r in the belt until the belt contains only v between f and f_r . It follows that all occurrences of v in the belt are consecutive. Let now v be singular. Then, the only two incident cut faces $f = f_\ell$ and f_r of v would share a cut edge $\{v, w\}$ that would not have been a cut edge before. Hence, w would have been a stopper of f to the right of v . \square

Note that the algorithm for computing the leftist canonical ordering can also be used to compute the rightist canonical ordering. In that case, we store for each cut face the leftmost stopper and we scan the belt from right to left.

Algorithm 2: Leftist Canonical Ordering

Input : $G = (V, E)$ planarly embedded triconnected undirected graph
 $v_1 \in V$ on the outer face of G

Output: leftist canonical ordering P_0, \dots, P_s of (G, v_1)

canonicalOrdering

```

replace each  $\{v, w\} \in E$  by  $(v, w)$  and  $(w, v)$ 
 $v_n \leftarrow$  clockwise neighbor of  $v_1$  on outer face
 $v_2 \leftarrow$  counterclockwise neighbor of  $v_1$  on outer face
for  $v \in V$  do CUTFACES( $v$ )  $\leftarrow$  0; CUTEDGES( $v$ )  $\leftarrow$  0
CUTFACES( $v_n$ )  $\leftarrow$  1
mark  $(v_1, v_2)$  and  $(v_2, v_1)$ ; BELT  $\leftarrow$   $\langle \langle (v_2, v_1), (v_1, v_2), (v_2, v_1) \rangle, \text{NIL} \rangle$ 
 $k \leftarrow -1$ ; CANDIDATE  $\leftarrow$  first item in BELT
while BELT  $\neq \emptyset$  do
|  $k \leftarrow k + 1$ 
|  $P_k \leftarrow$  leftmostFeasibleCandidate
| updateBelt

```

end

Algorithm 3: Skip infeasible candidates**list leftmostFeasibleCandidate**

```

FOUND  $\leftarrow$  false
repeat
| let  $\langle (z_0, z_1), (z_1, z_2), \dots, (z_p, z_{p+1}) \rangle :=$  CANDIDATE.CHAIN
| if  $z_0 \neq z_{p+1}$  then
| |  $j \leftarrow p$ 
| |  $\blacktriangleright^1$  while  $j > 0$  and not(forbidden( $z_j$ ) or singular( $z_j$ )) do
| | |  $j \leftarrow j - 1$ 
| | if  $j > 0$  then CANDIDATE.STOPPER  $\leftarrow z_j$ 
| |  $\blacktriangleright^2$  if  $j = 0$  or (singular(CANDIDATE.STOPPER) and  $p = 1$ )
| | then
| | | FOUND  $\leftarrow$  true
| | | for  $(v, w) \in$  CANDIDATE.CHAIN do mark  $(w, v)$ 
| if not FOUND then
| | CANDIDATE  $\leftarrow$  successor(CANDIDATE)
| | if CANDIDATE = NIL then HALT: illegal input graph
until FOUND
return  $\langle z_1, \dots, z_p \rangle$ 

```

end

Algorithm 4: Replace feasible candidate with incident faces

updateBelt

 ▼ **if** *singular*(CANDIDATE.STOPPER) **then**

| remove neighboring items with same singleton from BELT

 PRED \leftarrow *predecessor*(CANDIDATE); SUCC \leftarrow *successor*(CANDIDATE)

if SUCC \neq \emptyset **then** remove first edge from SUCC.CHAIN

 EXTENSION \leftarrow *BeltExtension*(CANDIDATE.CHAIN)

replace CANDIDATE by EXTENSION in BELT

if EXTENSION \neq \emptyset **then**

 | CANDIDATE \leftarrow first item of EXTENSION

else

 | CANDIDATE \leftarrow SUCC

if PRED \neq \emptyset **then**

 | remove last edge (v, w) from PRED.CHAIN

 | **if** $v = \text{PRED.STOPPER}$ **or** $w = \text{source}(\text{first edge of PRED.CHAIN})$

 | **then**

 | | PRED.STOPPER \leftarrow NIL; CANDIDATE \leftarrow PRED

end

Algorithm 5: Construct list of new belt items incident to P_k

list beltExtension(list $\langle e_0, \dots, e_p \rangle$)

 EXTENSION \leftarrow \emptyset
for $j \leftarrow 1, \dots, p$ **do** // scan for new cut faces incident to v_{start}

 | $v_{start} \leftarrow \text{source}(e_j)$; $v_{end} \leftarrow \text{target}(e_j)$

 | FIRST $\leftarrow e_j$

 | **repeat**

 | | FIRST = $(v, w) \leftarrow$ clockwise next in $N^+(v_{start})$ after FIRST

 | | CUTEDGES(w) \leftarrow CUTEDGES(w) + 1

 | | **if** FIRST *not marked* **then** // new cut face

 | | | CHAIN \leftarrow \emptyset

 | | | **repeat** // traverse clockwise

 | | | | mark (v, w) ; append CHAIN $\leftarrow (v, w)$

 | | | | CUTFACES(w) \leftarrow CUTFACES(w) + 1

 | | | | $(v, w) \leftarrow$ counterclockwise next in $N^+(w)$ after (w, v)

 | | | | **until** $w \in \{v_{start}, v_{end}\}$

 | | | | mark (v, w)

 | | | | append CHAIN $\leftarrow (v, w)$; append EXTENSION \leftarrow (CHAIN, NIL)

 | | **until** $w = v_{end}$

 | **return** EXTENSION

end

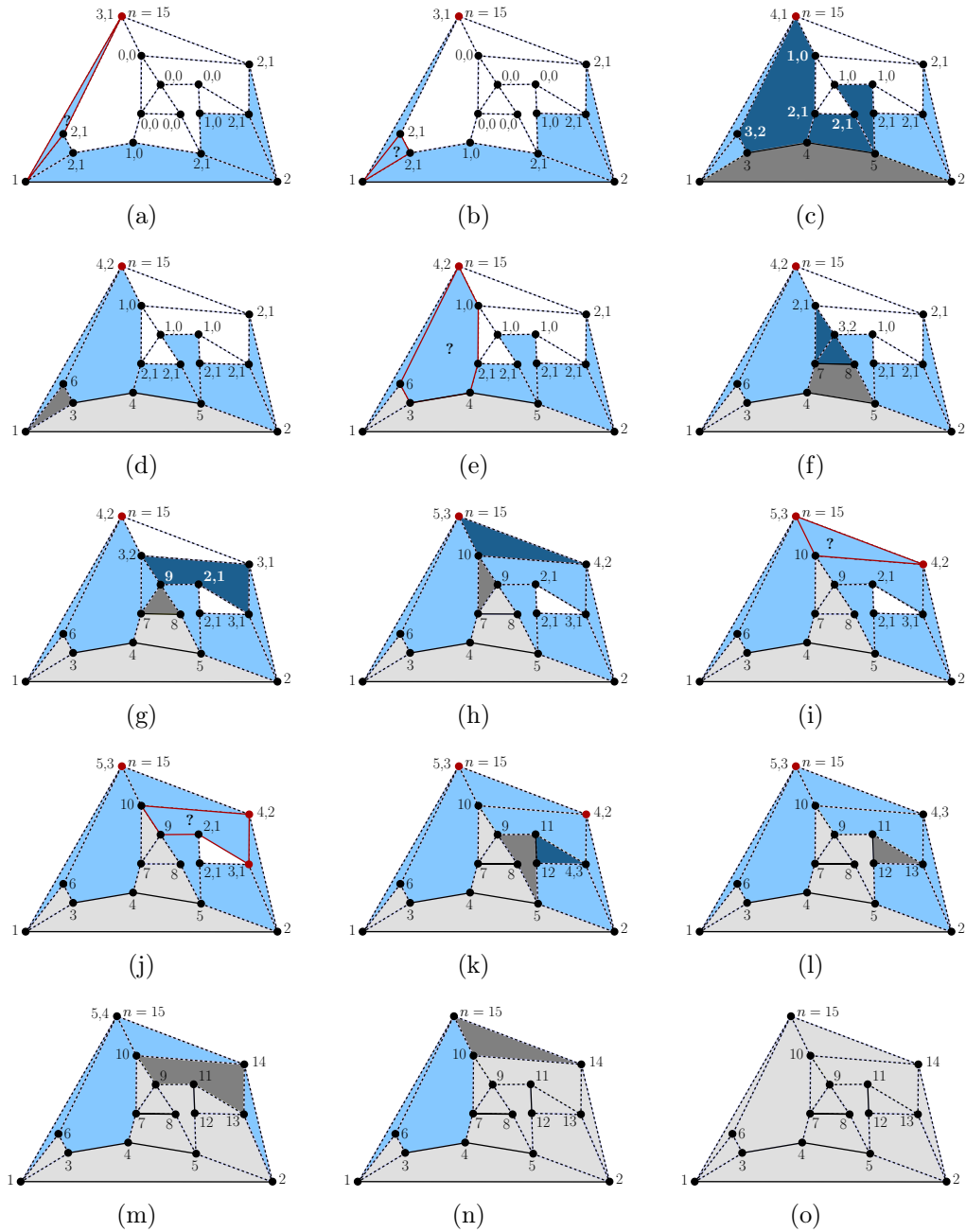


Figure 5.3: Illustration of Algorithm 2: The light blue faces are the cut faces of G_k , G_k is light gray. The leftmost feasible candidate is dark gray. Algorithm 4 substitutes the dark gray face by the dark blue faces, i.e., by the EXTENSION found by Algorithm 5. Black paths are chains, red vertices are forbidden. If a vertex v is labeled with a pair of numbers, the first number indicates $CUTFACES(v)$ and the second number indicates $CUTEDGES(v)$.

5.3 Applications

In this section, we summarize some applications of canonical ordering with focus on graph drawing but not restricted to it. Then, we concentrate on grid drawings and present **Kant**'s shift method that produces straight-line convex drawings of triconnected, planar graphs on a grid [**Kant, 1996**]. Finally, we briefly explain how to triangulate a biconnected graph while computing a canonical ordering [**Kant, 1993**, Section 6].

Beside grid drawings, canonical orderings are used in graph drawing to create

- visibility representations [**Nummenmaa, 1992, Fößmeier, Kant, and Kaufmann, 1997, Kant, 1997, Kant and He, 1997, Lin, Lu, and Sun, 2004**],
- curve embeddings [**Di Giacomo, Didimo, Liotta, and Wismath, 2003, 2005**]
- orthogonal drawings [**Biedl and Kaufmann, 1997**]
- radial drawings [**Di Giacomo, Didimo, and Liotta, 2008**]
- and other drawings [**Barequet, Goodrich, and Riley, 2004, Biedl, 1998, Djmović, Suderman, and Wood, 2005, Fößmeier, Kant, and Kaufmann, 1997, Goodrich and Wagner, 2000, Gutwenger and Mutzel, 1999**].

Further on, canonical orderings are found in

- graph encoding [**Barbay, Aleari, He, and Munro, 2007, Chuang, Garg, He, Kao, and Lu, 1998, He, Kao, and Lu, 1999**],
- used for the construction of realizers, spanners, or orderly spanning trees [**Bose, Gudmundsson, and Smid, 2005, Brehm, 2000, Chiang, Lin, and Lu, 2001, Di Battista, Tamassia, and Vismara, 1999, Miura, Azuma, and Nishizeki, 2005, Nakano, 2000, Schnyder, 1990**],
- and more [**de Fraysseix and Ossona de Mendez, 1995, He, 1999, Wada and Chen, 1998**].

5.3.1 Grid Drawings

In 1986, **Rosenstiehl and Tarjan** pose the question whether any planar graph has a planar, straight-line drawing on an $\mathcal{O}(n^k) \times \mathcal{O}(n^k)$ integer grid for a fixed k . It is first answered by **de Fraysseix, Pach, and Pollack** [1988, 1990] for maximal planar graphs. They present an algorithm for constructing a planar, straight-line drawing on a $(2n - 4) \times (n - 2)$ integer grid.

grid size	authors
$(2n - 4) \times (n - 2)$	De Fraysseix et al., 1990, Chrobak and Payne, 1995
$(n - 2) \times (n - 2)$	Chrobak and Kant, 1997
$\lfloor \frac{2(n-1)}{3} \rfloor \times (4 \lfloor \frac{2(n-1)}{3} \rfloor - 1)$	Chrobak and Nakano, 1998

Table 5.1: Grid size of different drawing algorithms for triangular graphs using canonical ordering.

Using this result, any planar graph can be drawn on an integer grid of polynomial size by adding a linear number of extra edges such that the graph is transformed into a maximal planar graph (as shown in Chapter 1.4). Then, the resulted graph is drawn and, finally, the extra edges are removed from the obtained drawing.

Until now, various algorithms to create straight-line drawings are known that are mainly based on two different methods. One class of algorithms is based on the shift method that is explained in detail in this chapter; the other one is based on the realizer method that is explained in the next chapter.

The *shift method* is introduced by de Fraysseix, Pach, and Pollack [1990] for maximal planar graphs and extended to triconnected, planar graphs by Kant [1996]. It finds various applications in the field of graph drawing and beyond and is precisely described in Section 5.3.2. Table 5.1 illustrates the progress in the grid size over the years for straight-line, convex drawings of triangular graphs.

Another question is whether it is possible to find drawings on smaller grids. However, de Fraysseix et al. [1990] show a lower bound on the grid size of $(\frac{2}{3}n - 1) \times (\frac{2}{3}n - 1)$ for this problem. Chrobak and Nakano [1998] show that each grid dimension has to be at least $\lfloor \frac{2}{3}(n - 1) \rfloor$.

Beside creating straight-line, convex grid drawings, some authors tend to achieve other esthetic criteria. For example, Goodrich and Wagner [2000] investigate an algorithm that is based on canonical ordering and that draws a triangular graph on an integer grid of size $(20n - 48) \times (10n - 24)$ with at most two bends per edge, where each edge is monotonically increasing or decreasing in both x - and y -coordinate. Not only the vertices but also the bends are on grid points. Further, the authors pay attention to the *minimum angle* that is $1/d$, where d is the maximum degree of any vertex of G , and to *edge separation*, i. e., the region around an edge that does not contain any other edge or vertex that is in this case one unit. In a second step, the edges can be replaced by curves while maintaining the desired esthetic criteria. Goodrich and Wagner mention that their algorithm can also be extended to triconnected, planar graphs.

grid size	authors
$(2n - 4) \times (n - 2)$	Kant, 1996
$(n - 2) \times (n - 2)$	Chrobak and Kant, 1997

Table 5.2: Grid size of different drawing algorithms for triconnected, planar graphs using canonical ordering.

In a next step, we extend Table 5.1 to triconnected, planar graphs that is illustrated in Table 5.2.

Also, in the triconnected scenario there are other esthetics to achieve. [Biedl and Kaufmann \[1997\]](#) draw a triconnected, planar graph orthogonally on a grid of size $(m - n + 1) \times (\min\{\frac{m}{2}, m - n + 1\})$ in linear-time with $m - n$ bends in total such that every edge has at most one bend.

Another linear-time algorithm based on the algorithm of [Kant](#) is due to [Cheng, Duncan, Goodrich, and Kobourov \[2001\]](#) who use at most two circular arcs per edge to create a drawing on an $\mathcal{O}(n) \times \mathcal{O}(n)$ grid with angular resolution $\Delta(\frac{1}{d(v)})$, where d is the maximum degree of a vertex. Further applications of the algorithm of [Kant](#) are outlined, e. g., in [Hong and Mader \[2009\]](#).

Beyond the shift method, [Kant](#) explored the *mixed model*, a method to create grid drawings of triconnected, planar graphs of size $(2n - 6) \times (3n - 9)$ with at most $5n - 15$ bends in total (at most three bends per edge), and with minimum angle greater than $\frac{2}{d}$, where d is the maximum degree of a vertex. This algorithm is extended by [Gutwenger and Mutzel \[1999\]](#) to compute a planar, polyline grid drawing of any plane graph with grid size $(2n - 5) \times (\frac{3}{2}n - \frac{7}{2})$, with at most $5n - 15$ bends, and with minimum angle greater than $\frac{2}{d}$.

5.3.2 Shift Method

[De Fraysseix, Pach, and Pollack \[1990\]](#) show that any triangular graph admits a straight-line drawing on a $(2n - 4) \times (n - 2)$ integer grid using a canonical ordering for triangular graphs. They present an $\mathcal{O}(n \log n)$ -time algorithm that is improved by [Chrobak and Payne \[1995\]](#) to linear time.

[Kant \[1996\]](#) extends the ideas of [de Fraysseix, Pach, and Pollack](#) to triconnected, planar graphs and shows that every triconnected, planar graph has a straight-line, convex drawing on an integer grid of size $(2n - 4) \times (n - 2)$. This result is strengthened by [Chrobak and Kant \[1997\]](#) to $(n - 2) \times (n - 2)$ integer grids using canonical ordering.

In this section, we describe a slightly different but conceptually equivalent variant of the algorithm of **Kant**, an extended version of the algorithm of **de Fraysseix et al.** that is also known as the *shift method* or *shift algorithm*. To my knowledge, this algorithm has nowhere been described in such a manner.

Let $G = (V, E)$ be a triconnected, planar graph with a vertex v_1 on the outer face and let $\Pi = (P_0 = \langle v_1, v_2 \rangle, \dots, P_s)$ be a canonical ordering of (G, v_1) . We use the same notations as in Chapter 2. Let $G_k = G[V_k] = (V_k, E_k)$ be the subgraph induced by $V_k = P_0 \cup \dots \cup P_k$ and let C_k be the outer face of G_k , $k = 0, \dots, s$. Again, we consider $v_1 = c_1, c_2, \dots, c_q = v_2$ to be the vertices from left to right on C_k . Let c_ℓ be the left neighbor of P_{k+1} on C_k and let c_r be the right neighbor of P_{k+1} on C_k .

The algorithm of **Kant** embeds one path after the other, following the canonical ordering, and maintaining a planar, straight-line, non-strictly convex grid embedding. Moreover, the following conditions are fulfilled for $k = 1, \dots, s$:

$$(C1) \quad v_1 = (-|V_k| + 2, 0), \quad v_2 = (|V_k| - 2, 0)$$

(C2) For the vertices $v_1 = c_1, c_2, \dots, c_q = v_2$ on C_k holds: $x(c_i) < x(c_{i+1})$, for $i = 1, \dots, q - 1$.

(C3) The edges $\{c_i, c_{i+1}\}$, $i = 1, \dots, q - 1$, have slope -1 , 0 , or $+1$. If an edge $\{c_i, c_{i+1}\}$ has slope 0 , then $x(c_i) + 2 = x(c_{i+1})$.

Initially, $P_0 = \langle v_1, v_2 \rangle$ and $P_1 = \langle v_3, \dots, v_p \rangle$ are placed such that $v_1 = (-p + 2, 0)$, $v_2 = (p - 2, 0)$, and $v_i = (2i - p - 3, 1)$, $i = 3, \dots, p$.

When a set of vertices is placed on the grid, some of the previously placed vertices are shifted to the left and some others are shifted to the right in order to maintain the above stated conditions for the currently outer face C_k , $k = 2, \dots, s$. Note that by Condition 3 the Manhattan distance between any two vertices of C_k is even.

Before we describe how to add the next path P_{k+1} to Γ_k , we explain which vertices have to be shifted. The idea is to shift vertices on the C_k to ensure that P_{k+1} can be added to Γ_k without introducing any edge crossings. Further, some inner vertices of Γ_k have to be shifted to guarantee that all inner faces remain non-strictly convex.

Let $c_\ell = c_{k_1}, \dots, c_{k_t} = c_r$ be the neighbors of P_{k+1} on C_k . Clearly, if P_{k+1} is a chain, then $t = 2$. Let $B_{k_j} = \langle c_{k_j}, \dots, c_{k_{j+1}} \rangle$, $j = 1, \dots, t - 1$, be a subpath of C_k such that c_{k_j} and $c_{k_{j+1}}$ are adjacent to a vertex of P_{k+1} and the inner vertices of the path B_{k_j} do not have any neighbors in any P_i , $i > k$. Let $c_{k_\alpha^j}$ and $c_{k_\beta^j}$ be the vertices with the smallest y -coordinate on the path B_{k_j} . We remark that by the properties of a canonical ordering and the construction of the drawing there are at most two such vertices. More precisely, each path B_{k_j} , $j = 1, \dots, t - 1$, has the following pattern:

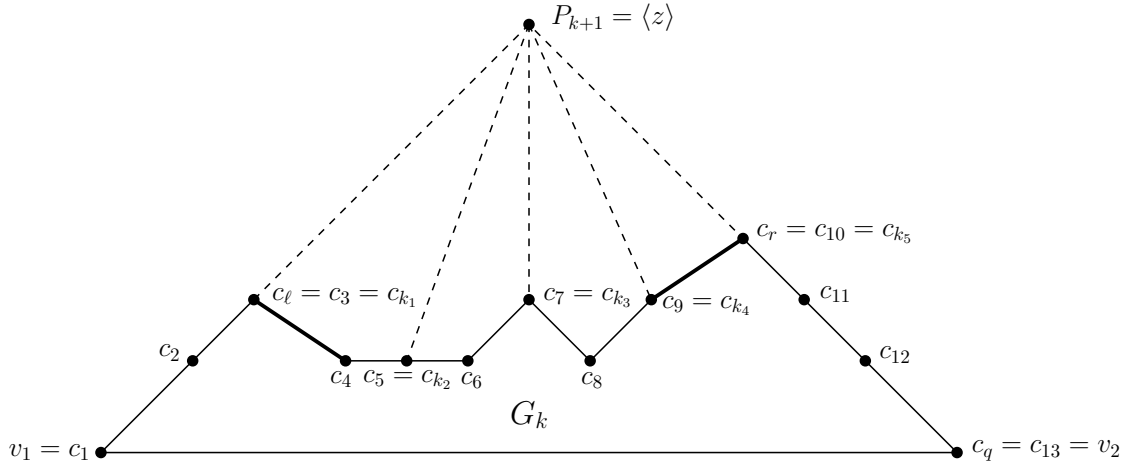


Figure 5.4: Adding P_{k+1} to the drawing of G_k . Edges $\{c_\ell, c_{\ell+1}\}$ and $\{c_{r-1}, c_r\}$ of $B_{k_j} = \langle c_{k_j}, \dots, c_{k_{j+1}} \rangle$ have slope unequal -1 and 1 . All edges on the outer face of G_{k+1} have slopes $-1, 0, +1$.

- A sequence of vertices $\langle c_{k_j}, \dots, c_{k_\alpha}^j \rangle$ with decreasing y -coordinates.
- A sequence of maximal two vertices $\langle c_{k_\alpha}^j, c_{k_\beta}^j \rangle$ with the same y -coordinate.
- A sequence of vertices $\langle c_{k_\beta}^j, \dots, c_{k_{j+1}} \rangle$ with increasing y -coordinates.

This is illustrated in Figures 5.4 and 5.5. Possibly, $c_{k_j} = c_{k_\alpha}^j$, $c_{k_{j+1}} = c_{k_\beta}^j$, or $c_{k_\alpha}^j = c_{k_\beta}^j$ for some $j \in \{1, \dots, t-1\}$. For example, in Figure 5.4, $c_4 = c_{k_\alpha}^1$, $c_{k_2} = c_{k_\beta}^1 = c_{k_\alpha}^2$, $c_8 = c_{k_\alpha}^3 = c_{k_\beta}^3$.

When shifting vertex z_i of P_{k+1} to the left and right, respectively, then also the subpaths $C_k^{\mathcal{L}} = \langle c_{k_1}, \dots, c_{k_\alpha^{t-1}-1} \rangle$ and $C_k^{\mathcal{R}} = \langle c_{k_\beta^1+1}, \dots, c_{k_t} \rangle$ of C_k have to be shifted to the left and right, respectively, in order to preserve planarity. This is shown in Figure 5.5. For example, in Figure 5.4, whenever z is shifted to the left and right, respectively, then also $C_k^{\mathcal{L}} = \langle c_3, \dots, c_8 \rangle$ and $C_k^{\mathcal{R}} = \langle c_6, \dots, c_{10} \rangle$ is shifted with the same value to the left and right, respectively.

To simplify the notation in the algorithm, we define $N_G^{\mathcal{L}}(z_i) = \{V(C_k^{\mathcal{L}}) \setminus \{c_\ell\}\}$ and $N_G^{\mathcal{R}}(z_i) = \{V(C_k^{\mathcal{R}}) \setminus \{c_r\}\}$.

Let Γ_k be a planar, straight-line, non-strictly convex grid drawing of G_k . Now, we describe how to add the next path P_{k+1} to Γ_k . We maintain for each vertex $v \in G_k$ a set of vertices $\mathcal{L}(v)$ that has to be shifted to the left whenever v is shifted to the left and a set of vertices $\mathcal{R}(v)$ that has to be shifted to the right whenever v is shifted to the right. Assume we add in the next step the path $P_{k+1} = \langle z_1, \dots, z_p \rangle$. Then, the following steps have to be carried out (compare Algorithm 6 for details):

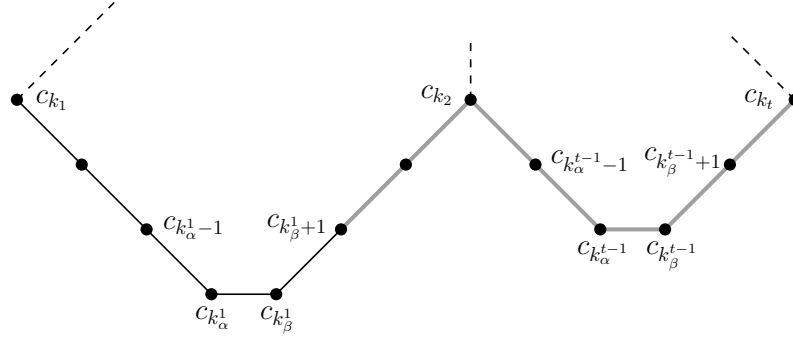


Figure 5.5: The gray path $C_k^r = \langle c_{k_\beta^1+1}, \dots, c_{k_t} \rangle$ has to be shifted to the right whenever $P_{k+1} = \langle z \rangle$ is shifted to the right.

- (S1) For each $v \in \bigcup_{i=1}^\ell \mathcal{L}(c_i)$, set $x(v) = x(v) - p$. (Vertices are shifted to the left by p .)
- (S2) For each $v \in \bigcup_{i=r}^q \mathcal{R}(c_i)$, set $x(v) = x(v) + p$. (Vertices are shifted to the right by p .)
- (S3) Let $(x(t), y(t)) = \mu(c_\ell, c_r)$, where $t = (x(t), y(t))$ is the intersection of the straight line through c_ℓ with slope $+1$ and the straight line through c_r with slope -1 (compare Section 1.2). Set $z_i = (x(t) - p - 1 + 2i, y(t) - p + 1)$, $i = 1, \dots, p$. (Set position for each vertex $z_i \in P_{k+1}$.)
- (S4) $\mathcal{L}(z_i) = \bigcup_{z \in N_{G_k}^{\mathcal{L}}} \mathcal{L}(z) \cup \{z_i\}$ and $\mathcal{R}(z_i) = \bigcup_{z \in N_{G_k}^{\mathcal{R}}} \mathcal{R}(z) \cup \{z_i\}$, $i = 1, \dots, p$. (Compute the set of vertices for each vertex $z_i \in P_{k+1}$ that has to be shifted whenever z_i is shifted.)

Shifting the sets of vertices in Steps 1 and 2 ensures that the vertices c_ℓ, \dots, c_r are visible from P_{k+1} and, thus, P_{k+1} can be added to the drawing Γ_k without creating any edge crossings as well as all inner faces are non-strictly convex. Clearly, all three conditions for the drawing are maintained.

Lemma 5.10. *The faces of G_k , $k = 1, \dots, s$, remain non-strictly convex during Algorithm 6.*

Proof. We prove this by induction on k , for $k = 1, \dots, s$. By construction, this clearly holds for $k = 1$.

So assume that $k > 1$. Let $P_k = \langle z_1, \dots, z_p \rangle$. When inserting P_k , the vertices c_1, \dots, c_ℓ are shifted to the left and the vertices c_r, \dots, c_q are shifted to the right. This yields that the inserted candidate faces are non-strictly convex.

Algorithm 6: Shift Method of **Kant**

Input : $G = (V, E)$ planarly embedded triconnected graph
 $v_1 \in V$ on the outer face of G
canonical ordering $\Pi = \langle P_0, \dots, P_s \rangle$ of (G, v_1)

Output: planar, straight-line drawing of G on a $(2n - 4) \times (n - 2)$ grid

ShiftMethod

```

 $P_0 \leftarrow \langle v_1, v_2 \rangle, P_1 \leftarrow \langle v_3, \dots, v_p \rangle$ 
 $v_1 = (-p + 2, 0), \mathcal{L}(v_1) \leftarrow \{v_1\}, \mathcal{R}(v_1) \leftarrow \emptyset$ 
 $v_2 = (p - 2, 0), \mathcal{R}(v_2) \leftarrow \{v_2\}, \mathcal{L}(v_2) \leftarrow \emptyset$ 
for  $i = 3, \dots, p$  do
   $v_i = (2i - p - 3, 1)$ 
   $\mathcal{L}(v_i) \leftarrow \{v_i\}, \mathcal{R}(v_i) \leftarrow \{v_i\}$ 
for  $k = 2, \dots, s$  do
   $P_k \leftarrow \langle z_1, \dots, z_p \rangle$ 
  for  $v \in \bigcup_{i=1}^{\ell} \mathcal{L}(c_i)$  do
     $x(v) = x(v) - p$ 
  for  $v \in \bigcup_{i=r}^q \mathcal{R}(c_i)$  do
     $x(v) = x(v) + p$ 
   $t = (x(t), y(t)) \leftarrow \mu(c_\ell, c_r)$ 
  for  $i = 1, \dots, p$  do
     $z_i = (x(t) - p - 1 + 2i, y(t) - p + 1)$ 
     $\mathcal{L}(z_i) \leftarrow \bigcup_{z \in N_{G_k}^{\mathcal{L}}} \mathcal{L}(z) \cup \{z_i\}$ 
     $\mathcal{R}(z_i) \leftarrow \bigcup_{z \in N_{G_k}^{\mathcal{R}}} \mathcal{R}(z) \cup \{z_i\}$ 
end

```

Reversely, when shifting a vertex z_i , $i = 1, \dots, p$, of P_k in a later step of the algorithm, then also $\mathcal{L}(z_i)$ and $\mathcal{R}(z_i)$, respectively, is shifted with the same value in the same direction. This yields the convexity of the inner faces of G_k . \square

Algorithm 6 can easily be implemented in quadratic time. De Fraysseix et al. [1990] show an $\mathcal{O}(n \log n)$ -implementation if the graph is triangular. Chrobak and Payne [1995] improve this result by describing a data structure that can be used to implement the algorithm in linear time, still if the graph is triangular. Instead of computing the x -coordinates of the vertices in every step, Chrobak and Payne calculate only relative positions of the vertices and, in a final step, the real x -coordinates are determined. A good description of the implementation can also be found in Nishizeki and Rahman [2004].

In order to achieve linear running-time also for triconnected, planar graphs, a leftmost canonical ordering is used. The main idea is the same as in the triangular scenario, i. e., that the exact coordinates for the vertices in the current drawing are only computed when they are necessary. See Kant [1996] for details. Further, Kant modifies Algorithm 6 slightly such that all inner faces are strictly convex.

Together with Lemma 5.10 we get the following theorem:

Theorem 5.11 (Kant, 1996). *Let G be a triconnected, planar graph. A planar, straight-line, strictly convex drawing of G on a $(2n-4) \times (n-2)$ grid can be computed in $\mathcal{O}(n)$ time and space.*

As mentioned above, this grid size is improved to $(n-2) \times (n-2)$ by Chrobak and Kant [1997]. Their algorithm also places the vertices following a canonical ordering and maintaining certain invariants for the contour of the drawing. Again, when installing a new set of vertices, some of the previously placed vertices have to be shifted in order to maintain the contour invariants. A description of the algorithm can be found, beside the original paper, in Nishizeki and Rahman [2004].

5.3.3 Triangulating a Planar Graph

In this section, we briefly review an algorithm of Kant [1993, Section 6] that triangulates a biconnected, plane graph while computing a canonical ordering at the same time. More about triangulating graphs can be found in Section 1.4.

Let $G = (V, E)$ be a biconnected, plane graph with a given vertex v_1 on the outer face. The algorithm follows the same idea as Algorithm 2 by successively adding vertices to G_k , $k = 2, \dots, n-1$, where $G_2 = (\{v_1, v_2\}, \{\{v_1, v_2\}\})$ and v_2 is the neighbor of v_1 on the outer face in counterclockwise direction.

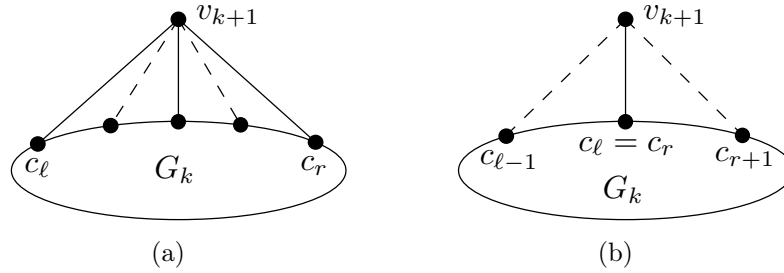


Figure 5.6: Dashed edges are added to the drawing in order to fulfill the invariant.

We use the same notations of *outgoing edges*, *left neighbor* c_ℓ , and *right neighbor* c_r as in Section 2.2.1. Again, let $v_1 = c_1, \dots, c_q = v_2$ be the vertices on the outer face C_k in clockwise direction, $k = 3, \dots, n$.

While triangulating the graph incrementally, we maintain the following invariant:

- (I) In each step $k = 3, \dots, n$, all inner faces of G_k are triangulated.

We choose the next vertex v_{k+1} that is added to G_k in such a way such that there exists at least one edge $\{v_k, c_i\}$, for $i = 1, \dots, q$. Let c_ℓ and c_r be the left and right neighbor of v_{k+1} on C_k , respectively. Note that possibly $\ell = r$.

If v_{k+1} has at least two neighbors on C_k , then by the planarity of G , none of the vertices $c_{\ell+1}, \dots, c_{r-1}$ has an outgoing edge to a vertex v_j , $j > k + 1$. Thus, we can add all edges $\{v_i, v_{k+1}\}$, $i = \ell + 1, \dots, r - 1$, if they are not yet present. This ensures that all faces that are added to G_k are triangles and the invariant is maintained. Figure 5.6(a) illustrates this.

If v_{k+1} has exactly one neighbor on C_k , then let v_{k+1} be the clockwise and counterclockwise neighbor of $c_{\ell-1}$ and c_{r+1} in the incidence list of $c_\ell = c_r$, respectively. Thus, we can add the edges $\{c_{\ell-1}, v_{k+1}\}$ and $\{c_{r+1}, v_{k+1}\}$. Again, if the invariant is fulfilled for G_k , then also for G_{k+1} . In Figure 5.6(b), v_{k+1} is the clockwise neighbor of $c_{\ell-1}$ as well as the counterclockwise neighbor of c_{r+1} in the incidence list of $c_\ell = c_r$.

Kant [1993] shows how to implement this algorithm in linear time.

Chapter 6

Schnyder Woods

Schnyder woods and synonymous concepts for triangular and triconnected, planar graphs were introduced in Chapter 3. In this chapter, we describe different algorithms for constructing Schnyder woods of triangular and triconnected, planar graphs, and applications of Schnyder woods in graph drawing.

In 1989 and 1990, Schnyder presents the first algorithm to construct a Schnyder wood of a triangular graph. His idea of contracting and expanding edges can already be found in Kampen [1976]. In 2001, Felsner extends Schnyder's construction to triconnected, planar graphs. Since both algorithms share the same principles, we only describe the more general version of Felsner [2001] in Section 6.2.2.

Di Battista, Tamassia, and Vismara [1999] give another approach to construct a Schnyder wood of a triconnected, planar graph using canonical ordering. It is described in Section 6.2.1. Nakano [2000] uses the same idea as Di Battista et al. [1999] but for triangular graphs.

We describe in Section 6.1 a variant of the algorithm of Brehm [2000] that directly outputs a Schnyder wood without clockwise and counterclockwise cycles, respectively. As we have seen in Chapter 3, some concepts are easier for triangular graphs than for triconnected, planar graphs. Therefore, we extend these ideas to triconnected, planar graphs in Section 6.2.3 [Badent et al., 2011].

Well-known applications of Schnyder woods in graph drawing are then presented in Section 6.3. More precisely, we describe the algorithm of Schnyder [1989, 1990] to create a straight-line embedding of triangular graphs on a grid of polynomial size, i. e., on an $(n - 2) \times (n - 2)$ grid. In this context, we review in tabular form the results of other grid drawing algorithms and explain the algorithm of Felsner [2001]. Finally, we sketch the connection of Schnyder woods to orthogonal surfaces and geodesic embeddings.

Beside the methods to construct a Schnyder wood that we explain in detail in this section, there are different approaches that are mentioned hereafter. [Fürer, He, Kao, and Raghavachari \[1992\]](#) compute a Schnyder wood of a triangular graph in parallel, in $\mathcal{O}(\log n \log \log n)$ time using $\frac{n}{\log n}$ processors on a CREW PRAM and using randomization in $\mathcal{O}(\log n)$ expected time using $\frac{n \log \log n}{\log n}$ processors on a CRCW PRAM. [He and Kao \[1993\]](#) extend these results to triconnected, planar graphs. They compute a canonical ordering via bidirectional realizer. A bidirectional realizer is similar to a Schnyder wood, however, face vertices are inserted and included in the three trees. It can be computed in $\mathcal{O}(\log^4 n)$ time using $\mathcal{O}(n^2)$ processors on a CREW PRAM and transformed into a canonical ordering in $\mathcal{O}(\log^2 n)$ time with $\mathcal{O}(n)$ processors on a CREW PRAM.

[Chiang, Lin, and Lu \[2005\]](#) construct a Schnyder wood via orderly spanning trees in linear time.

One further application of Schnyder woods in graph drawing that is not shown in the remainder of this section are visibility representations [[Lin et al., 2004](#)]. Beside graph drawing, Schnyder woods have a broad field of applications especially in graph encoding [[Aleardi et al., 2008, 2009](#), [Chuang et al., 1998](#), [Chiang et al., 2001](#)].

A related concept of Schnyder woods are regular edge labelings that were introduced in Section 2.4.2. They are used to construct rectangular duals [[He, 1993](#), [He and Kao, 1995](#), [Kant and He, 1997](#)] and visibility representations [[Kant and He, 1997](#)] of 4-connected, triangular graphs.

6.1 Triangular Graphs

To construct a Schnyder wood, [Schnyder \[1989, 1990\]](#) contracts edges that are incident to exterior vertices until the graph consists of a triangle only. Then, he expands the edges in reversing order while assigning labels and orientations to the edges. [Schnyder](#) proves that always a contractible edge exists. Moreover, his algorithm can generate every Schnyder wood and it runs in linear time.

A similar approach to construct a Schnyder wood of a triangular graph is due to [Brehm \[2000\]](#). However, instead of contracting edges, he chooses an *eligible* vertex on the outer face of the graph, i. e., a vertex that is not incident to a chord, assigns labels and orientations to all exterior edges of a certain cycle, and deletes the selected vertex. If only one edge is left, [Brehm](#) proves that the construction yields a Schnyder wood. He also shows that an eligible vertex exists in every step of his algorithm that runs in linear time. Moreover, the algorithm cannot only compute all possible Schnyder woods, but also, by selecting carefully the next eligible vertex, it constructs

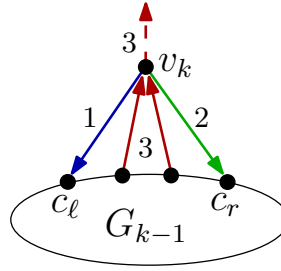


Figure 6.1: Labeling and orientation of the edges incident to v_k .

a special one, namely, the Schnyder wood without clockwise and counterclockwise cycles, respectively.

In this section, we describe an algorithm that combines the ideas of [Brehm \[2000\]](#) and [Di Battista et al. \[1999\]](#) to construct a Schnyder wood without clockwise and counterclockwise cycles, respectively. Our algorithm is based on the leftist (rightist) canonical ordering of a triangular graph and assigns labels and orientations to the edges at the same time when the leftist canonical ordering is computed. Also, it runs in linear time.

Let $G = (V, E)$ be a triangular graph and let v_1, v_2 , and v_n be the vertices on the outer face of G in counterclockwise direction. Let $\Pi = (v_1, v_2, \dots, v_n)$ be the leftist canonical ordering of (G, v_1) . Note that in the triangular case, every path of the ordering except $P_0 = \{v_1, v_2\}$ is a singleton. For $k = 1, \dots, n$, let $G_k = G[V_k] = (V_k, E_k)$ be the subgraph induced by $V_k = \{v_1, \dots, v_k\}$, and let C_k be the outer face of G_k . Again, let $v_1 = c_1, c_2, \dots, c_q = v_2$ be the vertices from left to right on C_{k-1} , $k = 3, \dots, n$. Let c_ℓ be the neighbor of v_k on C_{k-1} such that ℓ is as small as possible and let c_r be the neighbor of v_k on C_{k-1} such that r is as large as possible. We call c_ℓ the *left neighbor* and c_r the *right neighbor* of v_k .

Let (u, v) denote the directed edge from u to v and let $\text{label}(u, v) = i$ indicate that (u, v) has label i . A Schnyder wood can be constructed by processing the vertices in the leftist canonical ordering and assigning labels and orientations to the interior edges incident to v_k , $k = 3, \dots, n - 1$, as follows:

1. $\text{label}(v_k, c_\ell) = 1$
2. $\text{label}(v_k, c_r) = 2$
3. $\text{label}(c_i, v_k) = 3, i = \ell + 1, \dots, r - 1$

The interior edges incident to v_n receive $\text{label}(c_i, v_n) = 3$, for $i = \ell + 1, \dots, r - 1$. This procedure is also described in [Algorithm 7](#) and illustrated in [Figure 6.1](#).

Algorithm 7: Schnyder wood of a triangular graph without clockwise cycles

Input : $G = (V, E)$ triangular graph
 $v_1 \in V$ on the outer face of G
leftist canonical ordering $\Pi = (v_1, v_2, \dots, v_n)$ of (G, v_1)

Output: Schnyder wood of (G, v_1) without clockwise cycles

SchnyderWood

```

for  $k = 3, \dots, n - 1$  do
   $c_\ell, c_{\ell+1}, \dots, c_{r-1}, c_r \leftarrow$  neighbors of  $v_k$  on  $C_{k-1}$  from left to right
  label $(v_k, c_\ell) = 1$ 
  label $(v_k, c_r) = 2$ 
  for  $i = \ell + 1, \dots, r - 1$  do
    label $(c_i, v_k) = 3$ 
  all interior edges incident to  $v_n$  are incoming edges of  $v_n$  with label 3
end

```

We prove in the following that this construction yields a Schnyder wood without clockwise oriented triangles.

Lemma 6.1. *In Algorithm 7, no edge on C_k is labeled 3, $k = 2, \dots, n$.*

Proof. For $k = 2$ the statement is true since $e = \{v_1, v_2\}$ is not labeled at all. When adding a vertex v_k , only interior edges of the cycle $\{v_k, c_\ell, \dots, c_r, v_k\}$ are labeled 3. Thus, all edges on $C_k - e$ are labeled either 1 or 2, $k = 2, \dots, n - 1$. When adding v_n , the exterior edges incident to v_n are not labeled. \square

Theorem 6.2. *Let G be a triangular graph with vertex v_1 on the outer face. Algorithm 7 computes a Schnyder wood of (G, v_1) without clockwise oriented cycles in linear time and space.*

Proof. First, we show that Algorithm 7 computes a Schnyder wood of (G, v_1) .

By Lemma 6.1, every vertex on $C_k - \{v_1, v_2\}$ has exactly one outgoing edge with label 1, one outgoing edge with label 2, and no outgoing edge with label 3. Since we add the vertices in canonical ordering, for every vertex v_k there exists an edge $\{v_k, v_j\}$ with $v_j \notin G_k$, $j > k$ (compare Definition 2.3). This edge becomes either an outgoing edge for v_k with label 3 when v_j is added to G_{j-1} or, otherwise, since G is triangulated, v_k is incident to another edge $\{v_k, v_i\}$ with $v_i \notin G_k$, $i > j > k$. Let v_h be the neighbor of v_k such that h is as large as possible. Then, $\text{label}(v_k, v_h) = 3$. Also, the outgoing edges with label 1, 2, and 3 appear in counterclockwise order around each interior vertex of G .

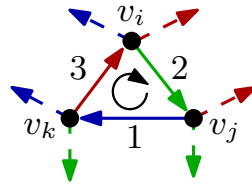


Figure 6.2: Clockwise oriented face.

For every vertex on C_k the possibly incoming edges with label 3 appear in the clockwise sector of the outgoing edges with label 2 and 1. Assume for a contradiction that there is an incoming edge $\{v_i, v_k\}$ of v_k with label 1 that appears in the adjacency list of v_k in the clockwise sector between the outgoing edge with label 1 and the outgoing edge with label 3. Since $\text{label}(v_i, v_k) = 1$, v_k is the left neighbor of v_i on C_{i-1} . As G is triangulated and C_k a simple cycle, this is a contradiction. The same argument holds also for the incoming edges of v_k with label 2.

It is easy to see that edges incident to the three exterior vertices are labeled and oriented correctly.

Using Lemma 3.5, it remains to show that G does not contain a directed face. Assume that we oriented and labeled the edges according to the leftist canonical ordering Π and, nevertheless, constructed a face oriented in clockwise direction as shown in Figure 6.2. Let v_k, v_j , and v_i be the vertices incident to this face such that $\text{label}(v_j, v_k) = 1$, $\text{label}(v_i, v_j) = 2$, and $\text{label}(v_k, v_i) = 3$. From this follows that $k < j < i$. When v_j is added to Π , it is the leftmost feasible candidate. This means that v_i is not feasible at that time and has, therefore, no neighbor left of v_k on C_{j-1} , or it has both neighbors left and right of v_k . Note that v_i cannot be incident to a feasible candidate left of v_i since v_j is the leftmost feasible candidate for step j . If v_i has no neighbor left of v_k on C_{j-1} , then $\text{label}(v_i, v_k) = 1$ which is a contradiction. If it has both neighbors left and right of v_k on C_{j-1} , then $\text{label}(v_j, v_i) = 3$ which is again a contradiction.

It is obvious that the algorithm can be carried out in linear time and space. \square

We gave a simple algorithm that uses the leftist canonical ordering to compute a Schnyder wood without clockwise oriented triangles. Also, its proof of correctness is very intuitive and does not make use of other concepts than canonical ordering. We point out that if in Algorithm 7 the rightist canonical ordering is used, then it computes a Schnyder wood without counterclockwise oriented triangles.

6.2 Triconnected Graphs

As already mentioned in Sections 3.4–3.6, the construction of a minimal Schnyder wood described above does not hold any more for triconnected, planar graphs.

We show how to generally compute Schnyder woods using canonical ordering [Di Battista et al., 1999] and edge contraction [Felsner, 2001], respectively. Finally, we adapt Algorithm 2 such that it outputs the leftist ordered path partition [Badent et al., 2011]. According to Theorem 3.47, this corresponds to the minimal Schnyder wood.

In this section, let $G = (V, E)$ be a triconnected, planar graph and let $\langle v_2, v_1, v_n \rangle$ be a path on the outer face of G in clockwise direction. We denote $v_1 = a_1$, $v_2 = a_2$, $v_n = a_3$ and assume on the labels $i = 1, 2, 3$ a cyclic structure so that $3 + 1 = 1$ and $1 - 1 = 3$.

6.2.1 Canonical Ordering

Di Battista, Tamassia, and Vismara [1999] construct a Schnyder wood of a triconnected, planar graph using canonical ordering. Their construction extends the one described in Section 6.1 and runs in linear time and space. However, as we have seen in Section 3.6, it is not possible to construct all Schnyder woods in this way. This led us to the definition of ordered path partitions (Definition 3.42).

Let $\Pi = (P_0, \dots, P_s)$ be a canonical ordering of (G, v_1) . Again, let $v_1 = c_1, c_2, \dots, c_q = v_2$ be the vertices from left to right on C_{k-1} . Let c_ℓ be the neighbor of P_k on C_{k-1} such that ℓ is as small as possible and let c_r be the neighbor of P_k on C_{k-1} such that r is as large as possible. We denote by (u, v) the directed edge from u to v and $\text{label}(u, v) = i$ indicates that (u, v) has label i .

A Schnyder wood can be constructed by processing the paths $P_k = \langle z_1, \dots, z_p \rangle$, $k = 1, \dots, s$, in canonical ordering and by assigning labels and orientations to the edges as follows:

1. $\text{label}(v_2, v_1) = 1$, $\text{label}(v_1, v_2) = 2$
2. $\text{label}(z_1, c_\ell) = 1$, $\text{label}(z_p, c_r) = 2$
3. $\text{label}(z_{i+1}, z_i) = 1$, $\text{label}(z_i, z_{i+1}) = 2$, $i = 1, \dots, p - 1$
4. If z_1 and z_p is the only neighbor of c_ℓ and c_r in $G - G_{k-1}$, respectively, then $\text{label}(c_\ell, z_1) = 3$ and $\text{label}(c_r, z_p) = 3$, respectively.
5. If $P_k = \langle z \rangle$ is a singleton, then $\text{label}(c_i, z) = 3$ for all neighbors c_i of z on C_{k-1} , $i = \ell + 1, \dots, r - 1$.

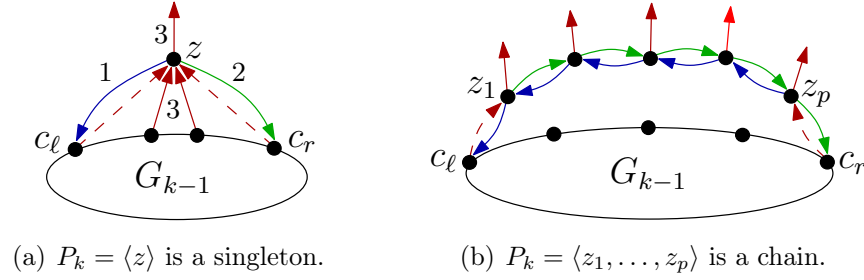


Figure 6.3: Labeling and orientation of the next path P_k .

This approach is described in Algorithm 8 and illustrated Figure 6.3.

In the following, we give an intuitive and simple proof that this construction yields a Schnyder wood by using only the properties of canonical ordering.

Theorem 6.3 (Di Battista et al., 1999). *Let G be a triconnected, planar graph with vertex v_1 on the outer face. Algorithm 8 computes a Schnyder wood of (G, v_1) in linear time and space.*

Proof. Note that we assume that the graph G is implicitly augmented to the closure G_∞ and that the implicit edges $\{a_i, v_\infty\}$ are oriented towards v_∞ and labeled i , $i = 1, 2, 3$. Thus, Property 3.19(2) is fulfilled. By construction, also Property 3.19(1) is satisfied.

Clearly, every vertex of G is incident to an outgoing edge with label 1 and 2. Once the last neighbor of a vertex is added to the canonical ordering, the vertex gets also incident to an outgoing edge labeled 3. Thus, every edge has outdegree one in each label.

Let $P_k = \langle z_1, \dots, z_p \rangle$. We remark that $p = 1$ is possible. Let c_ℓ be the left neighbor of P_k on C_{k-1} . Assume for a contradiction that there exists a vertex v such that $\text{label}(v, z_1) = 3$ and this edge appears in the adjacency list of z_1 in the clockwise sector between the outgoing edge with label 1 and the outgoing edge with label 3. Then, z_1 is the neighbor of v with the largest canonical ordering number. Also, v is left of c_ℓ on C_{k-1} . But then $\text{label}(z_1, v) = 1$. The same argumentation holds if an incoming edge with label 3 appears in the clockwise sector between the outgoing edges of label 3 and 2 of a vertex.

Assume for a contradiction that there exists a vertex v such that $\text{label}(v, z_1) = 1$. This edge appears in the clockwise sector between the outgoing edges with label 1 and 3. Let w be the endvertex of the outgoing edge of z_1 with label 3. Then, w appears after v in the canonical vertex ordering. Also, w and v are not part of the same path since this contradicts the definition of a canonical ordering. Let

Algorithm 8: Schnyder wood of a triconnected graph

Input : $G = (V, E)$ triconnected, planar graph
 $v_1 \in V$ on the outer face of G
 canonical ordering $\Pi = (P_0, \dots, P_s)$ of (G, v_1)

Output: Schnyder wood of (G, v_1)

SchnyderWood

```

label( $v_2, v_1$ ) = 1
label( $v_1, v_2$ ) = 2
for  $k = 1, \dots, s$  do
  if  $P_k = \langle z \rangle$  is a singleton then
     $c_\ell, c_{\ell+1}, \dots, c_{r-1}, c_r \leftarrow$  neighbors of  $z$  on  $C_{k-1}$  from left to right
    label( $z, c_\ell$ ) = 1
    label( $z, c_r$ ) = 2
    if  $c_\ell$  has no neighbor in  $G - G_k$  then
      label( $c_\ell, z$ ) = 3
    if  $c_r$  has no neighbor in  $G - G_k$  then
      label( $c_r, z$ ) = 3
    for  $i = \ell + 1, \dots, r - 1$  do
      if  $\{c_i, z\} \in E$  then
        label( $c_i, z$ ) = 3
  else if  $P_k = \langle z_1, \dots, z_p \rangle$  is a chain then
     $c_\ell \leftarrow$  left neighbor of  $P_k$ 
     $c_r \leftarrow$  right neighbor of  $P_k$ 
    label( $z_1, c_\ell$ ) = 1
    label( $z_p, c_r$ ) = 2
    for  $i = 1, \dots, p - 1$  do
      label( $z_{i+1}, z_i$ ) = 1
      label( $z_i, z_{i+1}$ ) = 2
    if  $c_\ell$  has no neighbor in  $G - G_k$  then
      label( $c_\ell, z_1$ ) = 3
    if  $c_r$  has no neighbor in  $G - G_k$  then
      label( $c_r, z_p$ ) = 3
end

```

v be part of path P_i , $i > k$. When adding P_i , z_1 is the left neighbor of v since $\text{label}(v, z_1) = 1$. Then, C_i is no simple cycle any more which is a contradiction. The same argumentation holds for an edge with label 2 that appears in the clockwise sector between the outgoing edges of a vertex with label 3 and 2.

This completes the requirements of Property 3.19(3).

From the canonical vertex ordering (Definition 2.7) follows Property 3.19(4), i. e., G has no cycle where all edges have the same label.

It is obvious that the algorithm can be carried out in linear time and space. \square

6.2.2 Edge Contraction

Felsner [2001] uses edge contractions to create Schnyder woods of triconnected, planar graphs. His construction extends the one of Schnyder [1989] for triangular graphs (Theorem 3.9). The brief outline of his method is as follows:

1. Choose an edge e of G and let G/e be the graph obtained by contracting e .
2. Recursively construct a Schnyder labeling of G/e .
3. Expand the labeling of G/e to a Schnyder labeling of G .

We proved in Lemma 1.18 that every triconnected graph G with at least five vertices has an edge e such that G/e is again triconnected. Such an edge is called *contractible*. Felsner extends this observation with the objective that a contractible edge has further properties and if none exists, another strategy has to be applied.

We remark again that our definition of Schnyder woods for triconnected, planar graphs (Definition 3.19) is different from the one in Felsner [2004a] and, thus, our construction, that is illustrated in Figure 6.4, is slightly easier.

Assume first that a_3 has a neighbor $x \notin C_n$ such that $e = \{a_3, x\}$ is contractible. Let a_3, x_1, \dots, x_i be the neighbors of x in counterclockwise order. Then, edge e is contracted into one vertex a_3 . By Corollary 3.23, all interior angles of vertex a_3 are labeled 3. The angles of the edge $\{a_3, x_j\}$ are labeled 1 and 2 at x_j in counterclockwise direction, $j = 1, \dots, i$.

When the edge e is expanded, the labeling of G/e is simultaneously extended to a labeling of G such that the labels of all faces that are not incident to e remain unchanged. This is done as follows. All angles of the edges $\{x, x_j\}$ at vertex x are labeled 3, $j = 2, \dots, i-1$. The edge $\{a_3, x\}$ is labeled 1 and 2 at x in counterclockwise direction. If there is an edge $\{a_3, x_1\}$ or $\{a_3, x_i\}$, then the angles at x_1 and x_i ,

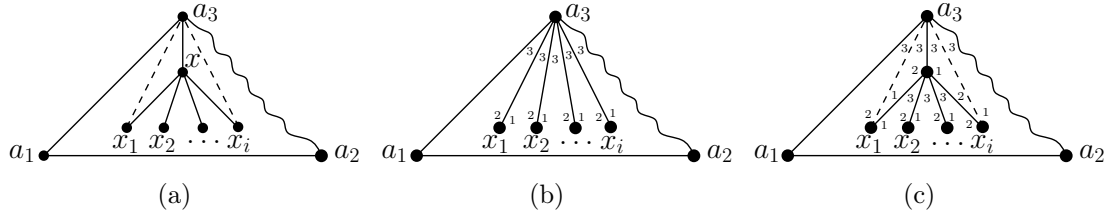


Figure 6.4: (a)-(b) Contraction of the edge $e = \{a_3, x\}$. (b)-(c) Expansion of the edge $e = \{a_3, x\}$ and labeling corresponding angles.

respectively, are labeled 1 and 2 in counterclockwise direction. The remaining labels at $x_j, j = 1, \dots, i$, remain unchanged.

Assume now that a_3 has no neighbor $x \notin C_n$ such that $e = \{a_3, x\}$ is contractible. Thus, G/e is biconnected and it exists a separation pair such that one vertex of it is a_3 . Let the other one be y . Then, $\{a_3, x, y\}$ is a separator of G . Let C'_1 and C'_2 be the two connected components of $G \setminus \{a_3, x, y\}$, and let $C_1 = (V(C'_1) \cup \{a_3, x, y\}, E(C_1) \cup \{\{a_3, y\}, \{x, y\}\})$ and $C_2 = (V(C'_2) \cup \{a_3, x, y\}, E(C_2) \cup \{\{a_3, y\}, \{x, y\}\})$ assuming the edges $\{a_3, y\}$ and $\{a_3, x\}$ are not present in C'_1 and C'_2 , respectively. Note that adding the edges $\{a_3, y\}$ and $\{a_3, x\}$ to each $C_i, i = 1, 2$, yields the triconnectivity of the components.

We want to assign angle labels to each component such that the union of both components together with the assigned labels results in a Schnyder labeling of the whole graph as shown in Figure 6.5.

Since $\langle a_2, a_1, a_3 \rangle$ is a path on the outer face, one component contains a_1, a_2 , and a_3 . Let this component be C_1 . Then, labeling all angles of C_1 yields that the triangle a_3, x, y has all three labels. Let x be the vertex with label 1 and let y be the vertex with label 2 in this triangle as shown Figure 6.5(a). When labeling the angles of C_2 , we treat x and y as the other two special vertices and construct a Schnyder labeling of C_2 . If the edges $\{a_3, y\}$ and $\{x, y\}$ have been present in G , then gluing the labelings of C_1 and C_2 together yields a Schnyder labeling of G .

If a face of G is split by inserting an edge, then we have to be more carefully. These case is illustrated in Figure 6.5(b). Assume that the edge $\{x, y\}$ splits a face f . Let f_1 be the part of f belonging to C_1 and let f_2 be the part of f belonging to C_2 . The case for the edge $\{a_3, y\}$ can be handled analogously.

Let x' be the neighbor of x on f in C_2 and let y' be the neighbor of y on f in C_2 . Since all angles of x are labeled 1 in C_2 (by Corollary 3.23), the angles of $\{x, x'\}$ at vertex x' are labeled 2 and 3 in counterclockwise order around x' . Analogously, since all angles of y are labeled 2 in C_2 , the angle of $\{y, y'\}$ at vertex y' are labeled 1 and 3 in clockwise order around y' . This is due to Lemma 3.22.

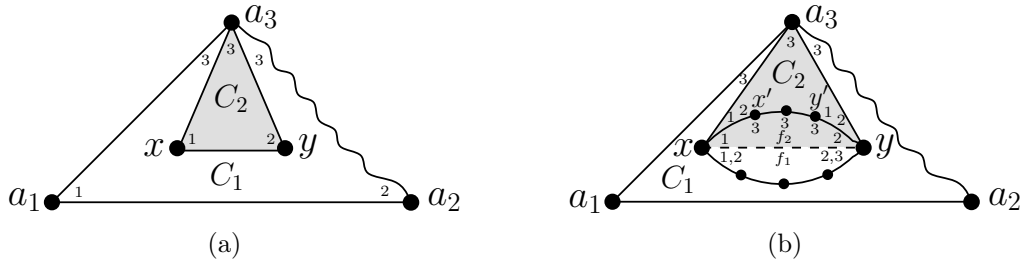


Figure 6.5: (a) Separate labeling of two components C_1 and C_2 . (b) Gluing two Schnyder labelings together.

Because of the rule of vertices, the angle at x in f_1 is either labeled 1 or 2; the angle at y is either labeled 2 or 3. Thus, taking the labels of f_1 for G yields a Schnyder labeling. Since Schnyder labelings are in one-to-one correspondence with Schnyder woods as shown in Section 3.2.2, this completes the construction.

6.2.3 Minimal Schnyder Wood

Fusy, Schaeffer, and Poulalhon [2008] describe a linear-time algorithm that computes the minimal α_0 -orientation of a triconnected, planar graph whose outer face is a triangle. Since α_0 -orientations are in bijection with Schnyder woods [Felsner, 2004b], their algorithm can be used to compute the minimal Schnyder wood.

We use the results of Section 3.6 and adapt Algorithm 2 such that it computes the leftist ordered path partition [Badent et al., 2011]. By Theorem 3.47 the leftist ordered path partition corresponds to the minimal Schnyder wood. Thus, our algorithm is an alternative method for computing the minimal Schnyder wood.

Replace line \blacktriangleright^1 in Algorithm 3 by

while $j > 0$ **and not** *forbidden*(z_j) **do**

 and line \blacktriangleright^2 in the same algorithm by

if $j = 0$ **then**

 Finally, replace the **if**-loop \blacktriangledown in Algorithm 4 by

let $\langle (z_0, z_1), (z_1, z_2), \dots, (z_p, z_{p+1}) \rangle := \text{CANDIDATE.CHAIN}$

if *singular*(z_p) **then**

 | remove neighboring items with z_p as singleton from BELT

Theorem 6.4. *The modification of Algorithm 2 as specified above computes the leftist ordered path partition of a triconnected, planar graph in linear time.*

Proof. The running time of Algorithm 2 is not affected by the changes.

The difference to a canonical ordering is that a path of the leftist ordered path partition can be a chain with an attached singleton to the right. This path would be split into a singleton and a chain in a canonical ordering.

The modifications in lines \blacktriangleright^1 and \blacktriangleright^2 in Algorithm 3 guarantee that the algorithm does not skip a candidate if it contains a singular vertex. Since we process the candidate faces from left to right and the vertices in a face from right to left, only the rightmost vertex of a path in the leftist ordered path partition can be singular. If a vertex is forbidden, the algorithm continues with the next face.

If the rightmost vertex of a path is singular, all neighboring items are still removed from the belt (**if**-loop \blacktriangledown in Algorithm 4). \square

6.3 Drawings

In this section, we briefly sketch some results about drawings of triangular and triconnected, planar graphs, respectively, that make use of Schnyder woods and related structures. Similar to the overview on grid drawings given in Section 5.3.1, we review the improvement on the grid size of different straight-line drawings that are created by using Schnyder woods for triconnected, planar graphs. This is illustrated in Table 6.1. The following notations are used: Let f denote the number of faces of the graph. Let Δ_0 be the number of counterclockwise oriented faces in the minimal Schnyder wood and let Δ be the number of faces that have a counterclockwise edge in each label in the minimal Schnyder wood.

grid size	authors
$(f - 2) \times (f - 2)$	Di Battista et al., 1999
$(f - 1) \times (f - 1)$	Felsner, 2001
$(n - 1 - \Delta_0) \times (n - 1 - \Delta_0)$	Zhang and He, 2003
$\mathcal{O}(n^{\frac{7}{2}}) \times \mathcal{O}(n^{\frac{7}{2}})$	Rote, 2005
$(n - 2 - \Delta) \times (n - 2 - \Delta), 0 \leq \Delta \leq \frac{n}{2} - 2$	Bonichon et al., 2005, 2007

Table 6.1: Grid size of different drawing algorithms using Schnyder woods.

6.3.1 Barycentric Representation of Triangular Graphs

Schnyder [1990] uses Schnyder woods to define a mapping of the vertices of a triangular graph onto the plane that yields a straight-line drawing.

The following introductory lemma helps to build an understanding of the subsequent results. Let $G = (V, E)$ be a triangular graph and let (v_1, v_2, v_3) denote the barycentric coordinates of vertex v as defined in Section 1.2.

Lemma 6.5 (**Schnyder, 1990**). *Let*

$$v \in V \rightarrow (v_1, v_2, v_3) \in \mathbb{R}^3$$

be a barycentric representation of a graph G . Then, given any three non-collinear points p , q , and r , the mapping

$$\Gamma: v \in V \rightarrow v_1p + v_2q + v_3r$$

is a straight-line embedding of G in the plane spanned by p , q , and r .

An edge $\{u, v\} \in E$ is represented by the straight line $\{\Gamma(u), \Gamma(v)\}$. Thus, each barycentric representation induces an embedding in the plane.

We require that the ordering of the three non-collinear points p , q , and r is counterclockwise and consider a triangular graph G together with a Schnyder wood. Let T_1 , T_2 , and T_3 be the three trees of the Schnyder wood according to Lemma 3.26.

In the first scenario, we assign coordinates that count triangles. In more detail, let v be an interior vertex of G and let v_i denote the number of elementary triangles in region $R_i(v)$, $i = 1, 2, 3$. Remember that the region of a vertex is defined in Section 3.2.3. Let v be an exterior vertex and the root of T_i . Then, for the three coordinates of v we define $v_i = 2n - 5$, $v_{i+1} = v_{i-1} = 0$. Again, the indices are modulo 3 such that $3 + 1 = 1$ and $1 - 1 = 3$.

A Schnyder labeling of a graph G is *induced* by a barycentric representation if $\text{label}(u, v) = i$ if and only if $u_i < v_i$ and $u_j > v_j$, $i, j = 1, 2, 3$, $i \neq j$.

Theorem 6.6 (**Schnyder, 1990**). *The function*

$$\Gamma: v \in V \rightarrow \frac{1}{2n-5}(v_1, v_2, v_3) \in \mathbb{R}^3$$

is a barycentric representation of G and the labeling of G that is induced by Γ is identical to the given labeling of G .

An example of a barycentric representation is given in Figure 6.6.

As the roots a_1 , a_2 , and a_3 of T_1 , T_2 , and T_3 are mapped to the reference points p , q , and r , the following corollary shows the relation of Theorem 6.6 and Schnyder woods using Lemma 6.5.

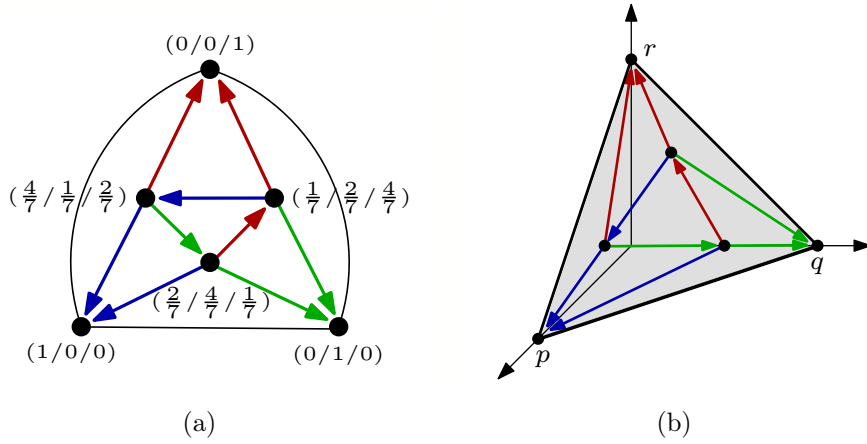


Figure 6.6: (a) Schnyder wood of a triangular graph. (b) Barycentric representation induced by the Schnyder wood of (a).

Corollary 6.7 (Schnyder, 1990). *Let $a_1, a_2,$ and a_3 be the roots of $T_1, T_2,$ and $T_3,$ the three trees of a Schnyder wood of a triangular graph. Then, for any choice of non-collinear points $p, q,$ and r such that a_1 is mapped to p, a_2 is mapped to $q,$ and a_3 is mapped to $r,$ the mapping*

$$v \in V \rightarrow \frac{1}{2n - 5}(v_1p + v_2q + v_3r)$$

is a straight-line embedding of G in the plane spanned by $p, q, r.$

Choosing the grid points $p = (0, 0), q = (2n - 5, 0),$ and $r = (0, 2n - 5),$ we obtain:

Proposition 6.8 (Schnyder, 1990). *The mapping*

$$v \in V \rightarrow (v_2, v_3)$$

is a straight-line embedding of G on the $(2n - 5) \times (2n - 5)$ integer grid.

Figure 6.7 shows an example of a straight-line grid drawing of the graph presented in Figure 6.6(a).

In the second scenario, we assign coordinates that count vertices. This leads to more compact drawings. We use the relaxed version of barycentric representations, namely, weak barycentric representations. Definitions were already given in Section 1.2. Note that Lemma 6.5 also applies to weak barycentric representations.

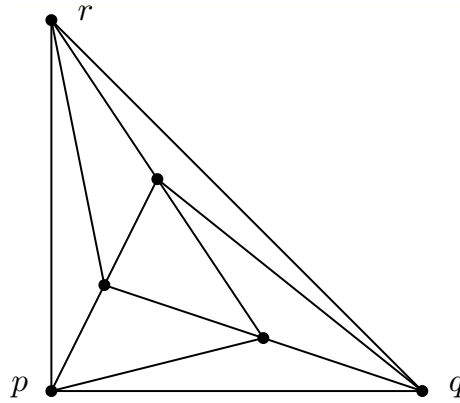


Figure 6.7: Straight-line grid drawing of the graph of Figure 6.6(a).

Again, consider a triangular graph G together with a Schnyder wood and its three trees T_1 , T_2 , and T_3 . For an interior vertex v of G , let $v'_i = |R_i(v)| - |P_{i-1}(v)|$. For the exterior vertices, we define $v'_i = n - 2$, $v'_{i+1} = 1$, $v'_{i-1} = 0$ for the root of T_i .

Schnyder shows that the function

$$v \in V \rightarrow (v'_1, v'_2, v'_3)$$

is injective and that

$$v \in V \rightarrow \frac{1}{n-2}(v'_1, v'_2, v'_3)$$

is a weak barycentric representation. Thus, Lemma 6.5 can be applied. Choosing $p = (0, 0)$, $q = (n - 1, 0)$, and $r = (0, n - 1)$ leads to the following theorem.

Theorem 6.9 (**Schnyder, 1990**). *The mapping*

$$v \in V \rightarrow (v'_2, v'_3)$$

is a straight-line embedding of G on the $(n - 2) \times (n - 2)$ integer grid.

From this, one can derive **Schnyder**'s main result:

Theorem 6.10 (**Schnyder, 1990**). *Every planar graph with $n \geq 3$ vertices has a straight-line embedding on an $(n - 2) \times (n - 2)$ integer grid.*

This theorem improves the bound of $(2n-4) \times (n-2)$ that is given by **de Fraysseix, Pach, and Pollack** [1990] using canonical ordering.

6.3.2 Convex Drawings of Triconnected Graphs

Tutte [1963] shows that every triconnected, planar graph G has a straight-line drawing where the boundary of each interior face is a convex polygon. However, **Tutte**'s drawings have some drawbacks such as a bad *angular resolution*, i. e., the size of the smallest angle between two edges that are incident to the same vertex is very small, or the ratio between the smallest and the largest distance between any two vertex positions is very large. Both aesthetics can become exponentially bad.

Felsner [2001] constructs convex grid drawings of triconnected, planar graphs with f faces on an $(f - 1) \times (f - 1)$ grid using Schnyder woods. In the following, we rephrase his construction and results that are an extension of the ones presented in Section 6.3.1. **Felsner** defines coordinate mappings that combine the properties of barycentric representations and Schnyder woods for triconnected, planar graphs. The theoretical basics were already settled in Section 3.2.3.

We follow the outline of **Felsner** [2004a]. Let $G = (V, E)$ be a triconnected, planar graph together with a Schnyder wood. We assign a *region vector* $(v_1, v_2, v_3) \in \mathbb{R}^3$ to every vertex $v \in V$ such that v_i denotes the number of faces in region $R_i(v)$ (compare also **Schnyder**'s first construction in Section 6.3.1). The three special vertices have region vectors $(f - 1, 0, 0)$, $(0, f - 1, 0)$, and $(0, 0, f - 1)$. Together with our knowledge about inclusions of regions, we obtain:

Definition 6.11 (coordinate mapping). *A coordinate mapping associates a vector $(v_1, v_2, v_3) \in \mathbb{R}^3$ with every vertex v such that:*

1. $\sum_{i=1}^3 v_i = f - 1$ for all $v \in V$
2. If $u \in R_i(v)$, then $u_i \leq v_i$; if $u \in R_i^O(v)$, then $u_i < v_i$.
3. If $\text{label}(u, v) = i$, then $u_i < v_i$, $u_{i+1} \geq v_{i+1}$, and $u_{i-1} \geq v_{i-1}$.
4. For every edge $\{u, v\}$ there are indices i and j such that $u_i < v_i$ and $u_j > v_j$, $i, j = 1, 2, 3$, $i \neq j$.

Again, let p , q , and r be three non-collinear points in the plane. We define a coordinate mapping

$$\Gamma: v \in V \rightarrow \frac{1}{f - 1}(v_1 p + v_2 q + v_3 r) \in \mathbb{R}^3.$$

Note that when choosing different points p , q , and r in coordinate mapping Γ and p' , q' , and r' in coordinate mapping Γ' , then there exists an affine function that maps one onto the other. Therefore, we sometimes ignore the base points. We denote the resulted drawing by $\Gamma(G)$. Then, we obtain the following result:

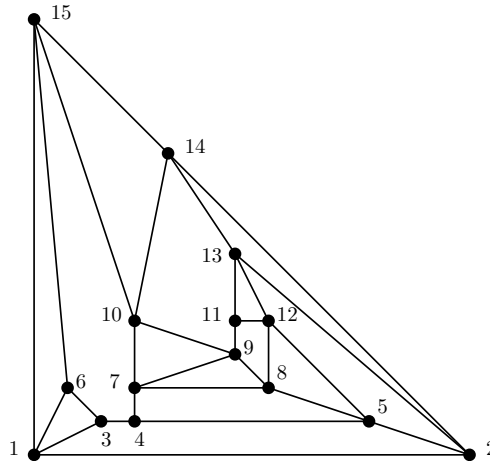


Figure 6.8: Straight-line grid drawing of the graph of Figure 2.3(c).

Theorem 6.12 (Felsner, 2001). *Let $G = (V, E)$ be a triconnected, planar graph together with a Schnyder wood. If the coordinate v_i of vertex $v \in V$ counts the number of faces in $R_i(v)$ with respect to the Schnyder wood of (G, v_1) , then $\Gamma(G)$ is a convex drawing of G .*

Choosing $p = (0, 0)$, $q = (f - 1, 0)$, and $r = (0, f - 1)$, every vertex $v \in V$ is mapped to an integer point on an $(f - 1) \times (f - 1)$ grid. This yields the main corollary of this section:

Corollary 6.13. *Let G be a triconnected, planar graph with f faces. Then, there exists a convex drawing of G on the $(f - 1) \times (f - 1)$ integer grid.*

An example is shown in Figure 6.8 where the underlying Schnyder wood is the Schnyder wood constructed by Algorithm 8 with the leftist canonical ordering as input canonical ordering (compare also Figure 2.3(c)).

Note that Corollary 6.13 is a version of Tutte's theorem (Theorem 1.16) that every triconnected, planar graph has a drawing with strictly convex interior faces.

Other Result Bonichon, Felsner, and Mosbah [2007] construct convex, straight-line drawings using Schnyder woods. Their obtained grid size is $(n - 2 - \Delta) \times (n - 2 - \Delta)$, where $\Delta \geq 0$ depends on the chosen Schnyder wood. They compute a sequence of maximal counterclockwise merges, i. e., redirecting and relabeling certain edges while deleting others, starting with a minimal Schnyder wood. They also apply the face counting method as described in Sections 6.3.1 and 6.3.2. At the end, they reinsert all edges that have been deleted and prove that the resulted drawing is planar and convex. To determine the grid size, they calculate the number of merges.

6.3.3 Orthogonal Surfaces and Geodesic Embeddings

The region vectors defined in Section 6.3.2 can also be used to create three-dimensional orthogonal surfaces. We summarize some results of Felsner [2003] that are also stated in Zickfeld [2007]. Most notations are already used in Miller [2002].

We consider \mathbb{R}^3 equipped with the *dominance order*, i. e., $u \leq v$ if and only if $u_i \leq v_i$ for each component i , $i = 1, 2, 3$, where $u = (u_1, u_2, u_3)$, $v = (v_1, v_2, v_3) \in \mathbb{R}^3$. We write $u \vee v$ and $u \wedge v$ to denote *join* (component-wise maximum) and *meet* (component-wise minimum), respectively.

Let $\mathcal{A} \subset \mathbb{R}^3$ be an *antichain*, i. e., a set of pairwise incomparable elements. The *filter* generated by \mathcal{A} in \mathbb{R}^3 is the set

$$\langle \mathcal{A} \rangle = \{ \alpha \in \mathbb{R}^3 \mid \alpha \geq v \text{ for some } v \in \mathcal{A} \}.$$

The boundary $\mathfrak{S}_{\mathcal{A}}$ of \mathcal{A} is the *orthogonal surface* generated by \mathcal{A} . An example is shown in Figure 4.22(h). An orthogonal surface is *axial* if it contains exactly three unbounded orthogonal arcs. This is also illustrated in Figure 4.22(h). If $u, v \in \mathcal{A}$ and $u \vee v \in \mathfrak{S}_{\mathcal{A}}$, then $\mathfrak{S}_{\mathcal{A}}$ contains the union of the two line segments joining u and v to $u \vee v$. Such arcs are called *elbow geodesics* of $\mathfrak{S}_{\mathcal{A}}$.

A planar drawing $G \rightarrow \mathfrak{S}_{\mathcal{A}}$ is a *geodesic embedding* if

1. there is a bijection between the vertices of G and \mathcal{A} ,
2. every edge of G is an elbow geodesic in $\mathfrak{S}_{\mathcal{A}}$ and every edge is drawn as an elbow geodesic of $\mathfrak{S}_{\mathcal{A}}$,
3. there are no crossing edges in the embedding of G on $\mathfrak{S}_{\mathcal{A}}$.

A geodesic embedding $G_{\infty} \rightarrow \mathfrak{S}_{\mathcal{A}}$ is *axial* if the three edges of G_{∞} incident to v_{∞} are mapped onto the three unbounded orthogonal arcs of $\mathfrak{S}_{\mathcal{A}}$.

Theorem 6.14 (Miller, 2002, Felsner, 2003, 2004a). *Let $\mathfrak{S}_{\mathcal{A}}$ be axial and let $G \rightarrow \mathfrak{S}_{\mathcal{A}}$ be a geodesic embedding. Then, the embedding induces a Schnyder wood of G_{∞} . Conversely, every Schnyder wood of G_{∞} induces an axial geodesic embedding.*

An example is shown in Figure 4.22(f).

Conclusion

In this thesis, we discussed the concepts canonical ordering and Schnyder woods, two important tools in planar graph drawing. These concepts are widely used in drawing algorithms, especially to create straight-line grid drawings.

A common approach for dealing with planar graphs is to demand that the considered graphs are triangulated since many concepts are simple for this class of graphs and triangulating a graph is easy and can be carried out in linear time. On the other hand, results are often not satisfying when this approach is used to apply an algorithm tailored for triangular graphs to general planar graphs. Therefore, we chose to examine the less restrictive class of triconnected, planar graphs. After we verified that many concepts that are simple for triangular graphs do not work for this class of graphs any more (Chapter 1), we concentrated on more powerful tools.

In Chapter 2 we presented definitions of canonical orderings for many kinds of planar graphs, and emphasized with rephrased definitions the connection of canonical ordering and *st*-ordering. We introduced the leftist canonical ordering, that is in contrast to previous concepts uniquely defined and, therefore, allows for deterministic results when used as tool in algorithms. Moreover, we proved that the dual of the leftist canonical ordering is the leftist canonical ordering of the dual graph.

It is well-known that canonical ordering is closely related to Schnyder woods. A closer look revealed that while this is indeed true for triangular graphs, it is complicated to establish this connection on the class of triconnected, planar graphs. Therefore, we introduced a novel approach which extends equivalence classes of canonical orderings of triangular graphs to equivalence classes of ordered path partitions for triconnected, planar graphs. Using these, we were able to prove that each of these concepts is in bijection with its corresponding set of Schnyder woods. These considerations are embedded in a thorough and consistent summary of other important properties of Schnyder woods in Chapter 3.

Chapter 4 was dedicated to triangle contact representations that can be constructed using Schnyder woods. We investigated two classes of graphs, namely, two-terminal series-parallel digraph and partial planar 3-tree, and proved that they

admit a homothetic triangle contact representation. The chapter is rounded off by the relation of triangle contact representation with its dual and Schnyder woods.

In Part II we presented algorithms for these concepts. In more detail, in Chapter 5 we developed a novel approach to compute the leftist canonical ordering and provided a detailed description of its linear-time implementation. In Chapter 6, we proposed algorithms to compute minimal Schnyder woods for triangular and triconnected, planar graphs, respectively. Both algorithms are based on the relation of Schnyder woods to certain equivalence classes of canonical ordering that nicely connects this chapter to the concepts introduced in Part I.

We conclude this thesis with a list of some open problems.

1. Investigate the connection of canonical ordering and barycentric representations for triconnected, planar graphs.

Barycentric representations for triangular graphs can be created using Schnyder woods as described in Section 6.3.1. Using the bijection between ordered path partitions and Schnyder woods, is it possible to directly determine the canonical ordering of a triconnected, planar graph from a barycentric representation?

2. Simplify the proof of correctness of the algorithm of Section 6.2.3 which computes the minimal Schnyder wood.

Fusy et al. [2008] use a complex distinction of cases to prove that their algorithm computes the minimal α_0 -orientation of a triconnected, planar graph whose outer face is a triangle. Our proof of correctness is based on this, however, a clearer, more direct proof might give additional insights.

3. Examine the lattice structure of the set of Schnyder woods more carefully.

Even if Felsner [2004b] proved that the set of Schnyder woods forms a distributive lattice, it is still open how join and meet look like. Therefore, it would be very interesting to gain more insight in the lattice structure of Schnyder woods. Further, given any lattice L , does there exist a graph whose set of Schnyder woods is in one-to-one correspondence to L ?

4. Can the presented concepts be applied to other combinatorial structures?

Eulerian orientations, spanning trees, and Schnyder woods are some examples that are in one-to-one correspondence with α -orientations, and, thus, carry a lattice structure. Can these insights be used to get a uniform view on different concepts of planar graphs?

Bibliography

Mohammad Mursalin Akon, Shah Asaduzzaman, and Md. Saidur Rahman. Proposal for *st*-Routing Protocol. *Telecommunication Systems*, 25(3–4):287–298, 2004.
Cited on page [38](#).

Md. Jawaherul Alam, Therese Biedl, Stefan Felsner, Michael Kaufmann, and Stephen G. Kobourov. Proportional Contact Representations of Planar Graphs. In Marc van Kreveld and Bettina Speckmann, editors, *Proceedings of the 19th International Symposium on Graph Drawing (GD'11)*, volume 7034 of *Lecture Notes in Computer Science*, pages 26–38. Springer, 2012.
Cited on page [99](#).

Luca Castelli Aleardi, Olivier Devillers, and Éric Fusy. Canonical Ordering for Triangulations on the Cylinder, with Applications to Periodic Straight-Line Drawings. In Walter Didimo and Maurizio Patrignani, editors, *Proceedings of the 19th International Symposium on Graph Drawing (GD'12)*. Springer. To appear.
Cited on page [39](#).

Luca Castelli Aleardi, Éric Fusy, and Thomas Lewiner. Schnyder Woods for Higher Genus Triangulated Surfaces. In *Proceedings of the 24th Annual ACM Symposium on Computational Geometry (SoCG'08)*, pages 311–319. ACM Press, 2008.
Cited on pages [60](#) and [146](#).

Luca Castelli Aleardi, Éric Fusy, and Thomas Lewiner. Schnyder Woods for Higher Genus Triangulated Surfaces, with Applications to Encoding. *Discrete and Computational Geometry*, 42(3):489–516, 2009.
Cited on page [146](#).

E. M. Andreev. On Convex Polyhedra in Lobačhevskiĭ Spaces. *Mathematics of the USSR - Sbornik*, 10(3):413–440, 1970.
Cited on page [97](#).

Fred D. Annexstein and Kenneth A. Berman. Directional Routing via Generalized *st*-Numbering. *SIAM Journal on Discrete Mathematics*, 13(2):268–279, 2000.
Cited on page [38](#).

- László Babai and D. Duffus. Dimension and Automorphism Groups of Lattices. *Algebra Universalis*, 12:279–289, 1981.
Cited on page [85](#).
- Melanie Badent, Carla Binucci, Emilio Di Giacomo, Walter Didimo, Stefan Fel-sner, Francesco Giordano, Jan Kratochvíl, Pietro Palladino, Maurizio Patrignani, and Francesco Trotta. Homothetic Triangle Contact Representations of Planar Graphs. In *Proceedings of the 19th Canadian Conference on Computational Ge-ometry (CCCG '07)*, pages 233–238. Carleton University, 2007.
Cited on pages [iii](#), [v](#), [2](#), [3](#), [100](#), [101](#), [103](#), [105](#), and [109](#).
- Melanie Badent, Michael Baur, Ulrik Brandes, and Sabine Cornelsen. Leftist Canon-ical Ordering. In David Eppstein and Emden R. Gansner, editors, *Proceedings of the 17th International Symposium on Graph Drawing (GD'09)*, volume 5849 of *Lecture Notes in Computer Science*, pages 159–170. Springer, 2010.
Cited on pages [iii](#), [iv](#), [v](#), [2](#), [3](#), and [125](#).
- Melanie Badent, Ulrik Brandes, and Sabine Cornelsen. More Canonical Ordering. *Journal of Graph Algorithms and Applications*, 15(1):97–126, 2011.
Cited on pages [iii](#), [iv](#), [v](#), [2](#), [3](#), [37](#), [60](#), [61](#), [125](#), [145](#), [150](#), and [155](#).
- Jérémy Barbay, Luca Castelli Aleardi, Meng He, and Ian Munro. Succinct Represen-tation of Labeled Graphs. In Takeshi Tokuyama, editor, *Proceedings of the 18th International Symposium on Algorithms and Computation (ISAAC'07)*, volume 4835 of *Lecture Notes in Computer Science*, pages 316–328. Springer, 2007.
Cited on pages [55](#) and [136](#).
- Gill Barequet, Michael T. Goodrich, and Chris Riley. Drawing Planar Graphs with Large Vertices and Thick Edges. *Journal of Graph Algorithms and Applications*, 8(1):3–20, 2004.
Cited on page [136](#).
- David W. Barnette and Branko Grünbaum. On Steinitz's Theorem Concerning Convex 3-Polytopes and on Some Properties of Planar Graphs. In Gary Chartrand and S. F. Kapoor, editors, *The Many Facets of Graph Theory*, volume 110 of *Lecture Notes in Mathematics*, pages 27–40. Springer, 1969.
Cited on pages [23](#), [29](#), [30](#), and [31](#).
- Seymour Benzer. On the Topology of the Genetic Fine Structure. *Proceedings of the National Academy of Science of the United States of America*, 45(11):1607–1620, 1959.
Cited on page [103](#).

- Therese Biedl and Franz J. Brandenburg. Partitions of Graphs into Trees. In Michael Kaufmann and Dorothea Wagner, editors, *Proceedings of the 14th International Symposium on Graph Drawing (GD'06)*, volume 4372 of *Lecture Notes in Computer Science*, pages 430–439. Springer, 2007.
Cited on page 60.
- Therese Biedl, Goos Kant, and Michael Kaufmann. On Triangulating Planar Graphs under the Four-Connectivity Constraint. *Algorithmica*, 19:427–446, 1997.
Cited on page 22.
- Therese C. Biedl. Drawing Planar Partitions I: LL-Drawings and LH-Drawings. In *Proceedings of the 14th Annual Symposium on Computational Geometry*, pages 287–296. ACM Press, 1998. URL <http://doi.acm.org/10.1145/276884.276917>.
Cited on page 136.
- Therese C. Biedl and Michael Kaufmann. Area-Efficient Static and Incremental Graph Drawings. In Gerhard J. Woeginger, editor, *Proceedings of the 5th Annual European Symposium on Algorithms (ESA'97)*, volume 1284 of *Lecture Notes in Computer Science*, pages 37–52. Springer, 1997.
Cited on pages 136 and 138.
- John Adrian Bondy and U. S. Murty. *Graph Theory with Applications*. Macmillan, 1976.
Cited on pages 7 and 31.
- Nicolas Bonichon, Stefan Felsner, and Mohamed Mosbah. Convex Drawings of 3-Connected Plane Graphs. In Pach [2005], pages 60–70.
Cited on page 156.
- Nicolas Bonichon, Stefan Felsner, and Mohamed Mosbah. Convex Drawings of 3-Connected Plane Graphs. *Algorithmica*, 47:399–420, 2007.
Cited on pages 156 and 161.
- Nicolas Bonichon, Cyril Gavoille, and Nicolas Hanusse. An Information-Theoretic Upper Bound on Planar Graphs Using Well-Orderly Maps. In Matthias Dehmer, Frank Emmert-Streib, and Alexander Mehler, editors, *Towards an Information Theory of Complex Networks: Statistical Methods and Applications*, pages 17–46. Birkhäuser Verlag, 2011.
Cited on page 58.
- Prosenjit Bose, Joachim Gudmundsson, and Michiel Smid. Constructing Plane Spanners of Bounded Degree and Low Weight. *Algorithmica*, 42(3–4):249–264,

2005.

Cited on page 136.

Ulrik Brandes. Eager *st*-Ordering. In Rolf H. Möhring and Rajeev Raman, editors, *Proceedings of the 10th Annual European Symposium on Algorithms (ESA'02)*, volume 2461 of *Lecture Notes in Computer Science*, pages 183–197. Springer, 2002.

Cited on page 37.

Ulrik Brandes and Sabine Cornelsen, editors. *Proceedings of the 18th International Symposium on Graph Drawing (GD'10)*, volume 6502 of *Lecture Notes in Computer Science*, 2011. Springer.

Cited on page 173.

Enno Brehm. 3-Orientations and Schnyder 3-Tree-Decompositions. Master's thesis, FU Berlin, 2000. URL <http://www.math.tu-berlin.de/~felsner/Diplomarbeiten/brehm.ps.gz>.

Cited on pages 44, 60, 65, 72, 73, 74, 88, 91, 136, 145, 146, and 147.

Graham R. Brightwell and Edward R. Scheinerman. Representations of Planar Graphs. *SIAM Journal on Discrete Mathematics*, 6(2):214–229, 1993.

Cited on page 97.

Heinz Bruggesser and G. Manic. Shellable Decompositions of Cells and Spheres. *Mathematica Scandinavica*, 29:197–205, 1971.

Cited on page 23.

Jérémie Chalopin and Daniel Gonçalves. Every Planar Graph is the Intersection Graph of Segments in the Plane. In Michael Mitzenmacher, editor, *Proceedings of the 41st Annual ACM Symposium on the Theory of Computing (STOC'09)*, pages 631–638. ACM Press, 2009.

Cited on page 100.

Chieh-Yu Chen, Ya-Fei Hung, and Hsueh-I Lu. Visibility Representations of Four-connected Plane Graphs with Near Optimal Heights. *Computational Geometry*, 42:865–872, 2009.

Cited on page 50.

Ho-Lin Chen, Chien-Chih Liao, Hsueh-I Lu, and Hsu-Chun Yen. Some Applications of Orderly Spanning Trees in Graph Drawing. In Michael T. Goodrich and Stephen G. Kobourov, editors, *Proceedings of the 10th International Symposium on Graph Drawing (GD'02)*, volume 2528 of *Lecture Notes in Computer Science*, pages 332–343. Springer, 2003.

Cited on page 57.

- C. C. Cheng, Christian A. Duncan, Michael T. Goodrich, and Stephen G. Kobourov. Drawing Planar Graphs with Circular Arcs. *Discrete and Computational Geometry*, 25(3):405–418, 2001.
Cited on page [138](#).
- Joseph Cheriyan and S. N. Maheshwari. Finding Nonseparating Induced Cycles and Independent Spanning Trees in 3-Connected Graphs. *Journal of Algorithms*, 9: 507–537, 1988.
Cited on page [59](#).
- Yi-Ting Chiang, Ching-Chi Lin, and Hsueh-I Lu. Orderly Spanning Trees with Applications to Graph Encoding and Graph Drawing. In S. Rao Kosaraju, editor, *Proceedings of the 12th Annual ACM–SIAM Symposium on Discrete Algorithms (SODA ’01)*, pages 506–515. ACM / SIAM, 2001.
Cited on pages [iv](#), [2](#), [57](#), [58](#), [136](#), and [146](#).
- Yi-Ting Chiang, Ching-Chi Lin, and Hsueh-I Lu. Orderly Spanning Trees with Applications. *SIAM Journal on Computing*, 34(4):924–945, 2005.
Cited on pages [iv](#), [2](#), [57](#), and [146](#).
- Marek Chrobak and Goos Kant. Convex Grid Drawings of 3-Connected Planar Graphs. *International Journal of Computational Geometry and Applications*, 7 (3):211–223, 1997.
Cited on pages [40](#), [137](#), [138](#), and [143](#).
- Marek Chrobak and Shin-Ichi Nakano. Minimum-Width Grid Drawings of Plane Graphs. *Computational Geometry*, 11(1):29–54, 1998.
Cited on page [137](#).
- Marek Chrobak and Thomas H. Payne. A Linear-Time Algorithm for Drawing a Planar Graph on a Grid. *Information Processing Letters*, 54(4):241–246, 1995.
Cited on pages [39](#), [137](#), [138](#), and [143](#).
- Richie Chih-Nan Chuang, Ashim Garg, Xin He, Ming-Yang Kao, and Hsueh-I Lu. Compact Encodings of Planar Graphs via Canonical Orderings and Multiple Parentheses. In Kim Guldstrand Larsen, Sven Skyum, and Glynn Winskel, editors, *Proceedings of the 25th International Colloquium on Automata, Languages and Programming (ICALP’98)*, volume 1443 of *Lecture Notes in Computer Science*, pages 118–129. Springer, 1998. Extended version with proofs: arXiv:cs/0102005v2 [cs.DS].
Cited on pages [iv](#), [2](#), [55](#), [57](#), [136](#), and [146](#).

- Hubert de Fraysseix and Patrice Ossona de Mendez. Regular Orientations, Arboricity, and Augmentation. In [Tamassia and Tollis \[1995\]](#), pages 111–118.
Cited on page [136](#).
- Hubert de Fraysseix and Patrice Ossona de Mendez. On Topological Aspects of Orientations. *Discrete Mathematics*, 229(1–3):57–72, 2001.
Cited on pages [60](#), [61](#), [64](#), and [71](#).
- Hubert de Fraysseix and Patrice Ossona de Mendez. Barycentric Systems and Stretchability. *Discrete Applied Mathematics*, 155:1079–1095, 2007.
Cited on page [117](#).
- Hubert de Fraysseix, János Pach, and Richard Pollack. Small Sets Supporting Fáry Embeddings of Planar Graphs. In Janos Simon, editor, *Proceedings of the 20th Annual ACM Symposium on the Theory of Computing (STOC'88)*, pages 426–433. ACM Press, 1988.
Cited on pages [39](#), [40](#), [49](#), [125](#), and [136](#).
- Hubert de Fraysseix, János Pach, and Richard Pollack. How to Draw a Planar Graph on a Grid. *Combinatorica*, 10(1):41–51, 1990.
Cited on pages [39](#), [40](#), [49](#), [125](#), [136](#), [137](#), [138](#), [139](#), [143](#), and [159](#).
- Hubert de Fraysseix, Patrice Ossona de Mendez, and Pierre Rosenstiehl. On Triangle Contact Graphs. *Combinatorics, Probability and Computing*, 3:233–246, 1994.
Cited on pages [v](#), [3](#), [98](#), [101](#), [103](#), [119](#), and [120](#).
- Hubert de Fraysseix, Patrice Ossona de Mendez, and Pierre Rosenstiehl. Bipolar Orientations Revisited. *Discrete Applied Mathematics*, 56(2–3):157–179, 1995.
Cited on page [38](#).
- Giuseppe Di Battista and Roberto Tamassia. Incremental Planarity Testing. In *Proceedings of the 30th Annual IEEE Symposium on Foundations of Computer Science (FOCS'89)*, pages 436–441. IEEE Computer Society, 1989.
Cited on page [26](#).
- Giuseppe Di Battista, Peter Eades, Roberto Tamassia, and Ioannis G. Tollis. *Graph Drawing - Algorithms for the Visualization of Graphs*. Prentice Hall, 1998.
Cited on page [16](#).
- Giuseppe Di Battista, Roberto Tamassia, and Luca Vismara. Output-Sensitive Reporting of Disjoint Paths. *Algorithmica*, 23(4):302–340, 1999.
Cited on pages [iv](#), [v](#), [2](#), [3](#), [59](#), [60](#), [75](#), [80](#), [81](#), [82](#), [83](#), [85](#), [136](#), [145](#), [147](#), [150](#), [151](#), and [156](#).

- Emilio Di Giacomo, Walter Didimo, Giuseppe Liotta, and Stephen K. Wismath. Drawing Planar Graphs on a Curve. In Hans L. Bodlaender, editor, *Proceedings of the 29th International Workshop on Graph-Theoretic Concepts in Computer Science (WG'03)*, volume 2880 of *Lecture Notes in Computer Science*, pages 192–204. Springer, 2003.
Cited on page 136.
- Emilio Di Giacomo, Walter Didimo, Giuseppe Liotta, and Stephen K. Wismath. Curve-Constrained Drawings of Planar Graphs. *Computational Geometry*, 30(2): 1–23, 2005.
Cited on page 136.
- Emilio Di Giacomo, Walter Didimo, and Giuseppe Liotta. Radial Drawings of Graphs: Geometric Constraints and Trade-Offs. *Journal of Discrete Algorithms*, 6(1):109–124, 2008.
Cited on page 136.
- Reinhard Diestel. *Graph Theory*. Graduate Texts in Mathematics. Springer, 2010.
Cited on pages 7, 13, 19, 23, and 36.
- Gabriel A. Dirac and S. Schuster. A Theorem of Kuratowski. *Indagationes Mathematicae*, 16:343–348, 1954.
Cited on page 32.
- Vida Dujmović, Matthew Suderman, and David R. Wood. Really Straight Graph Drawings. In Pach [2005], pages 122–132.
Cited on page 136.
- Jürgen Ebert. st -Ordering the Vertices of Biconnected Graphs. *Computing*, 30: 19–33, 1983.
Cited on page 37.
- Amr Elmasry, Kurt Mehlhorn, and Jens M. Schmidt. An $\mathcal{O}(n + m)$ Certifying Triconnectivity Algorithm for Hamiltonian Graphs. *Algorithmica*, 62:754–766, 2012.
Cited on page 28.
- David Eppstein. Nineteen Proofs of Euler’s Formula: $V - E + F = 2$, 2005. URL <http://www.ics.uci.edu/~eppstein/junkyard/euler/>.
Cited on page 19.
- Paul Erdős, Arnold Goodman, and Louis Pósa. The Representation of a Graph by Set Intersections. *Canadian Journal of Mathematics*, 18(1):106–112, 1966.
Cited on page 100.

- Kapali P. Eswaran and Robert E. Tarjan. Augmentation Problems. *SIAM Journal on Computing*, 5(4), 1976.
Cited on page 26.
- Shimon Even and Robert E. Tarjan. Computing an *st*-Numbering. *Theoretical Computer Science*, 2(3):339–344, 1976.
Cited on page 37.
- Shimon Even and Robert E. Tarjan. Corrigendum: Computing an *st*-Numbering. *Theoretical Computer Science*, 4(1):123, 1977.
Cited on page 37.
- István Fáry. On Straight line Representation of Planar Graphs. *Acta Scientiarum Mathematicarum (Szeged)*, 11(4):229–233, 1946.
Cited on pages 32 and 34.
- Stefan Felsner. Convex Drawings of Planar Graphs and the Order Dimension of 3-Polytopes. *ORDER*, 18(1):19–37, 2001.
Cited on pages iv, v, 2, 3, 60, 75, 76, 77, 79, 80, 145, 150, 153, 156, 160, and 161.
- Stefan Felsner. Geodesic Embeddings and Planar Graphs. *ORDER*, 20(2):135–150, 2003.
Cited on pages v, 3, 60, 78, 121, and 162.
- Stefan Felsner. *Geometric Graphs and Arrangements*. Vieweg, 2004a.
Cited on pages v, 2, 3, 35, 60, 61, 75, 76, 84, 153, 160, and 162.
- Stefan Felsner. Lattice Structure from Planar Graphs. *The Electronic Journal of Combinatorics*, 11(1), 2004b.
Cited on pages iv, 2, 60, 85, 86, 88, 89, 90, 155, and 164.
- Stefan Felsner and Mathew C. Francis. Contact Representations of Planar Graphs with Cubes. In Ferran Hurtado and Marc van Kreveld, editors, *Proceedings of the 27th Annual ACM Symposium on Computational Geometry (SoCG'11)*, pages 315–320. ACM Press, 2011.
Cited on pages 100 and 101.
- Stefan Felsner and Florian Zickfeld. Schnyder Woods and Orthogonal Surfaces. *Discrete and Computational Geometry*, 40(1):103–126, 2008.
Cited on page 60.
- Sergej Fialko and Petra Mutzel. A New Approximation Algorithm for the Planar Augmentation Problem. In Karloff [1998], pages 260–269.
Cited on page 27.

- Ulrich Fößmeier, Goos Kant, and Michael Kaufmann. 2-Visibility Drawings of Planar Graphs. In Stephen C. North, editor, *Proceedings of the 4th International Symposium on Graph Drawing (GD'96)*, volume 1090 of *Lecture Notes in Computer Science*, pages 155–168. Springer, 1997.
Cited on page [136](#).
- Delbert R. Fulkerson and O. A. Gross. Incidence Matrices and Interval Graphs. *Pacific Journal of Mathematics*, 15(3):835–855, 1965.
Cited on page [103](#).
- Martin Fürer, Xin He, Ming-Yang Kao, and Balaji Raghavachari. $\mathcal{O}(n \log \log n)$ -Work Parallel Algorithms for Straight-Line Grid Embeddings of Planar Graphs. In *Proceedings of the 4th Annual ACM Symposium on Parallel Algorithms and Architectures (SPAA'92)*, pages 410–419. ACM Press, 1992.
Cited on page [146](#).
- Éric Fusy, Gilles Schaeffer, and Dominique Poulalhon. Dissections, Orientations, and Trees with Applications to Optimal Mesh Encoding and Random Sampling. *ACM Transactions on Algorithms*, 4(2), 2008.
Cited on pages [60](#), [96](#), [155](#), and [164](#).
- Emden R. Gansner, Yifan Hu, Michael Kaufmann, and Stephen G. Kobourov. Optimal Polygonal Representation of Planar Graphs. In Alejandro López-Ortiz, editor, *Proceedings of the 9th Latin American Symposium on Theoretical Informatics (LATIN'10)*, volume 6034 of *Lecture Notes in Computer Science*, pages 417–432, 2010.
Cited on pages [99](#) and [116](#).
- Emden R. Gansner, Yifan Hu, and Stephen G. Kobourov. On Touching Triangle Graphs. In [Brandes and Cornelsen \[2011\]](#), pages 250–261.
Cited on page [99](#).
- Daniel Gonçalves, Benjamin Lévêque, and Alexandre Pinlou. Triangle Contact Representations and Duality. In [Brandes and Cornelsen \[2011\]](#).
Cited on pages [v](#), [3](#), [100](#), [101](#), [103](#), [115](#), [116](#), [117](#), [118](#), [120](#), and [121](#).
- Michael T. Goodrich and Christopher G. Wagner. A Framework for Drawing Planar Graphs with Curves and Polylines. *Journal of Algorithms*, 37(2):399–421, 2000.
Cited on pages [136](#) and [137](#).
- Jonathan L. Gross and Thomas W. Tucker. *Topological Graph Theory*. Wiley-Interscience Series in Discrete Mathematics and Optimization. Wiley, 1987.
Cited on page [15](#).

- Roberto Grossi and Elena Lodi. Simple Planar Graph Partition into Three Forests. *Discrete Applied Mathematics*, 84:121–132, 1998.
Cited on page 59.
- Carsten Gutwenger and Petra Mutzel. Planar Polyline Drawings with Good Angular Resolution. In Sue H. Whitesides, editor, *Proceedings of the 6th International Symposium on Graph Drawing (GD'98)*, volume 1547 of *Lecture Notes in Computer Science*, pages 167–182. Springer, 1999.
Cited on pages 136 and 138.
- Carsten Gutwenger and Petra Mutzel. A Linear Time Implementation of SPQR-Trees. In *Proceedings of the 8th International Symposium on Graph Drawing (GD'00)*, volume 1984 of *Lecture Notes in Computer Science*, pages 70–90. Springer, 2001.
Cited on page 26.
- Frank Harary. *Graph Theory*. Addison-Wesley, 1969.
Cited on page 7.
- David Harel and Meir Sardas. An Algorithm for Straight-Line Drawing of Planar Graphs. *Algorithmica*, 20:119–135, 1998.
Cited on pages iv, 2, 49, and 126.
- Xin He. On Finding the Rectangular Duals of Planar Triangular Graphs. *SIAM Journal on Computing*, 22:1218–1226, 1993.
Cited on page 146.
- Xin He. Grid Embedding of 4-Connected Plane Graphs. *Discrete and Computational Geometry*, 17(3):339–358, 1997.
Cited on pages 51 and 54.
- Xin He. On Floor-Plan of Plane Graphs. *SIAM Journal on Computing*, 28(6):2150–2167, 1999.
Cited on page 136.
- Xin He and Ming-Yang Kao. Parallel Construction of Canonical Ordering and Convex Drawing of Triconnected Planar Graphs. In K. W. Ng, Prabhakar Raghavan, and N. V. Balasubramanian, editors, *Proceedings of the 4th International Symposium on Algorithms and Computation (ISAAC'93)*, volume 762 of *Lecture Notes in Computer Science*, pages 303–312. Springer, 1993.
Cited on page 146.
- Xin He and Ming-Yang Kao. Regular Edge Labelings and Drawings of Planar Graphs. In Tamassia and Tollis [1995], pages 96–103.
Cited on pages 38 and 146.

- Xin He, Ming-Yang Kao, and Hsueh-I Lu. Linear-Time Succinct Encodings of Planar Graphs via Canonical Orderings. *SIAM Journal on Discrete Mathematics*, 12(3): 317–325, 1999.
Cited on pages [iv](#), [2](#), [55](#), and [136](#).
- Seok-Hee Hong and Martin Mader. Generalizing the Shift Method for Rectangular Shaped Vertices with Visibility Constraints. In Ioannis G. Tollis and Maurizio Patrignani, editors, *Proceedings of the 16th International Symposium on Graph Drawing (GD'08)*, volume 5417 of *Lecture Notes in Computer Science*, pages 278–283. Springer, 2009.
Cited on page [138](#).
- John E. Hopcroft and Robert E. Tarjan. Finding the Triconnected Components of a Graph. Technical Report TR 72-140, CS Dept., Cornell University, Ithaca, N.Y., 1972.
Cited on pages [25](#) and [26](#).
- John E. Hopcroft and Robert E. Tarjan. Dividing a Graph into Triconnected Components. Technical Report TR 74-197, CS Dept., Cornell University, Ithaca, N.Y., 1974.
Cited on page [26](#).
- Tsan-sheng Hsu and Vijaya Ramachandran. A Linear Time Algorithm for Triconnectivity Augmentation. In *Proceedings of the 32nd Annual IEEE Symposium on Foundations of Computer Science (FOCS'91)*, pages 548–559. IEEE Computer Society Press, 1991a.
Cited on page [26](#).
- Tsan-sheng Hsu and Vijaya Ramachandran. On Finding a Smallest Augmentation to Biconnect a Graph. In Min-Yao Hsu and Richard C. T. Lee, editors, *Proceedings of the 2nd International Symposium on Algorithms (ISA'91)*, volume 557 of *Lecture Notes in Computer Science*, pages 326–335. Springer, 1991b.
Cited on page [26](#).
- Toshimasa Ishii, Hiroshi Nagamochi, and Toshihide Ibaraki. Optimal Augmentation to Make a Graph k -Edge-Connected and Triconnected. In [Karloff \[1998\]](#), pages 280–289.
Cited on page [26](#).
- Alon Itai and Michael Rodeh. The Multi-Tree Approach to Reliability in Distributed Networks. *Information and Computation*, 79(1):43–59, 1988.
Cited on page [59](#).

- G. R. Kampen. Orienting Planar Graphs. *Discrete Mathematics*, 14(4):337–341, 1976.
Cited on pages 59, 67, and 145.
- Goos Kant. *Algorithms for Drawing Planar Graphs*. PhD thesis, Utrecht University, 1993.
Cited on pages v, 3, 22, 26, 27, 45, 47, 125, 136, 143, and 144.
- Goos Kant. Drawing Planar Graphs Using the Canonical Ordering. *Algorithmica*, 16(4):4–32, 1996.
Cited on pages v, 3, 40, 42, 43, 44, 45, 96, 125, 126, 136, 137, 138, 139, 142, and 143.
- Goos Kant. A More Compact Visibility Representation. *International Journal of Computational Geometry and Applications*, 7(3):197–210, 1997.
Cited on page 136.
- Goos Kant and Hans L. Bodlaender. Planar Graph Augmentation Problems. In Frank Dehne, Jörg-Rüdiger Sack, and Nicola Santoro, editors, *Proceedings of the 2nd International Workshop on Algorithms and Data Structures (WADS'91)*, volume 519 of *Lecture Notes in Computer Science*, pages 286–298. Springer, 1991.
Cited on pages 26 and 27.
- Goos Kant and Xin He. Regular Edge Labeling of 4-Connected Plane Graphs and its Applications in Graph Drawing Problems. *Theoretical Computer Science*, 172(1-2):175–193, 1997.
Cited on pages iv, 2, 50, 51, 53, 136, and 146.
- Howard Karloff, editor. *Proceedings of the 9th Annual ACM–SIAM Symposium on Discrete Algorithms (SODA'98)*, 1998. ACM / SIAM.
Cited on pages 172 and 175.
- Michael Kaufmann, Jan Kratochvíl, Katharina A. Lehmann, and Ashok Subramanian. Max-Tolerance Graphs as Intersection Graphs. In *Proceedings of the 17th Annual ACM–SIAM Symposium on Discrete Algorithms (SODA'06)*, pages 832–841. ACM Press, 2006.
Cited on page 103.
- A. K. Kelmans. Concept of a Vertex in a Matroid and 3-Connected Graphs. *Journal of Graph Theory*, 4(1):13–19, 1980.
Cited on page 36.
- Donald E. Knuth. *Fundamental Algorithms*, volume 1 of *The Art of Computer Programming*. Addison-Wesley, 2011.
Cited on page 38.

- Paul Koebe. Kontaktprobleme der konformen Abbildung. *Berichte über die Verhandlungen der Sächsischen Akademie der Wissenschaften zu Leipzig*, 88:141–164, 1936.
Cited on page 97.
- Casimir Kuratowski. Sur le problème des courbes gauches en Topologie. *Fundamenta Mathematicae*, 15:271–283, 1930.
Cited on pages 31, 32, and 34.
- Peter Läuchli. Generating All Planar 0-, 1-, 2-, 3-Connected Graphs. In Hartmut Noltemeier, editor, *Proceedings of the International Workshop on Graph-Theoretic Concepts in Computer Science (WG'80)*, Lecture Notes in Computer Science, pages 379–382. Springer, 1981.
Cited on pages 30 and 31.
- Katharina A. Lehmann, Michael Kaufmann, Stephan Steigle, and Kay Nieselt. On the maximal cliques in c -max-tolerance graphs and their application in clustering molecular sequences. *Algorithms for Molecular Biology*, 1(9), 2006.
Cited on page 103.
- Abraham Lempel, Shimon Even, and Israel Cederbaum. An Algorithm for Planarity Testing of Graphs. In Pierre Rosenstiehl, editor, *Proceedings of the International Symposium on the Theory of Graphs*, pages 215–232. Gordon and Breach, 1967.
Cited on page 38.
- Chien-Chih Liao, Hsueh-I Lu, and Hsu-Chun Yen. Compact Floor-Planning via Orderly Spanning Trees. *Journal of Algorithms*, 48:441–451, 2003.
Cited on page 57.
- Ching-Chi Lin, Hsueh-I Lu, and I-Fan Sun. Improved Compact Visibility Representation of Planar Graph via Schnyder's Realizer. *SIAM Journal on Discrete Mathematics*, 18(1):19–29, 2004.
Cited on pages 136 and 146.
- László Lovász. Geometric Representations of Graphs, 2009. URL www.cs.elte.hu/~lovasz/geomrep.pdf.
Cited on pages 24 and 98.
- Saunders Mac Lane. A Combinatorial Condition for Planar Graphs. *Fundamenta Mathematicae*, 28:22–32, 1937.
Cited on pages 31 and 36.
- Martin Mader. Planar Graph Drawing. Master's thesis, University of Konstanz, 2008.
Cited on page 26.

- Joseph Malkevitch. The First Proof of Euler's Formula. In *Coxeter-Festschrift*, volume 3 of *Mitteilungen aus dem Mathematischen Seminar Giessen*, pages 77–82. Selbstverlag des Mathematischen Instituts, 1984.
Cited on page [19](#).
- Terry A. McKee and F. R. McMorris. *Topics in Intersection Graph Theory*. Monographs on Discrete Mathematics and Applications. SIAM, 1999.
Cited on page [100](#).
- Karl Menger. Zur allgemeinen Kurventheorie. *Fundamenta Mathematicae*, 10:96–115, 1927.
Cited on page [13](#).
- Ezra Miller. Planar Graphs as Minimal Resolutions of Trivariate Monomial Ideals. *Documenta Mathematica*, 7:43–90, 2002.
Cited on page [162](#).
- Gary L. Miller and Vijaya Ramachandran. A New Graph Triconnectivity Algorithm and its Parallelization. *Combinatorica*, 12(1):53–76, 1992.
Cited on page [26](#).
- Kazuyuki Miura, Shin-Ichi Nakano, and Takao Nishizeki. Convex Grid Drawings of Four-Connected Plane Graphs. In *Proceedings of the 11th International Symposium on Algorithms and Computation (ISAAC'00)*, Lecture Notes in Computer Science, pages 254–265, 2000a.
Cited on page [54](#).
- Kazuyuki Miura, Shin-Ichi Nakano, and Takao Nishizeki. Grid Drawings of Four-Connected Plane Graphs. In *Proceedings of the 7th International Symposium on Graph Drawing (GD'99)*, volume 1731 of *Lecture Notes in Computer Science*, pages 145–154. Springer, 2000b.
Cited on pages [52](#), [53](#), and [54](#).
- Kazuyuki Miura, Machiko Azuma, and Takao Nishizeki. Canonical Decomposition, Realizer, Schnyder Labeling and Orderly Spanning Trees of Plane Graphs. *International Journal of Foundations of Computer Science*, 16(1):117–141, 2005.
Cited on pages [79](#) and [136](#).
- Bojan Mohar. Embedding Graphs in an Arbitrary Surface in Linear Time. In *Proceedings of the 28th Annual ACM Symposium on the Theory of Computing (STOC'96)*, pages 392–397. ACM Press, 1996.
Cited on page [15](#).

- Bojan Mohar. Circle Packings of Maps in Polynomial Time. *European Journal of Combinatorics*, 18(7):785–805, 1997.
Cited on page 97.
- Ugo G. Montanari. Separable Graphs, Planar Graphs and Web Grammars. *Information and Control*, 16(3):243–267, 1970.
Cited on page 31.
- Sayaka Nagai and Shin-Ichi Nakano. A Linear-Time Algorithm to Find Independent Spanning Trees in Maximal Planar Graphs. In Ulrik Brandes and Dorothea Wagner, editors, *Proceedings of the 26th International Workshop on Graph-Theoretic Concepts in Computer Science (WG'00)*, volume 1928 of *Lecture Notes in Computer Science*, pages 290–301. Springer, 2000.
Cited on pages iv, 2, and 55.
- Shin-Ichi Nakano. Planar Drawings of Plane Graphs. *IEICE Transactions on Information and Systems*, E83-D(3):384–391, 2000.
Cited on pages 136 and 145.
- Shin-Ichi Nakano, Md. Saidur Rahman, and Takao Nishizeki. A linear-time algorithm for four-partitioning four-connected planar graphs. *Information Processing Letters*, 62:315–322, 1997.
Cited on pages 52 and 54.
- Crispin St. Nash-Williams. London Mathematical Society. *Journal of the London Mathematical Society*, 36:445–450, 1961.
Cited on page 59.
- Crispin St. Nash-Williams. Decomposition of Finite Graphs into Forests. *Journal of the London Mathematical Society*, 39:12, 1964.
Cited on page 59.
- Walter Nef. Ein einfacher Beweis des Satzes von Euler-Schläfli. *Elemente der Mathematik*, 39(1), 1984.
Cited on page 23.
- Takao Nishizeki and Md. Saidur Rahman. *Planar Graph Drawing*, volume 12 of *Lecture Notes Series on Computing*. World Scientific Publishing, 2004.
Cited on pages 54 and 143.
- J. Nummenmaa. Constructing Compact Rectilinear Planar Layouts Using Canonical Representation of Planar Graphs. *Theoretical Computer Science*, 99(2):213–230, 1992.
Cited on page 136.

- P. V. O’Neil. A Short Proof of Mac Lane’s Planarity Theorem. *Proceedings of the American Mathematical Society*, 37:617–618, 1973.
Cited on page 36.
- Patrice Ossona de Mendez. *Orientations bipolaires*. PhD thesis, Ecole des Hautes Etudes en Sciences Sociales, Paris, 1994.
Cited on pages 74, 88, and 89.
- János Pach, editor. *Proceedings of the 12th International Symposium on Graph Drawing (GD’04)*, volume 3383 of *Lecture Notes in Computer Science*, 2005. Springer.
Cited on pages 167, 171, and 185.
- Achilleas Papakostas and Ioannis G. Tollis. Algorithms for Area-Efficient Orthogonal Drawings. *Computational Geometry: Theory and Applications*, 9(1–2):83–110, 1998.
Cited on page 38.
- Charalampos Papamanthou and Ioannis G. Tollis. Applications of Parameterized *st*-Orientations in Graph Drawing Algorithms. In Patrick Healy and Nikola S. Nikolov, editors, *Proceedings of the 13th International Symposium on Graph Drawing (GD’05)*, volume 3843 of *Lecture Notes in Computer Science*, pages 355–367. Springer, 2006.
Cited on page 38.
- Charalampos Papamanthou and Ioannis G. Tollis. Applications of Parameterized *st*-Orientations. *Journal of Graph Algorithms and Applications*, 14(2):337–365, 2010.
Cited on page 38.
- Ronald C. Read. A New Method for Drawing a Graph Given the Cyclic Order of the Edges at Each Vertex. *Congressus Numerantium*, 56:31–44, 1987.
Cited on page 22.
- Gerhard Ringel. Two Trees in Maximal Planar Bipartite Graphs. *Journal of Graph Theory*, 17:755–758, 1993.
Cited on page 60.
- Gerhard Ringel, Anna S. Lladó, and Oriol Serra. On the Tree Number of REgular Graphs. *Discrete Mathematics*, 165–166:587–595, 1997.
Cited on page 60.
- Fred S. Roberts. On the Boxicity and Cubicity of a Graph. In William T. Tutte, editor, *Recent Progresses in Combinatorics*, pages 301–310. Academic Press, 1969.
Cited on page 100.

- Pierre Rosenstiehl and Robert E. Tarjan. Rectilinear Planar Layouts and Bipolar Orientations of Planar Graphs. *Discrete and Computational Geometry*, 1(1):343–353, 1986.
Cited on pages [38](#), [45](#), and [136](#).
- Arnie Rosenthal and Anita Goldner. Smallest Augmentations to Biconnect a Graph. *SIAM Journal on Computing*, 6(1):55–66, 1977.
Cited on page [26](#).
- Günter Rote. Strictly Convex Drawings of Planar Graphs. In *Proceedings of the 16th Annual ACM–SIAM Symposium on Discrete Algorithms (SODA’05)*, pages 728–734. SIAM, 2005.
Cited on page [156](#).
- Horst Sachs. Coin Graphs, Polyhedra, and Conformal Mapping. *Discrete Mathematics*, 134:133–138, 1994.
Cited on page [97](#).
- Sadish Sadasivam and Huaming Zhang. NP-Completeness of st -Orientations for Plane Graphs. *Theoretical Computer Science*, 411(7–9):995–1003, 2010.
Cited on page [38](#).
- Edward R. Scheinerman. The Interval Number of a Planar Graph: Three Intervals Suffice. *Journal of Combinatorial Theory Series B*, 35(3):224–239, 1983.
Cited on page [100](#).
- Edward R. Scheinerman. *Intersection Classes and Multiple Intersection Parameters of Graphs*. PhD thesis, Princeton University, 1984.
Cited on page [100](#).
- Edward R. Scheinerman. Characterizing Intersection Classes of Graphs. *Discrete Mathematics*, 55(2):185–193, 1985a.
Cited on page [100](#).
- Edward R. Scheinerman. Irrepresentability by Multiple Intersection, or Why the Interval Number is Unbounded. *Discrete Mathematics*, 55(2):195–211, 1985b.
Cited on page [100](#).
- Ludwig Schläfli. Theorie der vielfachen Kontinuität. In *Gesammelte mathematische Abhandlungen*, volume 1. Birkhäuser Verlag, 1950.
Cited on page [23](#).
- Jens M. Schmidt. Construction Sequences and Certifying 3-Connectedness. In Jean-Yves Marion and Thomas Schwentick, editors, *Proceedings of the 27th International Symposium on Theoretical Aspects of Computer Science (STACS’10)*,

- pages 633–644. Dagstuhl Research Online Publication Server, 2010. URL <http://drops.dagstuhl.de/opus/volltexte/2010/2491/>.
Cited on page 30.
- Jens M. Schmidt. *Structure and Constructions of 3-Connected Graphs*. PhD thesis, Fachbereich Mathematik und Informatik, Freie Universität Berlin, 2011.
Cited on pages 22 and 28.
- Walter Schnyder. Planar Graphs and Poset Dimension. *ORDER*, 5(4):323–343, 1989.
Cited on pages iv, 2, 31, 34, 35, 59, 61, 67, 84, 145, 146, and 153.
- Walter Schnyder. Embedding Planar Graphs on the Grid. In *Proceedings of the 1st Annual ACM–SIAM Symposium on Discrete Algorithms (SODA ’90)*, pages 138–148. SIAM, 1990.
Cited on pages iv, v, 2, 3, 59, 60, 61, 66, 68, 136, 145, 146, 157, 158, 159, and 160.
- Oded Schramm. Existence and Uniqueness of Packings with Specified Combinatorics. *Israel Journal of Mathematics*, 73(3):321–341, 1991.
Cited on page 97.
- Oded Schramm. Combinatorically Prescribed Packings and Applications to Conformal and Quasiconformal Maps. Technical report, Princeton University, 2007. URL <http://arxiv.org/abs/0709.0710v1>. Modified version of PhD thesis, Princeton University, 1990.
Cited on pages 98 and 99.
- Angelika Steger. *Diskrete Strukturen Band 1. Kombinatorik, Graphentheorie, Algebra*. Springer, 2007.
Cited on page 19.
- S. K. Stein. Convex Maps. *Proceedings of the American Mathematical Society*, 2(3):464–466, 1951.
Cited on pages 32 and 34.
- Erich Steinitz. *Polyeder und Raumeinteilungen*. Encyklopädie der Wissenschaften mit Einschluss ihrer Anwendungen. Teubner, 1914.
Cited on page 22.
- Erich Steinitz and Hans Rademacher. *Vorlesungen über die Theorie der Polyeder*. Springer, 1934.
Cited on page 22.

- Kenneth Stephenson. *Introduction to Circle Packing: The Theory of Discrete Analytic Functions*. Cambridge University Press, 2005.
Cited on page 98.
- Roberto Tamassia and Ioannis G. Tollis. A Unified Approach to Visibility Representations of Planar Graphs. *Discrete and Computational Geometry*, 1:321–341, 1986.
Cited on pages 38 and 45.
- Roberto Tamassia and Ioannis G. Tollis, editors. *DIAMCS International Workshop*, volume 894 of *Lecture Notes in Computer Science*, 1995. Springer.
Cited on pages 170 and 174.
- Robert E. Tarjan. Two Streamlined Depth-First Search Algorithms. *Fundamenta Informaticae*, 9:85–94, 1986.
Cited on page 37.
- Carsten Thomassen. Planarity and Duality of Finite and Infinite Graphs. *Journal of Combinatorial Theory Series B*, 29(2):244–271, 1980.
Cited on pages 24, 28, 29, 32, 33, and 36.
- Carsten Thomassen. Kuratowski’s Theorem. *Journal of Graph Theory*, 5(3):225–241, 1981.
Cited on page 32.
- Carsten Thomassen. Plane Representations of Graphs. In John Adrian Bondy and U. S. Murty, editors, *Progress in Graph Theory*, pages 43–69. Academic Press, 1984.
Cited on pages 99 and 116.
- Carsten Thomassen. Interval Representation of Planar Graphs. *Journal of Combinatorial Theory Series B*, 40(1):9–20, 1986.
Cited on page 100.
- William Paul Thurston. *The Geometry and Topology of Three-Manifolds*, 2002.
URL <http://www.msri.org/publications/books/gt3m/>.
Cited on page 97.
- William T. Tutte. Convex Representations of Graphs. *Proceedings of the London Mathematical Society*, 10:304–320, 1960.
Cited on page 32.
- William T. Tutte. A Theory of 3-Connected Graphs. *Indagationes Mathematicae*, 23:441–455, 1961.
Cited on pages 28, 29, and 30.

William T. Tutte. How to Draw a Graph. *Proceedings of the London Mathematical Society*, s3-13(1):743–767, 1963.

Cited on pages [24](#), [32](#), [36](#), [160](#), and [161](#).

Jacobo Valdes, Robert E. Tarjan, and Eugene L. Lawler. The Recognition of Series Parallel Digraphs. *SIAM Journal on Computing*, 11(2):298–313, 1982.

Cited on page [105](#).

Koichi Wada and Wei Chen. Linear Algorithms for a k -Partition Problem of Planar Graphs. In Juraj Hromkovic and Ondrej Sýkora, editors, *Proceedings of the 24th International Workshop on Graph-Theoretic Concepts in Computer Science (WG'98)*, volume 1517 of *Lecture Notes in Computer Science*, pages 324–336. Springer, 1998.

Cited on page [136](#).

Klaus Wagner. Bemerkungen zum Vierfarbenproblem. *Jahresbericht der Deutschen Mathematiker-Vereinigung (DMV)*, 46:26–32, 1936.

Cited on pages [32](#) and [34](#).

Toshimasa Watanabe and Akira Nakamura. A Smallest Augmentation to 3-connect a Graph. *Discrete Applied Mathematics*, 28(2):183–186, 1990.

Cited on page [26](#).

Toshimasa Watanabe and Akira Nakamura. A Minimum 3-Connectivity Augmentation of a Graph. *Journal of Computer and System Sciences*, 46(1):91–128, 1993.

Cited on page [26](#).

Hassler Whitney. Non-Separable and Planar Graphs. *Transactions of the American Mathematical Society*, 34(2):339–338, 1932.

Cited on pages [19](#), [24](#), [31](#), [36](#), [38](#), and [60](#).

Hassler Whitney. A Set of Topological Invariants for Graphs. *American Journal of Mathematics*, 55:231–235, 1933.

Cited on page [24](#).

Avram Zehavi and Alon Itai. Three Tree-Paths. *Journal of Graph Theory*, 13(2):175–188, 1989.

Cited on page [59](#).

Bernd Thomas Zey. Algorithms for Planar Graph Augmentation. Master's thesis, TU Dortmund University, 2008.

Cited on pages [26](#) and [27](#).

- Huaming Zhang and Xin He. Compact Visibility Representation and Straight-Line Grid Embedding of Plane Graphs. In Frank Dehne, Jörg-Rüdiger Sack, and Michiel Smid, editors, *Proceedings of the 8th International Workshop on Algorithms and Data Structures (WADS'03)*, volume 2748 of *Lecture Notes in Computer Science*, pages 493–504. Springer, 2003.
Cited on pages [38](#), [60](#), and [156](#).
- Huaming Zhang and Xin He. Canonical Ordering Trees and Their Applications in Graph Drawing. *Discrete and Computational Geometry*, 33(2):321–344, 2005a.
Cited on pages [56](#), [58](#), and [71](#).
- Huaming Zhang and Xin He. Improved Visibility Representation of Plane Graphs. *Computational Geometry*, 30:29–39, 2005b.
Cited on page [38](#).
- Huaming Zhang and Xin He. New Theoretical Bounds of Visibility Representation of Plane Graphs. In [Pach \[2005\]](#), pages 425–430.
Cited on page [38](#).
- Huaming Zhang and Xin He. Visibility Representation of Plane Graphs via Canonical Ordering Tree. *Information Processing Letters*, 96(2):41–48, 2005d.
Cited on page [55](#).
- Huaming Zhang and Xin He. Optimal *st*-Orientations for Plane Triangulations. In *Proceedings of the 3rd International Conference on Algorithmic Aspects in Information and Management (AAIM'07)*, volume 4508 of *Lecture Notes in Computer Science*, pages 296–305. Springer, 2007.
Cited on page [38](#).
- Florian Zickfeld. *Geometric and Combinatorial Structures on Graphs*. PhD thesis, Fakultät II – Mathematik und Naturwissenschaften, Technische Universität Berlin, 2007.
Cited on pages [60](#), [71](#), [86](#), [88](#), and [162](#).
- Günter M. Ziegler. *Lectures on Polytopes*. Graduate Texts in Mathematics. Springer, 1995.
Cited on page [24](#).

List of Symbols

\prec	strict partial order
\preceq	total order or (non-strict) partial order
\subset	proper subgraph
\subseteq	subgraph
$a \vee b$	join of $a, b \in S$
$a \wedge b$	meet of $a, b \in S$
a	simple arc
\mathring{a}	interior of a
\mathcal{A}	antichain
$\langle \mathcal{A} \rangle$	filter generated by antichain \mathcal{A}
C_n	cycle of length n
\mathcal{C}	contact representation
∂S	boundary of an open or closed set $S \subseteq \mathbb{R}^2$
$\deg_G^-(v)$	indegree of vertex v in graph G
$\deg_G^+(v)$	outdegree of vertex v in graph G
$\dim(G)$	(order-)dimension of G
$d(p, q)$	distance of two points $p = (p_1, p_2) \in \mathbb{R}^2$ and $q = (q_1, q_2) \in \mathbb{R}^2$
$d_1(p, q)$	Manhattan distance of two points $p = (p_1, p_2) \in \mathbb{R}^2$ and $q = (q_1, q_2) \in \mathbb{R}^2$
$e = \{u, v\}$	undirected edge with endvertices u and v

$e = (u, v)$ directed edge with endvertices u and v

$E(G)$ edge set of graph G

$E(V_1, V_2)$ set of all V_1 - V_2 -edges in an edge set E

$\mathcal{E}(G)$ edge space of graph G

\mathbb{F}_2 field with two elements $\{0, 1\}$

$\mathcal{F} = \{S_1, \dots, S_n\}$ family of sets

f face of a graph G , or number of faces of a graph G

$F(G) \subseteq \mathbb{R}^2$ set of faces of a graph

$G = (V, E)$ graph

$G^* = (V^*, E^*)$ dual graph

$G^\times = (V^\times, E^\times)$ primal dual superimposition

$G \cup G'$ union of graphs

$G[V']$ induced subgraph of G

G/e edge e is contracted in graph G and multiple edges are replaced by a single edge

G/M_e edge e is contracted in graph G

$\gamma(G)$ genus of a graph G

Γ drawing

K_n complete graph on n vertices

$K_{n,m}$ complete bipartite graph

$L = (S, \preceq)$ lattice

m number of edges of a graph G

\mathbb{N} natural numbers including zero

$N_G(v)$ set of neighbors of a vertex v in G

n number of vertices of a graph G

- $\Pi = (P_0, \dots, P_s)$ canonical ordering or (ordered) path partition
 p, q points in the Euclidean plane
 $p = (p_1, p_2)$ vector $p \in \mathbb{R}^2$
 $p = (p_1, p_2, p_3)$ vector $p \in \mathbb{R}^3$
 $\|p\|$ length of a vector $p \in \mathbb{R}^2$
 $P = \langle v_1, \dots, v_k \rangle$ path
 $P = (S, \preceq)$ partially ordered set with a non-strict partial order
 $P = (S, <)$ partially ordered set with a strict partial order
 \mathcal{Q} contact system
 \mathbb{R} real numbers
 \mathbb{R}^2 Euclidean plane
 \mathbb{R}^3 Euclidean space
 \mathbb{R}^d d -dimensional vector space
 $R \subseteq S_1 \times \dots \times S_n$ relation
 \mathcal{R} family of total orders
 S set
 $[S]^n$ set of all n -element subsets of S
 $S_1 \times \dots \times S_n$ Cartesian product of S_1, \dots, S_n
 $\mathcal{S} = \{S_1, \dots, S_n\}$ partition
 \mathcal{S} Schnyder wood or bijective concept
 S_k surface of genus k
 $\mathfrak{S}_{\mathcal{A}}$ orthogonal surface generated by antichain \mathcal{A}
 $V(G)$ vertex set of graph G
 \mathcal{V} partition of a vertex set
 W_n wheel with $n + 1$ vertices

$(x(p), y(p))$ coordinates of $p \in \mathbb{R}^2$

$(x(p), y(p), z(p))$ coordinates of $p \in \mathbb{R}^3$

Index

A

Ackermann function 27
acyclic 12, 79
 α -orientation 59, 88
 feasible 88
 α_0 -orientation 85, 89
 minimal 90
ancestor 14
antichain 162
antisymmetric 9
arboricity 14, 59
augmentation problem 26
 general 26
 planar 26
automorphism 12

B

Barnette's and Grünbaum's construction
 sequence 30
barycentric representation 157
 weak 18, 158
belt 126, 127, 130
belt item 130, 131
binary relation *see* relation
bipolar orientation ... *see* *st*-orientation
bond 12, 25
 triple 25
boundary
 face 15
 set 8
boxicity 100
Brightwell-Trotter theorem 60

C

candidate 126
 feasible 43, 44, 126
 locally feasible 126
canonical ordering .. 37, 38, 75, 101, 150
 4-connected graphs 50
 biconnected graphs 49
 dual 47
 equivalent 69
 leftist 44, 61, 91, 125, 129
 leftmost 43
 triangular graphs 38
 triconnected graphs 40
 upper rightist 46
canonical ordering tree 55
canonical spanning tree ... *see* canonical
 ordering tree
Cartesian product 9
certifying algorithm 28
chain 41, 53, 55
 balanced 64
 face 53
 path 53
child 14
chord 16
 minimal 16
chordal path 16
circle packing theorem 97
closed unit interval 8
closure 75, 76
 dual 85
component
 split 25

- triconnected 25
 - connected component 12
 - connectivity
 - edge- 13
 - vertex- 13
 - contact point 8, 97
 - contact representation 97
 - primal dual 97, 117
 - tiling 117
 - contact system 97
 - of arcs 97
 - stretchable 117
 - convex hull 8
 - coordinate mapping 160
 - coordinates 7
 - cut 12
 - cut vertex 13
 - cutset 13
 - cycle 12, 72
 - simple 12
 - cycle space 36
- D**
- degree 11
 - digraph 11
 - two terminal series-parallel 104
 - disjoint 12
 - drawing 15
 - convex 17, 143, 158, 160, 161
 - equivalent 15
 - grid 17, 136, 143, 156, 158, 159, 161
 - planar 15, 98, 143, 158, 159, 161
 - polyline 17
 - straight-line ... 17, 98, 143, 158, 159, 161
- E**
- ear decomposition
 - open 38, 60
 - edge 10
 - bi-directed 11
 - bi-oriented 11
 - contractible 66, 153
 - contracting 27, 153
 - cut 127, 131, 132
 - directed 11
 - dummy 26
 - exterior 15
 - external *see* exterior edge
 - incoming 11
 - inner *see* interior edge
 - interior 15
 - internal *see* interior edge
 - multiple 11
 - outer *see* exterior edge
 - outgoing 11
 - undirected 11
 - uni-directed 11
 - unrelated 14
 - virtual 25
 - edge space 36
 - embedding 16
 - combinatorial 15, 16
 - geodesic 60, 162
 - axial 162
 - geometric 16
 - topological 15, 16
 - endpoint
 - arc 8
 - edge 11
 - endvertex
 - graph 11
 - path 12
 - Euclidean
 - distance 8
 - plane 7
 - space 7
 - Euler's formula 19, 77, 79
 - Euler-Poincaré 23
 - Eulerian orientations 60

F

face..... 15
 adjacent 15
 candidate..... 126
 cut 126, 131, 132
 external *see* outer face
 inner 15
 interior *see* inner face
 outer 15
 separation 46
 family
 of sets 100
 of total orders 35
 Fary's theorem 31, 32, 98
 feasible extension..... 45, 46
 feasible extension..... 46, 47
 filter..... 162
 forest 13
 spanning 14
 four-partition..... 54
 frontier *see* boundary

G

genus
 graph..... 15, 31
 surface 15, 60
 graph..... 10
 abstract dual 19
 biconnected 13
 bipartite..... 11
 complete 11
 connected 12
 dimension 35
 monotone 35
 directed 11
 disconnected 12
 dual 18, 85
 embedded 16
 finite 10
 grid 17

internally triconnected 16
 intersection..... 100
 interval 103
 isomorphic 12
 max-tolerance 103
 maximal plane 16
 merge 25
 multigraphs 11
 non-empty..... 10
 non-planar 15
 planar 15, 19
 plane 16
 polyhedral..... 8
 series-parallel..... 105, 114
 simple 11
 split 25
 triangular 16, 21
 triangulated 21
 triconnected 13, 22
 undirected..... 10
 greatest element 10, 74
 greatest lower bound *see* meet

H

handshaking lemma 20
 homothetic 103
 homothety..... 103
 center 103
 ratio..... 103

I

icosahedron 21
 indegree 11
 infimum *see* meet
 inner vertex
 path..... 12
 tree..... 13
 interior
 arc 8
 irreflexive..... 10

- isomorphism 12
- J**
- join 10, 162
- Jordan arc *see* simple arc
- Jordan curve ... *see* simple closed curve
- K**
- Koebe's theorem 97
- Kuratowski's theorem 32
- L**
- lattice 10, 60, 88
- distributive 10, 60, 89, 90
- leaf 13
- least element 10, 60, 74
- least upper bound *see* join
- length
- cycle 12
- path 12
- vector 8
- loop 11
- M**
- Mac Lane 36
- Manhattan distance 8, 139
- maximal element .. *see* greatest element
- maximum 10
- meet 10, 162
- minimal element *see* least element
- minimum 10
- N**
- n -sets 9
- n -subsets 9
- neighbors 11
- normal labeling... *see* Schnyder labeling
- O**
- open curve *see* simple arc
- order
- dominance 162
- partial 9
- total 9, 35
- order relation 89
- orderly spanning tree 57
- orthogonal surface 60, 121, 162
- axial 162
- orthogonal surfaces 162
- outdegree 11, 61, 62, 66
- outer chain 16
- P**
- parent 14
- partially ordered set 10
- partition 9, 126
- path 12
- straight 89
- path partition 91
- equivalent 92
- leftist 95, 96, 150, 155
- upper rightist 96
- planar dual *see* dual graph
- plane *see* Euclidean plane
- point
- grid 17
- in the plane 7
- poles 104
- polygon 8
- height 106
- inner 106
- polytope 8
- poset *see* partially ordered set
- primal dual superimposition 86, 90
- product set *see* Cartesian product
- R**
- realizer 34, 61
- reflexive 9
- region vector 160, 162

- regions of a vertex 80, 157
- regular edge labeling 51
- relation 9
- representation 15
 - barycentric 18
 - rubber band 24
 - touching 99
 - visibility 17
- root 13
- rotation system 15
- S**
- Scheinerman's conjecture 100
- Schnyder labeling 44, 59, 62, 63, 76, 85, 88, 153, 154, 157
- Schnyder realizer *see* Schnyder wood
- Schnyder wood 85
 - minimal 61, 90, 91, 96, 148, 155
 - triangular graph 61, 101, 118, 146
 - triconnected graph 74, 150, 160
- Schnyder's theorem 34
- separation class 25
- separation pair 13
- separator 13
- set
 - convex 8
- shift method 138
- side length of a triangle 106
- simple arc 8
- simple closed curve 8
- simple polygonal arc 8
- singleton 41, 53, 55
- size of a triangle 106
- source 11
- sparse 36
- st*-ordering 37, 38, 60
- st*-orientation 38, 60
- standard basis 36
- Steinitz's Theorem 22, 23
- Steinitz's theorem 31
- stereographic projection 32
- straight-line segment 8
- subdivision 32
- subgraph 11
 - induced 11
 - proper 11
- subpath 12
- support
 - left 49
 - legal 49
 - right 49
- supremum *see* join
- suspension 75, 76
- symmetric 10
- T**
- tangent 8
- target 11
- 3-orientation 62, 64, 66, 72
- tolerance 103
- topological ordering 37
- total 9
- transitive 9, 10
- traversal
 - inorder 15
 - postorder 14, 106, 109
 - preorder 14, 57, 58, 71
- tree 13
 - binary 14
 - decomposition 105
 - ordered 14
 - partial planar 3-tree 112
 - planar 3-tree 109
 - rooted 13, 68, 80
 - spanning 14, 59, 60
 - independent 14, 59
 - well-orderly 58
- triangle 11
 - separating 16
 - side length 106
 - size 106
- triangle contact representation

homothetic 103
 triangle contact system 101
 strict 101
 triangulation 143
 stacked 71, 109
 TTSP-digraph *see* two terminal
 series-parallel digraph
 Tutte's construction sequence 29
 Tutte's contraction sequence 28
 Tutte's theorem 24, 161

U

union of graphs 12
 unit interval *see* closed unit interval

V

valency 11
 vertex 10
 adjacent 11
 eligible 146
 exterior 15
 external *see* exterior vertex
 forbidden 128
 incident 11
 inner *see* interior vertex
 interior 15
 internal *see* interior vertex
 isolated 11
 outer *see* exterior vertex
 related 14
 simplicial 114
 singular 128, 129
 stopper 128, 129
 unrelated 14, 57

W

wheel 12, 29, 31
 Whitney's theorem 36